ELECTRON IMPACT STUDIES ON ORGANOMETALLIC COMPOUNDS

by

D.B. Chambers, B.Sc.

(Grey)

A Thesis submitted for the degree of Doctor of Philosophy in the University of Durham.

July, 1968.

ACKNOWLEDGEMENTS.

It is a pleasure to thank Prof. G.E. Coates, Dr. F. Glockling and Dr. M. Weston for their help and encouragement throughout the work described in this Thesis.

I am indebted to the Science Research Council for a maintenance grant, and to those members of the Chemistry Department, University of Durham, who so readily gave advice and assistance.

NOTE

The work described in this Thesis was carried out in the University of Durham between October 1965 and July 1968. The work has not been submitted for any other degree and is the original work of the author except where acknowledged by reference.

PUBLICATIONS

The work described in this Thesis has been the subject of the following publications:

"Mass Spectra of Organo-germanes and -stannanes", Chem. Comm., 1966, 282. (with F. Glockling, J.R.C. Light and M. Weston.)

"Mass Spectra of Organo-stannanes and -plumbanes", J. Chem. Soc., (A), 1967, 1759. (with F. Glockling and M. Weston.)

"Mass Spectra of Metal-Metal Bonded Compounds", J. Chem. Soc., (A), 1968, 735 (with F. Glockling.)

A review "Mass Spectra of Organometallic Compounds" has been accepted for publication by Quarterly Reviews. (with F. Glockling and J.R.C. Light.)

The author also gave a lecture "Electron Impact Behaviour and Bond Energies of Beryllium and Group IVb Organo- compounds" at the 3rd international Symposium on Organometallic Compounds, Munich, 1967. (with F. Glockling, J.R.C. Light and M. Weston.)

CONTENTS

SUMMARY

This thesis is concerned with electron impact studies on organoderivatives of beryllium, aluminium and Group IVb metals (mainly tin). The primary objectives of the research were:

i) To obtain, from appearance potential measurements, comparative and if possible absolute bond dissociation energies in both molecules and ions, together with other thermodynamic data.

ii) To examine the mass spectra of representative organometallic compounds with a view to determining the effect of the metal, changes in organic groups and spectrometer conditions.

From the appearance potentials of ions produced in the electron impact mass spectra of some organostannanes, bond dissociation energy differences, heats of formation of triphenyltin compounds and the dissociation energy of the bond $Ph_3Sn - X$ ($X = Me$, Et, Ph, I, $GeMe_3$, $SnMe_3$, $SnPh_3$) have been derived. The ionization potentials of beryllium dialkyls and the appearance potentials of the major beryllium - containing fragment ions have also been measured and bond dissociation energies in molecular and fragment ions evaluated.

In the mass spectra of organoderivatives of the Group IVb metals, the most abundant fragments are even-electron metal-containing ions in which the metal is three-co-ordinate. Parent ions are of low abundance and decompose mainly by radical elimination e.g.

$$R_4M^{+\cdot} \longrightarrow R_3M^{+} + R\cdot$$

Bond energy measurements suggest that the bond most readily cleaved in this decomposition is the weakest in the neutral molecule. In further

fragmentation even-electron ions maintain their even-electron character by molecule elimination.

Certain trends are attributable to the increasing metal-carbon bond strength from lead to silicon. Molecular ions decrease in the order Si > Ge > Sn > Pb while metal ions, $M^{+\bullet}$, are appreciable only for tin and lead. Ions formed by carbon-carbon or carbon-hydrogen cleavage, although always of low abundance, increase in importance from lead to silicon.

With beryllium dialkyls the abundance of all beryllium-containing ions but especially di-and tri-metallic ions falls with increasing source temperature due to dissociation of weak bridging bonds and thermal decomposition before ionization. The major di-and tri-metallic ions are even-electron and readily lose alkene. In contrast to Group IVb derivatives, odd-electron $C_aH_bBe^+$ ions are appreciable. Parent monomer ions, $(C_nH_{2n+1})_2Be^{+\bullet}$, decrease in abundance as the size of the alkyl group increases and major fragments are produced from the parent by elimination of the radical $C_nH_{2n+1}^{\bullet}$, and alkane, C_nH_{2n+2}.

Organoaluminium compounds give mass spectra which depend on source temperature. This is especially true for dimethyl- and diethyl-aluminium hydride which show thermal rearrangement above 100°C producing trimethyl- and triethyl-aluminium respectively. The decomposition modes of aluminium-containing ions are almost identical to those of Group IVb organoions.

1. INTRODUCTION.

1.1 Mass Spectra of Organometallic Compounds of the Main Groups.

1.2 Ionization and Appearance Potentials.

1.3 Derivation of Thermochemical Data from Appearance Potentials.

1. INTRODUCTION.

A mass spectrometer is an instrument which produces a beam of ions from a substance being investigated, sorts these ions into a spectrum according to their mass to charge ratios and records the relative abundance of each species of ions present. The theory and design of these instruments has been widely discussed [1,2] but a recent review sums up the salient points [3]. Most early studies in mass spectrometry employed single focussing instruments using a magnetic field to separate ions by their mass to charge ratio. The resolution of such instruments never exceeded one part in three thousand and recent developments have been with the aim of extending their mass range, versatility and precision. With a careful choice of design parameters electric and magnetic fields may be combined to increase the resolution by elimination of the two main aberrations limiting the resolution of magnetic sector instruments; a) the angular divergence of the ion beam and b) variations in the velocity of the ions.

Such high resolution mass spectrometers have brought a new dimension to the subject. Not only are these instruments capable of measuring ion masses, in some cases up to 1000 mass units, with a precision of a few parts per million, but they can also give ion abundance values to a high degree of accuracy. These instruments are thus able to provide at least in theory, data which can lead to the exact elemental analysis of every ion in the spectrum. Such information is often vital in structural analysis. For example the loss of 28 mass

units from an ion observed in a low resolution spectrum could be identified as CO, N_2, C_2H_4 or NCH_2 loss by the high resolution measurements.

Although the majority of mass spectrometric investigations resolve ions by magnetic deflection, there exist other techniques of growing importance. For example the time of flight method has been developed into a versatile technique and several commercial instruments are available [2].

Various methods are available for ion production [1] but that most widely used is electron bombardment of gaseous molecules when the generally accepted interaction occurs [1,4,5,6]:

$$e + XYZ \longrightarrow XYZ^+ + 2e$$

$$XYZ^+ \longrightarrow XY^+ + Z; \text{ or } YZ^+ + X; \text{ or } X^+ + YZ \text{ etc.}$$

The electron beam energy normally employed (about 50 or 70eV) is in excess of the minimum energy required to cause ionization. (Generally the ionization potential rarely exceeds 10eV and the bond dissociation energy 5eV so that the incident electron beam has more than three times the minimum energy needed for the above reactions).

Ions may also be formed by pre-ionization or pre-dissociation[7] when the interaction of an electron and a molecule does not lead directly to the formation of an ion but to a neutral excited molecule. The energy imparted to the molecule is postulated to be greater than, or at least as great as, the ionization potential so that the excited

molecule may subsequently decompose:-

$$XYZ^{*} \longrightarrow XYZ^{+} + e$$

$$XYZ^{*} \longrightarrow XY^{+} + Z + e$$

From the available evidence [8] indirect ion formation may compete with direct ionization.

The mass spectrum produced under specified ionization conditions is sometimes known as the cracking pattern, and is characteristic of the compound. This pattern will contain all possible combinations of ions as shown above, but it will also include ions of the type XZ^{+} which can only arise by a rearrangement process since in the original material the two constituents of this ion were separately attached to Y but not to each other.

One of the difficulties encountered in the analysis of spectra arises from the presence of these rearrangement ions. Although this interesting and difficult field has been the subject of extensive and detailed study for organic molecules with the aim of finding rules[1,4,5,9] which are broadly applicable, when the work described in this thesis was begun, there were only few published reports on the spectra of organometallic compounds. For example for the particular metal-compounds examined herein there were only two papers for tin, both describing the mass spectrum of tetramethyltin, and none for beryllium, aluminium or metal-metal bonded compounds of main group metals.

Most of the reported studies on organometallic compounds have involved mono-isotopic elements or elements containing one dominant isotope. Furthermore only low resolution spectra have been

recorded and so have been without direct confirmation of the elemental composition of ions in the spectra obtained. The present study has made considerable use of high resolution mass measurement which for polyisotopic metals is based on data specifically calculated for each polyisotopic unit considered. This need for repeated mass measurement has arisen for a number of reasons which are discussed in chapter 3., Calculation of Results.

1.1. Mass Spectra of Organometallic Compounds of the Main Groups.

A number of papers on the mass spectra of organometallic compounds of the main groups have appeared either during or since the completion of the present work. Those papers of immediate relevance and comparability to this research, which in some cases have provided confirmation of the results reported in this thesis are dealt with in Chapter 4.2. of the Discussion.

In the following review the mass spectra were produced by electron impact using 50 to 70 volt electrons. Ions in which the number of bonding electrons is odd are represented as $(ion)^{+\bullet}$, whereas even-electron ions are represented as $(ion)^{+}$. This distinction has been found in the present study to have considerable significance for main group organometallic compounds, though for transition metal complexes, where ionization may involve removal of an electron from a non-bonding orbital such considerations often have no relevance.

Group I Li.

The mass spectra of lithium alkyls are of interest since they contain ions of associated species. For example ethyl lithium vapour [10] gives $Et_5Li_6^+$, $Et_4Li_5^+$, $Et_3Li_4^+$, $Et_2Li_3^+$, $EtLi_2^+$ and Li^+. The appearance potentials of $Et_5Li_6^+$ and $Et_3Li_4^+$ are far lower than those of the other ions and from this it was tentatively deduced that the vapour of ethyllithium consisted of a mixture of hexamer and tetramer molecules (Et_6Li_6 and Et_4Li_4) which decomposed on ionization:

$$Et_nLi_n + e \longrightarrow Et_{n-1}Li_n^+ + Et^{\cdot} + 2e \quad n = 4 \text{ or } 6$$

Further evidence for the composition of the vapour came from a shift in the ratios of ion intensities as a result of varying the temperature of the vapour prior to ionization.

All other ions produced were due to decomposition of the $Et_{n-1}Li_n^+$ species.

$$Et_{n-1}Li_n^+ \longrightarrow Et_{n-x-1}Li_{n-x}^+ + (EtLi)_x$$

Lithiomethyltrimethylsilane $(LiCH_2SiMe_3)$ [11] vapour produced a spectrum showing ions which could have been derived from tetramer molecules (R_4Li_4) via the ionization and decomposition processes shown above.

Group II Zn,Hg.

The compounds Me_2Zn [12], $(t\text{-}Bu)_2Zn$ [13], Me_2Hg, Et_2Hg and $(n\text{-}Bu)_2Hg$ [14] have been examined. All give $MR_2^{+\cdot}$, MR^+ and $M^{+\cdot}$ ions (M = metal, R = alkyl) in high abundance, indicating that the major decomposition processes are bond cleavages:

$$R_2M^{+\cdot} \longrightarrow RM^+ \longrightarrow M^{+\cdot}$$

$RMH^{+\cdot}$ and MH^+ ions are present in low abundance. Hydrocarbon ions are major species in the spectra of the mercury compounds but may arise from thermal decomposition before ionization.

The ionic cyclopentadienyls $(C_5H_5)_2Mg$ and $(C_5H_5)_2Mn$ give similar spectra producing fragment ions, $C_5H_5M^+$ and $M^{+\cdot}$, formed by

metal-ring bond cleavages [15]. [$(C_5H_5)_2Mg^{+\cdot}$ 21%; $C_5H_5Mg^+$ 38%; $Mg^{+\cdot}$ 31% and $(C_5H_5)_2Mn^+$ 19%; $C_5H_5Mn^+$ 29%; Mn^+ 25%; abundances expressed as percentage of total ion current.] The bis-cyclopentadienyls of transition metals produce similar fragment ions although in different relative abundances and the molecular ion is generally the most intense ion [15,16].

Group III Al

Trimethylaluminium gives Al^+, $AlCH_3^{+\cdot}$; $AlMe_2^+$ and $AlMe_3^{+\cdot}$ as the most abundant metal containing species [12]. Rearrangement ions AlH_2^+ and $HAlMe^{+\cdot}$ are of low abundance.

From clastograms (Plots of ion current VS. Electron energy) and appearance potentials of the major ions it may be deduced that simple bond cleavage decomposition of the parent ion occurs.

$$AlMe_3^{+\cdot} \longrightarrow AlMe_2^+ \longrightarrow AlMe^{+\cdot} \longrightarrow Al^+$$

Although trimethylaluminium is known to be dimerie in the gas phase [17] $Al_2Me_5^+$ was the only bi-aluminium species detected in extremely low abundance. Work described in this thesis however shows that this is most probably due to a high source temperature ($\sim 200^{\circ}C$) an important instrument condition not specified by Winter and Kiser [12] in their study.

In contrast $(R_2AlNCPh_2)_2$, R = Me, or, Ph, [18] produce a weak peak corresponding to the molecular ion and $Ph_4(CN)_2Al_2R_3^+$ is the most abundant aluminium-containing ion. Weak ions

corresponding to monomer species were also observed but the major ion in the spectrum was $Ph_2CN^{+\cdot}$.

Group IV Si,Ge,Sn,Pb.

Although all the work published prior to 1966 is described below, some later papers are more appropriately dealt with in the Discussion of this thesis.

The mass spectra of a variety of organosilanes, mainly methylderivatives, have been described. All show low intensity molecular ions and major ions are produced by bond cleavage decompositions in the molecular ion. For example cyclic silicon organocompounds such as

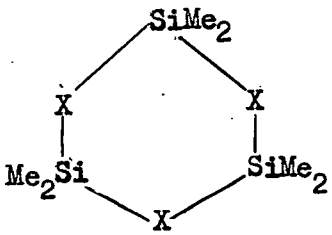

X = $-CH_2-$, $-NH-$, or $-O-$.

(I)

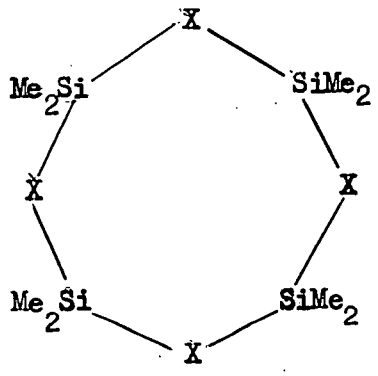

X = $-CH_2-$, or $-NH-$.

(II)

give similar spectra, loss of methyl from the molecular ion producing the most abundant ion [19,20,21,22,23]. The eight-membered ring compound II (X = $-CH_2-$) in addition gives ions of high abundance

resulting from ring fragmentation.

In general the cyclic compounds are more stable to electron impact induced fragmentation than linear compounds containing the same number of silicon atoms. Thus for Me_4Si, $Me_3Si{\cdot}CH_2{\cdot}SiMe_3$, $Me_3Si{\cdot}CH_2{\cdot}SiMe_2{\cdot}CH_2{\cdot}SiMe_3$ and $Me_3Si{\cdot}CH_2{\cdot}SiMe_2{\cdot}CH_2{\cdot}SiMe_2{\cdot}CH_2{\cdot}SiMe_3$ silicon-carbon bond cleavage takes the form of methyl radical loss for the lighter compounds but for Si_3 and Si_4 compounds fragmentation of the silicon-carbon skeleton occurs by cleavage of Si - CH_2 bonds. [19,24]

Substitution of the methylene hydrogen atoms in $Me_3Si{\cdot}CH_2{\cdot}SiMe_3$ by methyl or benzyl groups, increases the probability of the molecular ion decomposing by cleavage of the central Si - CR_2 bonds. [19] Such behaviour is perhaps not surprising being paralleled by alkanes which also tend to fragment at highly branched carbon atoms. [1,9] The observation is useful, however, in that it allows a clear distinction to be made between isomers of the type $H_2MeSi{\cdot}CH(Me){\cdot}SiMe_2H$ and $HMe_2Si{\cdot}CH_2{\cdot}SiMe_2H$. The stability of the skeleton to electron impact induced fragmentation is also reduced by increasing the number of methylene groups between silicon atoms. Thus $Me_3Si{\cdot}CH_2{\cdot}CH_2{\cdot}SiMe_3$ gives Me_3Si^+ as the most abundant ion whereas for $Me_3Si{\cdot}CH_2{\cdot}SiMe_3$, $(P\text{-}Me)^+$ i.e. (parent ion minus methyl) is the base peak. [19]

Replacing any or all of the methyl groups of I (X = CH_2) and $Me_3Si{\cdot}CH_2{\cdot}SiMe_3$ does not affect the lability of the molecular skeleton to fragment after ionization [21]. The loss of H· from fully methylated compounds is not generally observed but with $H_3Si{\cdot}CH_2{\cdot}SiH_3$ dissociation

of carbon-hydrogen bonds must occur at some stage since all the ions from $CH_7Si_2^+$ to CSi_2^+ are observed. When silicon-hydrogen bonds are present in a molecule $(P-H)^+$ ions are always observed in addition to $(P-Me)^+$ ions but methyl groups when present are lost preferentially. [24,21]

With alkylchlorosilanes R_3SiCl, R_2SiCl_2 and $RSiCl_3$ where R is CH_3 or C_2H_5, loss of both alkyl and chlorine from the molecular ion occurs but again cleavage of the silicon-carbon bond predominates. [25,26]

Rearrangement ions are often observed in the spectra of organosilanes. For example Phenylchlorosilanes, Ph_2SiCl_2 and $PhSiCl_3$ produce $Ph_2^{+\cdot}$ and $PhCl^{+\cdot}$ [25] and with Me_nSiH_{4-n} (n = 0,1,2,3,4) compounds [24] rearrangement ions are of high abundance, the elimination of a stable molecule from an ion often being accompanied by a metastable peak:

$$Me_3Si^+ \longrightarrow MeSiH_2^+ + C_2H_4$$

$$HSiMe_2^+ \longrightarrow H_3Si^+ + C_2H_4$$

$$HSiMe^{+\cdot} \longrightarrow Si^{+\cdot} + CH_4$$

Although no metastable peaks were reported in the mass spectra of silicon-methylene compounds [19,20,21], ions of low abundance were often observed especially for the cyclic compounds which could have resulted by emission of methane from $(P-Me)^+$ ions. Similarly silazanes [22] eliminate neutral molecules from $(P-Me)^+$ ions and in some cases metastable peaks are present. Thus $(Me_2SiNH)_3$ and $(Me_2SiNH)_4$ show loss of both CH_4 and NH_3 from $(P-Me)^+$ ions, the loss of NH_3 although requiring considerable rearrangement being confirmed [22] by a metastable peak. Similarly $Me_3Si{\cdot}NH{\cdot}SiMe_2Cl$ shows loss of HCl from $(P-Me)^+$ while $(MeO)Me_2Si{\cdot}NH{\cdot}SiMe_2(OMe)$ eliminates formaldehyde after losing a methyl group.

Though the molecular weight of an alcohol is often found from the mass spectra of its trimethylsilyl derivative (Me_3SiOR) which show a large $(P\text{-}Me\cdot)^+$ ion [27], the origins of the rearrangement ions were not elucidated [28] using deuterium labelling until 1967. The mechanisms involved are illustrated by the fragmentation of pentan-1-ol trimethylsilyl ether which exhibits peaks which appear in the spectra of practically all trimethylsilyl ethers

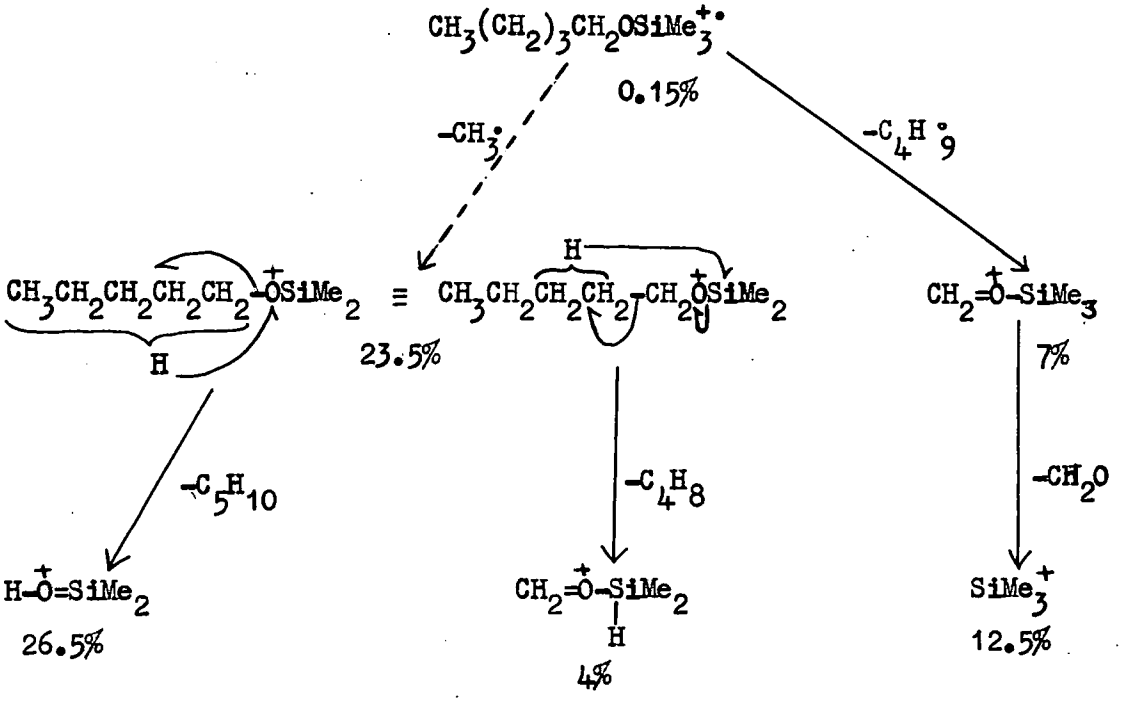

In the above solid straight arrows represent processes confirmed by metastable peaks and the numbers are the percentage of the total ion current carried by that ion. Curved fishhooks (↷) represent movement of one electron and curved arrows (↷) movement of two.

The trimethyl derivatives of secondary alcohols $Me_3Si\text{-}O\text{-}CH\begin{matrix}R'\\R\end{matrix}$; in addition give an intense peak corresponding to loss of the larger alkyl group R' or R.

An unusual feature of the methylsilalazanes, methylsiloxanes and methylsilicon methylene compounds is the production of multiply charged species often in quite high abundance. Thus

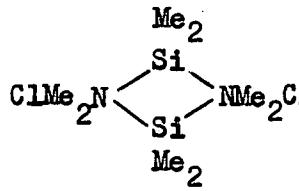

produces $(P-2Me\cdot)^{++}$ as the second most abundant ion and the cyclic siloxane $(Me_2SiO)_3$ shows $(P-2Me\cdot)^{++}$ and $(P-3Me\cdot)^{+++}$ Dibeler et. al. [23] first observed this high abundance of doubly charged ions when there were two silicon atoms present and triply charged ions when there were three and proposed that the most probable ionization process involved the removal of one electron and methyl group from each silicon atom within the molecule.

As with organosilanes, molecular ions of lead alkyls are of low abundance as are all ions heavier than $C_6H_{15}Pb^+$. With the compounds Me_4Pb, Me_3PbR (R=Et, n-Bu, s-Bu, t-Bu), Me_2PbEt_2, $MePbEt_3$ and Et_4Pb loss of the heaviest alkyl group from the molecular ion gives R_3Pb^+ as the most abundant ion in the spectrum.[29]

Rearrangement ions were very common. For example with tetra-n-propyl- and tetra-iso-butyl-lead, CH_3Pb^+ was the most abundant ion in their spectra. No metastable peaks were reported, however, that could indicate the mode of formation of these rearrangement ions even though some, such as hydride ions, were quite abundant.

The mass spectra of the tetramethylderivatives of carbon, silicon, germanium, tin and lead have been compared [30,111]. Again the

molecular ion is small and Me_3M^+ is the most abundant ion. This led to the suggestion that ionization occured by loss of a bonding electron between the central atom and a methyl group. The abundances of $M^{+\cdot}$, MR^+, and $MR_2^{+\cdot}$ increase from carbon to lead while ions resulting from the dissociation of hydrogen atoms decrease from carbon to lead.

Hydride ions $H_2MCH_3^+$ and H_3M^+ also decrease in abundance from silicon to lead and it was postulated that extrapolation of the abundances could give information concerning the origin of some of the peaks in the spectrum of tetramethylmethane. Thus the height of the H_3M^+ peaks varies from zero for tin and lead to 5.1% for Si (base peak for all compounds is Me_3M^+ = 100%) whereas the abundance of the methyl ion decreases from 12.4 in tetramethyllead to 5.07 in tetramethylsilicon. The abundance of the CH_3^+ peak has an intensity of 9.3% and it was argued that the trend observed with the other tetramethyl compounds showed that some of the CH_3^+ ions were in fact trihydrides of the central carbon. Measurements on $^{13}CMe_4$ showed [31] however, that no $^{13}CH_3^+$ ions occurs in the spectrum illustrating the unsatisfactory nature of the use of one element as a homologue of another.

Group V As, Sb, Bi.

For triphenylderivatives [32] molecular ion abundances diminish in the order As > Sb > Bi whereas metal ion abundances M^+ follow the reverse order, as expected from the variation of metal-carbon bond strengths within a group. Similar observations concerning M^+ ions

may be made for the trimethyl-compounds.[12,33]

Of these compounds trimethylantimony has been studied in most detail [12] and clastograms and appearance potential measurements on the major ions $Me_3Sb^{+\bullet}$ (78%), Me_2Sb^+ (100%), $MeSb^{+\bullet}$ (36%) and Sb^+ (37%) indicate simple bond cleavage decompositions

$$Me_xSb^+ \longrightarrow Me_{x-1}Sb^+ + Me^\bullet$$

Loss of H_2 (or $2H^\bullet$) from R_2M^+ ions is observed for all the arsenic and antimony compounds but not the bismuth.

1.2. Ionization and Appearance Potentials.

The first ionization potential of a molecule is defined as the energy difference between the ground state vibrational level of the lowest electronic state of the molecule and the molecular ion. This is sometimes refered to as the "adiabatic" ionization potential and is of importance in understanding the structure of molecules. Electrons of sufficient energy can ionize molecules by the process:-

$$e + AB \longrightarrow AB^{+} + 2e$$

The conditions under which ionization takes place are governed by the Franck-Condon principle since for electron bombardment ionization the time of interaction is so short (of the order of 10^{-15} sec.) compared to the time necessary for a vibration (10^{-12} to 10^{-13} sec.) that nuclei may be considered as fixed at their equilibrium distances during the ionization process. If the potential energy curves representing the molecule before the transition and the molecular ion after the transition are plotted, the points on these curves representing the conditions before and after ionization will correspond to the same nuclear separation and will thus lie on a line parallel to the energy axis. Such a transition is refered to as a vertical transition, and the ionization potential measured in this way as the vertical ionization potential. For the case of diatomic molecules various possibilities of electronic structures are shown in fig. 1.

It can be seem that ionization potentials of molecular ions which are obtained by electron impact measurements must be considered

Fig.1

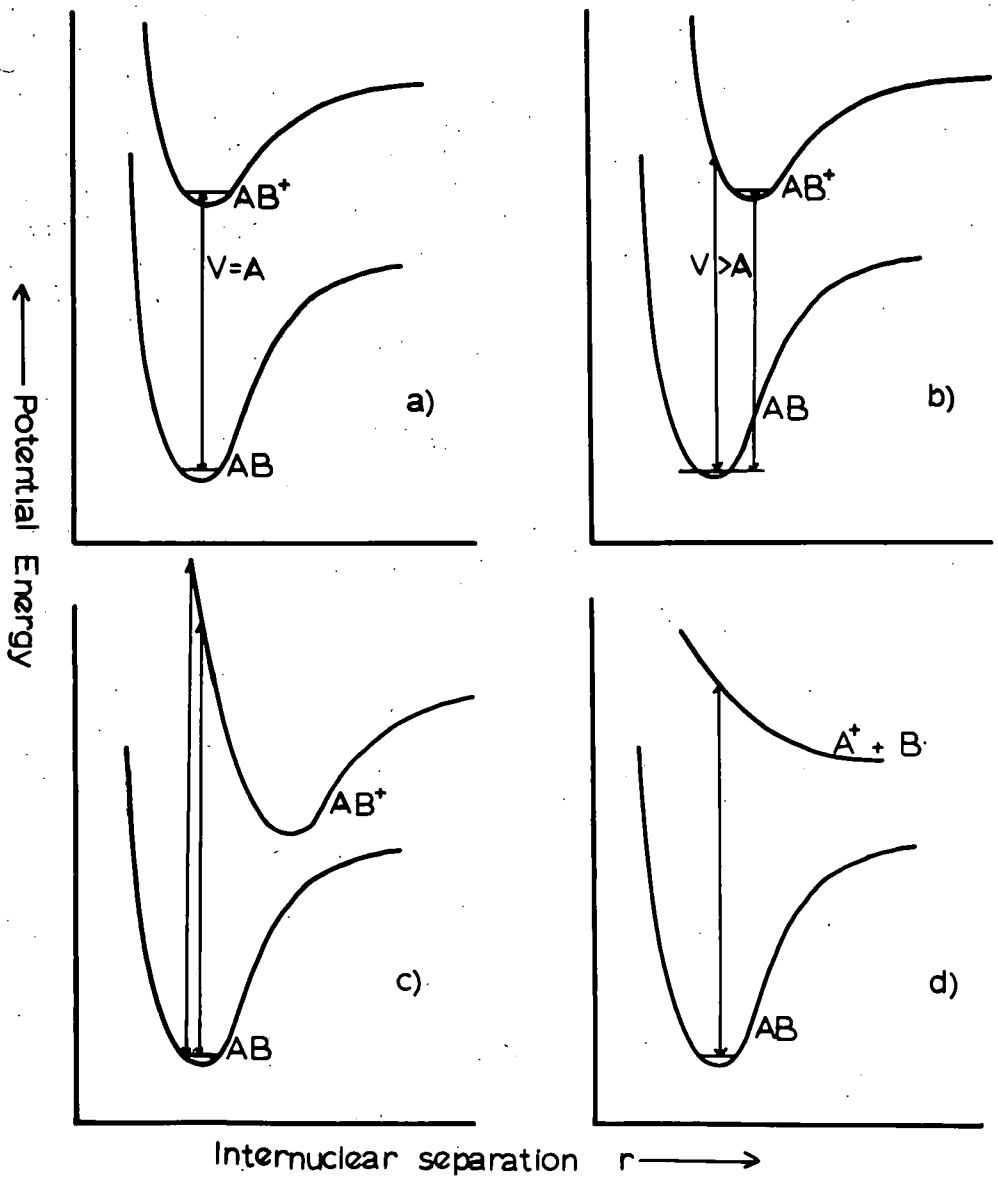

Potential energy curves showing:-

a) Equal vertical and "adiabatic" ionization potential V = A b) V ≠

c) Vertical ionization potentials leading to dissociation of the parent into fragments d) Upper potential energy curve repulsive with ionization leading to dissociation.

as upper limits of the "adiabatic" value. However even when the interatomic distances of the two possible states differ appreciably as in fig 1.b),c). there is still a finite possibility that ionization to the lowest vibrational level of the ionic state will occur. This suggests that in some cases the measured value of the ionization potential may depend on the sensitivity of the detecting apparatus used. Increasing the sensitivity is, in fact, equivalent to "broadening" the Franck-Condon region.

Fig. 1(d) shows a transition to a repulsive upper state. Fragmentation accompanies all such transitions and the excess energy of the fragments formed is given by the height of the transition region above the dissociation asymptote. Thus the appearance potentials of fragments obtained by methods involving vertical transitions also give values which are upper limits of the "adiabatic" or "true" value.

The experimental problem in measuring appearance potentials is to determine accurately the intercept, on the voltage axis, of graphs of ion current versus accelerating voltage of the ionizing electrons (ionization efficiency curve). The general shape of these curves is well established. With decreasing voltage the curve increases to a maximum value followed by a region of linear decrease. The curve then approaches the energy axis almost exactly exponentially, there being two reasons why this should be so.

Firstly, this behavior is inherent in the ionization process as may be understood from consideration of fig. 2.

Fig. 2.

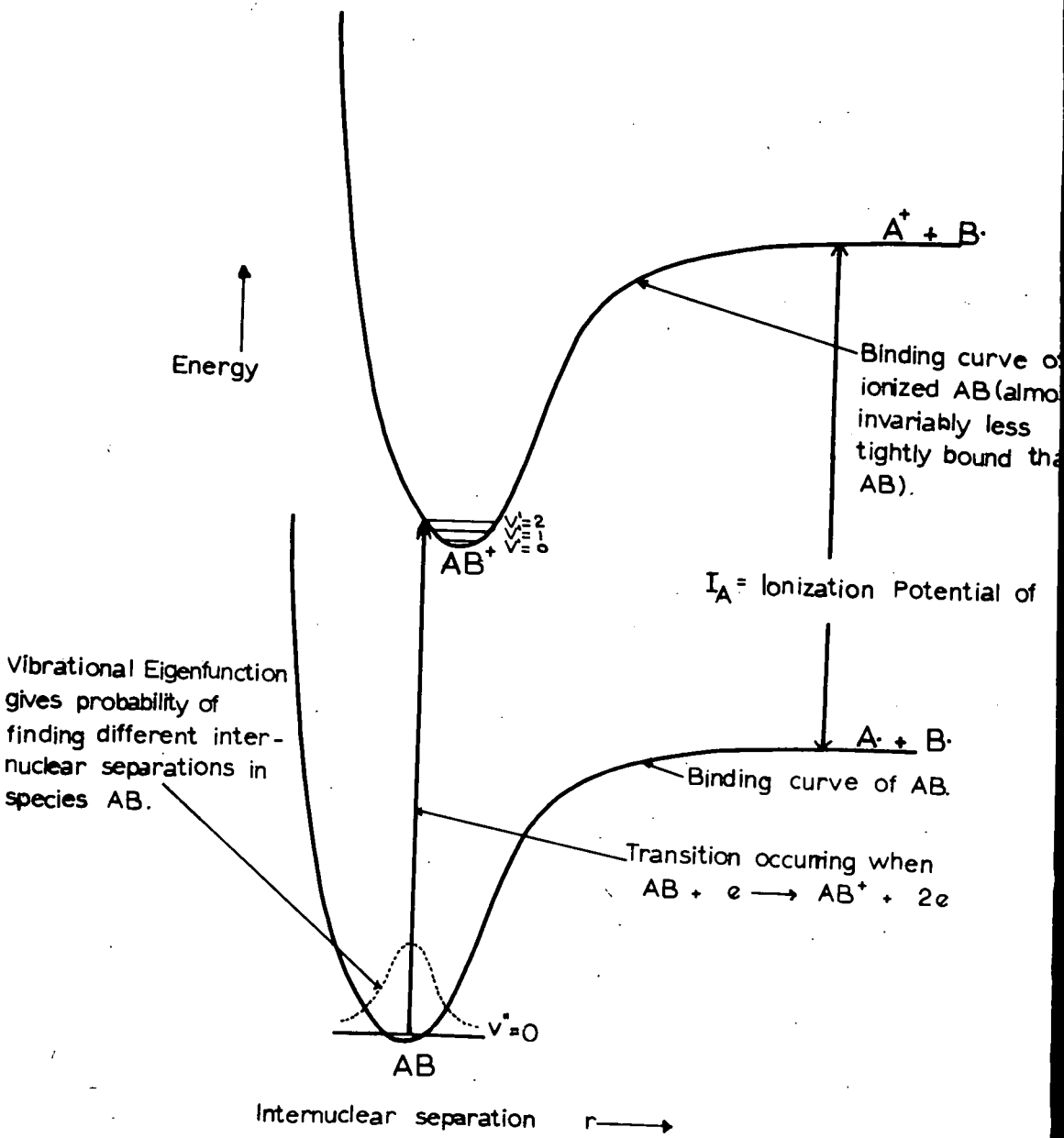
Energy
$A^+ + B\cdot$
Binding curve of ionized AB (almo invariably less tightly bound tha AB).
$V'=2$
$V'=1$
$V'=0$
AB^+
I_A = Ionization Potential of
Vibrational Eigenfunction gives probability of finding different inter-nuclear separations in species AB.
$A\cdot + B\cdot$
Binding curve of AB.
Transition occurring when $AB + e \longrightarrow AB^+ + 2e$
$V''=0$
AB
Internuclear separation r

Suppose that precisely monoenergetic electrons are used of energy equal to the energy of the transition shown on the diagram. As the energy is reduced so that there is only sufficient energy for transitions first to the $v' = 1$ and then $v' = 0$ levels, the requirements that the transition must be shown as vertical line means that the transition must originate from further to the right in the lower state. However the probability of finding AB molecules with such internuclear separations is decreasing, consequently the number of ionized AB^+ formed (i.e. ion current of AB^+) decreases following the shape of the probability curve of the $v'' = 0$ level.

Secondly, a non-monoenergetic electron beam causes further curvature of these graphs. Normally a mass spectrometer source forms the electron beam by acceleration of electrons emitted from a hot filament. The energy distribution of the emitted electrons will be essentially Maxwellian[34,35] and thus even when the minimum value of the electron energy is equal to the appearance potential of AB $\left[A\ (AB^+)\right]$ appreciable ion current persists because appreciable numbers of electrons with higher energies remain. Further reduction of the electron energy is required before the ion current at mass AB^+ disappears and the approximately exponential curvature of the energy distribution of the emitted electrons must lead to the ionization efficiency curve approaching the energy axis asymptotically.

In addition to difficulties arising from the shape of the ionization efficiency curve, other sources of error can enter into the measurement of appearance potentials by mass spectrometry. These have

been discussed by Waldron and Wood and are briefly outlined below.

The occurrence of a potential gradient within the ionization chamber will lead to the electrons being given an additional increment of energy and for this reason the ion repeller voltage is kept to a minimum. Provided the voltage of the repeller is kept constant however, this effect should not lead to an error in measuring the difference between two ionization potentials. The field within the ionization chamber is partly due to penetration of the ion accelerating field through the slit via which the ions emerge. Thus if the field within the ion chamber is to be the same for the examination of two ions of different mass, magnetic scanning must be used. The slit leading from the ionization chamber to the electron trap is usually relatively wide and the voltage of the trap can produce a considerable field penetration extending to the ionizing region. It is therefore ideal to work with the trap at the same potential as the ionization chamber. There is also the effect of the magnetic field in which the ionizing region is immersed. This will give rise to discriminations in that ions of different mass which are observed will originate in different regions of the ionization chamber and might thus receive different accelerations as they travel along the weak fields within the ionization chamber. This effect will be negligible if all the ions are formed in a region in which the lines of equipotential are parallel to the electron beam.

If the temperature of the filament, producing the electron beam, increases so does the energy spread in electron energy. It is therefore desirable that the filament temperature should be held constant

during measurement of a pair of ionization efficiency curves. Contact potentials within the ionization chamber may vary when a sample is introduced and for this reason it is usual to use an "internal standard" when measuring appearance potentials i.e. to introduce a second substance of known ionization potential whose ionization efficiency curve can be compared with that of the substance under investigation while they are both in the system and thus identical potential conditions.

The problem of determining the true origin of the ionization efficiency curve and hence the appearance potential has been critically discussed by Nicholson [37]. The early means of determining the true value for the ionization potential was the "initial break" i.e. extrapolating the curve back to its intersection with the energy axis [38,39]. The method is not very satisfactory because of the effect of the electron energy spread in making the curve asymptotic to the energy axis so that the point detected in this way will depend on the sample pressure, the number of bombarding electrons and the sensitivity of the detector employed. When a rare gas is introduced at the same time as the sample, differences in the electron energy corresponding to the minimum detectable current in each case can be used to obtain the appearance potential. There still remains the objection that the shapes of the curves may not be the same very near to the potentials at which the two currents vanish.

A second method, now little used, was introduced by Vought [40] who extrapolated the linear portion of the ionization efficiency curve to zero ion current using the extrapolated value as the ionization

potential. Its main disadvantage is due to using the current/voltage relationship comparatively far above the ionization potential where the ions may not be in their lowest energy states. The results obtained are generally higher than those from other methods especially when appearance potentials of fragment ions formed by complex reaction paths are being studied. It should be noted however that the method of Vought is practically the only one available for the determination of the potentials of second and higher breaks in the ionization efficiency curve.

An extension of the "initial break" method is due to Warren.[41] In this method, which uses an internal standard of known ionization potential, the ion current scales for the two graphs are adjusted so as to make the straight line portions parallel. The difference in voltage between corresponding ion currents on the curves is plotted against ion current and from the voltage difference at zero ion current the appearance potential is found. The same objections apply to this method as to the "initial break" but the method has the advantage of rendering differences in the shapes of the two curves clearly visible.

Several other methods which also depend for their success on the shapes of the two curves being compared being closely similar are classified by Nicholson as the "logarithmic" methods. The first of these due to Honig and Wannier[42] whilst not attempting to eliminate the electron energy spread accounts for it in an analytical expression which indicates that for about 1 eV below the ionization potential the curve will be approximately exponential. A semi-log plot of the ionization efficiency curve will give a slope of $\frac{2}{(3\,kT)}$ at the ionization potential. Dibeler and Reese[43]

measure the voltage difference between the particle being studied and a substance whose ionization potential is accurately known. The two graphs of ion current/electron voltage are plotted on the same scale so normalised that the two graphs are parallel. This normalisation is obtained by adjusting the partial pressure of the two components of the mixture until the ion current of each species is approximately equal with an electron beam of 50 - 70 eV energy. Another method similar to this is due to Lossing, Tickner and Bryce.[44] The pressure is again adjusted so as to get comparable intensities at 50eV, and a log. plot of peak heights, as percentages of the abundance at 50eV, against the electron energy yields parallel curves at the onset. Generally, voltage differences at 1% of the intensity at 50eV are taken as significant.

All the methods discussed give values which are usually reliable to 0.1eV for ions which give curves similar in form to those of the inert gas ions.

Morrison [45] has proposed an interesting analytical proceedure for treating ionization efficiency curves, which enabled him to remove at least partly the blurring effect of energy spread and to obtain from a given curve more information (particularly about excited states of ions). It is the derivative method. The method shows that if p(E), the probability of ionization to a given state, is a polynomial of the Kth degree, the (K + 1)th derivative represents the electron energy distribution, reversed with respect to the energy scale. An electronic device may be built to obtain automatically the derivative of the ionization

efficiency curve [46]. With this technique, Morrison was able to detect the appearance of excited states of ions and correlate them with known spectroscopic states. The technique is capable of giving interesting results, it has for instance allowed the estimation of relative probabilities for electronic transitions [47]. Ionization efficiency curves become easier to interpret if mono-energetic electrons are used since any fine structure which is smoothed out when there is a spread in electron energies is more easily observed. If, as is suggested by Nicholson[37] all errors arise from the fact that ionization efficiency curves do not have the same shape and differences in shape are due to different contributions of upper energy levels of the positive ions to the ionization efficiency curve, accuracy will be increased by any method which can detect fine structure in the curves. Clarke[48] using a beam of nearly mono-energetic electrons has shown that as the spread in electron energy is reduced the curves do, in most cases, become segmented straight lines with little curvature as the ionization potential is approached.

A quite different approach to the problem of obtaining the effect of mono-energetic electron beam has been made by Fox, Hickam, Kjeldaas and Grove[49,50] with their "retarding potential difference method". Ionization potentials determined by this method give results much closer to those calculated by spectroscopic methods than do the methods which do not employ "mono-energetic" electrons. This is especially so for molecules such as benzene [51,52,53,54] in which there are excited states of the ion close to the ground state [55,56]. Nevertheless there are some

difficulties in the results obtained by this method which have not been resolved [37].

In addition to the instrumental difficulties involved in reducing the electron energy spread, such reduction gives a correspondingly smaller electron current and therefore worse signal-to noise ratio in the final data. Morrison [57] has recently proposed an analytical method for reducing the effect of energy spread. This "deconvolution" method is based essentially on the use of Fourier transform relationships and communication theory and obtains a marked reduction in the scatter in the experimental data and reduces the effective electron energy spread by a factor of four or five times. Although an exact knowledge of the form of electron energy spread is not required, the better this knowledge the better the ultimate result. Tests made on several artificial examples and on two actual cases show that the methods are of some promise. Eland, Shepherd and Danby [58] used the same technique to obtain the ionization potentials of a series of aromatic amines. The method however does not mean that there is no advantage to be gained by using a beam of ionizing electrons with reduced energy spread. Morrison found it not possible to estimate an energy spread to a much greater accuracy than about $\frac{1}{4}$ to $\frac{1}{5}$ of its width, so that the smaller the width in the first place the better the ultimate result.

1.3. Derivation of Therochemical Data from Appearance Potentials

Appearance potentials may used in conjunction with ionization potentials, and/or calorimetric data allowing an estimation of certain thermodynamic quantities such as heats of formation and bond dissociation energies. Ionization by electron impact and subsequent fragmentation of the molecular ion by bond cleavage may be represented in a cycle of the form

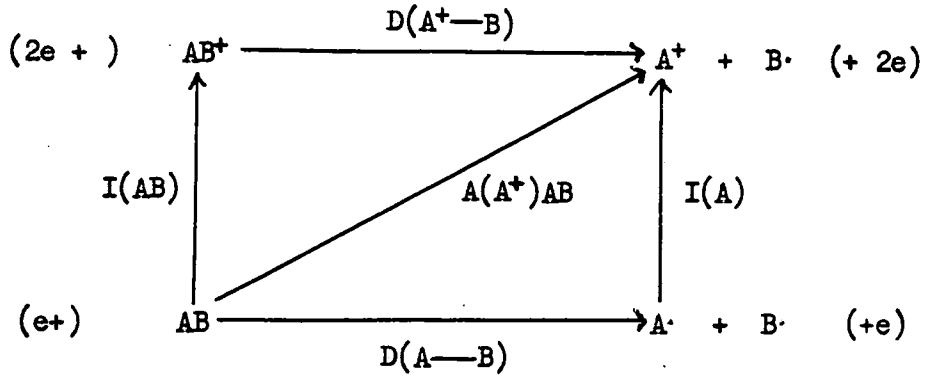

where $I(A\cdot)$ ionization potential of $A\cdot$

$A(A^+)AB$ appearance potential of A^+ from molecule AB

$D(A—B)$ dissociation energy of the bond A—B.

From this cycle the following relationships may be obtained.

$$A(A^+)AB = I(AB) + D(A^+—B) + E_1 \qquad 1.1$$

$$A(A^+)AB = I(A\cdot) + D(A—B) + E_2 \qquad 1.2$$

Here the terms E_1 and E_2 represent excess kinetic energy of the dissociation plus any excitation energy of the products A^+ and $B\cdot$.

The alternative products B^+ and $A\cdot$ may also be obtained leading to

$$A(B^+)\ AB = I(B\cdot) + D(A—B) + E_3 \qquad 1.3$$

$$A(B^+)\ AB = I(AB) + D(B^+—A) + E_4 \qquad 1.4$$

The values of E_1, E_2, E_3 and E_4 are not necessarily the same and in general will differ.

One simplfying assumption often made is that E_1, E_2; E_3, E_4 are zero i.e. that both the ion and the radical are produced in their ground state and that the kinetic energy term is zero. As $E_2 \neq E_3$ and $E_1 \neq E_4$, in general, this assumption will be true for only one of the two series of possible products. Stevenson [59], has pointed out that one might expect that ionization $e + XY \rightarrow X^+ + Y + 2e$ where $I(X\cdot) < I(Y\cdot)$ may lead to the formation of the ion and radical in their ground states. In many cases where the hypothesis that one of the excess energy terms is zero may be tested it has been found to hold [4,6]. A fairly extensive series of measurements has been made for singly substituted methane derivatives CH_3X and these are shown in table 1.3.1 along with the bond-dissociation energies estimated by other methods. The agreement between the values from electron impact studies and other methods is good, supporting the view that the fragments are produced in their electronic ground states and that E = 0. The use of equation 1.2. to estimate accurate bond dissociation energies requires an estimate of the ionization potential of the free radical. Few direct measurements of such quantities have been made for organometallic radicals and accurate estimations of bond

Table 1.3.1

Bond-dissociation energies $D(CH_3—X)$

X	Electron Impact (eV)	Other methods[c] (eV)
H	4.43 [a]	4.37
CH_3	3.99 [a]	3.60
NO_2	2.54 [a]	2,34
OH	3.95 [b]	3.90
Cl	3.40 [b]	3.47
Br	2.33 [b]	2.91
I	2.30 [b]	2.30

a) reference 6

b) R.I. Reed and W. Snedden, Trans. Faraday Soc., 54, 301, (1958).

c) "The strengths of Chemical Bonds", T.L. Cottrell, 2nd Edition, 1958, Butterworths, London. (1st Edition 1954.)

dissociation energies by other methods from which ionization potentials could be calculated by a combination with the appropriate appearance potentials are often lacking. For example various workers [60,61,62] have measured appearance potentials of the Me_3Si^+ ions from various trimethyl silyl compounds obtaining good agreement. Accurate bond dissociation energies for $Me_3Si—X$ bonds remained in doubt, until recently [63] because of different estimations of $D(Me_3Si—SiMe_3)$ from which $I(Me_3Si^\cdot)$ is calculated.

Relative bond dissociation energy measurements may still be calculated however without knowledge of ionization potentials. If for the compounds $L_nM—R$ the appearance potential of L_nM^+ is measured then by a subtraction of the two equations.

$$A(L_nM^+)L_nM—R_1 = I(L_nM^\cdot) + D(L_nM—R_1)$$

$$A(L_nM^+)L_nM—R_2 = I(L_nM^\cdot) + D(L_nM—R_2)$$

Bond dissociation energy differences are found.

$$D(L_nM—R_1) - D(L_nM—R_2) = A(L_nM^+)L_nM—R_1 - A(L_nM^+)L_nM—R_2 \qquad 1.5$$

Hess, Lampe and Sommer[60] have introduced an indirect method of estimating ionization potentials which is applicable to the organo-compounds of metals which form homonuclear metal-metal bonds. To explain the method equation 1.2 must be modified to involve other thermodynamic data. The bond dissociation energy D(A—B) is the heat of reaction

$$AB \rightarrow A^\cdot + B^\cdot$$

hence

$$D(A—B) = \Delta H_f^\circ (A\cdot) + \Delta H_f^\circ (B\cdot) - \Delta H_f^\circ (AB) \quad 1.6$$

where ΔH_f° represents the standard heat of formation.

Thus 1.2 becomes

$$A(A^+)AB = I(A\cdot) + \Delta H_f^\circ (A\cdot) + \Delta H_f^\circ (B\cdot) - \Delta H_f^\circ (AB) \quad 1.7$$

assuming

$$E_2 = 0$$

Also

$$I(A\cdot) = \Delta H_f^\circ (A^+) - \Delta H_f^\circ (A\cdot) \quad 1.8$$

and so

$$A(A^+)AB = \Delta H_f^\circ (A^+) + \Delta H_f^\circ (B\cdot) - \Delta H_f^\circ (AB) \quad 1.9$$

Suppose that for the compound AB, $\Delta H_f^\circ (AB)$ and $\Delta H_f^\circ (B\cdot)$ are known, then $\Delta H_f^\circ (A^+)$ can be found from the measurements of $A(A^+)AB$. With this value $A(A^+)$ can be measured from A—A. If $\Delta H_f^\circ (A—A)$ is known and it is assumed that any excess energy release associated with the formation of A^+ and $A\cdot$ is zero, the measurement permits a computation of $\Delta H_f^\circ (A\cdot)$. The ionization potential of $A\cdot$ can then be estimated using 1.8. Using this "indirect" method heats of formation and ionization potentials of the radicals $SiMe_3$ and $SnMe_3$ have been evaluated and bond dissociation energies $D(Me_3Si—R)$ [60] and $D(Me_3Sn—R)$ [64] found.

The high abundance of the metal ion (M^+) in the spectra of some organometallic compounds has prompted several workers [65,66,67] to measure the appearance potential of this ion in order to determine the heat of formation of the parent compound or mean metal-carbon bond

dissociation energies. Aside from instrumental errors, it will be apparent from the preceding discussion that the validity of using appearance potentials in the derivation of thermodynamic quantities depends primarily on the correct designation of the process involved in the threshold measurement. Since this may be difficult for processes involving extensive fragmentation, more reliance may generally be placed on values derived from appearance potentials of ions formed by less extensive dissociative processes. Even so quite accurate estimations of thermodynamic quantities have resulted from the appearance potential of M^+ for various transition metal carbonyls and cyclopentadienyl complexes.

Mean metal-carbon bond dissociation energies for a ML_n compound (M is metal and L ligand) may be calculated if we assume that the appearance potential of M^+ is the energy required for the decomposition

$$e + ML_n \longrightarrow M^+ + nL^\cdot + 2e \quad \triangle H = A(M^+)ML_n$$

Assuming no excess energy release the cycle below may be writtem:-

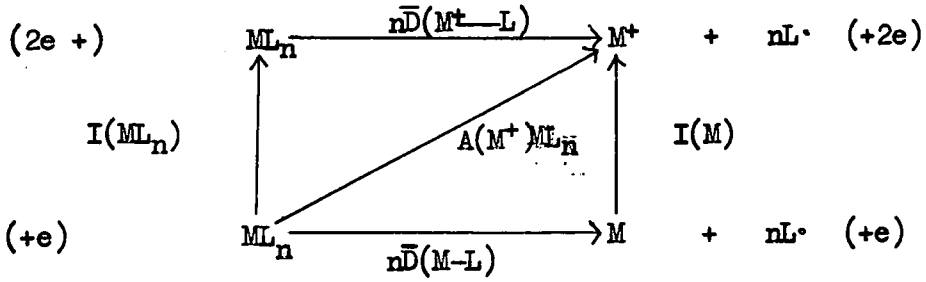

where $\bar{D}(M-L)$ = mean dissociation energy of M–L bond in ML_n

$\bar{D}(M^+-L)$ = mean dissociation energy of M–L bond in $ML_n^{+\cdot}$

From this

$$\bar{D}(M\text{-}L) = \frac{1}{n}\left[A(M^+)ML_n - I(M)\right] \qquad 1.10$$

$$\bar{D}(M^+\text{-}L) = \frac{1}{n}\left[A(M^+)ML_n - I(ML_n)\right] \qquad 1.11$$

Providing the appearance potential measurements can be accurately carried out then mean bond dissociation energies can be calculated in both the neutral molecule and molecular ion.

Some measurements for transition metal carbonyls are shown in Table 1.3.2. The appearance potential measurements give larger values for D(M-CO) than those calculated from heats of combustion. This discrepancy may be attributable to the failure of the negligible excess energy release assumption made in deriving equations 1.10 and 1.11.

Heats of formation may also calculated. If M^+ is formed by the process below with no excess energy release:-

$$L_nM + e \longrightarrow M^+ + nL + 2e \qquad \Delta H = A(M^+)ML_n$$

then $A(M^+)ML_n = \Delta H_f^\circ(M^+) + n\Delta H_f^\circ(L) - \Delta H_f^\circ(L_nM)$

from which $\Delta H_f^\circ(L_nM) = \Delta H_f^\circ(M^+) + n\Delta H_f^\circ(L) - A(M^+)ML_n$ 1.12

Since the heats of formation of metal ions in their ground states are known, then providing the heat of formation of the ligand L· is known, measurement of the appearance potential allows an estimation of the heat of formation of the parent molecule.[67]

Table 1.3.2

Mean metal-carbon bond dissociation energies in transition metal carbonyl molecules and ions

	Kcal. mole.$^{-1}$				
	Bidinosti et. al.[65]		Foffani et.al.[66]		Thermochemical[a]
	D(M—CO)	D(M^t—CO)	D(M—CO)	D(M^t—CO)	D(M—CO)
$Ni(CO)_4$	43	37			35.2
$Fe(CO)_5$	33	32	32	30	27.7
$Cr(CO)_6$	31	31	31	25	27.1
$Mo(CO)_6$	42	39	42	38	35.9
$W(CO)_6$	50	48	48	47	42.1
$V(CO)_6$	34	31			

a) F.A. Cotton, A.K. Fischer and G. Wilkinson, J. Amer. Chem. Soc., 1959, 81, 800.

Sometimes appearance potential data can also throw light onto the decomposition process occurring just above the threshold measurement. Winters and Kiser [68] measured the appearance potential of the metal ion from compounds of the type $(C_5H_5)\ M\ (CO)_x$ (M = Co, Mn,V). Heats of formation of the neutral molecules were calculated assuming in one instance metal ions to be formed by the decomposition

$$(C_5H_5)\ M\ (CO)_x + e \longrightarrow M^+ + C_3H_3 + C_2H_2 + x\ CO \qquad 1.13$$

and in another by

$$(C_5H_5)\ M\ (CO)_x + e \longrightarrow M^+ + C_5H_5 + x\ CO \qquad 1.14$$

Decomposition 1.13 was considered to be the most probable since the heat of formation obtained for this process agreed with values estimated from bond strength data of similar compounds.

2. EXPERIMENTAL.

2.1 Preparation of Compounds.

2.2 Recording Mass Spectra.

2.3 Measurement of Appearance Potentials.

2. EXPERIMENTAL

2.1 Preparation of Compounds

Et_4Sn: Prepared from the reaction of stannic chloride and ethylmagnesium bromide in ether [69,70]. The main impurity, triethyltin chloride was removed from an ether solution by agitating with aqueous/alcoholic potassium fluoride solution and filtering off the precipitated triethyltin fluoride [71]. Vapour phase chromatography [Pye 104 dual columns (5ft. 4 m.m. i.d.) dual flame ionization detectors. Stationary phase 10% Apiezon L on 100-200 mesh celite. Carrier gas N_2.] Temp. 200°C showed only one peak, b.pt = 174-176°C/760 m.m.

$(CH_2{:}CH)_4Sn$: The addition of anhydrous stannic chloride to vinylmagnesium bromide gave tetravinyltin in at least 60% yield [72]. b.pt. 160-163°C/760 m.m.

Ph_3SnCl: prepared from freshly distilled stannic chloride and tetraphenyltin by the redistribution reaction [73]

$$3SnPh_4 + SnCl_4 \longrightarrow 4SnPh_3Cl$$

Pure triphenyltin chloride was obtained by sohxlet extraction of the powdered product using ether [74]. m.pt. = 106-107°C

Ph_3SnBr: Prepared in the same way as triphenyltin chloride using anhydrous stannic bromide. m.pt. = 122°C.

Ph_3SnF: Triphenyltin chloride solution in hot ethanol was added to a hot aqueous/alcoholic solution of potassium fluoride. On cooling snow white fine crystals of triphenyltin fluoride formed [75] m.pt. = At 341°C the solid turned brown and at 355°C liquified.

Ph_3SnI: Sodium iodide (45 g.) in acetone (300 cc.) was added to triphenyltin chloride (19.2 g.) in acetone (50 cc.). The mixture was refluxed for 6 hr., decanted from sodium chloride and more sodium iodide (30 g.) added with further refluxing (8hr.). The crude iodide was purified by soxhlet extraction with light petroleum (b.pt. 40-60°C) from which it crystalised, m.pt. = 121°C.

$EtSnPh_3$: The reaction of triphenyltin chloride with ethylmagnesium bromide in anhydrous ether as described by Lesbre et. al. [76] gave ethyltriphenyltin in 63% yield.

The product was purified by alternatively recrystalising from ether and hexane until the mass spectrum showed no change after ten recrystalisations. m.pt. = 56°C.

$MeSnPh_3$: Prepared in an identical way to $EtSnPh_3$ using methylmagnesium bromide. Five alternate recrystalisations from hexane and ethanol were carried out. m.pt. = 58°C

Et_2SnPh_2: Diphenyltindibromide first prepared in the following manner. Tetraphenyltin (109 g. 0.5 mole) was suspended in ethylenedibromide

and bromide (80 g. 1 mole) in the same solvent added drop wise over a period of three hours. Ethylenedibromide and bromobenzene were removed by distillation at reduced pressure leaving a brown liquid. The distillate boiling at 156–170°C/1 m.m. was collected yielding diphenyltin dibromide (100g. 60%) Diethyldiphenyltin was prepared from the reaction of this bromide with ethylmagnesium bromide in ether [75]. Unforseen complications arose however because of the presence of chlorine even in analar bromine which resulted in the presence of some $PhEt_2SnBr$, $PhEt_2SnCl$ and Ph_3SnEt in the diethyldiphenyltin obtained.

Purification was effected by chromatography using a column of silica gel (100/200 mesh, activated by heating for 3 days at 120°C) and eluting with petroleum (b.pt. 40–60°C). Retention on the column was in the order $PhEt_2SnCl$, $PhEt_2SnBr > Ph_2SnEt_2 > Ph_3SnEt$. Using such a column (dimensions: length 18in. diameter 1in.) and by taking a middle cut of the petroleum fractions, 0.1 g. of pure diethyldiphenyltin was obtained from 1.5 g. of crude material. This sample gave only one peak by vapour phase chromatography using two stationary phases at 200°C (10% apiezon L on 100–200 mesh celite and N.G.A. ; carrier gas N_2) and showed no peaks in the mass spectrum corresponding to $PhEt_2SnCl$, $PhEt_2SnBr$ (i.e. $PhEtSnCl^+$ or $PhEtSnBr^+$) or Ph_3SnEt (i.e. Ph_3Sn^+).

Et_3SnPh: The preparation from tetraethyltin by the sequence $Et_4Sn \xrightarrow{Br_2}$

$\xrightarrow{Br_2}$ Et_3SnBr $\xrightarrow{PhMgBr}$ Et_3SnPh has been described [77]. Again the presence of chlorine in the bromine used resulted in the product being contaminated with Et_3SnBr, Et_3SnCl and Et_2SnPh_2. These were removed by silica gel column chromatography eluting with petroleum (b.pt. 40–60°C) (as for the diethyldiphenyltin purification described) followed by preparative scale vapour-phase chromatography using a 9ft. column of 10% apiezon L on celite and nitrogen as carrier gas.

It is interesting to note at this stage that an alumina column (Brockman No 1) and eluting with petroleum (b.pt. 40–60°C) would not separate either Et_2SnPh_2 or Et_3SnPh from their impurities.

Sn_2Et_6: Sodium amalgam (225 g. Hg + 1.13 g. Na) triethyltin chloride (11.7 g.) and cyclohexane (10 cc.) were shaken in a nitrogen purged flask for 14 days. No colour change was observed, but the mercury became more mobile and sodium chloride separated. Normal work-up gave two fractions, b.pt. 85–110°C/10 m.m. (3.6 g.) and b.pt. 148–150°C/10 m.m. (4.2 g.), both of which contained some Et_3SnCl which was not completely removed by shaking with aqueous/alcoholic KF or by chromatography on silica gel. The higher fraction was refluxed with potassium (3 g.) in benzene (50. cc.) for 10 hr. giving pure hexaethyldistannane (0.5 g.) b.pt. 100–151°C/15 m.m.

5 - Stannaspiro (4,4.) nonane: The di-Grignard reagent from 1,4 - dibromobutane (92 g.), magnesium (22 g.) and ether (400 cc.) was added to stannic chloride (26 g.) in ether (500 cc.) and the mixtures refluxed

for 10 hr. After hydrolysing with saturated ammonium chloride solution the two layers were separated and the aqueous layer extracted with more ether. The combined ether solutions were dried and the ether removed by distillation. The residue was distilled yielding 2.1 g. of colourless liquid b.pt. 108-110°C/30 m.m.. Its infra red spectrum showed no Sn-H absorption. (Found C58.9%; H4.7%; $C_8H_{16}Sn$ requires C58.8%; H4.9%).

Ph_3Sn-S-Ph: Thiophenol (12 g.) in dry methanol (20 cc.) was added to sodium methoxide (5.4 g.) in dry methanol (20 cc.) Triphenyltinbromide (42 g.) in tetrahydrofuran (50 cc.) was then added slowly. The mixture was boiled with reflux for 30 min. and filtered; the product crystalized from the filtrate. Recrystallisation from ethanol gave a colourless product (37 g. 82%) m.pt. 103°C (Found C 62.8%; H 4.5%; requires C 62.7%; H 4.4%.)

$Ph_3C \cdot CMe_3$: Tertiarybutylmagnesium chloride in diethylether was prepared from purified [78] tertiarybutylchloride. This was reacted with tritylbromide (1 mol.) (freshly prepared from triphenylcarbinol [79]) giving a 61% yield of tertiarybutyl-triphenylmethane m.pt. 175-177° .

Attempted preparation of tertiarybutyltriphenyltin: The reaction of tertiarybutylmagnesium bromide with triphenyltin chloride yielded only hexaphenylditin.

Metal-Metal bonded Compounds: These were prepared by the addition of the R_3 M Li derivative (M = Si, Ge, Sn; R = Me, Ph) to an equal number of

Table 2.1.1.

Products of reaction $R_3MLi + R'_3M'X$ (M,M = Si,Ge,Sn; X = Cl,Br)

Lithium Reagent	Halide	Solvent	Derivative and yield		M_2Ph_6 yield
Ph_3SnLi	Me_3SiCl	T.H.F.	-		62%
	Me_3SnBr	"	$Ph_3Sn{\cdot}SnMe_3$	14%	21%
	Et_3SiCl	"	-		51%
Ph_3SiLi	Me_3SiCl	T.H.F.	$Ph_3Si{\cdot}SiMe_3$	79%	-
	Et_3SnBr	"	-		66%
	Et_3SiCl	"	$Ph_3Si{\cdot}SiEt_3$	53%	-
Ph_3GeLi	Me_3SnBr	Et_2O	$Ph_3Ge{\cdot}SnMe_3$	67%	-
	Et_3SnBr	"	-		68%
	Et_3SiCl	"	$Ph_3Ge{\cdot}SiEt_3$	58%	7%
Me_3GeLi	Ph_3SnCl		$Ph_3Sn{\cdot}GeMe_3$	20%	present
Me_3SiLi	Ph_3SnCl		-		present

moles of $R'_3M'X$ (M' = Si,Ge,Sn; R' = Me or Et)

$$R_3MLi + R'_3M'X \rightarrow R'_3M'-MR_3 + LiX.$$

The results of these reactions are given in table 2.1.1. Because of halogen-metal exchange the symmetrical compounds R_6M_2 and $R'_6M'_2$ were often formed.

The preparations of a) Ph_3SnLi in tetrahydrofuran (T.H.F.) from Ph_3SnCl [80] b) Ph_3SiLi in T.H.F. from Ph_3SiCl [81] and c) Ph_3GeLi in diethylether from Ph_3GeH [82] have been described. Me_3GeLi and Me_3SiLi were prepared from the mercury derivative $(Me_3M)_2Hg$ by reaction with lithium under an atmosphere of nitrogen.

$Me_3GeSnPh_3$: m.pt. 110° - 111°C recrystalised from benzene.

$Me_3SnGePh_3$: m.pt. 81° recrystalised from 1:1 (V:V) mixture of petroleum (b.pt. = 40 - 60°C) and diethylether.

$(PhCH_2)_3GeSiMe_3$: [83] m.pt. 64°

$Me_3SiSiPh_3$: m.pt. 108°

$Et_3SiSiPh_3$: m.pt. 89 - 90°

$Et_3SiGePh_3$: m.pt. 91 - 91.5° all recrystalised from methanol

$Me_3SnSnPh_3$: m.pt. 106° separated from Sn_2Ph_6 by successive recrystalisations from diethylether.

$Ph_3SnSnPh_3$: m.pt. 237° recrystalised from benzene

$Ph_3SiSiPh_3$: m.pt. 365° recrystalised from benzene

Table 2.1.2.

Infra-red data for $A_3M - M B_3$ compounds.

	Metal-Phenyl[a] Characteristic Vibration	Methyl[b] deformation	Methyl[b] Rock	$CH_3 - M$[b] stretch asym.	sym.	$C_2H_5 - M$[84] characteristic symmetrical CH_2 deformation	
$Ph_3Si \cdot SiMe_3$	1102s	1253s	851s 835s	obscured			
$Ph_3Ge \cdot GeMe_3$	1083s	1230w	826s	564m	594s		
$Ph_3Ge \cdot SnMe_3$	1083s	1193w	771sb	508m	523s		
$Ph_3Sn \cdot GeMe_3$	1068s	1230w	824s	561m	544s		
$(PhCH_2)_3Ge \cdot SiMe_3$	-	1240m	847sh 837m	obscured			
$Ph_3Si \cdot SiEt_3$	1101s					1232w	956w
$Ph_3Ge \cdot SiEt_3$	1084s					1233w	956w

a) refs. 84,85,86,87.
b) refs. 84,88,89,90.

The spectra are quoted in cm $^{-1}$. Methyl rock, Methyl-metal stretching frequencies were recorded in cyclohexane and the metal-phenyl characteristic vibration and methyl deformation were recorded in pressed discs in potassium bromide.

w weak, m medium, s strong, b broad, sh shoulder.

Infra-Red Spectra of Metal-Metal bonded Compounds.

In order to establish that the compounds prepared were in fact of structure $A_3M - MB_3$ and not $A_2BM - MB_2A$ etc, infra-red spectra were recorded using a Grubb-Parsons spectromaster. The characteristic bands observed are shown in Table 2.1.2. from which it is immediately obvious that the infra-red data is consistent with structures $Ph_3M-M\,R_3$ with all the phenyl groups attached to a single metal.

Organoberyllium Compounds.

These were all prepared by P.D. Roberts, to whom my thanks are due, using the general methods [91] outlined below.

1. The dialkyls are obtained by the action of the Grignard reagent on beryllium chloride [92]

$$Cl_2Be(OEt_2)_2 + 2RMgX \longrightarrow R_2Be + MgX_2 + MgCl_2$$

The separation of the product from the reaction mixture presents some difficulties. The dimethyl may be obtained by a process of "ether distillation" at atmospheric pressure whereby ether continuously circulates carrying dimethylberyllium from the reaction mixture to a receiver which is kept well above room temperature, excess ether evaporating from the latter and returning to the reaction vessel via a condenser [93]. The higher alkyls should be distilled from the reaction mixture at reduced pressure at as low a temperature as possible (generally 50-80°) to minimise thermal decomposition. The use of non-ethereal Grignard reagents [94], or lithiumalkyls ~~alkyls~~ in

hydrocarbons, allows the preparation of ether free beryllium alkyls directly from beryllium chloride.

2. Dimethylberyllium [95] has been prepared by the action of the corresponding organomercury compound on metallic beryllium.

$$Me_2Hg + Be \longrightarrow Me_2Be + Hg$$

Organoaluminium Compounds.

These were available from Ethyl Corporation. After distillation the compounds were sealed in a tube containing a breakseal and attached to the direct evaporation line of the mass spectrometer.

2.2. Recording Mass Spectra

Spectra were recorded on an A.E.I. M.S.9 double focussing instrument. Routine measurements, such as high resolution mass measurements, were carried out as described in the instruction manual and unless otherwise stated ions were produced under the following conditions:

Ionizing electron beam voltage = 70eV

Trap Current (i.e. electron beam current) = 100 μ Amps

Ion repeller voltage = -2 to + 4 volts

Source temperature = 190 to 210°C

Since some difficulties were encountered with the methods of sample introduction, the production of reproducible spectra for abundance measurements, the detection of metastable peaks and measurement of appearance potentials these topics are discussed in detail.

2.2.1. Sample Handling Systems

Since electron impact sources require sample vapour at a pressure of about 10^{-5}m.m., the usual approach is to maintain a pressure of about 10^{-2}m.m. in a large reservoir from which vapour passes to the source through a leak which reduces the pressure by the requisite factor $\sim 10^{-3}$. The sample reservoir is filled according to the nature of the compound.

a) Permanent gases and compounds with room temperature vapour pressures of a few cm. or more use a "cold inlet" where by an aliquot of the gas/vapour (i.e. a volume of $\sim$ 10cc. of pressure $\sim$7 - 8 cm.) is

expanded into a 2 litre reservoir.

b) With relatively involatile liquids a volume of about a drop (i.e. handleable in a micropipette) is introduced, via a gallium covered sinter, into a reservoir whose volume can be 100 cc. or $\sim$ 1000 cc. The whole system can be heated to $\sim$ 200°C to cause vapourisation.

c) For very involatile liquids and solids the sample is introduced into a thimble where it may be frozen down in liquid nitrogen whilst the air in the thimble is evacuated. The sample is then given direct entry into the reservoir, and the thimble is heated in an oven until the vapour pressure reaches the required level. The oven and reservoir can be heated to $\sim$ 350°C.

Using this "heated inlet" system sometimes poses problems for solids because decomposition occurs: either the compound decomposes in the solid and it is the decomposition products that vapourise or else the vapour decomposes in the gas phase in the hot reservoir, possibly catalysed by the metal parts of the valves. A technique to minimise these troubles is the "direct insertion probe". A few micrograms of the solid are packed into a glass or ceramic probe. This is then introduced through a vacuum lock, directly into the source within a few m.m. of the electron beam. Sample vapourises from the probe under the influence of the source vacuum and source temperature ($\sim$ 200°C): If, under these conditions of vapourisation virtually directly into the electron beam, decomposition still occurs then it can probably never be eliminated.

To record mass spectra of solids the direct insertion probe

Fig. 3.

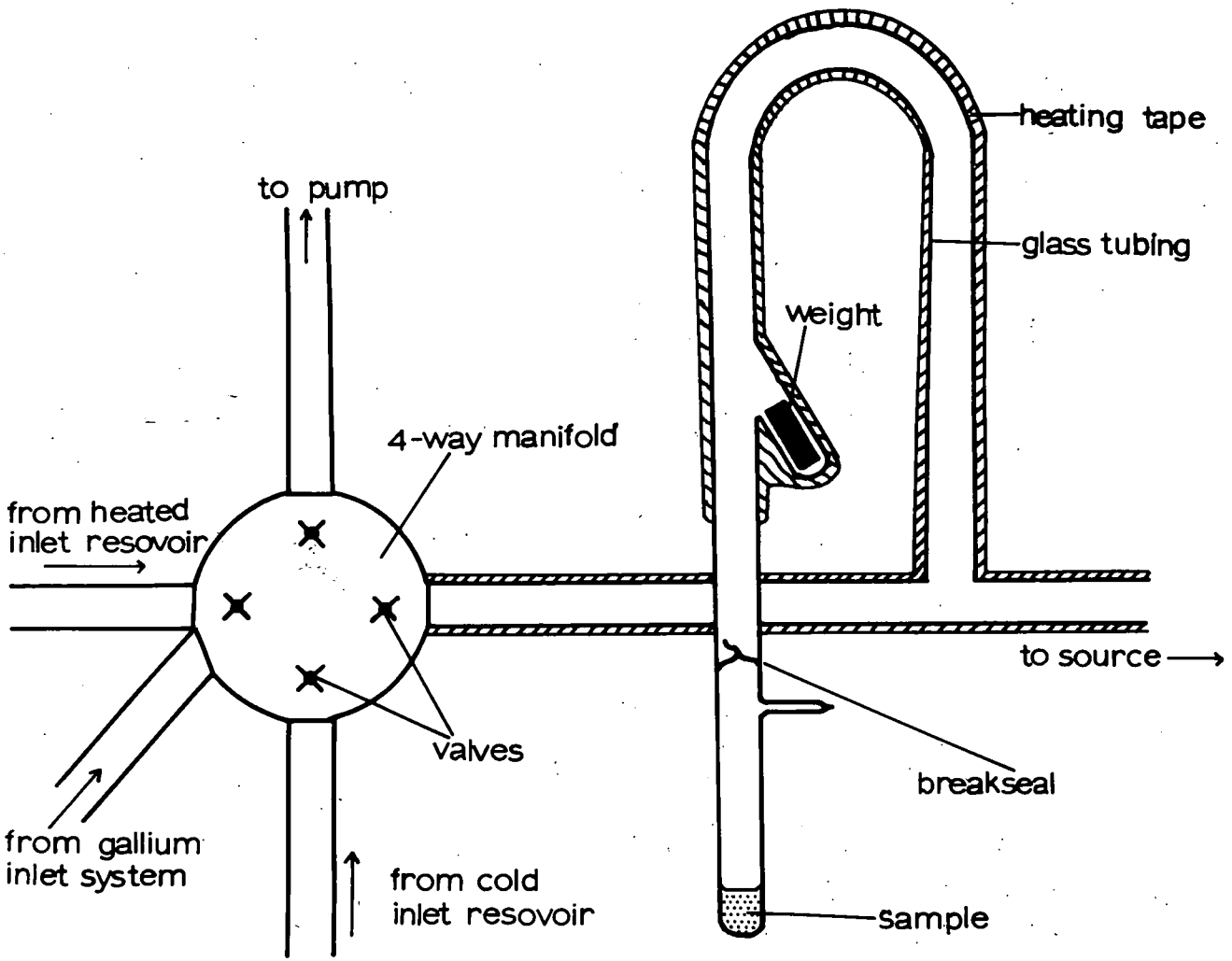

DIRECT EVAPORATION INLET SYSTEM.

was always used to introduce sample into the mass spectrometer.

With dialkylberyllium compounds in addition to difficulties encountered because of the highly reactive nature of these compounds to air and moisture, extensive decomposition of these compounds occurred whenever these inlet systems were used. Thus the volatile di-tertiary-butylberyllium decomposed giving mainly butene in the cold inlet system and dimethylberyllium, which does not thermally decompose until 200°C, produced a mass spectrum showing only peaks due to Me_3Sn^+, Me_3Ge^+ and hydrocarbon ions when introduced via the heated inlet system at 100°C. Such decomposition occurred even after the heated inlet system had been "baked" for 6 hours at 350°C before cooling to 100°C in order to remove any volatile residues that would react with the organoberyllium compound.

In case this decomposition was catalysed by metallic surfaces, an all glass inlet system was constructed; a schematic diagram of which is shown in Fig. 3. The rate evaporation of material into the source was controlled by altering the temperature of the sample. To give a reading on the source ionization guage of 2 to 8×10^{-6} m.m. the following sample temperatures (°C) were required for organo-beryllium and - aluminium compounds; Me_2Be 48°, Et_2Be 16.5°, $(i\text{-}Pr)_2Be$ 0°, $(n\text{-}Pr)_2Be$ 25°, $(i\text{-}Bu)_2Be$ 29° $(t\text{-}Bu)_2Be$ - 60°, Me_3Al - 25°, Et_3Al - 15°, Me_2AlH - 22°, Et_2AlH 22°. (temperatures in degrees centigrade). A disadvantage of this inlet system is that the beryllium or aluminium sample has to be sealed in a tube with a breakseal and then glass-blown onto the inlet line. To remove the sample, the source and inlet line to the 4 - way manifold

has to be let down to pure dry nitrogen and the sample tube and inlet-line sealed using a blow torch.

It was not possible to introduce di-n-butylberyllium through any of the sample inlet systems described because of its low volatility. Using the direct evaporation inlet system elimination of butene occurred when the sample was heated above 85°C. Prolonged heating at this temperature caused further decomposition and the sample turned to a grey viscous liquid. At no stage was the mass spectrum of di-n-butylberyllium recorded.

2.2.2. Obtaining Spectra for Abundance Measurements

These were recorded using a resolution of 1 part in 5,000 and a source pressure not so high that "sparking" of the high voltage employed in the source occurred. It is also important that a constant monitor current (i.e. a quantity proportional to the total ion current issuing from the ionization chamber found by intercepting part of the ion beam before it enters the magnetic sector) prevails while the spectra is recorded if meaningful abundances are to be obtained. With the inlet systems which employ a leak to regulate the flow of material into the source (i.e. the cold, heated and gallium systems) this is relatively easy but using the direct insertion probe some manipulation is necessary, especially with solids m.pt.$>$100°C, before constant evaporation into the source is obtained.

2.2.3. Detection of Metastable Peaks

For detection of such peaks an ion repeller voltage of + 20 to + 25 volts and a resolving power of one part in 500 to 1000 were used

since it has been shown [1] that the height of these peaks increases relative to the others under these conditions.

2.3. Measurement of Appearance Potentials

While an appearance potential is being measured it is essential that a constant monitor current prevails (i.e. for about thirty minutes) Thus whenever possible the cold, gallium, heated or direct evaporation inlet systems were used. However for some solids of high molecular weight, such as Ph_6Sn_2, decomposition ensued if the heated inlet system was used, and the direct insertion probe had to be employed. Even so it was found that by patient manipulation a constant monitor could be maintained for the duration of the measurements (Often, in fact, this constant monitor current occurred because material fell from the probe into the source, producing a background spectrum of the material and constant monitor current for several hours) The inlet systems used for the various elements and compounds for which appearance potentials of ions were measured were as follows:

Direct Evaporation: All dialkylberyllium compounds.

Heated Inlet: Ph_4Sn, Ph_3SnI, Ph_3SnEt, Ph_3SnMe, $Ph_3Sn{\cdot}GeMe_3$.

Gallium System: Et_4Sn, Et_3SnPh, Et_2SnPh_2, Et_6Sn_2.

Cold Inlet: All inert gases.

Direct Insertion Probe: Ph_6Sn_2, $Ph_3Sn{\cdot}SnMe_3$, $Ph_3Sn{\cdot}SMe$.

After the sample which produced an ion whose appearance potential (A.P.) was to be measured had been introduced via the appropriate inlet system, a standard compound was introduced through one of the remaining systems. (The required A.P. is measured relative to the A.P. of an ion

produced in the spectrum of the standard material, which was generally tetraethyltin for organotin compounds when $SnEt_3^+$ was the standard ion or the inert gases, argon, krypton or xenon, for organoberyllium compounds.)

The precautions taken in measuring appearance potentials may be illustrated from a specific example. For the measurement of $A(BeCH_3^+)BeMe_2$ argon was used as the standard. The CH_3Be^+ peak was first tuned, by adjusting the magnetic field, onto the collector meter and the ion beam focussed to its maximum value with the ion repellor voltage set within the limits - 1.0 to +5 volts (i.e. readings on the ion repeller dial of 1.35 to 3.30), the electron beam voltage at 20V. and the trap current at 10 μA for organotin compounds and 20 μA. for organoberyllium compounds. The electron beam voltage was then increased to 50V. and the ion currents given on the collector meter for the two ions, CH_3Be^+ and Ar^+, adjusted to give equal values by altering either the pressure of argon in the cold inlet reservoir or the temperature of dimethylberyllium in the direct evaporation system. (One scanned from the CH_3Be^+ peak to the Ar^+ peak and vice-versa by altering the magnetic field).

Since the accuracy of A.P. measurements depends on the sensitivity of ion detection this was made as great as possible by using:

a) A high source pressure produced by sample and standard compound vapour. The pressure normally used was $\sim 8 \times 10^{-6}$m.m. since it is important that this pressure is not so high that "sparking" occurs in the source. If "sparking" does occur while measurements are in progress then the A.P. determination must be restarted because potential gradients within

the source are altered.

b) Whenever possible the source slits were opened to give a resolution of only 1 part in 500. In practice this was not always possible. For example when measuring $A(C_2H_5Be^+)BeEt_2$ the ion $C_3H_2^+$ also occurred at the m/e value of 38. Since it is essential that the two ions were completely resolved a resolving power of 1 part in 1000 had to be used.

The electron beam was then reduced to 20 volts and the ion giving the largest ion current at this voltage tuned onto the collector meter. (In this case it was CH_3Be^+) The ion multiplier voltage was then increased so that the ion current was approximately 2 to 7 x 1000 units on the meter. In practice it was found that no advantage was gained by increasing this voltage above 2.8KV. (i.e. a reading on the ion multiplier dial of 6.00) Above this the collector meter reading was so unsteady for small ion currents that the advantage of increased sensitivity was annulled by a decreased accuracy of the readings.

Having made sure that the collector meter reads zero at an electron beam voltage of 5 volts (well below the appearance potential of ions under study) and the ion beam correctly focussed, the voltage was reduced in 0.2 volt steps and ion currents for CH_3Be^+ and $Ar^{+\cdot}$ measured after each step. The meter was zeroed periodically when no peak was tuned onto the collector meter and readings of ion currents discontinued when they became less than 0.5 x 1 units. A graph could then be drawn of ion current against electron beam energy (in eV) and the linear portion of the ionization efficiency curve established.

In measuring the same appearance potential again ion currents

were read in 0.4 volt steps while in this linear region and reduced to 0.2 volt steps only when tailing of the ionization efficiency curve commenced. When the two ions were no longer being formed the voltage was increased to 20 volts and ion currents again read and checked with those found at the start of the appearance potential measurements. If there was any discrepancy between the values then that particular set of data was discarded.

Appearance potentials were determined from at least four sets of measurements using methods described in Chapter 3.1. Calculation of Results.

3. CALCULATION OF RESULTS.

3.1 Evaluation of Appearance Potentials.

3.2 Identification of Ions.

3.3 Calculation of Abundances.

3.4 Assignment of Metastable Peaks.

3. CALCULATION OF RESULTS

3.1. Evaluation of Appearance Potentials

Two methods were used in the evaluation of appearance potentials from the data obtained following the experimental procedure described earlier (p. 50). Both methods are illustrated by reference to specific examples.

a) Modified Warren Method

Ionization efficiency curves for Me_2Be^+ and Ar^+ are shown in fig. 4,a). In the Warren [41] method of evaluation the linear portions of these curves are made parallel by multiplying the curve of steeper slope by the ratio of the slopes of the linear regions. In this case ion currents for $Ar^{+\cdot}$ are multiplied by 0.87. These standardised ion currents when plotted as log. (ion current) vs. electron energy give the graph shown in fig. 4b). The curves so produced also have linear portions, AB and A'B'. Within this region voltage differences ΔV(eV) are taken at corresponding ion currents and plotted to give graph 4c). From the voltage difference at zero ion current the ionization potential of Me_2Be is found.

b) Semi-logarithmic Method

Typical ionization efficiency curves for $SnPh_3^+$ (in this case from Ph_3SnI) and $SnEt_3^+$ (derived from $SnEt_4$) are shown in fig. 5a). In obtaining this experimental data ion currents of the two species at 50eV had been made equal and no further "standardisation" was carried out. In fig. 5b) log. (ion current) is plotted against electron energy producing the essentially straight line portions CD and C'D'. Voltage differences taken within this region at corresponding ion currents when

Fig. 4

Ionization Efficiency Curves for $Me_2Be^{+\cdot}$ and $Ar^{+\cdot}$.

Illustration of Appearance Potential Determination by Modified Warren Method.

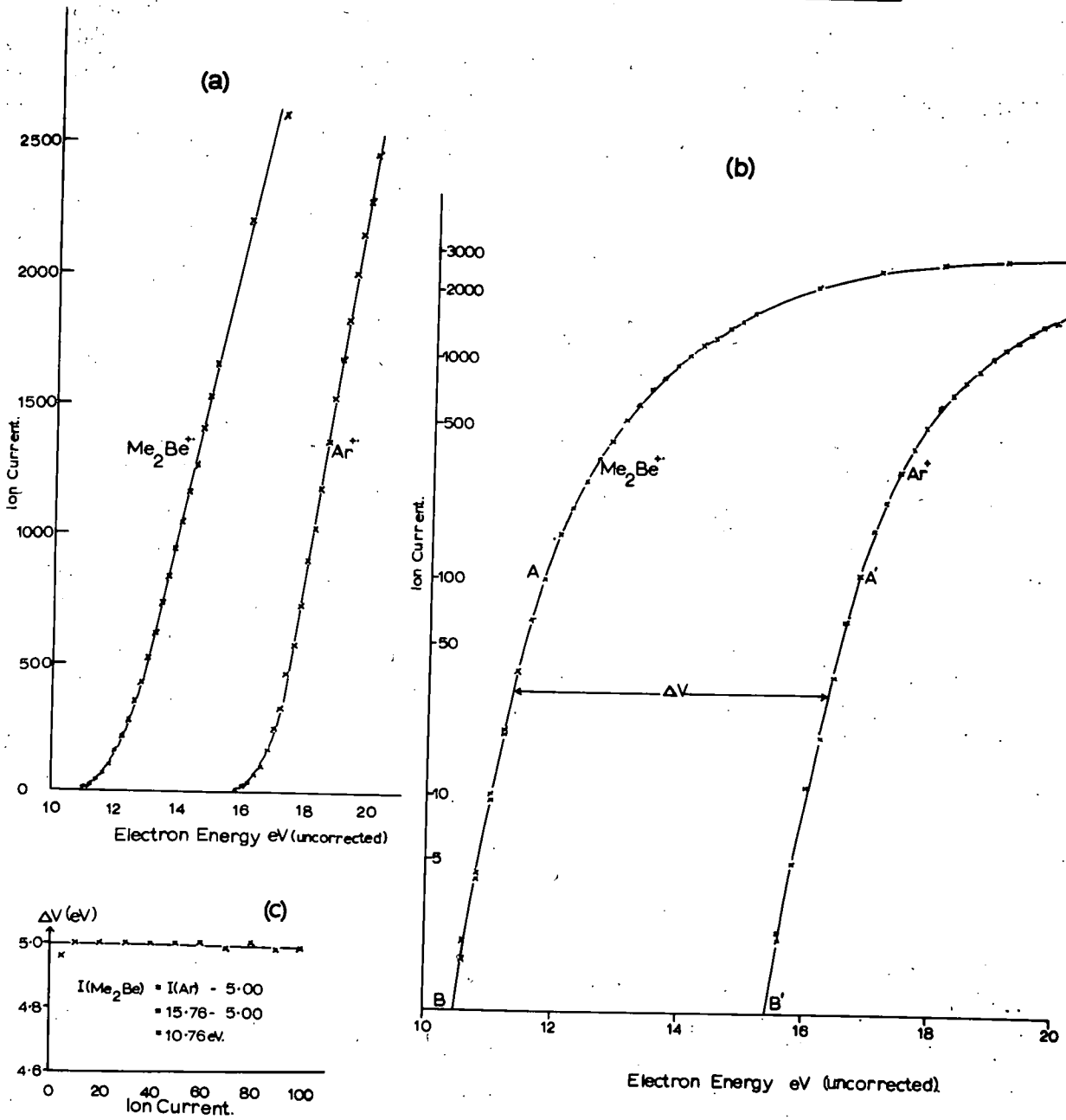

Fig. 2

Ionization Efficiency Curves for Ph_3Sn^+ from Ph_3SnI and Et_3Sn^+ from Et_4Sn. Illustration of Appearance Potential Determination by Semi-logarithmic Method.

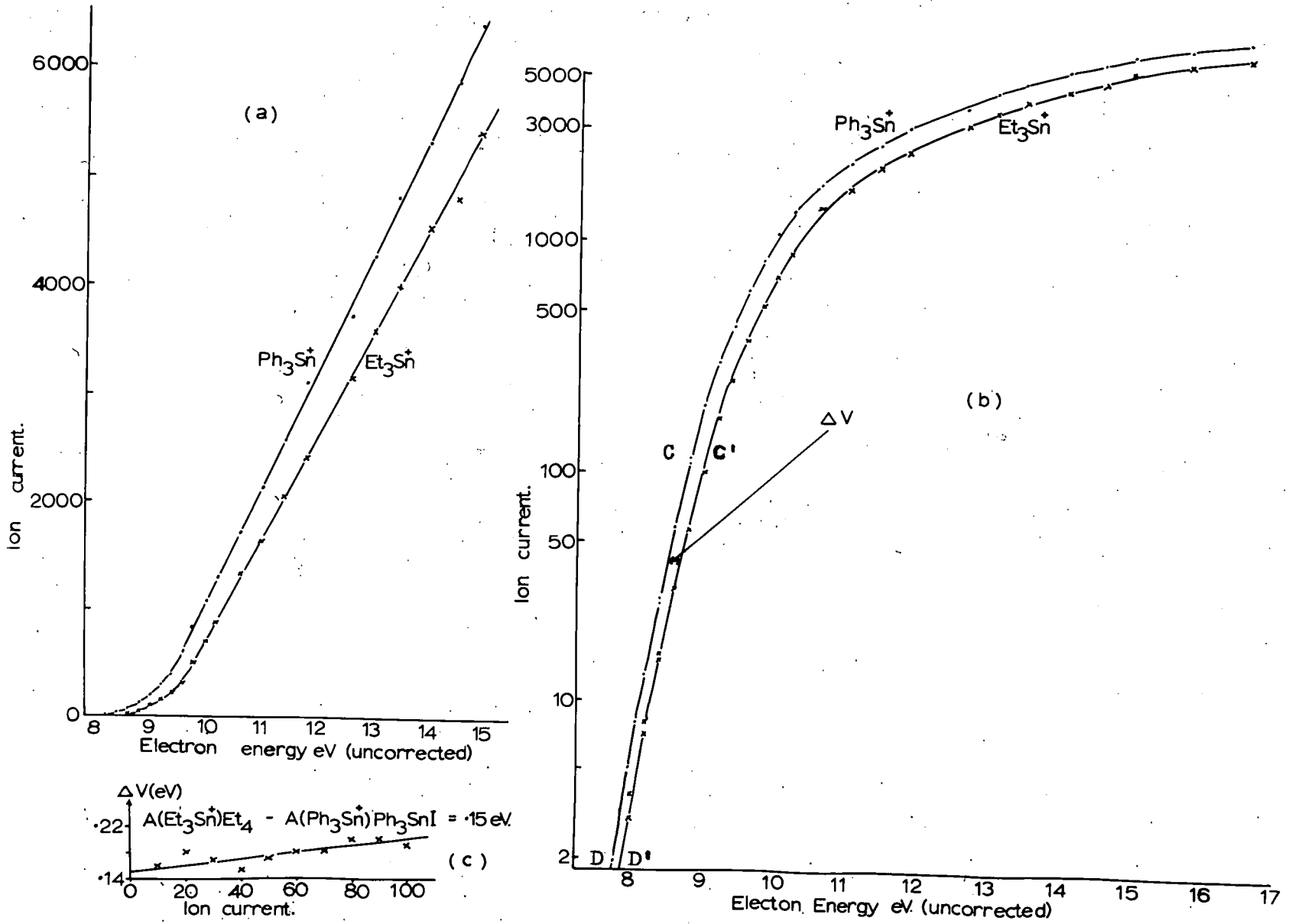

plotted to give graph 5c). The voltage difference at zero ion current allows $A(SnPh_3^+)Ph_3SnI$ to be found relative to $A(SnEt_3^+)SnEt_4$.

3.2. Identification of Ions

The mass spectra of Group IVb organometallic compounds, particularly germanium and tin, are complicated by the polyisotopic nature of these elements and characteristic patterns are produced for each metal containing ion which reflect the isotope abundances of the metal, as in the following illustration.

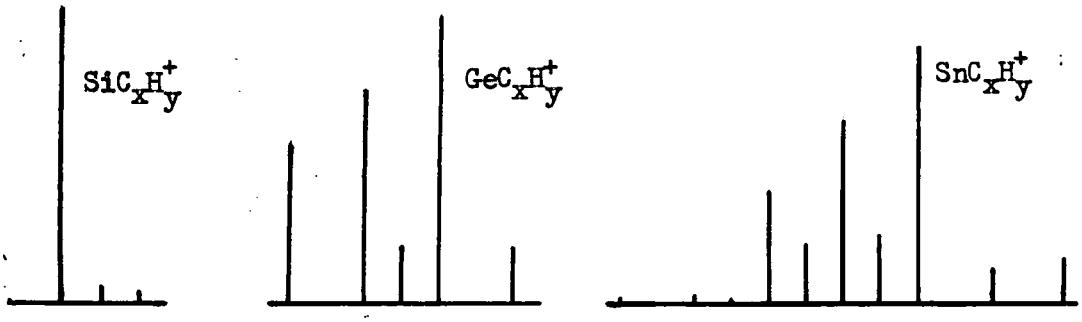

Even when x is as large as 18, the effects of ^{13}C are not sufficient to alter the visual appearance of these patterns.

Tin and lead isotope masses and abundances are given in Appendix 1. Since lead isotope abundances vary with sample origion these were calculated from the actual specimens of tetraethyl - and tetraphenyl-lead used.

Ions containing two or more polyisotopic elements produce a relatively high combined mass, extending over several mass units.

The combinations of isotopes for Ge_2 are shown below:-

Isotope Combination (mass numbers)		Mass	Abundance Product
70	70	139.848554	4.22714
72	70	141.846017	11.2751
73	70	142.847637	3.20325
74	70	143.845427	14.9965
76	70	145.845637-	3.19091
72	72	143.843480	7.51856
73	72	144.845099	4.27204
74	72	145.842890-	20.0001
76	72	147.842099	4.25558
73	73	145.846720-	.606841
74	73	146.844510	5.68203
76	73	148.844720	1.20901
74	74	147.842300	13.3006
76	74	149.842509	5.66014
76	76	151.842719	.602176

Number of combinations:- 15

The abundance product is the product of isotope abundances and factorial of total number of atoms, divided by the product of the factorial of numbers of each isotope present and is proportional to the probability of occurence of the isotope combination.

Those combinations which have the same nominal mass (such as $^{76}Ge\underline{\ ^{70}Ge}$, $^{74}Ge\underline{\ ^{72}Ge}$ and $^{73}Ge\underline{\ ^{73}Ge}$) cover a mass spread of less than 50 p.p.m (parts per million) and even with a maximum spectrometer resolution of 1:20,000 appear as a single peak corresponding to the weighted arithmetic mean of the exact masses of the contributing combinations. For example the precise mass of the peak at mass 146 is given by

$$\frac{145.84672 \times 0.606841 + 145.84289 \times 20.0001 + 145.845637 \times 3.19091}{0.606841 + 20.0001 + 3.19091}$$

$$= 145.843356.$$

The peak height of this mass is proportional to the sum of the relative abundances of the individual combinations (i.e. 0.606841 + 20.0001 + 3.19091).

The isotope abundance pattern for Ge_2 and the precise masses of the peaks are given below:-

Nominal Mass	multiplicity	spread (ppm.)	Peak Mass (wtd mean)	Relative Abundance
140	singlet		139.848554	17.7626
141	no combination			
142	singlet		141.846017	47.3786
143	singlet		142.847637	13.4602
144	2	14	143.844777	94.6093
145	singlet		144.845099	17.9513
146	3	26	145.843357	100.0000
147	singlet		146.844510	23.8762
148	2	5.4	147.842494	73.7720
149	singlet		148.844720	5.0803
150	singlet		149.842509	23.7842
151	no combination			
152	singlet		151.842719	2.5304

It will be observed that the most abundant peak does not occur at the sum of the mass numbers of the predominent germanium isotopes i.e. ^{74}Ge-^{74}Ge = 148. Often for combinations of elements which do not have one outstandingly predominant isotope, the integer mass of the most abundant peak does not correspond to the sum of the mass numbers of the predominant isotopes.

A computer programme has been written [96] to determine the mass and relative abundances of combinations of up to three different polyisotopic elements. Abundances and masses for Sn_2, SnGe, Ge_2, GeSi, SnCl and SnBr combinations, calculated using this programme are given in Appendix 1.

Fig. 6

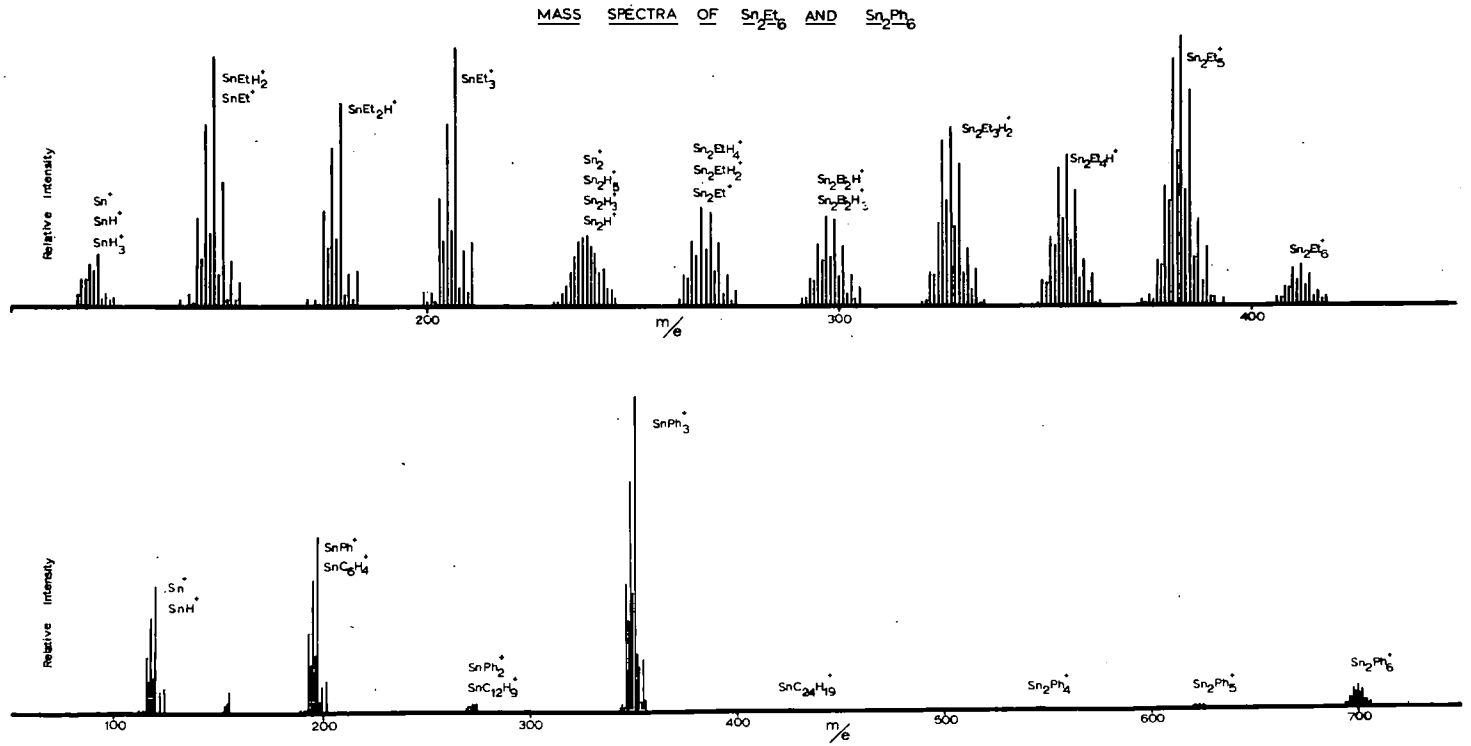
MASS SPECTRA OF Sn_2Et_6 AND Sn_2Ph_6
Relative Intensity
Sn^+
SnH^+
SnH_3^+
$SnEtH_2^+$
$SnEt^+$
$SnEt_2H^+$
$SnEt_3^+$
Sn_2^+
Sn_2H^+
$Sn_2H_3^+$
Sn_2H^+
$Sn_2EtH_4^+$
$Sn_2EtH_2^+$
Sn_2Et^+
$Sn_2B_2H^+$
$Sn_2B_2H_3^+$
$Sn_2Et_3H_2^+$
$Sn_2Et_4H^+$
$Sn_2Et_5^+$
$Sn_2Et_6^+$
200
300
400
m/e
Relative Intensity
Sn^+
SnH^+
$SnPh^+$
$SnC_6H_4^+$
$SnPh_2^+$
$SnC_{12}H_9^+$
$SnPh_3^+$
$SnC_{24}H_{19}^+$
$Sn_2Ph_4^+$
$Sn_2Ph_5^+$
$Sn_2Ph_6^+$
100
200
300
400
500
600
700
m/e

The characteristic patterns produced by ions containing a polyisotopic metal or metals are useful in allowing an immediate recognition of metal-containing ions and the determination of the number of metal atoms in an ion from the low resolution spectrum [see for example the spectrum of hexaethyldistannane and hexaphenyldistannane (Fig. 6).] However the pattern produced by a major ion often masks the presence of a low abundance ion only a few mass units different. As an example of this consider the group of peaks at m/e ~240 in the spectrum of hexaethyldistannane where four ion patterns overlap: $Sn_2^{+\cdot}$, Sn_2H^+, $Sn_2H_3^+$ and $Sn_2H_5^+$. Although it is possible to identify overlying ions from the low resolution pattern produced, the identification of ions present in a spectrum is more easily accomplished by measuring the precise masses of ions to 7 significant figures (using a resolving power of 1 part in 20,000).

This identification of overlying ions by precise mass measurement often poses problems especially in cases where mass differences between two peaks of the same high integer mass are small and barely resolved under high resolving conditions. With hexaethyldistannane the ions $^{240}Sn_2Et_2H_3^+$ and $^{242}Sn_2Et_2H^+$ are only just resolved having a mass difference of 45 p.p.m. For low abundance ions present under a group of peaks recourse must be made to the extremities of the peak pattern where peaks due to the more abundant ion may not be present. Thus $Sn_2H_5^+$ in the spectrum of Et_6Sn_2 was identified by a precise mass measurement of $^{244}Sn_2H_5^+$. With ions containing only one metal atom

similar difficulties sometimes occurred $^{120}SnC_{18}H_{19}^{+}$ and $^{119}SnPh_4^{+\cdot}$ are unresolved at high resolution differing in mass by only 23 p.p.m. and identification is achieved using the ^{112}Sn and ^{124}Sn isotopes respectively.

With organo-beryllium and - aluminium compounds it is essential to measure precisely the masses of each ion in the spectrum since the monoisotopicity of these metals means that metal-containing ions cannot be distinguished from hydrocarbon ions in the low resolution spectrum.

The empirical formulae of all ions described in this thesis were established by precise mass measurements. The agreement between measured and calculated mass was in all cases better than 6 p.p.m.

3.3. Calculation of Abundances

For ions containing monoisotopic elements abundances are found quite easily from peak heights produced by the ions in the low resolution spectra. Thus if A^+ is of peak height 4 arbitary units (a.u.), B^+ 3a.u., C^+ 2a.u., amd D^+ 1a.u., the abundance of A^+ as a percentage of total ion current is 40%. In comparing the abundances of ions containing polyisotopic elements with other types, contributions from each isotope combination must be summed. For example a spectrum showing three peaks of relative height 2:1:1 due to $^{127}I^+$, $^{81}Br^+$, and $^{79}Br^+$ corresponds to a 1:1 ratio of I^+ to Br^+. (^{81}Br = 49%; ^{79}Br = 51%) Similarly in the reported spectrum [97] of $(C_6F_5)_4Ge$ although $(C_6F_4)_2^+$ is the largest peak, when allowance is made for the presence of germanium isotopes $(C_6F_5)_3Ge^+$ is found to be the most abundant ion.

In calculating the abundances of ions allowance has also been made

for the presence of ^{13}C. The natural abundance of ^{13}C is 1% and for ions containing n carbon atoms n% of the ions will contain a ^{13}C atom. Thus if the effects of ^{13}C are neglected the abundances of ions containing a large number of carbon atoms will be underestimated.

In the following illustrations of the method of calculation of abundances the following symbols are used:-

i_n = peak height due to ions at m/e = n

$i_n(A_wC_xH_yM_z^+)$ = peak height at m/e = n carried by ion $A_wC_xH_yM_z^+$

$I(A_wC_xH_yM_z^+)$ = the sum of the peak heights of all A and M isotopic variants of the ion of composition $A_wC_xH_yM_z^+$

$It(A_wC_xH_yM_z^+)$ = $I(A_wC_xH_yM_z^+) + I(A_w{}^{13}CC_{x-1}H_yM_z^+)$

$i_n\left[{}^{13}C(n-1)\right]$ = contribution to peak height at m/e = n for one ^{13}C atom present in ionnor ions at m/e = (n-1).

$U(A_wC_xH_yM_z^+)$ = abundance of ion $A_wC_xH_yM_z^+$

For ions including only monoisotopic elements and for hydrocarbon ions it is obvious that

$$i_n(A_wC_xH_yM_z^+) = I(A_wC_xH_yM_z^+)$$

For the aluminium and beryllium compounds, where hydrocarbon ions were important, abundances have been calculated using the formula

$$U(A_wC_xH_yM_z^+) = \frac{It(A_wC_xH_yM_z^+)}{\sum It(A_wC_xH_yM_z^+)} \qquad - \quad 3.1$$

where the summation in the denominator is carried over all ions. For the metals silicon, germanium, tin and lead hydrocarbon ions generally comprised no more than 5% of the total ion current and abundances have

been found by restricting the summation in the denominator to metal-containing ions only.

Ion currents are measured in arbitary units (a.u.) which depend on sample pressure in source and on instrument sensitivity of ion detection while the spectrum is being recorded. Abundances on the other hand are dimensionless quantities and are hence not dependant, at least to a first approximation on instrument sensitivity.

When a single peak in a low resolution spectrum was known to include currents of two or more ionic species, the current at this mass number was divided amongst the ion species present in the ratio of the ion currents measured for the species when separated under high resolution (1:20,000).

For example in the spectra of diethylberyllium (70eV, source temp. 196°C) the ions $C_2H_6Be^{+\cdot}$ and $C_3H_3^+$ are present at m/e 39. High resolution measurements show that

$$i_{39}(C_2H_6Be^{+\cdot}) = 8.625 \times i_{39}(C_3H_3^+) \qquad 3.2$$

The current carried by ions at m/e = 39 is found from the low resolution spectra as 1.76 a.u.

$$1.76 \text{ a.u.} = i_{39}(^{13}C38) + i_{39}(C_2H_6Be^{+\cdot}) + i_{39}(C_3H_3^+) \qquad 3.3$$

$i_{39}(^{13}C38)$ is found from the peak height of m/e 38 which is 8.51 units.

$$i_{39}(^{13}C38) = i_{38} \times (^{13}C \text{ natural abundance}) \times (\text{no. of C atoms in } 38^+ \text{ ions})$$

$$= 8.51 \times 0.01 \times 2 = 0.170 \text{ a.u.}$$

hence from 3.3

$$1.59 \text{ a.u.} = i_{39}(C_2H_6Be^{+\cdot}) + i_{39}(C_3H_3^+) \qquad 3.4$$

from equations 3.2 and 3.4 it follows

$$i_{39}(C_3H_3^+) = 0.165 \text{ a.u.} = I(C_3H_3^+)$$

$$i_{39}(C_2H_6Be^{+\cdot}) = 1.425 \text{ a.u.} = I(C_2H_6Be^{+\cdot})$$

The contribution due to the presence of one ^{13}C atom is found as follows:

$$It(C_2H_6Be^{+\cdot}) = I(C_2H_6Be^{+\cdot}) + I(C^{13}CH_6Be^{+\cdot})$$

$$= 1.425 + 1.425 \times 0.01 \times 2$$

$$= 1.454 \text{ a.u.}$$

$$\text{Similarly } It(C_3H_3^+) = I(C_3H_3^+) + I(C_2{}^{13}CH_3^+)$$

$$= 0.168 \text{ a.u.}$$

The total ion current for diethylberyllium is 52.681 a.u. from which using 3.1

$$U(C_2H_6Be^{+\cdot}) = \frac{1.454 \times 100}{52.681} = 2.76$$

$$U(C_3H_3^+) = \frac{0.168 \times 100}{52.681} = 0.32$$

With polyisotopic metals the calculation is similar. In the spectrum of tetraethyltin the peak pattern produced in the region of m/e 150 is due to the overlap of $EtSn^+$ and $EtSnH_2^+$. High resolution mass measurements give

$$i_{151}(^{122}SnEt^+) = 0.0995\ i_{151}(^{120}SnEtH_2^+) \qquad 3.5$$

The current carried by ions at m/e 151 is found from the peak height of m/e 151 in the low resolution spectra.

$$3.105 \text{ a.u.} = i_{151}(^{120}SnEtH_2^+) + i_{151}(^{122}SnEt^+) + i_{151}(^{13}C150) \qquad - 3.6$$

$i_{151}(^{13}C150)$ is found from the peak height of m/e 150 which is 0.77 a.u.

$$i_{151}(^{13}C150) = 0.77 \times 0.01 \times 2 = 0.01 \text{ a.u.}$$

hence from equations 3.5 and 3.6

$$i_{151}(^{122}SnEt^+) = (3.105 - 0.01)\ 0.0995 = 0.28 \text{ a.u.}$$

$$i_{151}(^{120}SnEtH_2^+) = (3.105 - 0.01)\ 0.9005 = 2.815 \text{ a.u.}$$

$I(SnEt^+)$ and $I(SnEtH_2^+)$ is then found

$$I(SnEt^+) = i_{151}(^{122}SnEt^+) \times \frac{100}{\text{natural abundance of } ^{122}Sn}$$

$$= 0.28 \times \frac{100}{4.91} = 5.945 \text{ a.u.}$$

Similarly $I(SnEtH_2^+) = 8.540$ a.u.

Adding the contributions for the presence of one ^{13}C atom in these ions gives

$$It(SnEt^+) = 5.945 + 5.945 \times 0.01 \times 2 = 6.064 \text{ a.u.}$$

Similarly $It(SnEtH_2^+) = 8.711$ a.u.

Choosing another set of peaks the values of $It(SnEt^+)$ and $It(SnEtH_2^+)$ may be re-evaluated and mean taken. When ion currents of other metal containing ions have been found the abundances of the species are calculated using equation 3.1.

With ions containing 2 or more polyisotopic elements use is made of the calculated probabilities of occurrence of the various isotope combinations. (given in Appendix 1.) Thus if

$$i_{351}\left[^{197}(SnBr)Ph_2^+\right] = 9.73 \text{ a.u.}$$

$$I\left[SnBrPh_2^+\right] = 9.73 \times \frac{100}{\text{probability of occurrence of } ^{197}(SnBr) \text{ combination}}$$

$$= 9.73 \times \frac{100}{67.2} = 14.469 \text{ a.u.}$$

from which $It(SnBrPh_2^+) = 14.79 \times 1.12 = 16.216$ a.u.

3.4 Assignment of Metastable Peaks

The phrase "metastable peaks" is used for peaks arising in the mass spectra due to decomposition of metastable ions during their flight through the mass spectrometer tube [1,2]. They are recognisable not only from the fact that they appear at non-integral mass numbers but also because they are imperfectly focussed compared with peaks due to ions which travel the whole length of the spectrometer without decomposition. Because of the directional focussing properties of the sector magnetic field the decomposing ions most likely to be recorded are those which undergo the transition in the field free region preceding the magnetic analyser. For the decomposition

$$m_1^+ \longrightarrow m_2^+ + (m_1 - m_2)$$

with internal energy release TeV the position of maximum intensity for the observed metastable peak covers a mass range given by [98]

$$m^* = \frac{m_2^2}{m_1}\left[1 \mp \left(\frac{m_1 - m_2}{m_2} \cdot \frac{T}{eV}\right)^{\frac{1}{2}}\right]$$

where V is the accelerating voltage between the ionization chamber and entrance slit to the electrostatic analyser. For most metastable decompositions however the internal energy release is small enough to be neglected and the position of maximum intensity is given by

$$m^* = \frac{m_2^2}{m_1}$$

Although the shape of metastable peaks is generally roughly gaussian the peaks often differ widely in width and factors such as finite beam dimensions, angular spreading and kinetic energy of separation of fragments and discriminations against production must be considered

for a complete analysis [99].

The values m_1 and m_2 associated with any metastable peak m^* can usually be determined by a process of trial and error, remembering that the apparent mass is smaller than either of the masses of the ions giving rise to the peak and that the peaks at masses m_1 and m_2 will be much larger than the metastable peak. Of great help in this assignment are tables of m^* values that occur for various values of m_1 and m_2 ($m_1 \leqslant 500$ and $500 \geqslant m^* \geqslant 1$)[100].

With polyisotopic elements present in an ion, metastable peaks produced by the decomposition of such an ion eliminating a neutral species consisting of essentially monoisotopic elements (e.g. a hydrocarbon) must follow the peak pattern of the daughter and parent ions. For example 7a) and b) show metastable peaks for decomposition of Sn_2CxHy^+ and $SnCxHy^+$ ions respectively. When a polyisotopic element is lost as a neutral fragment, the ion formed will have a different peak pattern from its precurser. The resulting metastable peaks may merge because of their diffuse nature producing a single broad metastable peak. Examples of such are shown in fig.7c) and d). Fig.7e) shows the approximate metastable peak envelope for the decomposition

$$Ph_6Sn_2^{+\bullet} \longrightarrow Ph_3Sn^+ + Ph_3Sn^\circ$$

This has been calculated by considering all the possible decompositions for $Ph_6Sn_2^{+\bullet}$ ions containing the abundant tin isotopes.

Fig. 7

Metastable Peaks

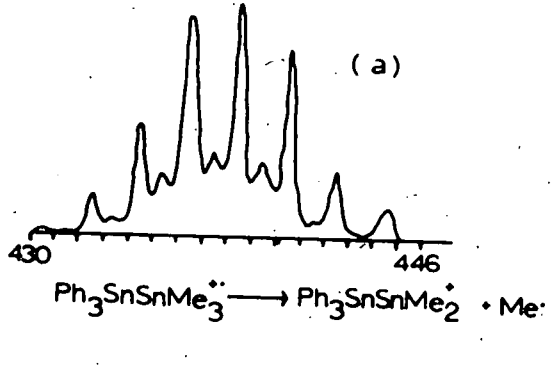

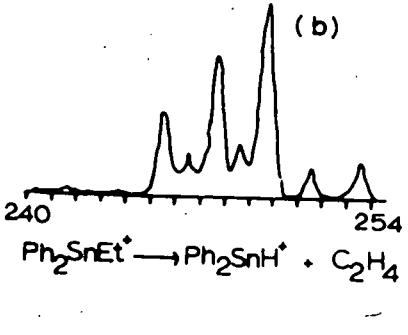

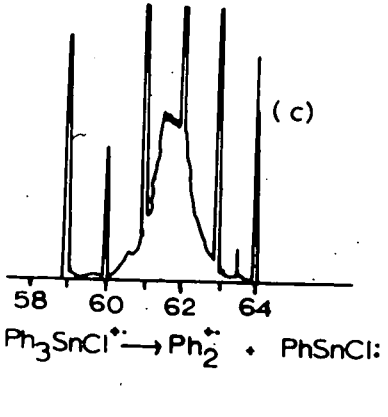

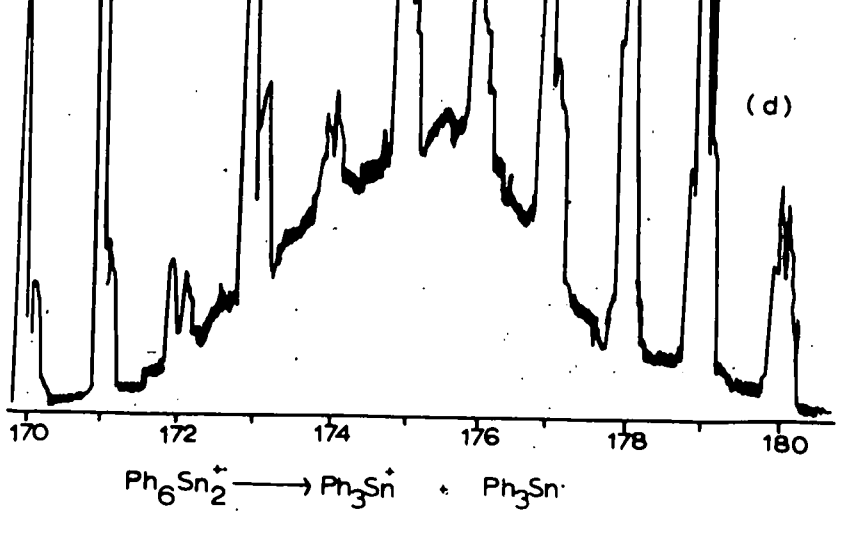

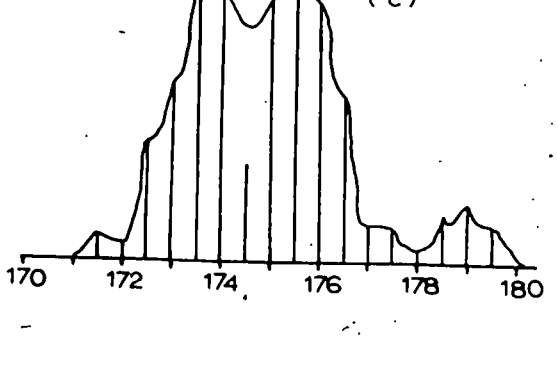

Metastable peaks for $Ph_3Sn.SnPh_3^{+\bullet} \rightarrow Ph_3Sn^+ + Ph_3Sn^\bullet$

Tin isotopes in $Ph_3Sn \cdot SnPh_3^{+\bullet}$ (m^+_1)		Tin isotope in Ph_3Sn^+ (m^+_2)	$\left(= \frac{m^*}{\frac{m_2^2}{m_1}}\right)$	abundance of m^*
116	116	116	173.5	1
		116	173.5	1
116	117	116	173.25	1
		117	174.25	1
116	118	116	173.0	3.5
		118	175.0	3.5
117	118	117	173.7	2
		118	174.7	2
116	119	116	172.8	1
		119	175.8	1
118	118	118	173.5	3
		118	173.5	3
116	120	116	172.5	4.5
		120	176.5	4.5
117	119	117	173.5	0.5
		119	175.5	0.5
117	120	117	173.3	2.5
		120	176.3	2.5
118	119	118	174.3	2
		119	175.3	2
118	120	118	174	8
		120	176	8
116	122	116	172	0.5
		122	178	0.5
119	119	119	175	0.5
		119	175	0.5
119	120	119	174.8	3
		120	175.8	3
117	122	117	172.8	0.5
		122	178.8	0.5
120	120	120	175.5	5.5
		120	175.5	5.5
118	122	118	173.5	1
		122	177.5	1
116	124	116	171.5	1
		124	179.5	1
119	122	119	173.5	0.5
		122	177.3	0.5
117	124	117	172.3	0.5
		124	179.3	0.5
120	122	120	175	1.5
		122	177	1.5
118	124	118	173	1.5
		124	179	1.5

119	124	119	173.8	0.5
		124	178.8	0.5
120	124	120	174.5	2
		124	178.5	2

The relative abundance of the metastable peak produced is found from the relative abundance of the isotope combination of the "parent" m_1^+ ion. For example the relative abundance of the $^{116}Sn^{118}Sn$ combination is 7 and hence the relative abundance of the metastable peak formed by decomposition of $Ph_3{}^{116}Sn^{118}SnPh_3^{+\cdot}$ to $Ph_3{}^{118}Sn^+$ or $Ph_3{}^{116}Sn^+$ is 3.5. The m/e values at which the various metastable peaks occur were rounded off to the nearest 0.5 and plotted against relative abundance as shown in fig. 7e). The approximate metastable peak envelope was then drawn bearing in mind the guassian shape of metastable peaks.

It will be apparent that the shape of the metastable peak for a decomposition

$$MM'C_aH_b^+ \longrightarrow MC_eH_d^+ \quad + \quad M'C_{a-e}H_{b-d}$$

depends on the polyisotopic nature of M and M'.

4. RESULTS AND DISCUSSION.

4.1 Appearance Potentials and Derivation of Bond Dissociation Energies and Heats of Formation.

4.2 Mass Spectra of Organocompounds of Silicon, Germanium, Tin and Lead.

4.3 Mass Spectra of Beryllium Dialkyls.

4.4 Mass Spectra of Organoaluminium Compounds.

Table 4.1.1.

Comparison of measured ionization potentials (I.P.s) with literature values.

	Standard used	Individual determinations eV. Warren method	Individual determinations eV. Semi-log method	Measured I.P. eV.	Literature values for I.P. eV. [3]
Argon	Krypton I.P = 14.00eV	15.80 15.80 15.76	15.76 15.74 15.78	15.77 ±.01	15.755 spectroscopic
Benzene	Krypton	9.50 9.50 9.52	9.56 9.52	9.53 ±.01	9.52 ±.10 9.38 ±.10 electron-impact 9.247 spectroscopic 9.245 photo-ionization
Nitrogen	Argon I.P. = 15.76eV	15.60 15.58 15.64	15.60 15.60	15.60 ±.01	15.60 ±.01 electron impact 15.58 ±.02 spectroscopic

Source temperature 185 - 195°C

Ion repeller voltage 0.4 - 2.0 volts.

4. RESULTS AND DISCUSSION

4.1 Appearance Potentials and Derivation of Bond Dissociation Energies and Heats of Formation.

4.1.1. Accuracy of Appearance Potential Measurements.

To test the accuracy of the appearance potential measurements, ionization potentials of argon, nitrogen and benzene were measured using the logarithmic and Warren method. Different sets of experimental data were used for each method of calculation. The results of these measurements together with published values of the ionization potentials are presented in table 4.1.1.

The values obtained for argon and nitrogen agree well with the values obtained by other workers and it is apparent in this case that the adiabatic and vertical ionization potential are one and the same. With benzene the measured ionization potential agrees well with the values found by other workers using electron impact methods but is some 0.28eV higher than values obtained by photo ionization or spectroscopic methods.

Both methods of evaluation hence give good estimations of vertical ionization potentials.

4.1.2. Appearance Potentials and Bond Dissociation Energies for Organotin Compounds.

i) Appearance Potentials

Since R_3Sn^+ ions from mono-metallic compounds give similar ionization efficiency curves and under this condition the most accurate determinations of appearance potentials are obtained [101],

Fig. 8

Ionization efficiency curves for Et_3Sn^+ from Et_4Sn and Ph_3Sn^+ from $Ph_3Sn{\cdot}GeMe_3$

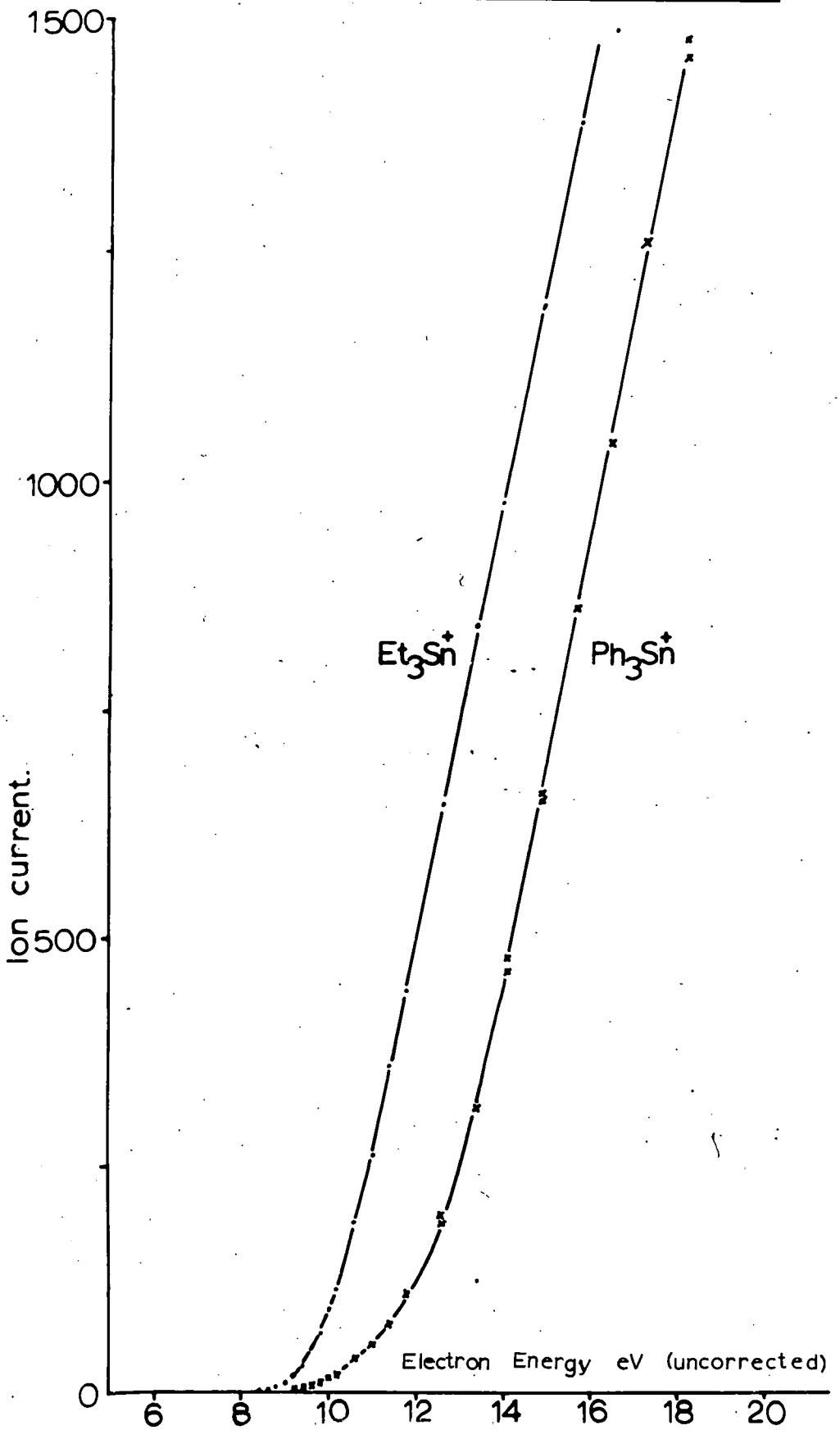

Et_3Sn^+ from Et_4Sn was used as standard except for $PhSnEt_3$ which produced this ion in its mass spectrum. For this compound Ph_3Sn^+ from triphenylethyl - or tetraphenyl-tin was used. The relationship between $A(Ph_3Sn^+)Ph_3SnR$ - $A(PhSnEt_2^+)PhSnEt_3$ then enabled $A(Et_3Sn^+)Et_4Sn$ - $A(PhSnEt_2^+)PhSnEt_3$ to be found.

The ionization efficiency curve for a typical R_3Sn^+ ion is shown in fig. 5 (p. 56) "Tailing" of the ionization efficiency curves often associated with excess energy was observed only for Ph_3Sn^+ ions derived from $Ph_3Sn{\cdot}SnPh_3$, $Ph_3Sn{\cdot}SnMe_3$ and $Ph_3Sn{\cdot}GeMe_3$. The extent of this tailing is shown in fig. 8. where the ionization efficiency curve for Ph_3Sn^+ derived from $Ph_3Sn{\cdot}GeMe_3$ is shown. A similar long tail has been observed with the ionization efficiency curve of Me_3Si^+ obtained from hexamethyldisilane. [62]

The appearance potentials of R_3Sn^+ and $R_4Sn^{+\cdot}$ ions relative to that of Et_3Sn^+ from tetraethyltin are shown in tables 4.1.2. and 4.1.3. Separate sets of experimental data were used for each method of calculation.

$A(Et_3Sn^+)Et_3SnPh$ was not measured since this ion was of too low abundance.

The reproducibility of the measurements is good, the standard error of the mean being always less than $\pm$ 0.05eV and generally $<$ 0.03eV. In calculating dissociation energy differences an error of twice the maximum observed standard error of the mean has been used (i.e. $\pm$ 0.10eV)

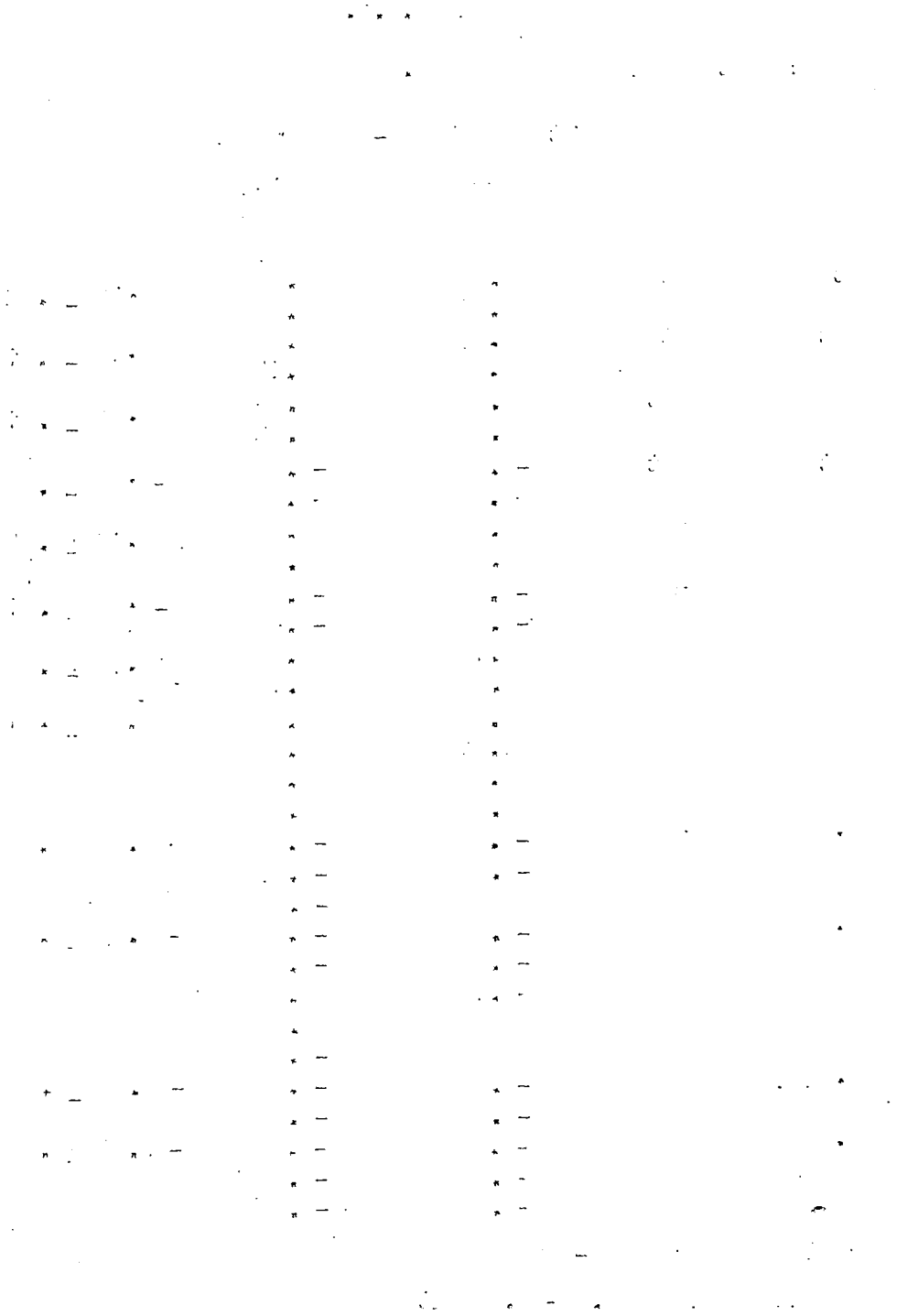

Table 4.1.2.

Appearance potentials of R_3Sn^+ ions.

		$A(Et_3Sn^+)Et_4Sn - A(R_3Sn^+)$ eV		
	R_3Sn^+	Warren method	Semi-log method	Mean
$PhSnEt_3$	$PhSnEt_2^+$	0.17	0.14	0.19 ± .02
		0.21	0.22	
Ph_2SnEt_2	$PhSnEt_2^+$	0.17	0.13	0.15 ± .01
		0.17	0.14	
	Ph_2SnEt^+	0.12	0.13	0.14 ± .01
		0.15	0.14	
Ph_3SnEt	Ph_2SnEt^+	-0.31	-0.30	-0.27 ± .02
		-0.21	-0.27	
	Ph_3Sn^+	0.15	0.17	0.13 ± .02
		0.15	0.05	
Ph_4Sn	Ph_3Sn^+	-0.90	-0.90	-0.90 ± .01
		-0.88	-0.92	
Ph_3SnI	Ph_3Sn^+	0.10	0.05	0.10 ± .02
		0.10	0.15	
Ph_3SnMe	Ph_3Sn^+	0.0	0.02	0.04 ± .01
		0.01	0.03	
		0.06	0.06	
		0.05	0.08	
$Ph_3Sn{\cdot}SPh$	Ph_3Sn^+	-0.40	-0.30	- 0.31 ± .03
		-0.35	-0.23	
			-0.28	
$Ph_3Sn{\cdot}SnPh_3$	Ph_3Sn^+	-0.02	-0.07	- 0.03 ± .02
		-0.08	-0.10	
		-0.10	+0.04	
			+0.13	
			-0.02	
$Ph_3Sn{\cdot}GeMe_3$	Ph_3Sn^+	-0.40	-0.29	- 0.38 ± .05
		-0.33	-0.48	
$Ph_3Sn{\cdot}SnMe_3$	Ph_3Sn^+	-0.36	-0.28	- 0.24 ± .03
		-0.27	-0.17	
		-0.18	-0.20	

Source temperature 195 - 210°C

Ion repeller voltage 0.4 - 2.0 volts

Table 4.1.3.

Ionization Potential (I.P.) of Et_4Sn and Ph_2SnEt_2

$A(Et_3Sn^+)Et_4Sn$ - I.P. eV

	Warren	Semi-log	Mean
Et_4Sn	0.58 0.60	0.63 0.59	0.60 ± .01
Ph_2SnEt_2	0.57 0.49	0.62 0.54	0.56 ± .03

Source temperature 200°C

Ion repeller voltage 0.4 - 2.0 volts.

ii) Bond Dissociation Energy Differences.

These have been derived using:

$$A(R_3Sn^+)R_3SnR = I(R_3Sn\cdot) + D(R_3Sn\text{-}R) + E \qquad 4.1$$

where $I(R_3Sn\cdot)$ = Ionization potential of $R_3Sn\cdot$

$D(R_3Sn\text{-}R)$ = dissociation energy of bond $R_3Sn - R$

E = excess energy associated with R_3Sn^+ and $R\cdot$

In all calculations E has been taken as zero. By Stevenson's rule [59] this will probably be a correct assumption provided $I(R_3Sn\cdot) < I(R\cdot)$. The low abundance of R^+ compared to R_3Sn^+ is consistent with this and as mentioned earlier tailing of the ionization efficiency curve was observed only with metal-metal bonded compounds. For $Ph_3Sn\cdot$ it can be shown that $I(Ph_3Sn\cdot) < I(R\cdot)$ (p. 89). It must be emphasised however that possession of the lower ionization potential together with a simple appearance potential curve does not ensure the absence of excess energy so that calculated bond dissociation energies must be regarded as upper limits.

Bond dissociation energy differences are calculated directly from the differences in appearance potentials of the same ions produced from different compounds. Thus using eqn. 4.1 assuming E = 0

$$A(Ph_3Sn^+)Ph_4Sn = I(Ph_3Sn\cdot) + D(Ph_3Sn - Ph)$$

$$A(Ph_3Sn^+)Ph_3SnR = I(Ph_3Sn\cdot) + D(Ph_3Sn - R)$$

and by subtraction

$$A(Ph_3Sn^+)Ph_4Sn - A(Ph_3Sn^+)Ph_3SnR = D(Ph_3Sn\text{-}Ph) - D(Ph_3Sn\text{-}R)$$

Even though appearance potentials are known only relative to $A(SnEt_3^+)Et_4Sn$ appearance potential differences may still be found.

Table 4.1.4.

Bond energy data.

Bond dissociation energy differences (Kcal. mole $^{-1}$)

Tolerance = ± 3.2 Kcal. mole $^{-1}$.

$D(Ph_3Sn - Ph) - D(Ph_3Sn - Et) = 23.8$

$D(Ph_2EtSn - Ph) - D(Ph_2EtSn - Et) = 10.4$

$D(PhEt_2Sn - Ph) - D(PhEt_2Sn - Et) = 1.2$

Values of the difference ($\triangle$) $D(Ph_3Sn - Ph) - D(Ph_3Sn - R)$

where:-

R	$\triangle$
$GeMe_3$	12.0
SPh	13.6
$SnMe_3$	15.2
$SnPh_3$	20.1
Me	21.7
I	23.1
Et	23.8

Dissociation energies in molecular ions Kcal.mole^{-1}

$D(Et_3Sn^+ - Et) = 13.9 \pm 2.3$

$D(Ph_2EtSn^+ - Et) = 9.7 \pm 3.2$

$D(Ph_2EtSn^+ - Ph) = 9.5 \pm 3.2$

Thus

$$A(Et_3Sn^+)Et_4Sn - A(Ph_3Sn^+)Ph_3SnEt = 0.13eV$$

$$A(Et_3Sn^+)Et_4Sn - A(Ph_3Sn^+)Ph_4Sn = -.90eV$$

which by subtraction gives:

$$A(Ph_3Sn^+)Ph_4Sn - A(Ph_3Sn^+)Ph_3SnEt = 1.03eV$$

which is also $D(Ph_3Sn - Ph) - D(Ph_3Sn - Et)$.

In this way the bond dissociation energies differences shown in table 4.1.4. were calculated.

The decrease in the difference in the energies of dissociation $D(Et_nPh_{3-n}Sn - Ph) - D(Et_nPh_{3-n}Sn - Et)$ as n increases from 0 to 2 emphasises the well known unacceptability of the simple model of constant, transferable and additive bond energy terms. A similar variation occurs with methylphenyl tin compounds.

$$D(Me_3Sn - Ph) - D(Me_3Sn - Me)^{64} = 8 \pm 6 \text{ Kcal. mole}^{-1}$$

and $$D(Ph_3Sn - Ph) - D(Ph_3Sn - Me) = 22 \pm 3 \text{ Kcal. mole}^{-1}$$

This may indicate a general rule that the energy difference in removing an alkyl or phenyl group from gaseous $(alkyl)_nSnPh_{4-n}$ becomes less with increasing alkyl content.

The bond dissociation energies in table 4.1.4. have been extremely useful (see page 105) in interpreting the nature of the mass spectra of these organometallic compounds.

iii) Bond Dissociation Energies in Molecular Ions.

These were obtained using the relationship

$$A(R_3Sn^+)R_4Sn = I(R_4Sn) + D(R_3Sn^+ - R)$$

assuming the excess energy associated with the formation of R· and R_3Sn^+

Table 4.1.5.

Appearance potential of Et_3Sn^+ derived from Et_4Sn (eV)

	Warren	Semi-log	Mean
$A(Et_3Sn^+)Et_4Sn$	8.66	8.48	8.70 ± 0.09
	8.93	8.73	

Source temperature 195°C Standard used Xe I.P. = 12.13eV.

Appearance potentials of Ph_3Sn^+ ions and heats of formation of triphenyltin compounds.

	$A(SnPh_3^+)$ eV (± .2eV)	$\Delta H_f^\circ (SnPh_3R)_g$ Kcal. mole $^{-1}$
Ph_4Sn	9.6	114 ± 1 [103]
Ph_3SnEt	8.6	91 ± 7
Ph_3SnI	8.6	91 ± 7
Ph_3SnMe	8.7	97 ± 7
$Ph_3Sn{\cdot}SPh$	9.0	103
$Ph_3Sn{\cdot}GeMe_3$	9.1	-
$Ph_3Sn{\cdot}SnMe_3$	8.9	92 ± 8
$Ph_3Sn{\cdot}SnPh_3$	8.7	-

to be negligible. Again appearance potentials measured relative to $A(Et_3Sn^+)Et_4Sn$ yield values for these energies viz:

$$A(SnEt_3^+)Et_4Sn = I(Et_4Sn) + D(Et_3Sn^+ - Et)$$

Since $A(SnEt_3^+)Et_4Sn - I(Et_4Sn) = 0.6eV$ (table 4.1.3. p. 77)

If follows that

$$D(Et_3Sn^+ - Et) = 0.6eV$$

Similarly $D(Ph_2EtSn^+ - Et)$ and $D(PhEt_2Sn^+ - Ph)$ were evaluated the results being displayed in Table 4.1.4. Other dissociation energies in parent ions were not measured, because in these cases the parent ion was of such low abundance that the appearance potential could not be measured. The low Sn - C bond energies in $R_4Sn^{+\bullet}$ ions compared with those in the molecule (see Table 4.1.6.) are consistent with a bonding electron being removed from an Sn - C bond.

iv) Heats of Formation of Triphenyltin Compounds.

To determine heats of formation the absolute values of appearance potentials are required. Thus $A(Et_3Sn^+)Et_4Sn$ was measured using xenon as standard $I(Xe\bullet) = 12.13eV$ [102] giving the result shown in Table 4.1.5. In the determination of heats of formation an error of $\pm 0.2eV$ which is twice the standard error of the mean has been assumed. Using this value of $A(Et_3Sn^+)Et_4Sn$ ($8.7 \pm 0.2eV$) appearance potentials of Ph_3Sn^+ ions were derived using Table 4.1.2. and are shown in Table 4.1.5.

Heats of formation have been calculated assuming the occurrence of a simple dissociative process involving no excess energy:-

$$Ph_3SnR + e \longrightarrow Ph_3Sn^+ + R\bullet + 2e$$

It follows that

$$A(Ph_3Sn^+)Ph_3SnR = \Delta H_f^\circ(Ph_3Sn^+) + \Delta H_f^\circ(R\cdot) - \Delta H_f^\circ(Ph_3SnR)_g$$

from which

$$\Delta H_f^\circ(Ph_3SnR)_g = \Delta H_f^\circ(Ph_3Sn^+) + \Delta H_f^\circ(R\cdot) - A(Ph_3Sn^+)Ph_3SnR \quad - 4.2$$

First $\Delta H_f^\circ(Ph_3Sn^+)$ must be evaluated from a calorimetric estimation of $\Delta H_f^\circ(Ph_4Sn)$ gaseous (114.3 ± 1 Kcal. mole.$^{-1}$)[103], $A(Ph_3Sn^+)$ and $\Delta H_f^\circ(Ph\cdot)$ gaseous (72 ± 2 Kcal. mole.$^{-1}$)[104]. This quantity (263 ± 5 Kcal.mole.$^{-1}$) combined with the appropriate appearance potential and standard radical (gaseous) heats of formation ($CH_3\cdot$ 34 ± 1 [104]; $C_2H_5\cdot$ 26 ± 1 [104]; PhS· 50[104]; $Me_3Sn\cdot$ 35 ± 4[64]; I· 25.54 ± 0.01[102] Kcal. mole.$^{-1}$) gives the standard heats of formation for triphenyltin compounds shown in table 4.1.5.

v) Ph_3Sn - R Bond Dissociation Energies.

For absolute evaluation of these dissociation energies the ionization potential of $Ph_3Sn\cdot$ is required. Since it is possible to evaluate this quantity from the appearance potential measurements provided $\Delta H_f^\circ(Ph_6Sn_2)$ (gaseous) is known [64] a calculation of this quantity using the Franklin group parameter method [105] was attempted.

It was shown for hydrocarbons that ΔH_f° was an additive function of the groups making up the molecule and ΔH_f° values for many characteristic hydrocarbon groups were calculated from known heats of formation for various hydrocarbons. Unmeasured heats of formation could then be estimated by the addition of these group values although for highly branched molecules correction factors had to be applied.

The ΔH_f° group value for tetravalent tin can be found from the standard heats of formation of gaseous organotin compounds using:

$$\Delta H_f^\circ (R_4Sn)_g = 4 \times G(R\cdot) + G(Sn\cdot)$$

where $G(R\cdot)$ is the ΔH_f° group value for R.

$G(Sn)$ is the ΔH_f° group value for tetravalent Sn.

Using ΔH_f° group values for R· given by Franklin [105] [In Kcal.mole^{-1} at 298°K $G(CH_3\cdot) = -10.1$; $G(-CH_2-) = -4.9$; $G(-CH{:}CH_2) = 15.00$; $G(C_6H_5\cdot) = 22.1$] and the calorimetrically determined standard heats of formation for nine R_4Sn compounds [106], G(Sn) is evaluated at 298°K as 38 ± 3 Kcal. mole^{-1}.

Using this group value the following heats of formation were estimated at 298°K. $\Delta H_f^\circ (Ph_3SnEt)_g$ = 89 ± 3 Kcal. mole^{-1} and $\Delta H_f^\circ (Ph_3SnMe)_g$ = 94 ± 3 Kcal. mole^{-1}. which agree with the experimentally determined values in table 4.1.5. [i.e. $\Delta H_f^\circ (Ph_3SnEt)_g$ = 91 ± 7; $\Delta H_f^\circ (Ph_3SnMe)_g$ = 97 ± 7 Kcal. mole^{-1}.]

Because a correction factor may apply to compounds containing a tin-tin bond calculated heats of formation of such compounds (obtained using the above ΔH_f° group values) were compared with experimentally determined values.

	Calculated Kcal. mole^{-1}.	Measured Kcal. mole^{-1}.	Difference Kcal. mole^{-1}.
$\Delta H_f^\circ (Me_6Sn_2)_g$	15 ± 6	-7.6 ±2 [106]	22.6
$\Delta H_f^\circ (Et_6Sn_2)_g$	-13 ± 6	-37 ± 3 [106]	24
$\Delta H_f^\circ (Ph_3Sn\cdot SnMe_3)_g$	112 ± 6	92 ± 8	20

From these it follows that 22 Kcal. mole^{-1}. should be subtracted from the calculated heat of formation for a ditin compound. $\Delta H_f^\circ (Ph_6Sn_2)_g$ was thus estimated as 186 ± 6 Kcal. mole^{-1}.

From equation 4.2 it follows that:-

Table 4.1.6.

Bond dissociation energies.

R	Kcal. mole $^{-1}$. $D(Ph_3Sn - R)$ This work	$D(Me_3Sn - R)$ Ref. 64.	$D(Me_3Si - R)$ Ref. 63.
Ph	83 ± 10	81 ± 5	
Et	60 ± 10	68 ± 4	
T	60 ± 10	80 ± 4	69 ± 2
Me	62 ± 10	73 ± 4	76 ± 2
SPh	69 ± 10		
$GeMe_3$	71 ± 10		
$SnMe_3$	67 ± 10	76.0	
$SnPh_3$	62 ± 10		
$SiMe_3$			67 ± 2

$$\Delta H_f^\circ (Ph_3Sn\cdot) = \Delta H_f^\circ (Ph_6Sn_2) + A(Ph_3Sn^+)Ph_6Sn_2 - \Delta H_f^\circ(Ph_3Sn^+)$$
$$= 124 \pm 9 \text{ Kcal. mole}^{-1}.$$

The ionization potential of the triphenylstannyl radical is hence:-

$$I(Ph_3Sn\cdot) = \Delta H_f^\circ (Ph_3Sn^+) - \Delta H_f^\circ (Ph_3Sn\cdot)$$
$$= 139 \pm 10 \text{ Kcal. mole}^{-1}.$$
$$= 6.0 \pm 0.4 \text{ eV}.$$

Values for $D(Ph_3Sn - R)$ determined from this ionization potential and $A(Ph_3Sn^+)Ph_3SnR$ (using eqn. 4.1) are given in table 4.1.6.

$\bar{D}(Sn-Ph)$ has been calculated as 61.4 ± 2 Kcal. mole^{-1} from $\Delta H_f^\circ (Ph_4Sn)g.$[103] using the relationship

$$\bar{D}(Sn-Ph) = \tfrac{1}{4}\Delta H_f^\circ (Sn)g. + \Delta H_f^\circ (Ph\cdot) - \tfrac{1}{4}\Delta H_f^\circ (Ph_4Sn)g.$$

giving $D(Ph_3Sn-Ph) = \bar{D}(Sn-Ph) + 22 \pm 10$ Kcal. mole^{-1}. A similar relationship has also been found with tetramethyltin where $D(Me_3Sn-Me) = \bar{D}(Sn-Me) + 21 \pm 4$ Kcal. mole^{-1}.[64] Thus it appears that one should not attempt to approximate a bond dissociation energy with a mean bond dissociation energy for organotin compounds. With silicon the picture is somewhat confusing. $D(Me_3Si-Me)$ is about the same as the value ~77 Kcal. mole^{-1}. for $\bar{D}(Si-Me)$ calculated from $\Delta H_f^\circ (Me_4Si)g.$[107] and $\Delta H_f^\circ (Si)g.$[102]. But with alkylsilanes $D(H_3Si-R)$ are higher than mean $\bar{D}(Si-R)$ values calculated assuming that the values for $\bar{D}(C-H)$ and $\bar{D}(Si-H)$ determined for CH_4 and SiH_4 can be carried over to $RSiH_3$ compounds.[108]

Even though $\bar{D}(M-C)$ values for group IVb organometallic compounds increase steadily from lead to carbon,[106] $D(Me_3Si - Me)$ is only slightly larger than $D(Me_3Sn - Me)$ and $D(Ph_3Sn - Me)$. Surprisingly the metal-metal bond strength in hexamethyldisilane is equal or even weaker than the

tin-tin bond in ditin compounds.

Comparison of $D(Me_3Sn - R)$ and $D(Ph_3Sn - R)$ shows that the strengths of tin-alkyl, tin-phenyl and tin-tin bonds are very similar for the two sets of compounds. The tin-iodine bond however is far weaker in the triphenyltin iodide and this is difficult to explain. $p\pi - d\pi$ interaction between silicon and halogen atoms has been invoked to explain the variation of $D(Me_3Si - X)$ from X = Cl to X = I, this interaction being greatest for iodine [109]. If such interaction occurs for tin it may be that with Ph_3SnI the π - electron cloud of the phenyl groups interact with d - orbitals of tin and prevent any $p\pi - d\pi$ interaction between tin and iodine so producing a weaker Sn - I bond than found in $Me_3Sn - I$. Alternatively there may be steric interaction between iodine atoms and the bulky phenyl groups.

It is interesting to compare the ionization potentials of Group IVb $R_3M^{\bullet}$ radicals and Me_4M molecules.

	C	Si	Ge	Sn	Pb
Me_4M	10.29eV [102]	9.8 ±.15eV [111]	9.2 ±.2eV [111]	8.25 ±.15eV [111]	8.00 ±.4eV [111]
$Me_3M^{\bullet}$	7.42eV [102]	7.1eV [63]	-	6.54eV [64]	-
$Ph_3M^{\bullet}$	7.23eV [110]	-	-	6.00 ±.4eV	-

The ionization potentials decrease with both increase in atomic number of the central atom and with increasing phenyl content. This allows an approximate estimation of ionization potentials:- $I(Me_3Ge^{\bullet}) \sim 6.8eV.$, $I(Me_3Pb^{\bullet}) \sim 6.2eV.$, $I(Ph_3Si^{\bullet}) \sim 6.8eV.$, $I(Ph_3Ge^{\bullet}) \sim 6.4eV.$ and $I(Ph_3Pb^{\bullet}) \sim 5.6eV.$

Table 4.1.7.

Ionization potentials of dialkylberyllium compounds.

	Ionization Potential eV	Values of Individual Determinations eV	Standard Used	Ion Repeller Voltage	Source Temp. °C
Me_2Be	10.67 ± 0.07	10.64	Argon	0	217
		10.76	"	-0.2	193
		10.50	"	-0.2	187
		10.76	"	-0.2	183
		10.88	"	+0.2	183
		10.46	"	0	220
Et_2Be	9.46 ± 0.05	9.66	Krypton	-1	230
		9.50	"	0.4	213 - 230
		9.36	"	0.4	197 - 213
		9.48	"	-1	230
		9.38	"	0.4	197
		9.38	"	0.4	195
$(n\text{-}Pr)_2Be$	8.71 ± 0.06	8.52	Argon	5	180
		8.76	"	5	180
		8.60	"	5	180
		8.84	"	5	180
		8.84	"	5	180
$(i\text{-}Pr)_2Be$	8.80 ± 0.02	8.80	Krypton	-0.7	205
		8.88	"	-0.7	205
		8.80	"	-0.7	205
		8.80	"	-0.7	205
		8.72	Argon	-0.5	210
$(i\text{-}Bu)_2Be$	8.74 ± .05	8.69	Xenon	5.0	205
		8.71	"	5.0	205
		8.89	"	2.4	198 - 205
		8.89	"	5.0	205
		8.71	"	5.0	205
		8.57	"	5.0	205

These estimates and values for the ionization potentials of other radicals [102] ($I(CH_3^{\bullet}) = 9.86eV$, $I(C_2H_5^{\bullet}) = 8.80eV.$, $I(C_6H_5^{\bullet}) = 9.4eV.$ and $I(I^{\bullet}) = 10.45eV.$) verify the validity of the assumption made earlier that for the molecule Ph_3SnR, $I(Ph_3Sn^{\bullet}) < I(R^{\bullet})$.

4.1.3. Ionization Potentials and Bond Dissociation Energies of Dialkylberyllium Compounds.

i) Ionization Potentials of Dialkyberyllium Compounds.

Appearance potentials of $R_2Be^{+\bullet}$ ions produced in the spectra of dialkylberyllium compounds have been measured. At the high source temperature used during these measurements (c.f 200°C) electron deficient associated species such as R_4Be_2 are almost totally decomposed to monomer R_2Be. Thus it is most likely that $R_2Be^{+\bullet}$ ions are formed by ionization of R_2Be molecules rather than decomposition of ions containing more than one beryllium atom. The appearance potential of this ion is hence most probably a measure of the vertical ionization potential of unassociated berylliumdialkyls.

The ionization efficiency curves for these ions were very similar to those produced for the inert gases and in fig. 4 (p. 55) typical curves obtained are illustrated. Values of the ionization potentials obtained by the Warren method are given in table 4.1.7. As with measurements on organotin compounds the reproducibility of the determination is good.

The determination of $I(i\text{-}Bu_2Be)$ is probably high because the intensity of the ion $i\text{-}Bu_2Be^{+\bullet}$ was low so making the sensitivity of ion detection low.

Table 4.1.8.

Vertical ionization potentials of main group organometallic compounds.

	R	I.P.(eV.)	Ref
Group IIb			
R_2Zn	Me	8.86±.15	12
R_2Hg	Me	8.90±.2	111
		9.1 ±.1	112
	Et	8.5 ±.1	112
	i-Pr	7.6 ±.1	112
Group IIIb			
R_3B	Me	8.8 ±.2	113
	Et	9.0 ±.2	113
R_3Al	Me	9.09±.3	12
Group IVb			
$RSiH_3$	Et	10.18±.05	114
	i-Pr	9.85±.1	114
	t-Bu	9.5 ±.2	114
$RSiCl_3$	Me	11.36±.03	114
	Et	10.74±.04	114
	i-Pr	10.28±.1	114
$RSiMe_3$	H	9.8 ±.3	111
	Me	9.8 ±.15	111
		9.98±.03	60
	Et	9.70±.01	60
	i-Pr	9.50±.03	60
	t-Bu	9.34±.06	60
	$SiMe_3$	8.79±.08	60
	$OSiMe_3$	9.59±.04	60
$RSiMe_3$	OMe	9.79±.04	60
	F	10.55±.06	60
	Cl	10.58±.04	60
	Br	10.24±.02	60
	NEt_2	8.06±.02	60
R_4Ge	Me	9.2 ±.2	111
R_4Sn	Me	8.25±.15	111
	Et	8.1 ±.2	115
Et_2SnPh_2		8.1 ±.2	115
R_4Pb	Me	8.0 ±.2	111
Group Vb			
R_3As	Me	8.3 ±.1	116
	CF_3	11.0 ±.1	116
	H	10.6 ±.1	116
	Cl	11.7 +.1	116
$RAsH_2$	Me	9.7 ±.1	116
$RAsCl_2$	Me	10.4 ±.1	116
$RAs(CF_3)_2$	Me	10.5 ±.1	116
	H	10.9 ±.1	116
	Cl	11.0±.1	116
$RAsMe_2$	CF_3	9.2 ±.1	116
	H	9.0 ±.1	116
	Cl	9.9 ±.1	116
R_3Sb	Me	8.04±.16	12

The most apparent trend is the lowering of the ionization potential as the size of the attached group is increased, the largest drop being 1.21eV between I(Me_2Be) and I(Et_2Be). A similar variation occurs with the vertical ionization potentials of other organometallic compounds (see table 4.1.8.) of the main group.

The physical basis for such a result is the macroscopic view that in removing an electron from a molecule the resultant charged species can distribute the charge at least partially over its surface. Consequently the repulsive energy due to the net charge will be less as the surface increases. Another point of view is that any charged species will induce a dipole in any uncharged species and hence be attracted to it. Thus the work in removing an electron will be less if another species is in its neighbourhood.

The ionization potential of Me_2Be is higher than any other fully alkylated organometallic compound. If the dimethylcompounds of group IIa vary in the same way as those of IVb, this ionization potential will also be higher than those of Me_2Mg and Me_2Ca. Such a trend is however not apparent in group IIb where the ionization potentials of both Me_2Zn and Me_2Hg are about 8.9eV and in group IIIb the ionization potential of Me_3B is lower than that of Me_3Al.

ii) Appearance Potentials of Fragment Ions and Bond Dissociation Energies in Ions.

The appearance potential curves for $C_4H_9Be^+$ and $C_4H_8Be^{+\cdot}$ produced from di-iso-butylberyllium are shown in fig. 9. The curves produced are typical of those given by ions $C_nH_{2n+1}Be^+$ and $C_nH_{2n}Be^{+\cdot}$ produced from $(C_nH_{2n+1})_2Be$. It is immediately apparent that some "tailing"

Fig. 9

Ionization Efficiency Curves for $C_4H_9Be^+$ and $C_4H_8Be^+$ produced from $^tBu_2Be$.

Evaluation of Appearance Potential by Modified Warren Method.

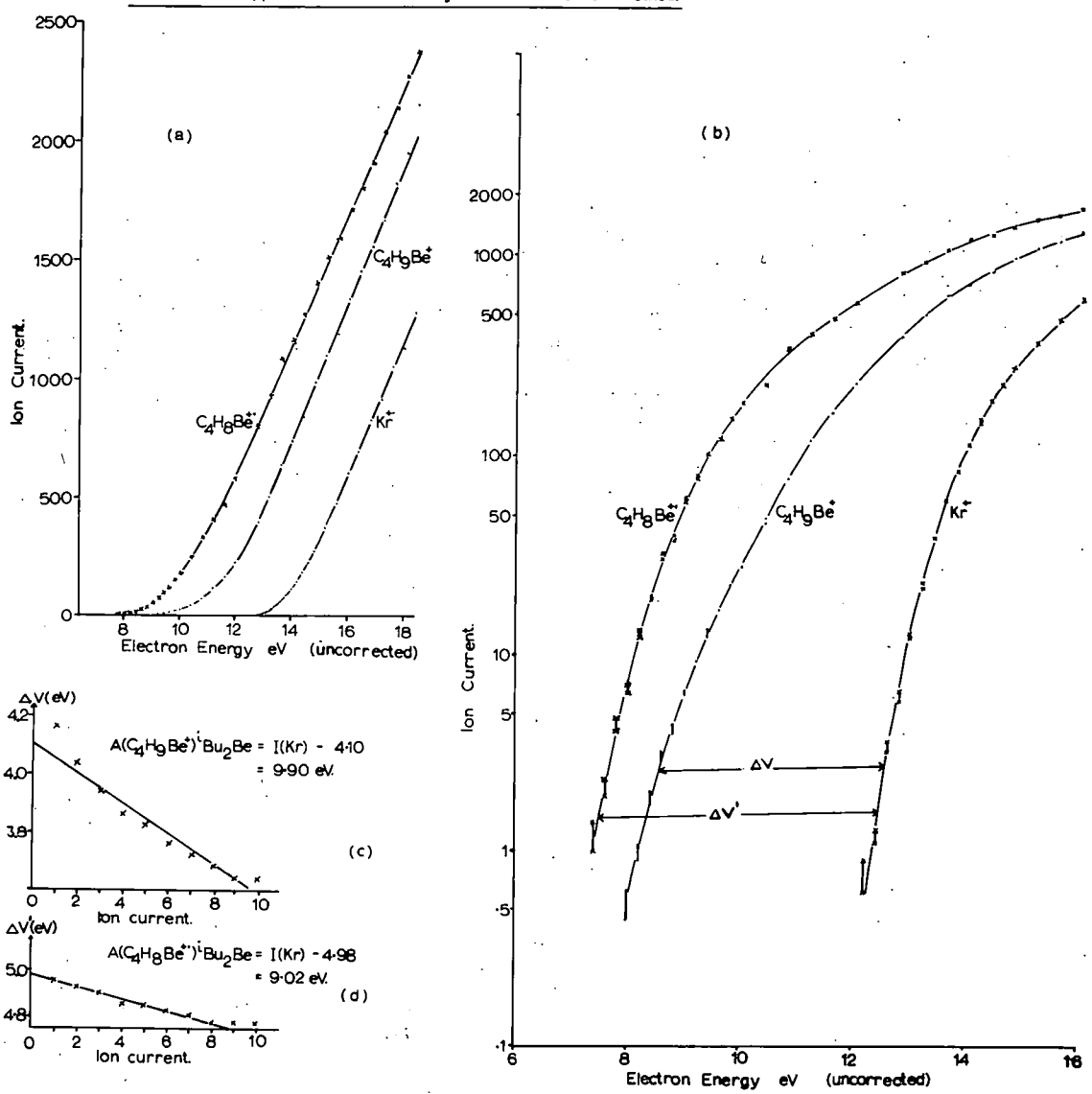

Table 4.1.9.

Appearance potentials of major ions in spectra of beryllium dialkyls.

	Appearance Potential eV.	Values of Individual Determinations eV.	Standard Used	Ion Repeller Voltage	Source Temp. °C.
Me_2Be					
$CH_2Be^{+\cdot}$	11.92 ± .05	11.92,11.96,12.02	Argon	-0.2	193
		12.01	Me_2Be	0	199
		11.70	Argon	0.1	210
CH_3Be^{+}	12.67 ± .02	12.70,12.70,12.68	Argon	-0.2	193
		12.71	Me_2Be	0	194
		12.58	Argon	0.1	210
Et_2Be					
$C_2H_4Be^{+\cdot}$	10.35 ± .03	10.42,10.26,10.26	Argon	1.4	220
		10.44,10.28,10.38	"	0.2	200
		10.42	"	0.5	225
$C_2H_5Be^{+}$	11.51 ± .05	11.50,11.76,11.34	Argon	1.4	220
		11.32,11.52,11.64	"	0.2	200
		11.52	"	0.5	225
$(i\text{-}Pr)_2Be$					
$C_3H_6Be^{+\cdot}$	9.60 ± .01	9.57,9.56,9.66	Argon	-0.5	205
		9.70,9.51	"	1.0	190
$C_3H_7Be^{+\cdot}$	10.65 ± .01	10.59,10.68,10.67	Argon	-0.5	205
		10.75,10.54	"	1.0	190
$(n\text{-}Pr)_2Be$					
$C_3H_6Be^{+\cdot}$	9.86 ± .05	9.92,9.98,9.76	Argon	+ 4.6	185
		9.72,9.92	"	+ 4.6	185
$C_3H_7Be^{+\cdot}$	10.81 ± .05	10.92,10.92,10.72	Argon	+ 4.6	185
		10.72,10.76	"	+ 4.6	185
$(i\text{-}Bu)_2Be$					
$C_4H_8Be^{+\cdot}$	9.14 ± .03	9.14,9.02	Krypton	5.0	205
		9.20	"	2.5	198
		9.16	"	3.0	205
		9.16	"	2.4	205
$C_4H_9Be^{+}$	10.00 ± .05	10.18,9.90	Krypton	5.0	205
		10.04	"	2.5	198
		9.94	"	3.0	205
		9.96	"	2.5	205

occurs with these fragment ions especially for the $C_nH_{2n+1}Be^+$ ion (i.e. in fig. 9, $C_4H_9Be^+$).

In table 4.1.9. the values of the appearance potentials as determined by the Warren method are given. Again the reproducibility of measurement was good and the standard error of the mean of estimations never exceeded ± 0.05eV. In calculating bond-dissociation energies an error of twice the maximum observed standard error of the mean has been used (± 0.1eV).

If the ion RBe^+ from R_2Be (R = alkyl) is formed by the simple dissociative process:-

$$R_2Be + e \longrightarrow RBe^+ + R\cdot + 2e$$

involving no excess energy then

$$D(RBe^+-R) = A(RBe^+)R_2Be - I(R_2Be) \qquad 4.3$$

The excess energy term is most likely to be zero if $I(RBe\cdot) < I(R\cdot)$. The low abundance of R^+ in comparison to RBe^+ at low source temperatures (when hydrocarbon ions are less likely to be formed by thermal decomposition of beryllium dialkyls prior to ionization) is consistent with this. The occurrence of "tailing" of the ionization efficiency curves is however not consistent with a negligable excess energy term and so all derived bond dissociation energies must be regarded as upper limits.

Using equation 4.3 bond dissociation energies shown in table 4.1.10 have been derived.

Table 4.1.10.

Bond dissociation energies in dialkylberyllium molecular ions.

R	$D(RBe^{+}-R)$ Kcal. mole.$^{-1}$ *(error = ± 3.2 Kcal. mole.$^{-1}$)
Me	46.1
Et	47.3
i-Pr	48.7
n-Pr	42.7
i-Bu	29.1

* error calculated assuming a tolerance of ± 0.1eV in the appearance potential measurements.

The low value obtained for $D(i\text{-}BuBe^{+}-i\text{-}Bu)$ probably results from the estimation of $I(i\text{-}Bu_2Be)$ being too high (see p. 89)

Beryllium-carbon bond strengths in molecular ions of the dialkyls are much stronger than the tin-carbon bond strengths in $Et_4Sn^{+\bullet}$ or $Ph_2SnEt_2^{+\bullet}$ which were of the order of 10 Kcal. mole.$^{-1}$. Other metal-carbon bond strengths in molecular ions may be evaluated from appearance potentials published in the literature assuming the decomposition

$$R_nM + e \longrightarrow R_{n-1}M^{+} + R\bullet + 2e$$

to occur with no excess energy release. Values are given in table 4.1.11.

The Be-C bond dissociation energy is most similar to that for zinc-methyl in $Me_2Zn^{+\bullet}$. For dimethyl zinc the metal-carbon bond in the molecule is almost the same as in the ion indicating the removal of an essentially non-bonding electron upon ionization i.e. $D(MeZn-Me)$[106]

Table 4.1.11.

Bond dissociation energies in molecular ions (Kcal.mole.$^{-1}$)

$D(MeZn^{+}—Me)$[12]	53		
$D(RHg^{+}—R)$	32 (Me)[111,112]	27 (Et)[112]	35 (i-Pr)[112]
$D(R_2B^{+}—R)$[117]	35 (Me)	14 (Et)	
$D(Me_2Al^{+}—Me)$[12]	23		
$D(Me_2Sb^{+}—Me)$[12]	58		

= 47.2 ± 1 Kcal. mole.$^{-1}$ With dimethylmercury however the Hg-C bond strength in the ion is lower than in the molecule and in this case the electron comes from a bonding orbital i.e. $D(MeHg—Me)$[106] = 51.5 ± 2 Kcal. mole.$^{-1}$; $D(EtHg—Et)$[106] = 42.5 ± 2 Kcal. mole.$^{-1}$.

With beryllium dialkyls it is difficult to envisage removal of anything but a bonding-electron upon ionization in which case the beryllium carbon dissociation energy in the molecule D(RBe—R) will be greater then ∿ 45 Kcal. mole.$^{-1}$. It would be interesting to compare this value with a mean beryllium-carbon bond dissociation energy to see whether the beryllium dialkyls resemble dimethylmercury in which $D(MeHg—Me)$ = 51.5 ± 2 Kcal. mole.$^{-1}$ and $D(Hg—Me)$ = 6.9 ± 3 Kcal. mole.$^{-1}$[106] or dimethylzinc where the difference between the two dissociation energies is much less $D(MeZn—Me)$ = 47.2 ± 1 Kcal. mole.$^{-1}$ and $D(Zn—Me)$ = 36.8 ± 3 Kcal. mole.$^{-1}$[106]. Unfortunately however no calorimetric data is available for beryllium dialkyls.

A metastable peak present for berylliumdialkyls shows that the $C_nH_{2n}Be^{+\cdot}$ ion is formed by the process

$$e + (C_nH_{2n+1})_2Be \rightarrow C_2H_{2n}Be^{+\cdot} + C_nH_{2n+2} + 2e$$

Table 4.1.12.

Enthalpy change (ΔH) for reaction:

$$C_nH_{2n+1}Be^+ + C_nH_{2n+1}\cdot \longrightarrow C_nH_{2n}Be^{+\cdot} + C_nH_{2n+2}$$

					ΔH(Kcal. mole.$^{-1}$) error ± 3.2 Kcal. mole.$^{-1}$
CH_3Be^+	+ $CH_3\cdot$	$\longrightarrow$	$CH_2Be^{+\cdot}$	+ CH_4	-17.30
$C_2H_5Be^+$	+ $C_2H_5\cdot$	$\longrightarrow$	$C_2H_4Be^{+\cdot}$	+ C_2H_6	-26.8
n-$C_3H_7Be^+$	+ n-$C_3H_7\cdot$	$\longrightarrow$	$C_3H_6Be^{+\cdot}$	+ C_3H_8	-21.9
i-$C_3H_7Be^+$	+ i-$C_3H_7\cdot$	$\longrightarrow$	$C_3H_6Be^{+\cdot}$	+ C_3H_8	-24.2
i-$C_4H_9Be^+$	+ $C_4H_9\cdot$	$\longrightarrow$	$C_4H_8Be^{+\cdot}$	+ C_4H_{10}	-19.8

error calculated assumed a tolerance of ± .1eV for appearance potential measurements.

Table 4.1.13.

Bond dissociation energies D($BeC_nH_{2n}^+$——H) (Kcal. mole.$^{-1}$)

D($BeCH_2^+$—H)	86.7 ± 3.4
D($BeC_2H_4^+$—H)	71.5 ± 3.4
D(Be-i-$C_3H_6^+$—H)	76.0 ± 3.8
D(Be-n-$C_3H_6^+$—H)	70.7 ± 3.4
D(Be-i-$C_4H_8^+$—H)	77.7 ± 3.8

Hence

$$A(C_nH_{2n}Be^{+\cdot}) = \Delta H_f^o(C_nH_{2n}Be^{+\cdot}) + \Delta H_f^o(C_nH_{2n+2}) - \Delta H_f^o (C_nH_{2n+1})_2Be$$

and $$A(C_nH_{2n+1}Be^{+}) = \Delta H_f^o(C_nH_{2n+1}Be^{+}) + \Delta H_f^o(C_nH_{2n+1}\cdot) - \Delta H_f^o (C_nH_{2n+1})_2Be$$

by subtraction

$$\Delta H = A(C_nH_{2n}Be^{+\cdot}) - A(C_nH_{2n+1}Be^{+}) = \Delta H_f^o(C_nH_{2n}Be^{+\cdot}) - \Delta H_f^o(C_nH_{2n+1}Be^{+}) + \Delta H_f^o(C_nH_{2n+2}) - \Delta H_f^o(C_nH_{2n+1}\cdot)$$

Thus ΔH is the enthalpy change for the reaction

$$C_nH_{2n+1}Be^{+} + C_nH_{2n+1}\cdot \longrightarrow C_nH_{2n}Be^{+\cdot} + C_nH_{2n+2} \quad \Delta H \qquad 4.4.$$

These values of ΔH are illustrated in table 4.1.12. The reaction 4.4. ... is exothermic in all cases to the extent of -22 Kcal. mole.$^{-1}$.

From eqn. 4.4. it also follows:

$$\Delta H_f^o(C_nH_{2n}Be^{+\cdot}) - \Delta H_f^o(C_nH_{2n+1}Be^{+}) = \Delta H - \Delta H_f^o(C_nH_{2n+2}) + \Delta H_f^o(C_nH_{2n+1}\cdot)$$

and so the dissociation energy

$$C_nH_{2n+1}Be^{+} \longrightarrow C_nH_{2n}Be^{+\cdot} + H\cdot$$

may be found

$$D(BeC_nH_{2n}^{+}\text{——}H) = \Delta H - \Delta H_f^o(C_nH_{2n+2}) + \Delta H_f^o(C_nH_{2n+1}\cdot) + \Delta H_f^o(H\cdot)$$

These dissociation energies are given in table 4.1.13. In this calculation the following heats of formation were used (expressed in Kcal. mole.$^{-1}$):

$\Delta H_f^o(CH_3\cdot)^{104} = 34 \pm 1$; $\Delta H_f^o(Et\cdot)^{104} = 26 \pm 1$; $\Delta H_f^o(n\text{-}Pr\cdot)^{104} = 21 \pm 2$;

$\Delta H_f^o(i\text{-}Pr\cdot)^{104} = 17.6 \pm 1$; $\Delta H_f^o(i\text{-}Bu\cdot)^{104} = 14 \pm 2$; $\Delta H_f^o(CH_4)^{118} = 17.9$;

$\Delta H_f^o(C_2H_6)^{118} = -20.2$; $\Delta H_f^o(C_3H_8)^{118} = 24.8$; $\Delta H_f^o(\text{n-butane})^{118} = -29.8$;

$\Delta H_f^o(\text{2 methyl propane})^{118} = -31.4$.

Excepting for $D(BeCH_2^{+}\text{——}H)$ these ion dissociation energies are very similar at around 74 Kcal. mole.$^{-1}$. This exception for the CH_3Be^{+} ion can be explained if some stabilising rearrangement is assumed for

$C_nH_{2n}Be^{+\cdot}$ ions containing more than one carbon atom. Thus the structure of the ethyl compound may be 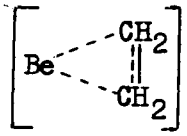 rather than 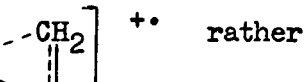

(where each dotted line represents a bond containing only one electron)

and similarly $C_3H_6Be^{+\cdot}$ ions may be 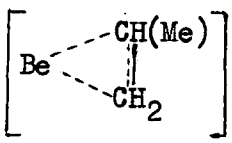 . Alternatively

the structure 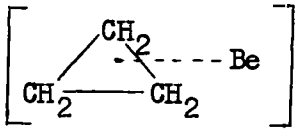 may be proposed which bears similarities to the cationated cyclopropane rings which have been postulated to explain the breakdown [119] of t-butyl-benzene - α - ^{13}C and the structure [120] of $C_3H_7^+$ ions which are abundant in so many hydrocarbon spectra. Similar structures may be drawn for $C_4H_8Be^{+\cdot}$ ions;

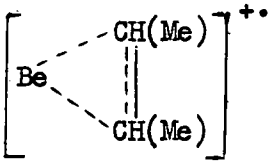 or 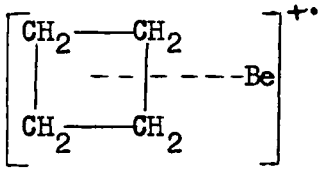

With the methyl compound it may not be possible for $CH_2Be^{+\cdot}$ to attain a ring structure and hence the hydrogen atom in CH_3Be^+ is more tightly bound.

4.2. Mass Spectra of Organocompounds of Silicon, Germanium, Tin and Lead.

4.2.1. Organo-stannanes.

Since no data was initially available on the electron impact induced fragmentation of organo-tin compounds other than tetramethyltin[30,111], a mass spectroscopic study of the following tin-compounds was undertaken: Ph_nSnEt_{4-n} (n=0,1,2,3,4), $Ph_3Sn\,R$ (R = SPh, CH_2CH_2Ph), spiro - $(CH_2)_4\rangle Sn\langle(CH_2)_4$, Ph_3SnX (X = F,Cl,Br,I), R_6Sn_2 (R = Et, Ph). The abundances of ions (calculated as described in the calculation of results section) are given in tables 4.2.1., 4.2.2., and 4.2.3.

An electron energy of 70eV was mainly used to obtain spectra but for some compounds (given in table 4.2.1.) 20 volt electrons were also used. Other ionizing conditions are given in chapter 2.2 of the Experimental. (p.45).

The assignment of metastable peaks allows the decomposition modes of organotin compounds to be classified and these are outlined below. Throughout m^* refers to the observed mass of a metastable peak. The shapes of metastable peaks for processes in which a polyisotopic element is eliminated has already been commented upon. (chapter 3.3.). The experimental values quoted for such peaks are the mass spread of the metastable peaks and its mass at maximum intensity. In all other cases m^* refers to the most abundant isotope or combination of isotopes. The agreement between observed and calculated values of m^* was always better than $\pm$ .1 a.m.u.

Decomposition Modes of Organostannanes at 70eV.

Metal-containing ions are generally the most abundant, accounting

Table 4.2.1.

Ion abundance relative to total tin-containing ions

$SnPh_4$ Ion+	ev 70	ev 20
$SnPh_4$	0·11	0·17
$SnPh_3$	42·26	53·78
$SnPh_2$	10·74	25·22
SnPh	17·55	5·84
SnH	0·36	0·1
Sn	18·61	13·06
$SnC_{24}H_{18}$	0·03	0·03
$SnC_{12}H_9$	1·53	1·40
$SnC_{12}H_8$	0·10	—
SnC_6H_5	0·14	—
SnC_6H_4	0·00	0·50
SnC_6H_3	0·41	—
SnC_6H	0·17	—
SnC_6H	1·09	—

$SnPh_3Et$ Ion+	ev 70	ev 20
$SnPh_3Et$	0·05	0·05
$SnPh_3$	62·27	89·99
$SnPh_2Et$	0·47	1·02
$SnPh_2H$	1·26	1·06
$SnPh_2$	0·18	0·32
SnPh	17·67	4·20
SnH	0·74	0·04
Sn	13·35	2·66
$SnPh_2Me$	0·09	0·08
$SnC_{12}H_9$	0·61	0·27
$SnC_{12}H_7$	0·10	—
SnC_6H_5	0·16	—
SnC_6H_4	0·73	0·40
SnC_6H_3	0·60	—
SnC_6H	0·24	—
SnC_6H	1·48	—

$SnPh_2Et_2$ Ion+	ev 70	ev 20
$SnPh_2Et_2$	1·35	1·38
$SnPh_2Et$	50·52	68·97
$SnPhEt_2$	1·14	0·94
$SnPh_2H$	14·19	18·26
SnPh(Et)H	0·53	0·94
$SnPhH_2$	0·89	0·89
SnPh	16·46	5·33
SnEt	0·23	0·20
SnH	1·07	0·15
Sn	9·61	2·21
$SnC_{12}H_9$	0·65	0·30
$SnC_{12}H_7$	0·18	—
SnC_6H_{10}	0·09	—
SnC_6H_5	0·14	—
SnC_7H_9	0·09	0·20
SnC_6H_4	0·58	0·32
SnC_6H_3	0·51	—
SnC_6H	0·18	—
SnC_6H	1·59	—

$SnPhEt_3$ Ion+	ev 70	ev 20
$SnPhEt_3$	0·26	0·50
$SnPhEt_2$	30·37	53·17
$SnEt_3$	0·62	<0·1
SnPh(Et)H	13·77	24·07
$SnPhH_2$	10·76	12·31
$SnEt_2H$	0·35	<0·1
$SnEtH_2$	0·20	<0·1
SnPh	19·59	9·89
SnEt	3·15	<0·1
SnH	5·20	—
Sn	9·83	—
SnC_6H_{10}	1·26	<0·1
SnC_6H_9	0·11	<0·1
SnC_6H_3	0·89	—
SnC_6H	0·33	—
SnC_6H	3·31	—

$SnEt_4$ Ion+	ev 70	ev 20
$SnEt_4$	0·97	2·76
$SnEt_3^+$	26·18	48·29
$SnEt_3H^+$	24·16	32·68
$SnEtH_3$	17·24	14·77
SnH_3	1·31	0·42
SnEt	11·93	—
SnH	12·13	0·27
Sn	4·89	—
$SnEt_3Me$	0·12	0·64
SnC_2H_5	0·16	—
$SnCH_3$	0·47	—
$SnCH_3$	0·46	0·27

$SnPh_3(CH_2CH_2Ph)$ Ion+	70 ev
$SnPh_3(CH_2CH_2Ph)$	0·01
$SnPh_3CH_2Ph$	0·74
$SnPh_3$	0·01
$SnPh_2(CH_2CH_2Ph)$	0·01
$SnPh_2(CH_2Ph)$	0·23
$SnPh_2$	61·60
$SnPh_2H$	0·13
$SnPh_2$	0·18
SnPh	18·85
SnH	0·49
Sn	15·35
$SnC_{12}H_9$	0·52
$SnC_{12}H_7$	0·07
SnC_6H_5	0·11
SnC_6H_3	0·40
SnC_6H	0·18
SnC_6H	1·12

Sn_2Ph_6 Ion+	70 ev
Sn_2Ph_6	6·51
Sn_2Ph_5	1·48
Sn_2Ph_4	0·68
Sn_2Ph_3	0·05
$SnPh_3$	43·26
$SnPh_2$	1·23
SnPh	24·59
SnH	0·38
Sn	18·42
$SnC_{24}H_{18}$	0·42
$SnC_{12}H_9$	0·88
$SnC_{12}H_7$	0·10
SnC_6H_5	0·14
SnC_6H_4	0·80
SnC_6H_3	0·35
SnC_6H	0·07
SnC_6H	0·59

Sn_2Et_6 Ion+	70 ev 200°*	70 ev 100°*
Sn_2Et_6	1·94	4·48
Sn_2Et_5	19·74	15·42
Sn_2Et_4H	10·00	12·33
$Sn_2Et_3H_2$	12·54	10·65
$Sn_2Et_2H_2$	3·86	3·59
Sn_2Et_4H	2·78	3·13
Sn_2EtH_4	0·95	0·11
Sn_2EtH_3	5·21	5·40
Sn_2EtH_2	2·88	3·71
Sn_2H_3	0·38	0·39
Sn_2H_2	2·63	2·74
Sn_2H	2·31	2·41
Sn_2	3·77	3·92
$SnEt_3$	9·36	8·01
$SnEt_2H$	8·01	7·23
$SnEtH_2$	3·94	4·87
SnH_3	0·18	0·25
SnEt	6·22	7·32
SnH	1·82	2·38
Sn	0·73	0·95
$SnEt_3Me$	0·24	0·21
SnC_2H_5	0·17	0·16
$SnCH_3$	0·20	0·25
$SnCH_3$	0·04	0·04

* Temperature of ionisation chamber.

spiro$[CH_2]_4$>Sn<$[CH_2]_4$ Ion+	70 ev
SnC_6H_{10}	10·19
SnC_6H_{12}	8·04
SnC_6H_9	20·80
SnC_6H_6	35·29
SnH_3	0·73
SnH	7·46
Sn	16·59

Table 4.2.2.

Abundances of ions in triphenyl tin halides at 70 ev relative to total tin-containing ions

Ion +	F	Cl	Br	I
$SnPh_3X$	0·81	1·22	1·40	0·05
$SnPh_2X$	44·44	46·96	46·28	3·70
$SnPh_3$	3·59	1·51	5·16	52·63
$SnPh_2$	0·50	0·19	0·13	0·20
SnPhX	1·48	2·10	3·90	0·08
SnPh	12·08	10·12	4·75	19·89
SnX	25·03	27·61	26·22	5·55
SnH	0·35	0·37	0·47	0·49
Sn	5·13	5·10	6·59	11·94
$SnPh_2C_6H_4X$	0·23	0·63	0·10	—
$SnPh_2C_6H_4$	2·12	0·77	1·09	1·61
$SnPhC_6H_4$	1·30	0·52	1·15	0·54
$SnC_{10}H_7$	0·11	0·05	0·15	0·05
SnC_6H_5	0·10	0·09	0·07	0·09
SnC_6H_4	0·57	0·60	0·26	0·97
SnC_4H_3	0·27	0·35	0·36	0·43
SnC_4H	0·25	0·15	0·34	0·28
SnC_2H	1·02	1·06	1·36	1·45

Table 4.2.3.

Ion abundances * in thiophenyltriphenyltin at 70eV.

Ion$^+$	
$Ph_3SnSPh^\bullet$	3.56
Ph_2SnSPh	1.21
Ph_3SnS	
Ph_3Sn	47.24
$Ph_2Sn^\bullet$	0.62
$PhSnSPh^\bullet$	1.99
$Ph_2SnS^\bullet$	
PhSSn	3.63
PhSnS	
PhSn	22.16
HSn	0.54
$Sn^\bullet$	12.97
$C_{12}H_9Sn$	0.56
$C_{10}H_7Sn$	0.77
C_8H_5Sn	0.09
C_6H_4Sn	1.06
C_4H_3Sn	0.32
C_4HSn	0.36
C_2HSn	1.11

* Expressed as % of total tin-containing ions.

for about 95% of the total ion current. The electronegativity of carbon is greater than that of tin [121] and it is apparent that the charge is most likely to remain on the metal-containing fragment formed when an ion decomposes. The work confirms the influence of the odd bonding - or even bonding-electron character of an ion on its dissociation reactions [5] and in all cases the even-electron ions R_3M^+ and RM^+ are the most abundant. Parent ions, which are of low abundance decompose mainly by elimination of odd-electron fragments and even-electron ions tend to maintain themselves even-electron by eliminating an even-electron molecule.

i) Radical Elimination by Bond Cleavage.

This is a dominant process for odd-electron ions: Thus parent ions eliminate a group attached to the metal producing an even-electron ion in high abundance.

$Ph_3SnX^{+\bullet} \longrightarrow Ph_2SnX^+$	+	$Ph^\bullet$	m^*	232	X = F
			m^*	247.4	X = Cl
			m^*	291.7	X = Br
			m^*	336.4	X = I
$Ph_3SnI^{+\bullet} \longrightarrow Ph_3Sn^+$	+	$I^\bullet$	m^*	257.7	
$Et_4Sn^{+\bullet} \longrightarrow Et_3Sn^+$	+	$Et^\bullet$	m^*	181.6	
$Et_6Sn_2^{+\bullet} \longrightarrow Et_5Sn_2^+$	+	$Et^\bullet$	m^*	358.0	
$Ph_6Sn_2^{+\bullet} \longrightarrow Ph_5Sn_2^+$	+	$Ph^\bullet$	m^*	556.4	
$\searrow Ph_3Sn^+$	+	$Ph_3Sn^\bullet$	m^*	173.5 - 176 max.,= 175	
$Ph_3SnSPh^{+\bullet} \longrightarrow Ph_3Sn^+$	+	$PhS^\bullet$	m^*	267.8	

With unsymmetrical compounds different groups may be lost from the parent ion producing different three co-ordinate ions. The mixed ethylphenylstannanes produce two R_3Sn^+ ions the more abundant being

Table 4.2.4.

Abundances of $SnR_4^{+\bullet}$ and SnR_3^+ ions relative to total tin-containing ions for ethyl-phenyl tin compounds at 70 ev

Compound	$SnR_4^{+\bullet}$	SnR_3^+				
		$SnPh_3^+$	$SnPh_2Et^+$	$SnPhEt_2^+$	$SnEt_3^+$	$SnPh_2(CH_2{\cdot}CH_2Ph)^+$
$SnPh_4$	0·11	42·26				
$SnPh_3Et$	0·05	62·27	0·47			
$SnPh_2Et_2$	1·35		50·52	1·14		
$SnPhEt_3$	0·26			30·37	0·62	
$SnEt_4$	0·97				26·18	
$SnPh_3(CH_2{\cdot}CH_2Ph)$	0·01	61·60				0·01

Table 4.2.5.

Abundances of SnR_3^+ ions making allowances for subsequent decompositions of the SnR_3^+ ions. Abundances relative to total tin-containing ions

Compound	SnR_3^+			
	$SnPh_3$	$SnPh_2Et^+$	$SnPhEt_2^+$	$SnEt_3^+$
$SnPh_4$	83·15 [a]			
$SnPh_3Et$	64·14 [b]	1·73		
$SnPh_2Et_2$		94·61	4·04	
$SnPhEt_3$			90·22 [c]	1·17
$SnEt_4$				99·03

[a] Abundance of $SnPh_3^{+\bullet}$ ignored since process $SnPh_4^{+\bullet} \longrightarrow SnPh_3^{+\bullet} + Ph_2$ occurs. [b] Abundance of $SnPh^+$ and all derivative ions ignored since the decompositions $SnPh_2H^+ \longrightarrow SnPh^+ + C_6H_6$ and $SnPh_3^+ \longrightarrow SnPh^+ + Ph_2$ occur. Thus both $SnPh_2Et^+$ and $SnPh_3^+$ are sources of $SnPh^+$. [c] $SnEt^+$ and SnH^+ ignored since $SnPhEt_2^+$ and $SnEt_3^+$ are both sources of these ions.

Table 4.2.6.

Dependance of hydride ion formation on the number of Sn–Et bonds present. Abundances (%) relative to total tin-containing ions

	Sn^+	$(SnH^+ + R_2SnH^+)$ *	$RSnH_2^+$	SnH_3^+
$SnPh_4$	18·61	0·36		
$SnPh_3Et$	13·35	2·00		
$SnPh_2Et_2$	9·61	16·79	0·89	
$SnPhEt_3$	9·83	19·92	10·96	
$SnEt_4$	4·89	36·29	17·24	1·31

* $RSnH^+$ and R_3SnH^+ absent.

that containing the greater proportion of phenyl groups. (table 4.2.4.) This could be due to the ease with which further decompositions of ions containing Sn - Et groups occurs, but in table 4.2.5. an attempt has been made to allow for the subsequent fragmentation of R_3Sn^+ ions, using the decomposition diagrams fig. 10. (p.118), thereby giving an estimate of the ratio of the two $Ph_nSnEt_{3-n}^+$ ions initially formed from the ethylphenyl stannanes.

Even when these allowances are made, the ion containing the greater proportion of phenyl groups is always the more abundant. The relative probabilities of the dissociative processes available depends on the relative bond strengths in the molecular ion and also on the relative stabilities of the radicals and ions produced. Appearance potential measurements discussed earlier were not sensitive enough to distinguish between $D(Ph_2EtSn^+ - Ph)$ and $D(PhEt_2Sn^+ - Ph)$ and the high abundance of the R_3Sn^+ ion containing the greater proportion of phenyl groups may not be due entirely to bond strengths but also to more effective delocalisation of positive charge in the R_3Sn^+ ion having the greater proportion of phenyl groups.

In the neutral molecules, however, the indications are that a tin-phenyl bond is stronger than a tin-ethyl although in some cases the difference is small.

$D(Ph_3Sn - Ph) - D(Ph_3Sn - Et) = 23.1 \pm 3.2$ Kcal. mole.$^{-1}$

$D(Ph_2EtSn - Ph) - D(Ph_2EtSn - Et) = 10.4 \pm 3.2$ "

$D(PhEt_2Sn - Ph) - D(PhEt_2Sn - Et) = 1.2 \pm 3.2$ "

$D(Me_3Sn - Ph) - D(Me_3Sn - Et)$[64] $= 13 \pm 6$ "

Thus it appears that the radical most readily lost is that which would be

expected to be most weakly bonded to tin in the neutral molecule. With hexaphenyldistannane less than 10% of the total ion current is carried by ions containing a tin-tin bond. Appearance potential measurements given earlier showed that the Sn - Sn bond in hexaphenyldistannane was some 20.1 Kcal. mole.$^{-1}$ weaker than the tin-phenyl bond in tetraphenyltin. Also in the spectra of ethylmethylstannanes [122] the major ion is produced by ethyl loss and known bond dissociation energies give $D(Me_3Sn - Me) > D(Me_3Sn - Et)$.[64]

Loss of R· from an $R_2Sn^{+\cdot}$ ion has never been observed. $PhSn^+$ is the only even-electron ion which shows a bond-cleavage process.

$$PhSn^+ \longrightarrow Sn^{+\cdot} + Ph\cdot \qquad m^* = 73.1$$

The odd electron metal ion, $Sn^{+\cdot}$, is of high abundance for all the tin compounds studied.

Ions formed by cleavage of C - C or C - H bonds are always of very low abundance. This probably reflects the weakness of tin-carbon bond strengths relative to C - C or C - H. Loss of a hydrogen atom is observed only for tetraphenyltin and the triphenyltin halides. In each case low abundance ions are produced, e.g.

$$Ph_4Sn^{+\cdot} \longrightarrow C_{24}H_{19}Sn^+ + H\cdot$$

Major Rearrangement Decompositions.

ii) Alkene Elimination. $>Sn^+ - Et \longrightarrow Sn^+ - H + C_2H_4$

This process which is probably general for even-electron ions containing the grouping $R_2CH\cdot CH_2M$, has been observed with tetraethyl - and ethylphenyltin compounds. The percentage ion-current carried by hydride ions increases with the number of Sn - Et bonds (table 4.2.6. p. 104) and with the strength of the metal-hydrogen bond (table 4.2.7.)

Table 4.2.7.

Hydride ion abundances relative to total tin-containing ions in MEt_4 at 70eV.

	M^+	MH^+ and Et_2MH^+	$EtMH_2^+$	H_3M^+	Total
Et_4Ge^{123}	1.8	41.30	15.40	2.4	59.1
Et_4Sn	4.89	36.29	17.24	1.31	53.53
Et_4Pb*	10.33	11.95	0.79	-	12.74

* See table 4.2.10. p. 123.

Metastable confirmed decompositions of this type are

Et_4Sn	$Et_3Sn^+ \longrightarrow Et_2SnH^+ + C_2H_4$	m^*	154.8
Et_4Sn	$Et_2SnH^+ \longrightarrow EtSnH_2^+ + C_2H_4$	m^*	127.4
$PhSnEt_3$	$Et_2SnPh^+ \longrightarrow EtSn(H)Ph^+ + C_2H_4$	m^*	202
$PhSnEt_3$	$EtSn(H)Ph^+ \longrightarrow H_2SnPh^+ + C_2H_4$	m^*	174.5
Ph_2SnEt_2	$EtSnPh_2^+ \longrightarrow Ph_2SnH^+ + C_2H_4$	m^*	249.5

It seems probable that transfer of a hydrogen from a β - carbon atom is involved since ethylene elimination readily occurs from ions containing only one Sn - Et bond.

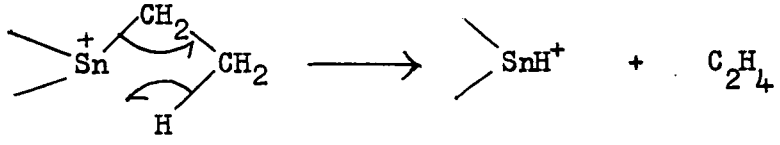

(here fishhooks ⌒ represent movement of one electron)

In the spectrum of tetraethyltin the presence of H_3Sn^+ can be explained by ethylene loss from H_2SnEt^+ which is of high abundance.

Elimination of ethylene from odd-electron molecular ions has never been observed and by the above mechanism would require a pentaco-ordinate transition intermediate which may be energetically

unfavourable compared with loss of an R radical. With hexaethyldistannane, loss of ethylene from the parent ion is not observed but it must occur from tetraco-ordinate tin at some stage although this may not involve a pentaco-ordinate intermediate.

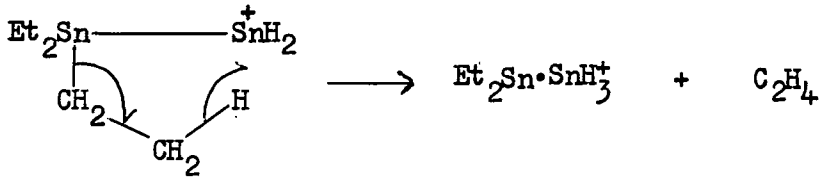

$$Et_2Sn\cdot SnH_3^+ + C_2H_4$$

Et_6Sn_2	$Et_5Sn_2^+$	$\longrightarrow$	$Et_4Sn_2H^+$	+ C_2H_4	m^*	331
Et_6Sn_2	$Et_4Sn_2H^+$	$\longrightarrow$	$Et_3Sn_2H_2^+$	+ C_2H_4	m^*	303.2
Et_6Sn_2	$Et_3Sn_2H_2^+$	$\longrightarrow$	$Et_2Sn_2H_3^+$	+ C_2H_4	m^*	275.4

Labelling studies would provide valuable information concerning the above mechanisms.

Alkene elimination from other alkyltin compounds has also been observed.[124] The decompositions

$$R_3Sn^+ \longrightarrow R_2SnH^+ \longrightarrow RSnH_2^+$$

give metastable peaks when R = n-Pr, n-Bu and $-CH{=}CH_2$. Whether alkene elimination from alkyl groups is a specific rearrangement is a question which can only be satisfied by deuterium labelling.

iii) Elimination of RR' from $-SnR'R^+$.

This process has been observed when R and R' are H, Ph, halogen or vinyl. Metastable peaks corresponding to loss of $C_6H_5\cdot C_2H_5$ and $C_2H_5\cdot C_2H_5$ have been searched for but none found.

Tetraphenyltin, hexaphenyldistannane and tetravinyltin show[124] this process from odd-electron ions.

$$Ph_4Sn^{+\cdot} \longrightarrow Ph_2Sn^{+\cdot} + Ph_2 \qquad m^* \; 175.4$$

$$Ph_2Sn^{+\cdot} \longrightarrow Sn^{+\cdot} + Ph_2 \qquad m^* \; 52.6$$

$$Ph_6Sn_2^{+\cdot} \longrightarrow Ph_4Sn_2^{+\cdot} + Ph_2 \qquad m^* \; 427.8$$

$$(CH_2{:}CH)_2Sn^{+\cdot} \longrightarrow Sn^{+\cdot} + C_4H_6 \qquad \text{ref. } 124$$

The elimination of biphenyl from $Ph_6Sn_2^{+\cdot}$ leads to a product ion which may be formulated as $Ph_3SnSnPh^{+\cdot}$ or $Ph_2SnSnPh_2^{+\cdot}$.

$\triangle H_f^o(Sn^{+\cdot})$ calculated from the appearance potential[124] of $Sn^{+\cdot}$ in the spectrum of tetraphenyltin agrees with biphenyl elimination.

$$Ph_4Sn + e \longrightarrow Sn^{+\cdot} + 2Ph_2 + 2e$$

Since the abundance of $Ph_2Sn^{+\cdot}$ is only just detectable for a variety of triphenyltin compounds which show a strong Ph_3Sn^+ ion it may be inferred that biphenyl loss from $Ph_4Sn^{+\cdot}$ is the major process leading to $Ph_2Sn^{+\cdot}$, and that loss of a phenyl radical from Ph_3Sn^+ occurs to only a minor extent. It also follows that reactions such as

$$Ph_3SnEt^{+\cdot} \longrightarrow Ph_2Sn^{+\cdot} + Ph{\cdot}Et$$

do not occur to any significant extent.

Elimination of RR' molecules from even-electron ions $X\text{-}SnR'R^+$ is a major process. Thus for all triphenyltin compounds examined the decomposition

$$Ph_3Sn^+ \longrightarrow PhSn^+ + Ph_2 \qquad m^* = 110.6$$

is observed. Diphenyltin halide ions eliminate both biphenyl and halogenobenzene

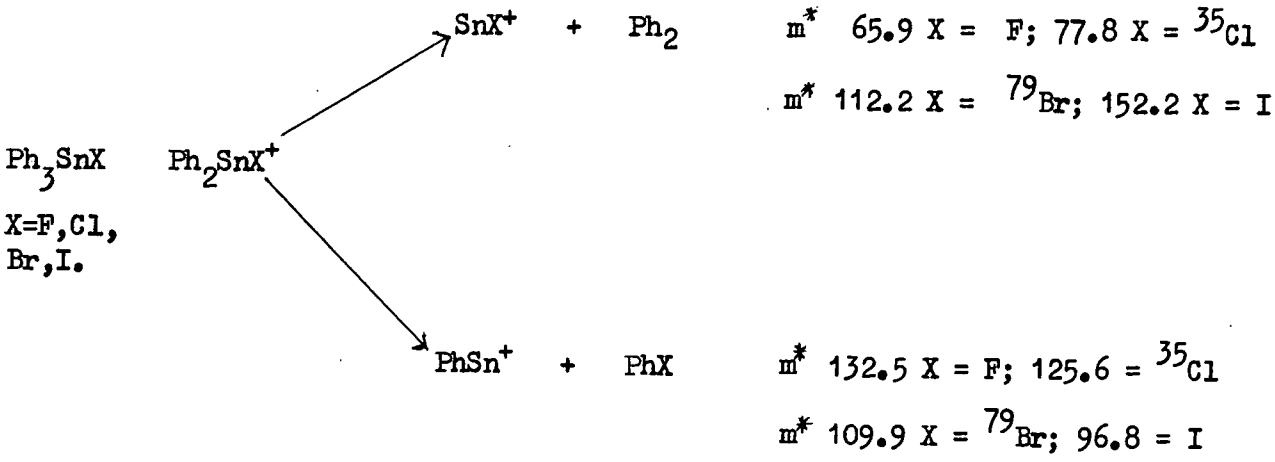

The diphenyltin hydride ion, from diethyldiphenyltin decomposes by elimination of benzene whilst loss of hydrogen is observed from $-SnH_2^+$ ions derived from tetraethyltin and hexaethyldistannane.

Ph_2SnEt_2	$Ph_2SnH^+ \longrightarrow PhSn^+ + C_6H_6$	m*	141.1
Et_4Sn	$EtSnH_2^+ \longrightarrow EtSn^+ + H_2$	m*	147.0
Et_6Sn_2	$Et_2Sn_2H_3^+ \longrightarrow Et_2Sn_2H^+ + H_2$	m*	293
	$EtSn_2H_2 \longrightarrow EtSn_2^+ + H_2$	m*	263

The elimination of ethane has been observed in the spectrum of triethyltin chloride[125].

$$Et_2SnH^+ \longrightarrow EtSn^+ + C_2H_6$$

This elimination of RR' molecules could proceed via a 3 centre transition intermediate.

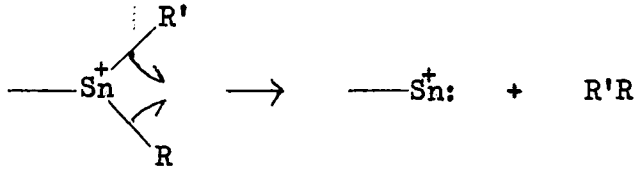

Here fishhooks( ) represent movement of one electron.

Minor Rearrangement Decompositions.

iv) Molecule Elimination by Cleavage of One Sn X Bond.

Such a process is observed in the spectra of $Ph_3Sn{\cdot}SPh$,

Ph_3SnEt, Ph_4Sn and triphenyltin halides producing ions of low abundance

$$Ph_3Sn^+ \longrightarrow PhSnC_6H_4^+ + C_6H_6 \qquad m^* \ 212.3$$

$$Ph_2SnCl^+ \longrightarrow ClSnC_6H_4^+ + C_6H_6 \qquad m^* \ 172.6$$

It would be interesting to determine the hydrogen atom which is transfered in this process. This could be accomplished by deuterium labelling in specific positions in the phenyl group. It seems plausable that a σ - hydrogen may be involved with formation of a 5 - centre transition intermediate.

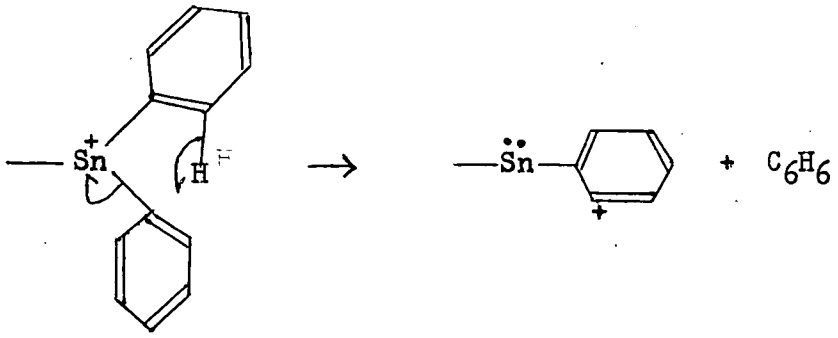

Here fishhooks (⌒) represent movement of one electron.

These product ions might involve a σ - bonded phenyl group from which a hydrogen atom has been removed, or they could be formulated as

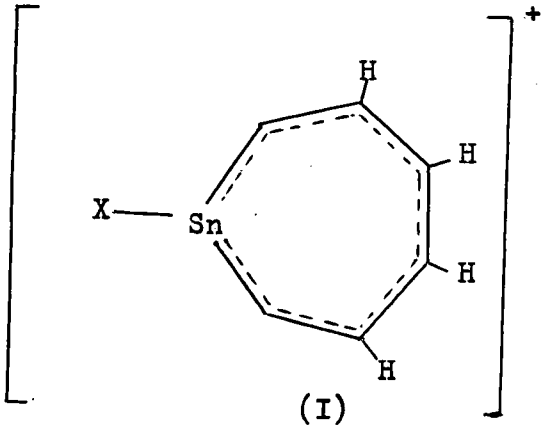

(I)

each dotted line represents 1 and 1/7 electrons.

Here the tin is trico-ordinate and extensive delocalisation of positive charge is possible. The high stability of trico-ordinate tin ions (tables 4.2.4. and 4.2.5. p. 104) is one of the dominant features revealed in this work.

The elimination of HX from $Ph_3SnX^{+\bullet}$ producing the ion $Ph_2SnC_6H_4^{+\bullet}$ in low abundance has been metastable confirmed for the fluorotin compound.

$$Ph_3SnF^{+\bullet} \longrightarrow Ph_2SnC_6H_4^{+\bullet} + HF \qquad m^* \ 331$$

With 5 - stannaspiro (4,4) nonane elimination of ethylene from the parent ion and $C_4H_8Sn^{+\bullet}$ may involve cleavage of a tin-carbon bond.

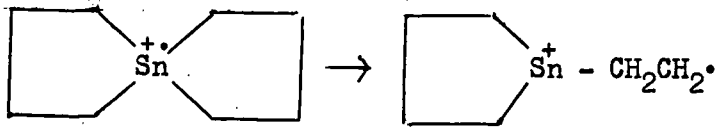

or $+ C_2H_4$ $\quad m^* \ 179.4$

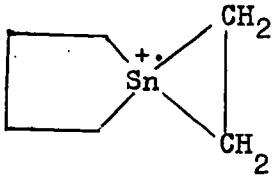

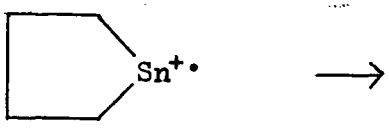

$\longrightarrow \quad SnCH_2CH_2^{+\bullet}$

or $+ C_2H_4$ $\quad m^* \ 124.5$

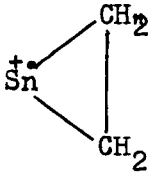

Similar ethylene eliminations have been observed with sila [126] - and germa - [127]

cydoalkanes. With the germanium compound deuterium labelling shows that Ge - C cleavage is involved.

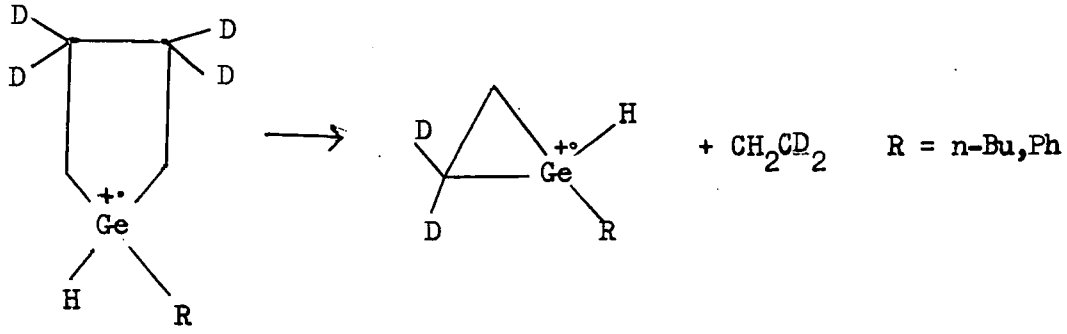

v) Fragmentation of Phenyl Groups Attached to Tin:

Such processes require considerable energy and disappear from the spectrum at 20eV. Phenyltin ions fragment by successive loss of acetylene and, although these transitions are not metastable supported for tin, they are for germanium and silicon (see p. 136)

$$PhSn^+ \xrightarrow{-C_2H_2} C_4H_3Sn^+ \xrightarrow{-C_2H_2} C_2HSn^+$$

$$C_4H_3Sn^+ \xrightarrow{-H_2} C_4HSn^+$$

Tetraphenyltin and compounds of the type Ph_3SnX and Ph_2SnX_2 produce the ion $C_{12}H_9Sn^+$ which can be formulated as the trico-ordinate ion (I). Whenever $C_{12}H_9Sn^+$ is present so are ions which are probably derived from it by successive loss of acetylene.

$$C_{12}H_9Sn^+ \longrightarrow C_{10}H_7Sn^+ \longrightarrow C_8H_5Sn^+$$

The analogous decomposition from silicon and germanium ions is confirmed by the presence of metastable peaks (see p. 136).

It is significant that ring fragmentation processes involving loss of acetylene from Ph_3Sn^+ are not observed. This may be because of other more favourable modes of decomposition available to Ph_3Sn^+

(i.e. such as biphenyl or benzene loss). Alternatively a certain minimum positive charge may be necessary on a phenyl group to cause C_2H_2 elimination. The triphenyltin halides, which produce $XSnC_6H_4^+$ ions in low abundance, also do not show ring fragmentation products $XSnC_4H_2^+$ or $XSnC_2^+$; this may be due to a mesomeric effect of the halogen atom reducing the positive charge on the organic group.

vi) Methylene Elimination from $SnCH_2CH_3^+$

All ethyltin compounds and triphenylethyltin show low abundance ions ascribable to a methylene elimination reaction

$$Et_3Sn^+ \longrightarrow Et_2SnCH_3^+ + CH_2:$$

$$Ph_2SnEt^+ \longrightarrow Ph_2SnCH_3^+ + CH_2:$$

Since for tetraethyl - and ethyltriphenyl - tin the ion currents of the product ions vary linearly with those of $Et_4Sn^{+\cdot}$ and Ph_3Sn^+, respectively, the above unimolecular process is favoured, but this does not exclude the possibility of slow (rate determining) methyl loss followed by rapid hydrogen attachment. The ethylbromide used in the preparation of ethyltin compounds was free from methyl halides thus excluding the possibility that the ethyltin compounds contained traces of methyltin compounds. Moreover the mass spectrum of tetraethyltin showed no change in abundance of Et_2SnMe^+ over the temperature range 20 - 200°C, indicating that the ion is not produced by thermal rearrangement. Corresponding ions which could result from methylene elimination are observed with tetraethyl-germane [123] and - lead (table 4.2.10. p. 123) and ethyltriphenylgermane [123]. With triphenylphenethyltin methylene elimination must occur. $Ph_4Sn^{+\cdot}$ could be formed by ethylene elimination

from the parent ion involving transfer of a phenyl group rather than a hydrogen atom if the mechanism given on p. 107 applies.

$$PhCH_2CH_2SnPh_3^{+\bullet} \longrightarrow PhCH_2SnPh_3^{+\bullet} \longrightarrow Ph_4Sn^{+\bullet}$$

$$PhCH_2CH_2SnPh_3^{+\bullet} \xrightarrow{-C_2H_4} Ph_4Sn^{+\bullet}$$

The compounds Et_6Sn_2 and Ph_2SnEt_2 also show ions which could result by methylene elimination:

$$Et_3Sn^+ \longrightarrow Et_2SnCH_3^+$$

$$PhSnEt_2^+ \longrightarrow PhSnMeEt^+$$

$$PhSnEt(H)^+ \longrightarrow PhSn(H)Me^+$$

In the last example the ion $PhSn(H)Me^+$ could also be produced by ethylene elimination from $PhSn(Me)Et^+$. Methylene elimination has also been observed with ethyltrimethylstannane where the decomposition gives a metastable peak [122]

$$Me_3Sn^+ \longrightarrow Me_2SnH^+ + CH_2: \qquad m^* \ 138.2$$

vii) Elimination of $C_{18}H_{15}$ from Ph_3Sn^+

Compounds which produce a high abundance of Ph_3Sn^+ ion show a weak metastable peak corresponding to the transition

$$Ph_3Sn^+ \longrightarrow Sn^{+\bullet} + C_{18}H_{15} \qquad m^* \ 41.0$$

This may occur in one step but it could also result from the consecutive reactions

$$Ph_3Sn^+ \longrightarrow PhSn^+ + Ph_2$$

$$PhSn^+ \longrightarrow Sn^{+\bullet} + Ph^\bullet$$

occurring in the field free region between the magnetic and electrostatic analysers. The presence of a metastable peak does not mean that the observed elimination occurs in a single step. [128]

viii) Fragmentation involving Formation of Hydrocarbon Ions.

With the triphenyltin halides the $Ph_2^{+\cdot}$ ion is of unusually high abundance (i.e. accounts for about 10% of the total ion current) and is produced by elimination of PhSnX from the parent ion.

$$Ph_3SnX^{+\cdot} \longrightarrow Ph_2^{+\cdot} + PhSnX: \qquad m^* \ 60.2 - 63, \ \text{max., } 61.6X = Cl$$

$$m^* \ 54.5 - 56.5, \ \text{max., } 55.3X = Br$$

$$m^* \ 64 - 65.5, \ \text{max., } 64.3X = F$$

This decomposition is identical to process iii) (p.108)

$$-SnR'R^+ \longrightarrow -Sn^+ + R'R$$

except that the charge is retained by the hydrocarbon fragment. This expulsion reaction in which two moieties not directly bonded in the molecule are found combined in the fragment ion are now known to be quite common for organic compounds.[129]

The triphenyltin halides, with the exception of the iodide, also produce the ion $C_{18}H_{15}^+$ in about 0.5% abundance. For the chloride a metastable peak is present corresponding to the decomposition:

$$Ph_3SnCl^{+\cdot} \longrightarrow C_{18}H_{15}^+ + SnX\cdot \qquad m^* \ 136.5 - 141, \ \text{max., } 138.6$$

Identical eliminations have been observed with triphenylhalogermanes.[123] Such a process involves considerable rearrangement and a variety of complex structures are possible for $C_{18}H_{15}^+$. In view of this rearrangement the elimination of the radical $C_{18}H_{15}\cdot$ from Ph_3Sn^+ should be regarded as a distinct possibility.

Mass Spectra of Ph_nSnEt_{4-n}, Et_6Sn_2, Ph_6Sn_2 and $(CH_2)_4 \rangle Sn \langle (CH_2)_4$

Using the observed decomposition modes for organostannanes, the probable decomposition processes for these compounds are shown in fig. 10.

For all the compounds the molecular ions are of very low abundance. At 20eV many of the fragment ions formed from ethylphenylstannanes virtually dissapear; for example phenyl group fragmentation is no longer observed. With the exception of tetraphenyltin 90% of the ion current is carried by R_3Sn^+ ions (table 4.2.1. p. 101). For Et_4Sn and Et_3SnPh the ions $Sn^{+\cdot}$, SnH^+ and $EtSn^+$ fall to very low values. This is most readily ascribed to the non-occurrence of the process

$$EtSnH_2^+ \longrightarrow EtSn^+ + H_2$$

Hexaethyldistannane contrasts with hexaphenyldistannane in that almost 70% of the total ion current is carried by Sn_2 species. The earlier observation that the bond most likely to be cleaved on decomposition of the molecular ion was the one which would be expected to be the weakest in the neutral molecule can be used to explain this since $D(Ph_3Sn - SnMe_3)$ is about 8 Kcal. mole.$^{-1}$ weaker than $D(Ph_3Sn - Et)$ and $D(Me_3Sn - SnMe_3)$ is about 8 Kcal. mole.$^{-1}$ weaker than $D(Me_3Sn - Et)$.[64] The ion $Et_5Sn_2^+$ can then decompose further by successive eliminations of ethylene producing hydride ions.

There is some evidence that hexaethyldistannane undergoes partial thermal decomposition at an ionization chamber temperature of 200°C since at 100°C the abundance of the parent ion is doubled, with a decrease in the abundance of both $Et_5Sn_2^+$ and Et_3Sn^+. (table 4.2.1.)

Tetraphenyltin, hexaphenyldistannane and the triphenyltin halides show the tin hydride ions SnH^+ which do not feature in fig. 10. and are not

Fig. 10.

Decomposition diagram for organostannanes.

Fig. 10. continued

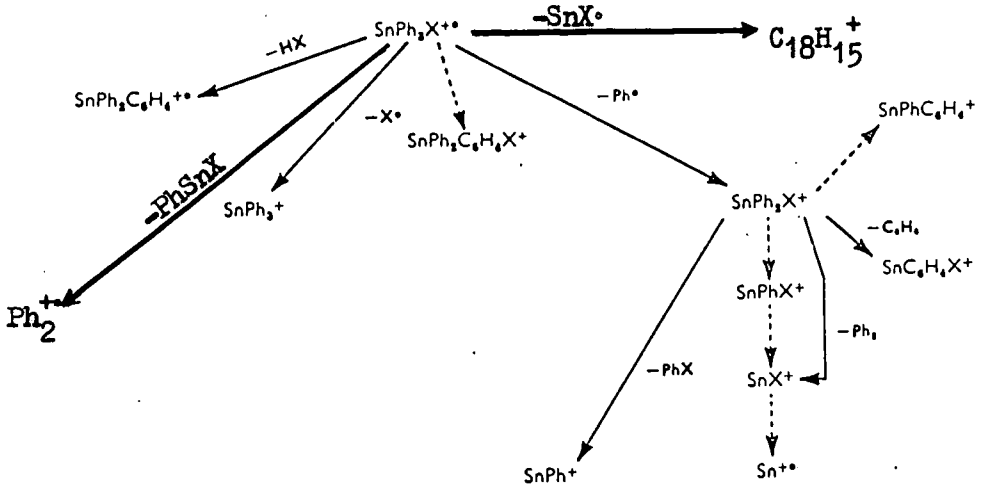

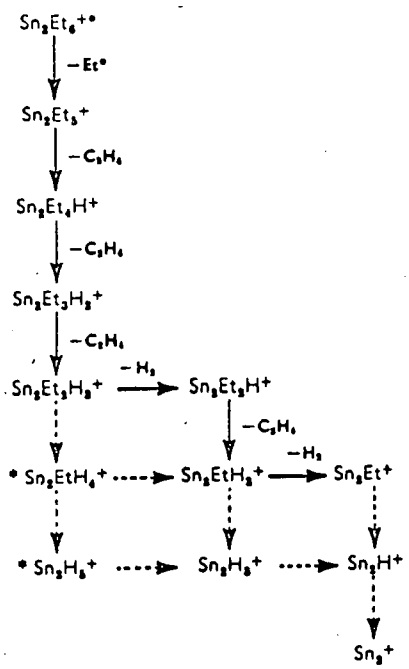

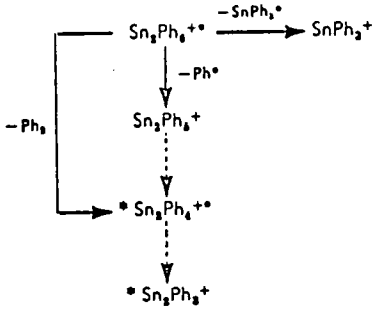

Fragmentation of ions common to two or more compounds are shown only once.

Solid arrows indicate metastable confirmed transitions.

* Abundance < 1% of total tin-containing ions.

explicable by any of the fragmentation modes discussed earlier. The abundance of SnH^+ varies linearly with that of $Sn^{+\bullet}$, hence it is probably not produced by hydrogen attachment but by processes such as $C_2HSn^+ \longrightarrow SnH^+ + C_2$ and $PhSn^+ \longrightarrow SnH^+ + C_6H_4$.

An interesting feature of the spectra of Ph_6Sn_2 is the occurrence of $C_{24}H_{19}Sn^+$ (i.e. $Ph_3SnC_6H_4^+$). Since its abundance varied linearly with that of the parent ion it is best explained in terms of the transfer of an organic group from one tin atom to the other with cleavage of the tin-tin bond. Such transformations, which are clearly more readily studied when the two metals are dissimilar, are described in more detail in the following chapter 4.2.2.

In the mass spectrum of 5 - stannaspiro (4,4) nonane the molecular ion and first bond cleavage product have the same mass and cannot be distinguished. Similarly a number of reasonable structure can be assigned to the fragment $C_6H_{12}Sn^+$.

Mass Spectra of Triphenyltin Halides

The decomposition diagram for these compounds is given in fig.10. The cracking patterns are very similar except for the iodide, where cleavage of the Sn-I bond is the important process. This probably implies that $D(Ph_2ISn\text{-}Ph) > D(Ph_3Sn\text{-}I)$ whereas for the other triphenyltin halides the order is reversed.

4.2.2. Metal-Metal Bonded Compounds $A_3M\text{-}M'B_3$ (M = Si,Ge and Sn) and Organoplumbanes.

The mass spectrum of hexaphenyldistannane showed the presence of an ion ($SnC_{24}H_{19}^+$;) in which transfer of an organic group from one metal to the other had occurred. To investigate this rearrangement more fully the mass spectra of a variety of $A_3M\text{-}M'B_3$ compounds were recorded at 70eV. The specific compounds studied and the abundances of their decomposition products are shown in table 4.2.8.

Since it was apparent that the modes of decomposition found for the organo-tin ions applied equally well to organo-silicon and - germanium ions, the mass spectra of tetraethyl - and tetraphenyl - lead, tetraphenylmethane and t-butyltriphenylmethane were also recorded for comparison. The abundance of ions produced for these compounds are shown in tables 4.2.9., 4.2.10., and fig. 11. The spectrum of tetraethyllead shows minor differences from earlier observations [14] which may be attributed to different source temperatures and spectrometers.

Modes of Decomposition at 70eV.

The major feature of the mass spectra of $A_3M\text{-}M'B_3$ compounds (M,M' = Si,Ge,Sn; A,B = phenyl, methyl, ethyl, benzyl) is the presence of ions, often in high abundance where transfer of organic groups between metal atoms has occurred (table 4.2.11.) Apart from this these compounds and the organoplumbanes studied decompose under electron impact in ways very similar to those observed for organostannanes (chapter 4.2.1.). Metal-containing ions are always the most abundant accounting for ~95% of the total ion current. Again this is not surprising since the electronegativity of carbon is greater than for the other group IV elements.

Table 4.2.8.

Ion abundances *

$(PhCH_2)_3Ge{\cdot}SiMe_3$		$Ph_3Ge{\cdot}SiEt_3$		$Ph_3Sn{\cdot}GeMe_3$		$Me_3Sn{\cdot}GePh_3$		$Ph_3M{\cdot}MMe_3$	Sn	M Ge	Si	$Et_3Si{\cdot}SiPh_3$		$Ph_3Si{\cdot}SiPh_3$	
$(PhCH_2)_3Me_3GeSi^+$	0·05	$Ph_3Et_3GeSi^+$	3·99	$Ph_3Me_3SnGe^+$	0·91	$Ph_3Me_3SnGe^+$	1·68	$Ph_3M_2Me_3$	1·83	4·09	9·14	$Et_3Ph_3Si_2^+$	6·72	$Ph_3Si_2^+$	14·87
								$C_{21}H_{23}M_3$			0·07	$C_{21}H_{23}Si_3$	0·03	$C_{24}H_{23}Si_3$	0·07
$(PhCH_2)_3Me_2GeSi$	0·73	Ph_3Et_2GeSi	3·98	Ph_3Me_3SnGe	1·29	Ph_3Me_3SnGe	15·56	$Ph_3Me_3M_2$	12·89	2·10	4·01	$Ph_3Et_2Si_2$	0·95		
		$Ph_3Et(H)GeSi$	0·64			$C_{14}H_{13}SnGe^+$	0·33	$C_{20}H_{18}M_2$			0·04	$Ph_3Et(H)Si_2$	1·11		
		Ph_3H_2GeSi	0·48			Ph_3SnGe	0·10	$C_{14}H_{14}M_2$			0·12	$Ph_3Si_2H_2$	2·61		
		Ph_3GeSi	0·33					Ph_3MeM_2	0·24			$C_{18}H_{13}Si_2$	0·24		
								Ph_3M_2	0·14						
$(PhCH_2)_2Me_4GeSi$	28·00	Ph_2Et_2GeSi	0·10	Ph_2Me_4SnGe	0·75	Ph_2Me_2SnGe	0·16	$Ph_2Me_4M_2$	0·26	0·20	0·53	$Ph_2Et_2Si_2$	0·07	Ph_2Si_2	0·07
$C_{15}H_{22}GeSi^+$	0·50	$Ph_2Et_2(H)GeSi$	0·12	$C_{13}H_{12}SnGe^+$	0·17	$C_{14}H_{12}SnGe$	0·06	$C_{15}H_{14}M_2^+$			0·34	$Ph_2Et_2HSi_2$	0·05	$C_{28}H_{24}Si_2^+$	0·04
$(PhCH_2)_2Me_2GeSi^+$	0·27	$Ph_2Et(H)_2GeSi$	0·28			$C_{13}H_{11}SnGe$	0·10	$C_{15}H_{13}M_2$			0·34			$Ph_2Si_2^+$	0·02
$C_{14}H_{15}GeSi$	3·72					$C_{12}H_9SnGe$	0·06	$Ph_2Me_2M_2^+$	0·04						
$(PhCH_2)Me_5GeSi^+$	0·31							$C_{14}H_{13}M_2$	0·07						
								Ph_2MeM_2	0·07						
$(PhCH_2)Me_3GeSi$	0·67							$Ph_2M_2^+$	0·04						
								$C_{13}H_9M_2$	0·04						
								$PhMe_2M_2^+$	0·14					$C_{24}H_{19}Si$	0·05
$(PhCH_2)_2Ge$	2·85	Ph_3Ge	9·83	Ph_3Sn	10·06	Ph_3Ge	26·81	Ph_2M	11·97	40·50	40·60	Ph_2Si	34·77	Ph_2Si	69·45
$C_{21}H_{18}Ge$	0·05	$C_{18}H_{15}Ge$	0·28			$C_{18}H_{15}Ge$	0·28	$C_{15}H_{13}M$		0·23	0·04	$C_{14}H_{12}Si$	0·87	$C_{14}H_{12}Si$	1·30
								$C_{15}H_{15}M$			0·31	$C_{15}H_{15}Si$	0·37	$C_{15}H_{15}Si$	0·04
$C_{14}H_{12}Ge$	0·30	C_6H_4GePh	3·84	C_6H_4SnPh	1·20	C_6H_4GePh	2·21	C_6H_4MPh	0·27	5·04	6·52	C_6H_4SiPh	6·28	C_6H_4SiPh	5·47
$C_{13}H_{11}Ge$	0·06	$C_6H_3GePh^+$	1·71			$C_6H_3GePh^+$	0·15	$C_{13}H_9M^+$		1·02	2·32	$C_{12}H_9Si^+$	2·00	$C_{12}H_9Si^+$	1·75
								$C_{12}H_9M$			0·55	$C_{12}H_9Si$	0·61	$C_{12}H_9Si$	0·05
								$C_{12}H_8M^+$			0·11	$C_{12}H_8Si^+$	0·08	$C_{12}H_8Si^+$	0·01
		$PhGeC_4H_9$	0·25	$PhSnC_4H_9$	0·11	$PhGeC_4H_9$	0·54	$PhMC_4H_9$	0·11	0·28	1·42	$PhSiC_4H_9$	1·49	$PhSiC_4H_9$	1·31
		$PhGeC_3$	0·16	$PhSnC_3$	0·10	$PhGeC_3$	0·22	$PhMC_3$	0·05	0·19	0·62	$PhSiC_3$	0·64	$PhSiC_3$	0·05
		Ph_3Ge^+	28·92	Ph_3Sn^+	17·46	Ph_2Ge^+	0·89	Ph_2M^+	1·81	3·65	3·41	Ph_3Si^+	1·72	Ph_3Si^+	1·29
		Ph_3GeH	0·59	Ph_3SnH	0·15			Ph_2MH	0·14	0·76	0·39	Ph_2SiH	3·64	Ph_2SiH	0·43
												$PhSiH^+$	0·76		
$(PhCH_2)GeH_3$	0·85	$PhGeH_2$	0·46					$PhMH_2$	0·08	0·36	0·22	$PhSiH_2$	3·10		
$(PhCH_2)Ge$	15·03	PhGe	6·47	PhSn	17·75	PhGe	11·28	PhM	27·83	11·56	5·01	PhSi	8·21	PhSi	3·48
$C_7H_7Ge^+$	0·04	$C_6H_4Ge^+$	0·34	$C_6H_4Sn^+$	0·45	$C_6H_4Ge^+$	0·11	$C_6H_4M^+$	0·61	2·00	1·92	$C_6H_4Si^+$	0·13	$C_6H_4Si^+$	0·02
C_7H_6Ge	0·08	C_6H_3Ge	0·59					C_6H_3M		0·19	0·62	C_6H_3Si	0·77	C_6H_3Si	0·05
C_6H_4Ge	0·87														
C_6H_3Ge	1·34	C_4H_3Ge	0·59	C_4H_3Sn	0·20	C_4H_3Ge	1·21	C_4H_3M	0·26	1·21	0·75	C_4H_3Si	0·10	C_4H_3Si	0·05
$C_3H_4Ge^+$	0·35			C_4HSn	0·12			$C_4H_2M^+$			0·64	$C_4H_2Si^+$	0·03	$C_4H_2Si^+$	0·02
								C_4HM	0·14		0·21	C_4HSi	0·02	C_4HSi	0·01
C_3H_2Ge	0·42	C_2HGe	0·43	C_2HSn	0·68	C_2HGe	0·94	C_2HM	0·56	1·04	1·21	C_2HSi	1·10	C_2HSi	0·07
$C_3H_2Ge^+$	0·14														
C_2HGe	0·57											H_3Si	0·72		
HGe	0·14	HGe	0·11	HSn	0·17	HGe	0·09	HM	0·40	0·27	0·18	HSi	0·16	HSi	0·02
Ge	0·08	Ge^+	0·15	Sn^+	19·04	Ge^+	0·28	M^+	10·78	0·36	0·07	Si^+	0·09	Si^+	0·01
Me_3Si	11·24	Et_3Si	2·61	Me_3Ge	3·95	Me_3Sn	1·11	Me_3M	1·76	3·69	3·30	Et_3Si	3·30		
C_3H_7Si	0·01			$C_6H_3Ge^+$	0·17							$C_6H_{11}Si^+$	0·58		
C_3H_5Si	0·04														
Me_2SiH	1·07	Et_2SiH	8·69	Me_2GeH	0·22										
Me_2Si^+	0·10	Et_2Si^+	0·26	Me_2Ge^+	0·76	Me_2Sn^+	0·44	Me_2M^+	0·53	0·63		Et_2SiH	6·41		
C_2H_5Si	0·10	C_6H_5Si	0·10			C_2H_5Sn	0·04	C_2H_5M	0·04	0·23		Et_2Si^+	0·67		
												C_2H_5Si	0·10		
$MeSiH_3$	2·56	$EtSiH_3$	5·49	$MeGeH_3$	0·54			$MeMH_3$		1·27	0·87	$EtSiH_3$	5·09		
MeSi	0·82	EtSi	1·11	MeGe	0·33	MeSn	2·25	MeM	1·77	1·34	0·89	EtSi	0·72		
MeSiH	0·12					CH_3Sn^+	0·04	CH_3M^+	0·13	0·37		$EtSiH^+$	1·21		
		H_3Si	0·40												
		HSi	0·06	HGe	0·45	HSn	0·06								
		Si	0·02	Ge	0·45	Sn	1·48								

Rearrangement ions by group transfer

$(PhCH_2)_3GeMe$	0·04	Ph_3GeEt	0·42	Ph_3SnMe	0·65	Ph_2GeMe	13·00	Ph_2MMe	17·36	12·03	7·33	Ph_2SiEt	1·01		
$C_{14}H_{13}Ge$	0·13					$C_{13}H_{12}Ge^+$	0·07	$C_{13}H_{12}M^+$		0·03	0·69				
						$C_{13}H_{11}Ge$	0·30	$C_{13}H_{11}M$		0·27					
$(PhCH_2)GeMe_3$	0·19	$PhGeEt_2$	1·49	$PhSnMe_3$	0·65	$PhGeMe_3$	1·47	$PhMMe_3$	7·17	4·64	3·09	$PhSiEt_2$	0·52		
		PhGeH(Et)	0·74			$PhGeMe^+$	0·11	$PhMMe^+$	0·43	0·45	0·25	PhSi(Et)H	0·53		
		EtGe	0·09					PhM(Me)H	0·08	0·12	0·23	C_6H_9Si	0·22		
Me_3Ge	0·90			Me_3Sn	0·39	Me_3Ge	0·90	C_7H_7M			0·62				
$MeGeH_3$	0·40			MeSn	0·13	MeGe	0·36								
MeGe	1·80	Ph_3Si	0·49	Ph_3Ge	0·97	Ph_3Sn	0·12								
$(PhCH_2)_3SiMe$	3·89	Ph_3SiEt	0·36	Ph_3GeMe	5·50	Ph_3SnMe	0·48								
				$C_{13}H_{11}Ge$	0·04										
				$C_{13}H_{11}Ge$	0·16										
		$PhSiC_6H_4$	0·29	$PhGeC_6H_4$	0·22	$PhSnC_6H_4$	0·12								
		$C_{13}H_9Si^+$	0·16												
		Ph_2Si^+	1·15	Ph_2Ge^+	0·22	Ph_2Sn^+	0·02								
		Ph_2SiH	2·07												
		$PhSiC_4H_9$	0·11	$PhGeC_4H_9$	0·33										
		$PhSiC_3$	0·07	$PhGeC_3$	0·06										
$(PhCH_2)SiMe_3$	12·23	$PhSiEt_3$	0·86	$PhGeMe_3$	9·02	$PhSnMe_3$	1·67								
$C_9H_{13}Si^+$	0·12	$PhSiEt(H)$	1·64	$PhGeMe^+$	0·36	$PhSnMe^+$	0·07								
$C_9H_{11}Si$	0·10	$PhSiH_3$	5·04												
$(PhCH_2)SiH_3$	0·87														
		PhSi	0·89	PhGe	3·38	PhSn	12·07								
		$C_6H_5Si^+$	0·05			C_6HSn^+	0·21								
		C_6H_5Si	0·17	C_6H_5Ge	0·18	C_6H_5Sn	0·19								
		C_6HSi	1·01	C_6HGe	0·19	C_6HSn	0·40								

* Percentage of metal-containing ions.

Table 4.2.9.

Ion abundances and metastable transitions in tetraphenylmethane at 70 ev relative to total carbon-containing ions

Ion+	Abundance	Ion+	Abundance
$C_{25}H_{20}$	12·60	$C_{12}H_9$	0·23
$C_{25}H_{19}$	2·53	$C_{12}H_8$	0·54
$C_{25}H_{18}$	0·23	$C_{12}H_7$	0·41
$C_{19}H_{15}$	32·98	$C_{25}H_{20}^{++}$	1·07
$C_{19}H_{14}$	0·87	$C_{25}H_{19}^{++}$	0·15
$C_{19}H_{13}$	2·61	$C_{11}H_7$	0·61
$C_{19}H_{12}$	0·46	$C_{11}H_6$	0·26
$C_{19}H_{11}$	2·40	$C_{11}H_5$	0·10
$C_{19}H_{10}$	0·20	$C_{19}H_{15}^{++}$	0·18
$C_{19}H_9$	0·41	$C_{19}H_{14}^{++}$	0·64
$C_{18}H_{12}$	1·84	C_9H_7	1·15
$C_{18}H_{11}$	0·46	C_9H_5	0·20
$C_{18}H_{10}$	0·84	$C_{13}H_{10}^{++}$	0·08
$C_{17}H_{11}$	1·41	C_6H_6	3·30
$C_{17}H_{10}$	0·15	C_6H_5	0·95
$C_{17}H_9$	0·43	C_6H_4	0·28
$C_{16}H_{11}$	0·20	C_6H_3	1·74
$C_{16}H_{10}$	0·84	C_6H_2	0·26
$C_{16}H_9$	0·15	C_5H_5	0·28
$C_{16}H_8$	0·20	C_5H_3	0·28
$C_{15}H_9$	0·38	C_4H_4	0·56
$C_{15}H_8$	0·10	C_4H_3	0·89
$C_{15}H_7$	0·13	C_4H_2	0·54
$C_{14}H_{10}$	1·41	C_4H	0·10
$C_{14}H_8$	0·28	C_3H_3	0·84
$C_{13}H_{11}$	1·43	C_3H_2	0·18
$C_{13}H_{10}$	2·35	C_3H	0·13
$C_{13}H_9$	13·91	C_2H_4	0·10
$C_{13}H_8$	0·77	C_2H_3	0·10
$C_{13}H_7$	0·59	C_2H_2	0·10
$C_{12}H_{10}$	0·56	CH_4	0·03

		m*
$C_{25}H_{20}^{+\bullet} \longrightarrow$	$C_{19}H_{15}^{+} + C_6H_5^{\bullet}$	184·6
$C_{19}H_{15}^{+} \longrightarrow$	$C_{13}H_9^{+} + C_6H_6$	112·0
$C_{19}H_{15}^{+} \longrightarrow$	$C_{18}H_{12}^{+\bullet} + CH_3^{\bullet}$	214·0
$C_{19}H_{15}^{+} \longrightarrow$	$C_{19}H_{14}^{+\bullet} + H^{\bullet}$	241·0
$C_{19}H_{14}^{+\bullet} \longrightarrow$	$C_{19}H_{13}^{+} + H^{\bullet}$	240·0
$C_{19}H_{15}^{+} \longrightarrow$	$C_{19}H_{13}^{+} + H_2$	239·0
$C_{19}H_{14}^{+\bullet} \longrightarrow$	$C_{19}H_{12}^{+\bullet} + H_2$	238·0
$C_{19}H_{13}^{+} \longrightarrow$	$C_{19}H_{11}^{+} + H_2$	237·0
$C_{13}H_{10}^{+\bullet} \longrightarrow$	$C_{13}H_9^{+} + H^{\bullet}$	164·0
$C_{13}H_9^{+} \longrightarrow$	$C_{13}H_8^{+\bullet} + H^{\bullet}$	163·0

Table 4.2. 10.

$PbEt_4$ and $PbPh_4$ ion abundances at 70 ev relative to total lead-containing ions

$PbEt_4$		$PbPh_4$	
Ion+	Abundance	Ion+	Abundance
$PbEt_4$	0·42	$PbPh_4$	0·05
PbC_6H_{19}	0·27	$PbC_{24}H_{19}$	0·02
$PbEt_3$	35·00	$PbPh_3$	33·80
PbC_4H_{13}	0·02	$PbPh_2$	0·37
$PbEt_2H$	2·20	$PbC_{12}H_9$	0·60
$PbEt_2$	6·51	PbPh	33·30
PbC_3H_9	0·01	PbC_2H	0·14
PbC_3H_7	0·18	PbH	0·16
$PbEtH_2$	0·79	Pb	31·56
PbEt	33·17		
$PbCH_3$	0·17		
$PbCH_2$	1·16		
PbCH	0·02		
PbH	9·75		
Pb	10·33		

Fig. 11.

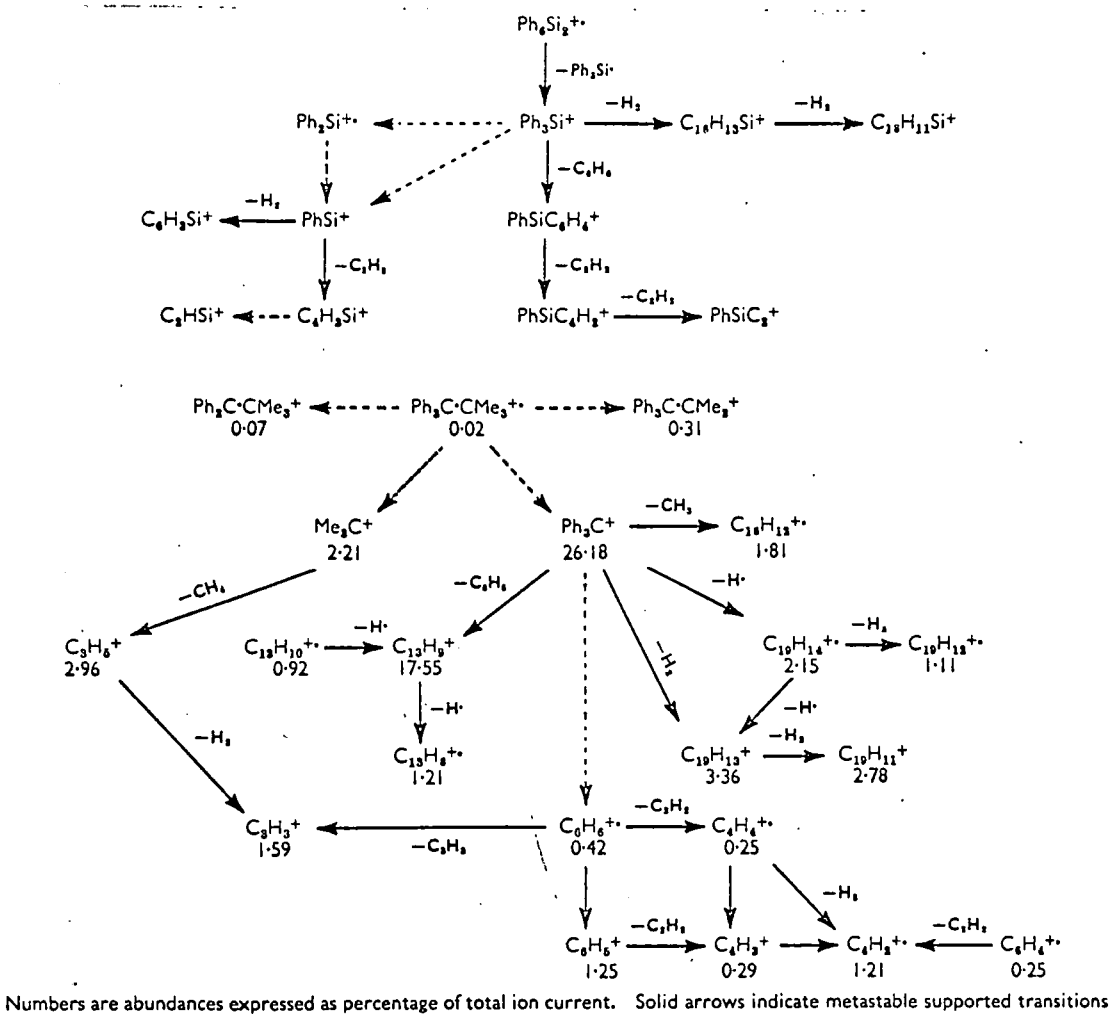

Numbers are abundances expressed as percentage of total ion current. Solid arrows indicate metastable supported transitions

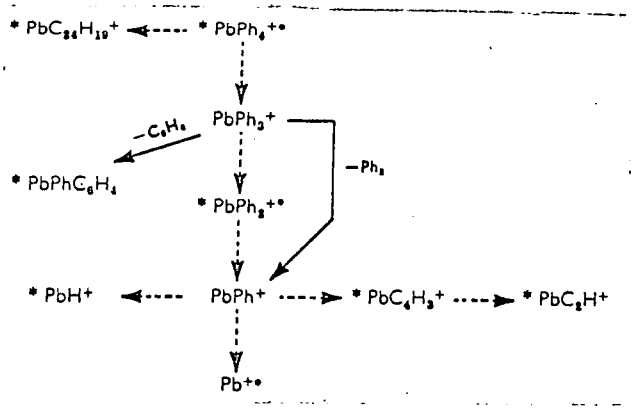

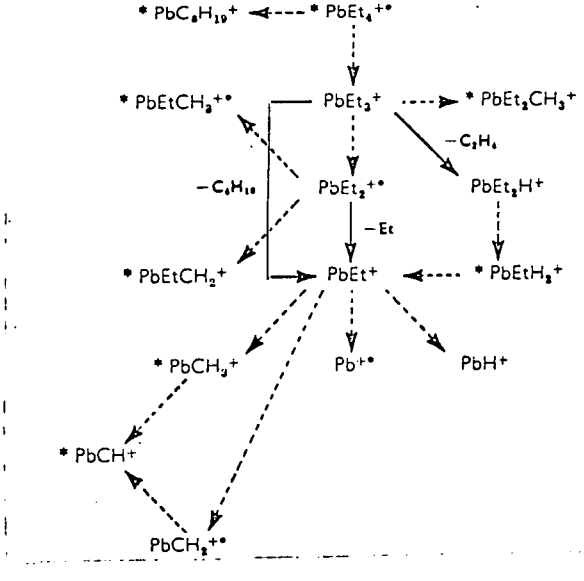

* abundance < 1% of total lead-containing ions.

Fig. 12.

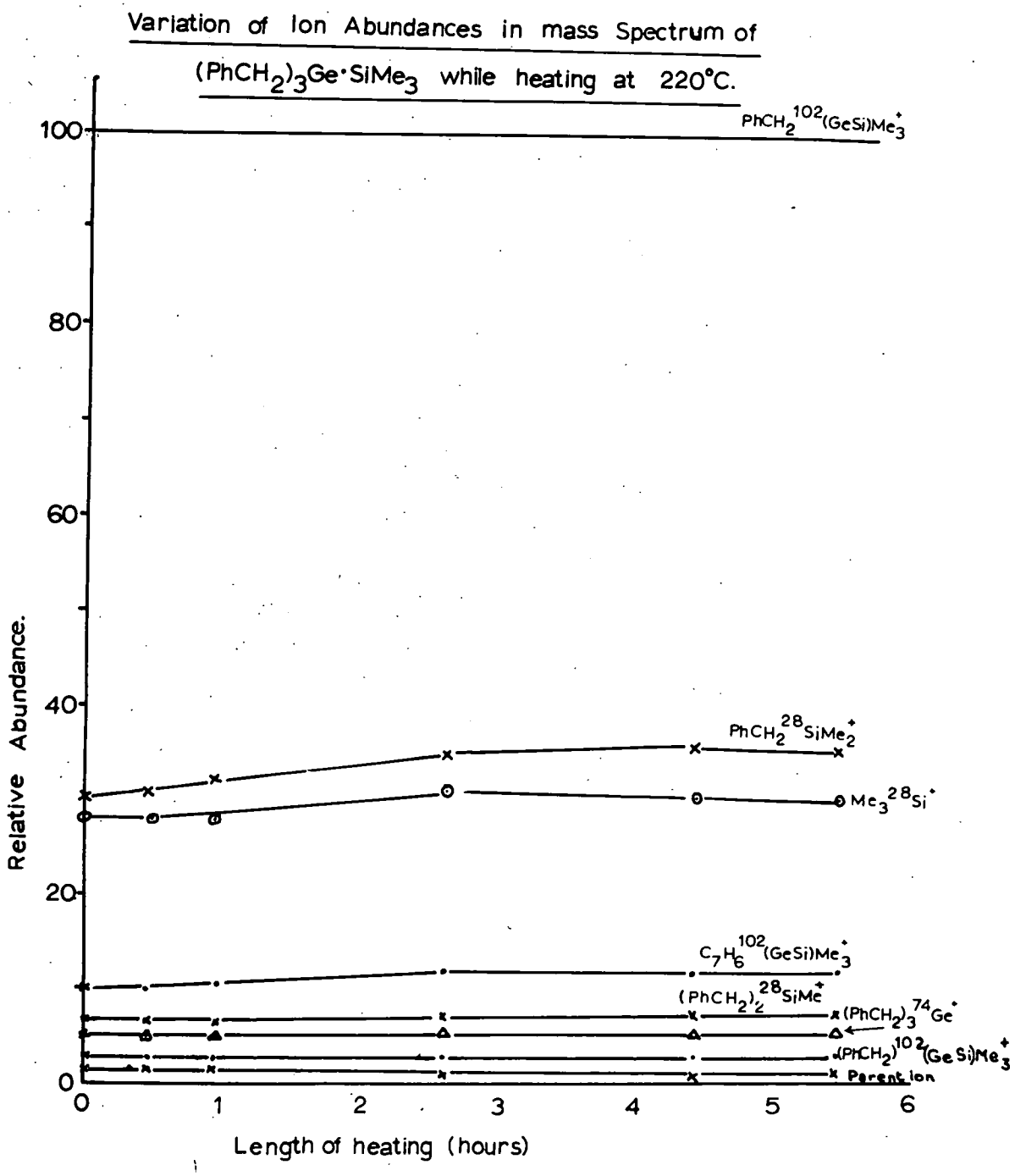
Variation of Ion Abundances in mass Spectrum of
(PhCH2)3Ge·SiMe3 while heating at 220°C.
PhCH2 102(GeSi)Me3+
PhCH2 28SiMe2+
Me3 28Si+
C7H6 102(GeSi)Me3+
(PhCH2)2 28SiMe+
(PhCH2)3 74Ge+
(PhCH2) 102(GeSi)Me3+
Parent Ion
Relative Abundance.
Length of heating (hours)
0
20
40
60
80
100
0
1
2
3
4
5
6

Table 4.2.11.

Abundances of rearrangement ions formed by group transfer across the metal-metal bond.

$Me_3M{\cdot}MPh_3$	Me_2MPh^+	$MeMPh_2^+$	Sum of abundances of all group transfer ions.
$Me_3Si{\cdot}SiPh_3$	3.09	7.33	12.21
$Me_3Ge{\cdot}GePh_3$	4.64	12.03	17.54
$Me_3Sn{\cdot}SnPh_3$	7.17	17.36	25.04

$A_3M{\cdot}M'B_3$	A_2MB^+	AMB_2^+	B_3M^+	$B_2M'A^+$	$BM'A_2^+$	$A_3M'^+$	
$Ph_3Ge{\cdot}SnMe_3$	Ph_2GeMe	$PhGeMe_2$	Me_3Ge	Me_2SnPh	$MeSnPh_2$	Ph_3Sn	
	13.00	1.47	0.90	1.67	0.48	0.12	31.56
$Me_3Ge{\cdot}GePh_3$	Me_2GePh	$MeGePh_2$	Ph_3Ge	Ph_2SnMe	$PhSnMe_2$	Me_3Sn	
	9.02	5.50	0.97	0.65	0.65	0.39	22.45
$Me_3Si{\cdot}GeBz_3$	Me_2SiPh	$MeSiBz_2$	Bz_3Si	Bz_2GeMe	$BzGeMe_2$	Me_3Ge	
	12.33	3.89	-	0.04	0.19	0.90	17.10
$Et_3Si{\cdot}GePh_3$	Et_2SiPh	$EtSiPh_2$	Ph_3Si	Ph_2GeEt	$PhGeEt_2$	Et_3Ge	
	0.87	0.35	0.49	0.42	1.49	-	
C_2H_4 corrected	7.54	2.43	0.49	0.42	1.62	-	26.67

Loss of a radical from parent ions by cleavage of a M-C bond is a dominant process and in general even-electron ions are the major species and maintain themselves even-electron by eliminating a neutral molecule.

i) Migration of Organic Groups across a Metal-Metal Bond.

Ions formed by such migration are of high abundance for all $A_3M{\cdot}M'B_3$ compounds studied (table 4.2.11.). It is doubtful that rearrangement occurs prior to ionization. The infra-red spectra (p.43) give no indication that different groups are attached to the same metal. Thermal decomposition of $Me_3Sn{\cdot}SnEt_3$ has been studied [130] and found to be free of dissociation when heated for several hours at 170°C. At 190°C general decomposition occurred with formation of Me_4Sn, Et_4Sn and traces of Me_6Sn_2 and Et_6Sn_2. The mass spectra of $A_3MM'B_3$ compounds did not show ions corresponding to these symmetrical compounds. Furthermore only slight changes were observed in the mass spectrum of $(PhCH_2)_3GeSiMe_3$ when heated at 220°C for a period of 6 hours (fig. 12.)

These rearrangement processes make the identification of isomeric compounds of the type A_3B_3MM'(M = Si,Ge,Sn) by mass spectrometry somewhat ambiguous.

For $Me_3M{\cdot}MPh_3$ compounds the Ph_2MMe^+ ion is always the most abundant rearrangement ion of this type and the abundances of these ions decrease in the order Si < Ge < Sn. With $Me_3C{\cdot}CPh_3$ no ions resulting from the transfer of Me· or Ph· are present.

Each of the compounds $A_3M{\cdot}M'B_3$ show all six rearrangement ions.

$$A_3M{\cdot}M'B_3^{+\cdot} \longrightarrow A_2MB^+ + AMB_2^+ + MB_3^+ + B_2M'A^+ + BM'A_2^+ + M'A_3^+$$

Concerning the relative abundances of these ions the observation may be made that if M is the lighter metal (i.e. forms stronger M-C bonds) in the compound $A_3M{\cdot}M'B_3$ then ions formed by migration of groups are most common for M, the most abundant being A_2MB^+ followed by AMB_2^+ (table 4.2.11 p.126). In this table since metal-ethyl groups in $Et_3Si{\cdot}GePh_3$ have a highly favourable mode not available in metal-phenyl or -methyl compounds (Si^+-Et $\rightarrow$ SiH^+ + C_2H_4), allowance has been made to correct for ethylene elimination in obtaining the abundances of ions containing ethyl groups.

There is evidence that rearrangement occurs in the molecular ion either prior to elimination of a neutral species or as a synchronous process.

$$Ph_3Et_3Si_2^{+\cdot} \longrightarrow Ph_2SiEt^+ + PhSiEt_2\cdot \qquad m^* \ 119.$$

For this rearrangement to occur in the molecular ion would require a 5 - co-ordinate intermediate, probably with d - orbital participation, and this may explain why the hydrocarbon $Ph_3C{\cdot}CMe_3$ does not show these types of rearrangement ions. If exchange of groups occurs in the molecular ion it is difficult to see why this should not lead to all possible isomeric ions of the type $A_3B_3MM'^{+\cdot}$; the proportion of each would be strongly influenced by relative bond energy considerations.

The formation of these rearrangement ions from $A_2M{\cdot}MB_3^+$ ions has been confirmed in a few cases:

<u>$Ph_3Si{\cdot}SiMe_3$</u>

$$Ph_3Me_2Si_2^+ \longrightarrow Ph_2SiMe^+ + PhSiMe: \qquad m^* \ 122.4$$

$Ph_3Sn \cdot SnMe_3$

$$Ph_3Me_2Sn_2^+ \longrightarrow Ph_2SnMe^+ + PhSnMe: \qquad m^* \quad 162 - 169.5 \text{ max., } 166$$

$(PhCH_2)_3Ge \cdot SiMe_3$

$$(PhCH_2)_2Me_3Si{:}Ge^+ \longrightarrow (PhCH_2)SiMe_2^+ + MeGeCH_2Ph: \quad m^* \quad 66.9 - 69 \text{ max., } 66.8$$

$$(PhCH_2)_2Me_3Ge \cdot Si^+ \longrightarrow (PhCH_2)_2SiMe^+ + Me_2Ge: \quad m^* \quad 154 - 157 \text{ max., } 154$$

$$(PhCH_2)_3Me_2Ge \cdot Si^+ \longrightarrow (PhCH_2)GeMe_2^+ + (PhCH_2)_2Si: \quad m^* \quad 94.2$$

$Ph_3Ge \cdot SnMe_3$

$$Ph_3Me_2Ge \cdot Sn^+ \longrightarrow Ph_2GeMe^+ + PhSnMe: \qquad m^* \quad 126.5 - 131.5 \text{ max., } 130$$

and/or

$$PhGeMe_2^+ \longrightarrow PhGeH_2^+ + C_2H_4$$

All these ions could have structures such that the products are simply the result of cleavage of the metal-metal bond; the necessary rearrangement having occurred in the parent ion. However there seems no reason why rearrangement should not also occur in fragment ions when d-orbital participation by the metal need not be invoked since at least one metal atom will be less than 4-co-ordinate. If rearrangement occurs in $A_2M \cdot MB_3^+$ ions then the abundance of A_2MB^+, AMB_2^+ etc. ions will be influenced by the rate of formation of $A_2M \cdot MB_3^+$ from the parent ion, the lifetime of $A_2M \cdot MB_3^+$ which must be long enough to allow rearrangement to occur, the activation energy for the rearrangement and the stabilities of the resulting ion and fragment. With the carbon compound $Ph_3C \cdot CMe_3$ the major decomposition of the parent ion is formation of Ph_3C^+ and Me_3C^+. Any rearrangement ions formed from $Ph_2C \cdot CMe_3^+$ or $Ph_3C \cdot CMe_2^+$ will thus also

be of low abundance.

In $Et_3Si{\cdot}SiPh_3$ the rearrangement ions Et_2SiPh^+ and $EtSiPh_2^+$ are present but of low abundance. The hydride ions $Et(H)SiPh^+$, H_2SiPh^+ and $HSiPh_2^+$ may arise by hydrogen transfer from one silicon atom to the other or by ethylene elimination.

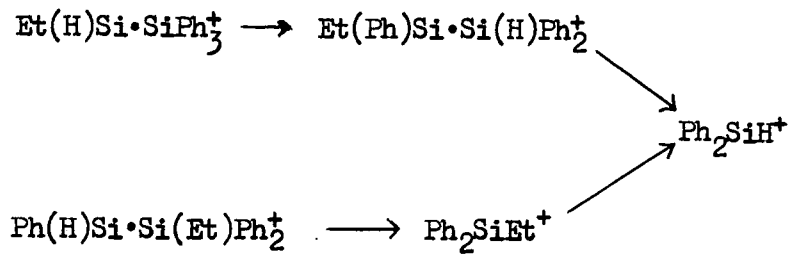

In $Ph_3Ge{\cdot}SnMe_3$ the $PhSn^+$ ion is of high abundance and a metastable peak shows that it is produced largely by the reaction.

$$Ph_3Me_2Ge{\cdot}Sn^+ \longrightarrow PhSn^+ + Ph_2GeMe_2 \qquad m^* \ 82 - 86.5 \ \text{max.}, 85.2$$

ii) <u>Radical Elimination by Bond Cleavage.</u>

This is the major mode of decomposition for molecular ions:

$Ph_3Sn{\cdot}SnMe_3^{+\cdot}$	$\longrightarrow$	$Ph_3Sn{\cdot}SnMe_2^+$	+	$Me{\cdot}$	m^* 484.4
$Ph_3Ge{\cdot}SnMe_3^{+\cdot}$	$\longrightarrow$	$Ph_3Ge{\cdot}SnMe_2^+$	+	$Me{\cdot}$	m^* 440.5
	$\longrightarrow$	$Ph_2Ge{\cdot}SnMe_3^+$	+	$Ph{\cdot}$	m^* 428.6
	$\longrightarrow$	Ph_3Ge^+	+	$Me_3Sn{\cdot}$	m^* 194–199 max., 198
$Ph_3Ge{\cdot}GeMe_3^{+\cdot}$	$\longrightarrow$	Ph_3Ge^+	+	$Me_3Ge{\cdot}$	m^* 216–220 max., 220
$Ph_3Si{\cdot}SiMe_3^{+\cdot}$	$\longrightarrow$	Ph_3Si^+	+	$Me_3Si{\cdot}$	m^* 202
$Ph_3Si{\cdot}SiEt_3^{+\cdot}$	$\longrightarrow$	Ph_3Si^+	+	$Et_3Si{\cdot}$	m^* 179.4
	$\longrightarrow$	$Ph_3Si{\cdot}SiEt_2^+$	+	$Et{\cdot}$	m^* 318.2
$Ph_3Ge{\cdot}SiEt_3^{+\cdot}$	$\longrightarrow$	$Ph_3Ge{\cdot}SiEt_2^+$	+	$Et{\cdot}$	m^* 364
$Ph_3Si{\cdot}SiPh_3^{+\cdot}$	$\longrightarrow$	Ph_3Si^+	+	$Ph_3Si{\cdot}$	m^* 129.5

As with organostannanes discussed in chapter 4.2.1. it appears that bond cleavage of the molecular ion proceeds largely in the direction expected for the weakest bond in the molecule, although all four product ions are observed. Thus ions containing metal-metal bonds are abundant only for those compounds where the metal-metal bond is expected to be stronger than any metal-carbon bonds in the neutral molecule. For example with $Ph_3Ge{\cdot}SnMe_3$ and $Ph_3Ge{\cdot}SnMe_3$ cleavage of an Sn-Me bond in the parent ion gives ions of high abundance and the available bond dissociation energies suggest that this is the weakest bond in the molecule.

$D(Ph_3Sn\text{-}Ph) - D(Ph_3Sn\text{-}Me) = 21.7 \pm 3.2$ Kcal. mole.$^{-1}$

$D(Ph_3Sn\text{-}SnMe_3) - D(Ph_3Sn\text{-}Me) = 6.5 \pm 3.2$ "

$D(Ph_3Sn\text{-}GeMe_3) - D(Ph_3Sn\text{-}Me) = 9.7 \pm 3.2$ "

$D(Me_3Sn\text{-}SnMe_3)$[64] = 76 Kcal. mole.$^{-1}$ $D(Me_3Sn\text{-}Me)$[64] = 73 ± 4 Kcal. mole.$^{-1}$

$D(Me_3Sn\text{-}Ph)$[64] = 81 ± 5 Kcal. mole.$^{-1}$

Also $Me_3Si{\cdot}SiPh_3$ and $Ph_3Si{\cdot}SiEt_3$ give $C_xH_ySi^+$ species as the major ions and the strength of the silicon-alkyl bond is stronger than the silicon-silicon bond in these compounds.[62,131] Ions resulting from phenyl-metal bond cleavage from the parent are always of low abundance.

Parent ion decomposition by metal-metal bond cleavage can give two ions:

$$A_3M{\cdot}M'B_3^{+\cdot} \longrightarrow A_3M^+ \quad \text{or} \quad B_3M'^+$$

If A is phenyl and B methyl then Ph_3M^+ is always the more abundant. This may be due to several factors: the ionization potential of $Ph_3M{\cdot}$ radicals may be lower than $R_3M{\cdot}$ radicals; charge delocalisation in Ph_3M^+ will tend to stabilise the ion, and in individual cases there may be fewer low energy decomposition routes available for Ph_3M^+ than R_3M^+ ions.

Table. 4.2.12.

Molecule elimination by cleavage of two M–X bonds (M = Si, Ge, or Sn)		
$Ph_3Sn{\cdot}GeMe_3$, $Ph_3Sn{\cdot}SnMe_3$	$Ph_3Sn^+ \longrightarrow PhSn^+ + Ph_2$	110·6
$Ph_3Ge{\cdot}SnMe_3$, $Ph_3Ge{\cdot}GeMe_3$, $Ph_3Ge{\cdot}SiEt_3$	$Ph_3Ge^+ \longrightarrow PhGe^+ + Ph_2$	74·8
$(PhCH_2)_3Ge{\cdot}SiMe_3$	$(PhCH_2)_3Ge{\cdot}SiMe_2^+ \longrightarrow PhCH_2Ge^+ + PhCH_2{\cdot}SiMe_2$	82·7
$Ph_3Sn{\cdot}SnMe_3$, $Ph_3Sn{\cdot}GeMe_3$	$Ph_2Sn^{+\cdot} \longrightarrow Sn^{+\cdot} + Ph_2$	52·5
Alkene elimination		
$(PhCH_2)_3Ge{\cdot}SiMe_3$	$(PhCH_2)SiMe_2^+ \longrightarrow PhCH_2{\cdot}SiH_2^+ + C_2H_4$	98·4
$(PhCH_2)_3Ge{\cdot}SiMe_3$	$Me_3Si^+ \longrightarrow MeSiH_2^+ + C_2H_4$	27·7
$Ph_3Si{\cdot}SiMe_3$		
$Ph_3Sn{\cdot}GeMe_3$, $Ph_3Ge{\cdot}GeMe_3$	$Me_3Ge^+ \longrightarrow MeGeH_2^+ + C_2H_4$	69·6
$Ph_3Si{\cdot}SiMe_3$	$PhSiMe_2^+ \longrightarrow PhSiH_2^+ + C_2H_4$	84·8
$Ph_3{\cdot}SiSiEt_2$	$Et_3Si^+ \longrightarrow Et_2SiH^+ + C_2H_4$	65·8
	$Et_2SiH^+ \longrightarrow EtSiH_2^+ + C_2H_4$	40·0
	$PhSiEt_2^+ \longrightarrow PhSiEt(H)^+ + C_2H_4$	111·9
	$PhSiEt(H)^+ \longrightarrow PhSiH_2^+ + C_2H_4$	84·8
	$Ph_2SiEt^+ \longrightarrow Ph_2SiH^+ + C_2H_4$	158·7
$Ph_3{\cdot}SiSiEt_3$	$Ph_3Et_2Si_2^+ \longrightarrow Ph_3Et(H)Si_2^+ + C_2H_4$	291·3
	$Ph_3Et(H)Si_2^+ \longrightarrow Ph_3H_2Si_2^+ + C_2H_4$	263·5
$Ph_3Ge{\cdot}SiEt_3$	$Ph_3Et_2GeSi^+ \longrightarrow Ph_3Et(H)GeSi^+ + C_2H_4$	337
	$Ph_3Et(H)GeSi^+ \longrightarrow Ph_3H_2GeSi^+ + C_2H_4$	309·3
	$Ph_2GeEt^+ \longrightarrow Ph_2GeH^+ + C_2H_4$	204·1
Molecule elimination by cleavage of one M–X bond (M = Si, Ge, or Sn)		
Ph_6Si_2, $Ph_3Si{\cdot}SiMe_3$, $Ph_3Si{\cdot}SiEt_3$	$Ph_3Si^+ \longrightarrow C_{12}H_9Si^+ + C_6H_6$	126·5
$Ph_3Ge{\cdot}SnMe_3$, $Ph_3Ge{\cdot}GeMe_3$, $Ph_3Ge{\cdot}SiEt_3$	$Ph_3Ge^+ \longrightarrow C_{12}H_9Ge^+ + C_6H_6$	168·9
$Ph_3Sn{\cdot}GeMe_3$, $Ph_3Sn{\cdot}SnMe_3$	$Ph_3Sn^+ \longrightarrow C_{12}H_9Sn^+ + C_6H_6$	212·4
$(PhCH_2)_3Ge{\cdot}SiMe_3$	$(PhCH_2)_2Me_3GeSi^+ \longrightarrow C_{10}H_{15}GeSi^+ + C_7H_8$	170·8
Molecule eliminations without M–X bond cleavage		
$(PhCH_2)_3Ge{\cdot}SiMe_3$	$(PhCH_2)_2SiMe^+ \longrightarrow C_9H_{11}Si^+ + C_6H_6$	96·0
	$(PhCH_2)_2SiMe^+ \longrightarrow C_{15}H_{15}Si^+ + H_2$	221
	$(PhCH_2)_3Ge^+ \longrightarrow C_{21}H_{19}Ge^+ + H_2$	343
	$C_7H_7Ge^+ \longrightarrow C_5H_5Ge^+ + C_2H_2$	117
$Ph_3Ge{\cdot}SnMe_3$, $Ph_3Ge{\cdot}GeMe_3$	$Ph_2GeMe^+ \longrightarrow C_{13}H_{11}Ge^+ + H_2$	239
$Ph_3Si{\cdot}SiMe_3$	$Ph_2SiMe^+ \longrightarrow C_{13}H_{11}Si^+ + H_2$	193·1
$Ph_3Si{\cdot}SiMe_3$	$PhSiMe(H)^+ \longrightarrow C_7H_7Si^+ + H_2$	117·0
$Ph_3Si{\cdot}SiMe_3$	$PhSi^+ \longrightarrow C_6H_5Si^+ + H_2$	101
$Ph_3Si{\cdot}SiEt_3$	$Ph_3Si^+ \longrightarrow C_{18}H_{13}Si^+ + H_2$	255
Ph_6Si_2	$C_{18}H_{13}Si^+ \longrightarrow C_{18}H_{11}Si^+ + H_2$	253
$Ph_3Ge{\cdot}SiEt_3$	$Ph_3SiH^+ \longrightarrow C_{12}H_9Si^+ + H_2$	179·4
$Ph_3Si{\cdot}SiEt_3$	$PhSiH_2^+ \longrightarrow C_6H_5Si^+ + H_2$	103
$Ph_3Ge{\cdot}SiEt_3$	$Ph_3H_2Ge{\cdot}Si^+ \longrightarrow C_{18}H_{15}Ge{\cdot}Si^+ + H_2$	331
$Ph_3Si{\cdot}SiEt_3$	$Ph_3H_2Si_2^+ \longrightarrow C_{18}H_{15}Si_2^+ + H_2$	285

Loss of H• or 2H• by cleavage of C-H bonds becomes increasingly important for $Ph_3M{\bullet}MMe_3$ compounds in the order C > Si > Ge > Sn (table 4.2.8. and fig. 11 p. 122 and 124) which probably reflects the strength of the M-C bonds (C > Si > Ge > Sn). With the lead compounds (table 4.2.10. p. 123.) hydrogen loss does not give abundant ions.

Bond cleavage decompositions in even-electron ions also occur:

$(PhCH_2)_3Ge{\bullet}SiMe_2^+$	⟶ $(PhCH_2)_3Ge^+$	+	Me_2Si:	m^* 293-300 max., 297
$(PhCH_2)_2GeMe^+$	⟶ $(PhCH_2)_2Ge^{+\bullet}$	+	Me•	m^* 242
$PhSn^+$	⟶ $Sn^{+\bullet}$	+	Ph•	m^* 73.1
$Ph_3Ge{\bullet}SnMe_2^+$	⟶ Ph_3Ge^+	+	Me_2Sn:	m^* 201-206.5 max., 204.5
Ph_2GeMe^+	⟶ $Ph_2Ge^{+\bullet}$	+	Me•	m^* 214
$Ph_3Si{\bullet}SiH_2^+$	⟶ Ph_3Si^+	+	H_2Si:	m^* 232.1

The metal ions $M^{+\bullet}$ are of high abundance only for the tin and lead compounds. This is probably a reflection of the energy to remove all the groups from the metal decreasing in the order Si > Ge > Sn > Pb. [106]

iii) <u>Ethylene Elimination</u>. $>M^+—Et \longrightarrow M^+—H + C_2H_4$

$-MMe_2^+ \longrightarrow M^+—H + C_2H_4$

Metastable confirmed decompositions for this process are shown in table 4.2.12. Loss of ethylene occurs from even-electron ions containing an M^+—Et bond and the mechanism is probably similar to that previously discussed for tin (p. 106). Other even-electron ethyl-germanium [123] and - silicon [132] ions show ready loss of ethylene.

With the ions Me_3Ge^+ and Me_3Si^+ ethylene elimination also occurs. Although such a process may involve rearrangement to an ethylmetal hydride, loss of this molecule may also occur by concerted cleavage of two M-C bonds.

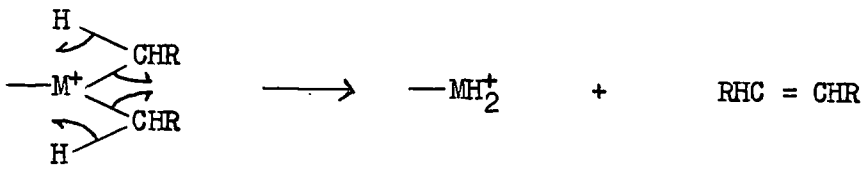

A similar elimination of stilbene [123] occurs from $(PhCH_2)_3Ge^+$.

iv) Molecule Elimination by Cleavage of two M—X Bonds.

Such decomposition of parent ions has been noted for tetraphenyl-tin and -germane [123] as being responsible for the formation of $Ph_2M^{+\bullet}$ in high abundance. With tetraphenyllead $Ph_2Pb^{+\bullet}$ is of low abundance and no metastable peak corresponding to biphenyl elimination from the parent ion was observed.

With $Ph_3Ge{\cdot}SiEt_3$ and $Ph_3Sn{\cdot}GeMe_3$ a similar decomposition occurs giving an odd-electron ion in high abundance.

$Ph_3Ge{\cdot}SiEt_3^{+\bullet}$	$\longrightarrow$	$Ph_2Ge^{+\bullet}$	+ $PhSiEt_3$	m^*	123.8
$Ph_3Sn{\cdot}GeMe_3^{+\bullet}$	$\longrightarrow$	$Ph_2Sn^{+\bullet}$	+ $PhGeMe_3$	m^*	156.5 - 161.2 max., 160.

In the second process a Ge-Ph bond is produced by cleavage of a weaker Sn-Ph and Sn-Ge bond (the metal-metal bond since this is the weakest in the molecule will probably be one-electron and hence very weak). A similar situation occurs with $Ph_3Ge{\cdot}SiEt_3$ when a stronger Ph-Si bond is formed by cleavage of the weaker Ph-Ge and Ge-Si. In both cases the ions $Et_2Si^{+\bullet}$ and $Me_2Ge^{+\bullet}$, which would result from elimination of Ph_3GeEt and Ph_3SnMe, respectively, are of very low abundance. However the selectivity of this elimination process will also depend on the stability of the resulting odd-electron ion. The bond energy argument applied to $Ph_3Ge{\cdot}SnMe_3^{+\bullet}$ would favour a process giving $Me_2Sn^{+\bullet}$, but this ion is not observed and $Ph_2Ge^{+\bullet}$ is of very low abundance. Compounds of the type

$Ph_3M{\cdot}MMe_3$(M = Si,Ge, or Sn) also fail to show this elimination.

Elimination of RR' molecules from even-electron ions are very common and examples observed with metal-metal bonded compounds are given in table 4.2.12. Biphenyl elimination from Ph_3M^+ ions is observed for M = Ge,Sn, and Pb but not M = Si, or C.

$$Ph_3M^+ \longrightarrow PhM^+ + Ph_2 \qquad m^* \; 74.8 \; (M = Ge), \; 110.6 \; (M = Sn), \; 185 \; (M = Pb)$$

This is probably a reflection of the greater Si-Ph and C-Ph bond strengths in these ions. This type of decomposition may occur however from other silicon ions.

$$PhSiH_2^+ \longrightarrow C_6H_5Si^+ + H_2 \qquad m^* \; 103$$

$$Ph_3H_2Si_2^+ \longrightarrow C_{18}H_{15}Si_2^+ + H_2 \qquad m^* \; 285$$

$$Ph_3H_2Si{\cdot}Ge^+ \longrightarrow C_{18}H_{15}SiGe^+ + H_2 \qquad m^* \; 331$$

On the other hand these decompositions may not involve hydrogen atoms not attached to silicon.

In tetraethyllead the elimination of butane from Et_3Pb^+ ions occurs.

$$Et_3Pb^+ \longrightarrow EtPb^+ + C_4H_{10} \qquad m^* \; 190.4$$

Such elimination is not observed with triethyl-silyl, - germyl or -stannyl ions. A similar decomposition occurring from the parent ion of tetraethyllead could also explain the high abundance of $Et_2Pb^{+\cdot}$ which contrasts with the low-abundance of $Et_2M^{+\cdot}$ ions for tetraethyl-tin and - germane.[123]

$$Et_4Pb^{+\cdot} \longrightarrow Et_2Pb^{+\cdot} + C_4H_{10}$$

A metastable peak for this process was not observed however.

v) Molecule Elimination by Cleavage of one M-X Bond.

Benzene elimination from Ph_3M^+ ions gives a metastable peak for

all group IV elements C,Si,Ge,Sn,Pb;

$$Ph_3M^+ \longrightarrow PhMC_6H_4^+ + C_6H_6 \qquad m^* \quad \begin{matrix} 112.0 & M = C \\ 126.5 & M = Si \\ 168.9 & M = Ge \\ 212.4 & M = Sn \\ 297.0 & M = Pb \end{matrix}$$

With $Ph_3M{\cdot}MMe_3$ compounds the abundance of the resulting ion decreases in the order C > Si > Ge > Sn (table 4.2.8. and fig. 11. p.124). With Ph_4M compounds the ion $PhMC_6H_4^+$ is less abundant for Pb than Sn.

A somewhat similar elimination is loss of toluene from benzyl ions (table 4.2.12. p. 131).

In some trimethyl compounds, $Me_3M{\cdot}M'R_3$, ions are produced in low abundance which can be explained as successive loss of methane, e.g.,

$$Me_3Ph_2Ge{\cdot}Sn^+ \rightarrow C_{14}H_{15}Ge{\cdot}Sn^+ \rightarrow$$

$$C_{13}H_{11}Ge{\cdot}Sn^+ \longrightarrow C_{12}H_7Ge{\cdot}Sn^+$$

vi) Fragmentation of Phenyl Groups attached to Metal.

Ions which could result by successive elimination of acetylene by fragmentation of phenyl groups attached to metal are present in the triphenyl derivatives of silicon, germanium and tin.

$$PhMC_6H_4^+ \longrightarrow PhMC_4H_2^+ + C_2H_2 \qquad m^* \; 132.7 \; M = Si; \; 178 \; M = Ge$$

$$PhMC_4H_2^+ \longrightarrow PhMC_2^+ + C_2H_2 \qquad m^* \; 107.4 \; M = Si; \; 152.4 \; M = Ge$$

$$PhM^+ \longrightarrow C_4H_3M^+ + C_2H_2 \qquad m^* \; 59.4 \; M = Si; \; 103.5 \; M = Ge$$

$$C_4H_3M^+ \longrightarrow C_2HM^+ + C_2H_2$$

In phenyltin compounds these processes are not metastable confirmed. In tetraphenyllead only C_2HPb^+ was observed and then in very low abundance. (table 4.2.10.)

Table 4.2.13.

Abundances of $PhMC_6H_4^+$, PhM^+ and ions produced by C_2H_2 elimination

	$PhMC_6H_4^+$	$PhMC_4H_2^+$	$PhMC_2^+$	PhM^+	$C_4H_3M^+$	C_2HM^+
$Ph_3Si\cdot SiEt_3$	6.28	1.49	0.64	8.21	0.10	1.10
$Ph_3Si\cdot SiMe_3$	6.52	1.42	0.62	5.01	0.75	1.21
$Ph_3Ge\cdot GeMe_3$	5.04	0.28	0.19	11.56	1.21	1.04
$Ph_3Sn\cdot SnMe_3$	0.27	0.11	0.05	27.83	0.26	0.56

From table 4.2.13. it will be observed that the fragment ions decrease in abundance in the order Si > Ge > Sn, which is probably a reflection of the change in metal-carbon bond strength.

vii) Loss of Hydrogen H· or H_2

Some of the H_2 eliminations e.g.

$$Ph_3H_2Si_2^+ \longrightarrow C_{18}H_5Si_2^+ + H_2$$

may well be decompositions of category iv) (p. 134) and have been discussed there. Others such as

$$PhSi^+ \longrightarrow C_6H_3Si^+ + H_2$$

probably do not involve metal-hydrogen cleavage and are shown in table 4.2.12. (p. 132)

Decomposition modes of organo-silicon, - germanium, - tin and - lead compounds have been shown to be very similar for a variety of ions containing M-Me, M-Et and M-Ph bonds. From a detailed study of the mass spectra of organogermanes [123] it is apparent that similarities to organostannanes extend over a wide variety of compounds.

The abundances of parent ions show some trends for group IV organometallic compounds. For example the abundances at 70eV of parent ions for the following compounds are:

	Si	Ge	Sn	Pb
Ph_6M_2	14.87%	8.9%	6.51%	
$Ph_3M^{\bullet}MMe_3$	9.14%	4.00%	1.83%	
Ph_4M		2.00%	0.11%	0.05%
Et_4M		2.00%	0.97%	0.42%

Such a trend is probably due to the increase in M–C bond strength in the order Si > Ge > Sn > Pb. The increase in abundance of ions resulting from C–H or C–C cleavage in the order C > Si > Ge > Sn > Pb is also probably because of the variation of M–C bond strength.

The decrease in abundance of RM^+ and $M^{+\bullet}$ ions in going from analogous compounds of lead and silicon may also be related to the decreasing energy required to strip organic groups from the metal in going from silicon to lead.[106] Gielen, Nasielski and Boue[133] relate the intensity of RM^+ fragments primarily to the stability of the M^{II} oxidation state which increases in going from silicon to lead. These authors also regard parent ions as M^V species and $R_2M^{+\bullet}$ as M^{III} species. The high abundance of the even-electron ions RM^+ and R_3M^+ is attributed not primarily to the even-electron character but to the stability of M^{II} and M^{IV} oxidation states relative to M^{III} and M^{IV}.

Rearrangement processes involving hydrogen migration are prevalent with these compounds especially when metal–alkyl bonds are present. Alkene elimination from even-electron ions containing alkyl groups with formation of metal hydride ions is particularly very favourable. Such hydrogen migrations are also well known in the mass spectra of organic compounds, for example the rearrangement of a ~~odd-e~~ hydrogen to a polar functional group is often observed[9]. e.g.

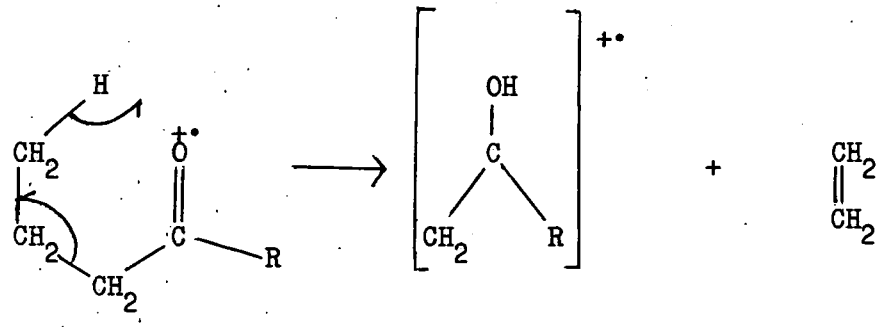

Rearrangements where migration of a functional group occurs, although common for the organometallic compounds discussed in this chapter, has only recently been shown to occur with organic compounds.[129]

$$[A—B—C]^{+} \longrightarrow \left[\begin{array}{c} C \\ A \cdots B \end{array}\right]^{+} \longrightarrow A—C^{+} + B$$

With transition metal complexes which have been widely investigated such rearrangement processes are well known.

Thus the iron-tin complex $\pi - C_5H_5(CO)_2Fe{\cdot}SnPh_3$ shows the metastable confirmed rearrangement.[134]

$$C_5H_5(Ph)Fe{\cdot}Sn^{+} \longrightarrow PhFe^{+} + C_5H_5Sn^{\cdot}$$
$$C_5H_5(Ph)Fe{\cdot}Sn^{+} \longrightarrow C_5H_5Sn^{+} + PhFe^{\cdot}$$

Similarly $PhMn^{+}$ is observed in low abundance in the spectrum of $Ph_3Sn{\cdot}Mn(CO)_5$.[134] Transfer of an initially π- bonded cyclopentadienyl group from a transition metal to a non-transition-metal is a common process and for $\left[\pi - C_5H_5(CO)_2Fe\right]_2SnCl_2$ the ion $C_5H_5Sn^{+}$ is the most abundant ion in the spectrum. Trialkylgermyl-molybdenum and - tungsten complexes, $\pi - C_5H_5(CO)_3M{\cdot}GeR_3$ behave similarly in forming $C_5H_5Ge^{+}$.[135] Similar migrations are observed with platinum-germanium phosphine complexes.[136]. The μ- mercaptide, μ- alkoxo and μ- dialkylamido derivatives of chromium, iron and nickel produce rearrangement ions, a metastable peak for the

compound 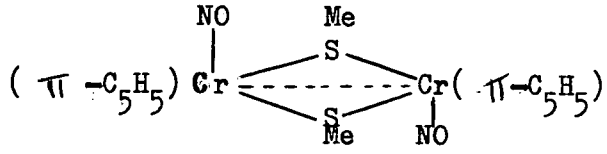 indicating the process:-

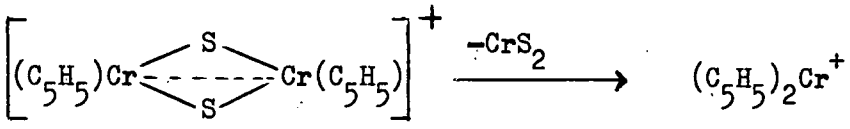

The migration of carbonyl groups across a metal-metal bond seems to be uncommon. However with $Re_2(CO)_{10}$,[138] $ReMn(CO)_{10}$[139] and $HRe_3(CO)_{14}$[138] it must occur since the ion $M(CO)_6^+$ is produced in very low abundance. Sometimes however ions observed may result from thermal decomposition followed by ionization, as in $Hg[Mn(CO)_5]_2$[140] where 42% of the total in current is due to ions $Mn_2(CO)_{0-7}^+$.

Such migration reactions are not confirmed to metal-metal bonded compounds. A variety of compounds involving two metals π-bonded to the same ligand (such as

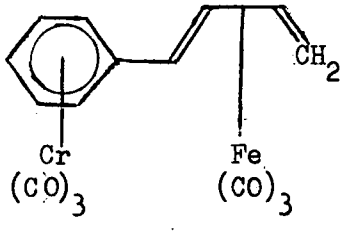 and 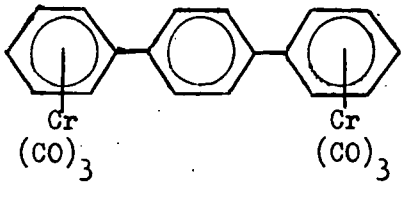)

produce $M-M^+$ ions.

Migration of groups from carbon to metal has also been observed. The spectra of some substituted π - bonded arene complexes[142]

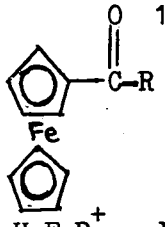

produce ions resulting from transfer of R to the metal i.e. $C_5H_5FeR^+$ and FeR^+.

Trimethylsilyl derivatives of benzylalcohol and benzylamine

(Me_3SiOCH_2Ph and $Me_3SiNHCH_2Ph$) produce phenylsilyl ions although this rearrangement is only a minor feature of the corresponding sulphur compound.[28]

Group migration reactions are common in fluorocarbon metal compounds, presumably because of the high strength of metal-fluorine bonds. Tetrakis(pentafluorophenyl)germane [97] produces $(C_6F_5)_2GeF^+$ in high abundance contrasting with the low abundance of Ph_2GeH^+ derived from tetraphenylgermane.[123] Similar migrations of fluorine are observed with fluorocarbon derivatives of silicon [97], arsenic [143] iron [97,144,145,146] manganese [140,147] and rhenium [147], and elimination of neutral metal fluoride is often observed.

$$(C_6H_5)_3Ge^+ \longrightarrow C_{18}F_{12}^{+\bullet} + GeF_3\bullet$$

$$(F_3C)_2AsCF_2^+ \longrightarrow C_3F_5^+ + AsF_3$$

4.3. Mass Spectra of Beryllium Dialkyls.

Since most dialkyls of beryllium form electron deficient associated molecules in liquid and vapour phases [91] the mass spectra of these compounds are of considerable interest because of the possibility of forming ions from these associated molecules in high abundance. The following beryllium dialkyls were investigated using an ionizing electron beam of 70, 15 or 12 volts and various source temperatures:- Me_2Be; Et_2Be; $(i\text{-}Pr)_2Be$; $(n\text{-}Pr)_2Be$; $(i\text{-}Bu)_2Be$ and $(t\text{-}Bu)_2Be$. Ion abundances for these compounds are given in Appendix 2.

The method of sample introduction for beryllium dialkyls has been discussed in chapter 2.2.1. p. 48. It is worth commenting here, however, that the temperature of the sample required for di-tert-butylberyllium reflects its monomeric structure [153]. Thus whereas di-iso-butylberyllium required a sample temperature of 0°C to give a source pressure reading of 5×10^{-6} m.m., a similar source pressure was obtained for the tertiary-butyl compound when the sample was solid at -60°C.

4.3.1. Effect of Source Temperature.

This was most apparent for diethylberyllium and fig. 13 shows the 70eV spectrum recorded at various source temperatures. As the temperature rises the abundance of monomeric ions, $C_xH_yBe^+$, increases whereas that of trimeric ions, $C_aH_eBe_3^+$, and the much more abundant dimeric ions, $C_aH_bBe_2^+$, decreases (fig. 14 and table 4.3.1.). Such behavior can be explained by increased dissociation of associated molecules to monomers at higher source temperatures prior to ionization.

Fig. 13.

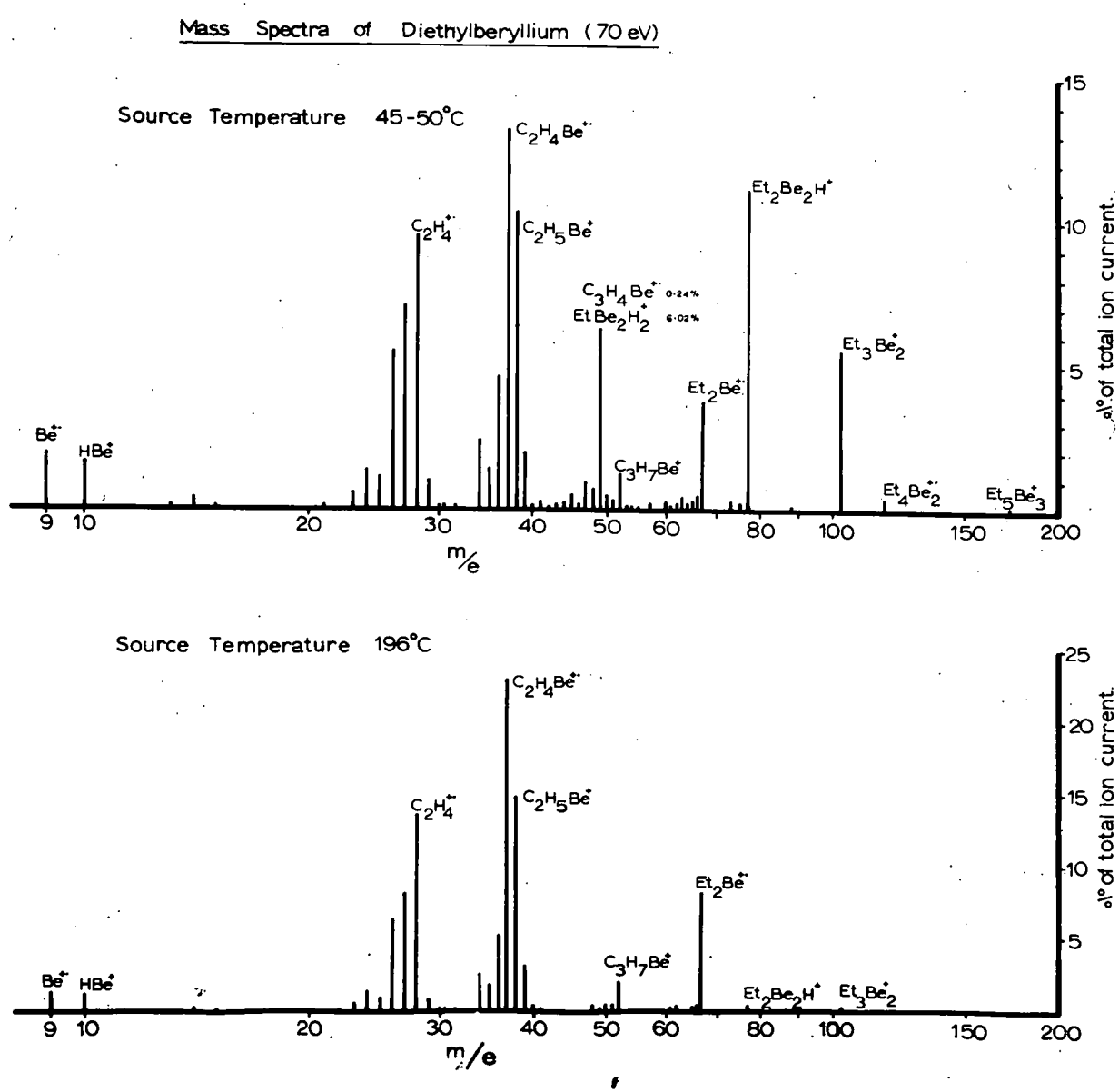
Mass Spectra of Diethylberyllium (70 eV)
Source Temperature 45-50°C
$C_2H_4Be^{+\cdot}$
$Et_2Be_2H^+$
$C_2H_4^{+\cdot}$
$C_2H_5Be^+$
$C_3H_4Be^{+\cdot}$ 0·24%
$EtBe_2H_2^+$ 6·02%
$Et_3Be_2^+$
$Et_2Be^{+\cdot}$
$Be^{+\cdot}$
HBe^+
$C_3H_7Be^+$
$Et_4Be_2^{+\cdot}$
$Et_5Be_3^+$
9 10 20 30 40 50 60 80 100 150 200
m/e
% of total ion current.
15 10 5
Source Temperature 196°C
$C_2H_4Be^{+\cdot}$
$C_2H_4^{+\cdot}$
$C_2H_5Be^+$
$Et_2Be^{+\cdot}$
$C_3H_7Be^+$
$Be^{+\cdot}$
HBe^+
$Et_2Be_2H^+$
$Et_3Be_2^+$
9 10 20 30 40 50 60 80 100 150 200
m/e
% of total ion current.
25 20 15 10 5

Fig. 14.

Variation of Ion Abundances with Source Temperature for Diethylberyllium.

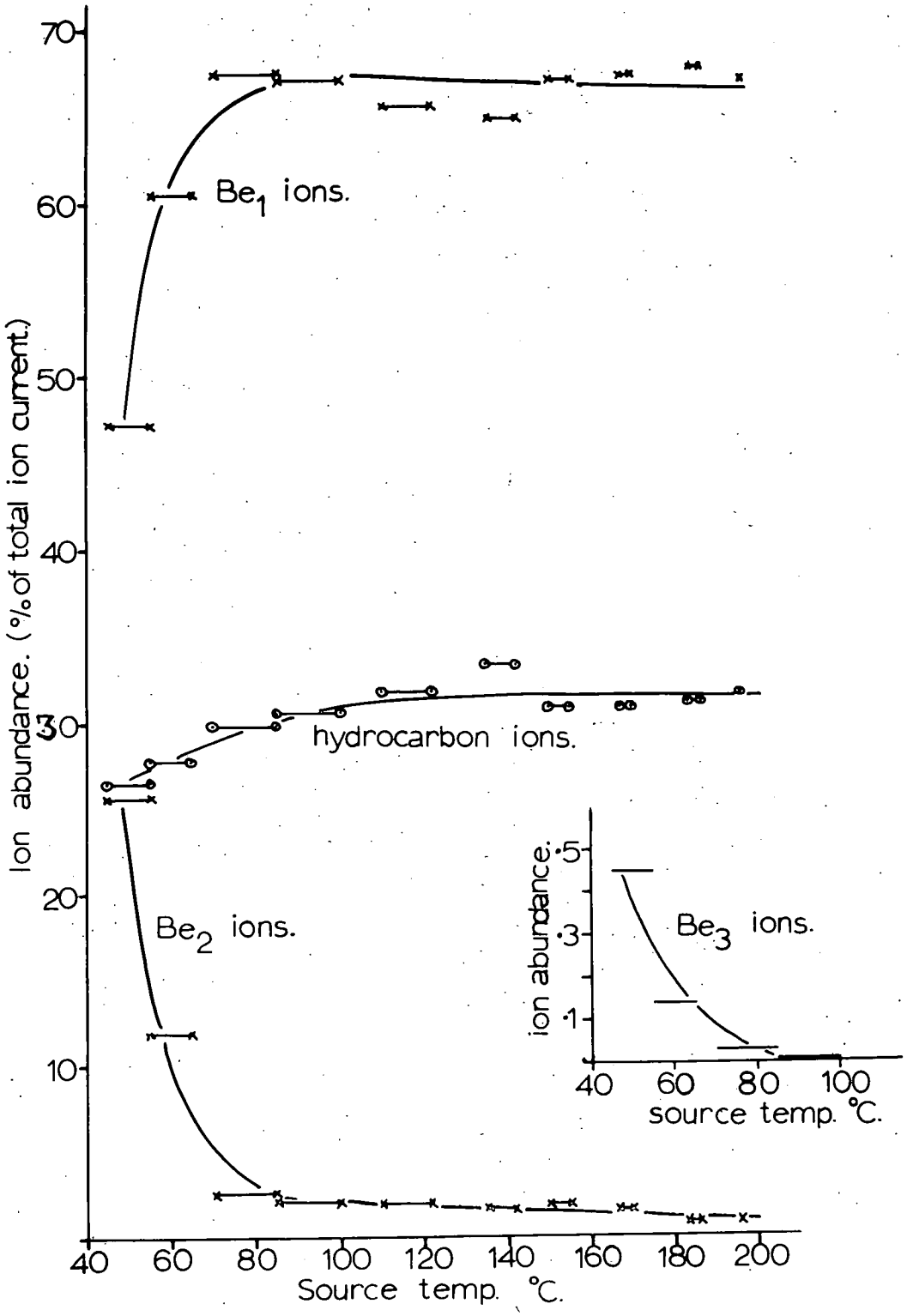

Fig. 15.

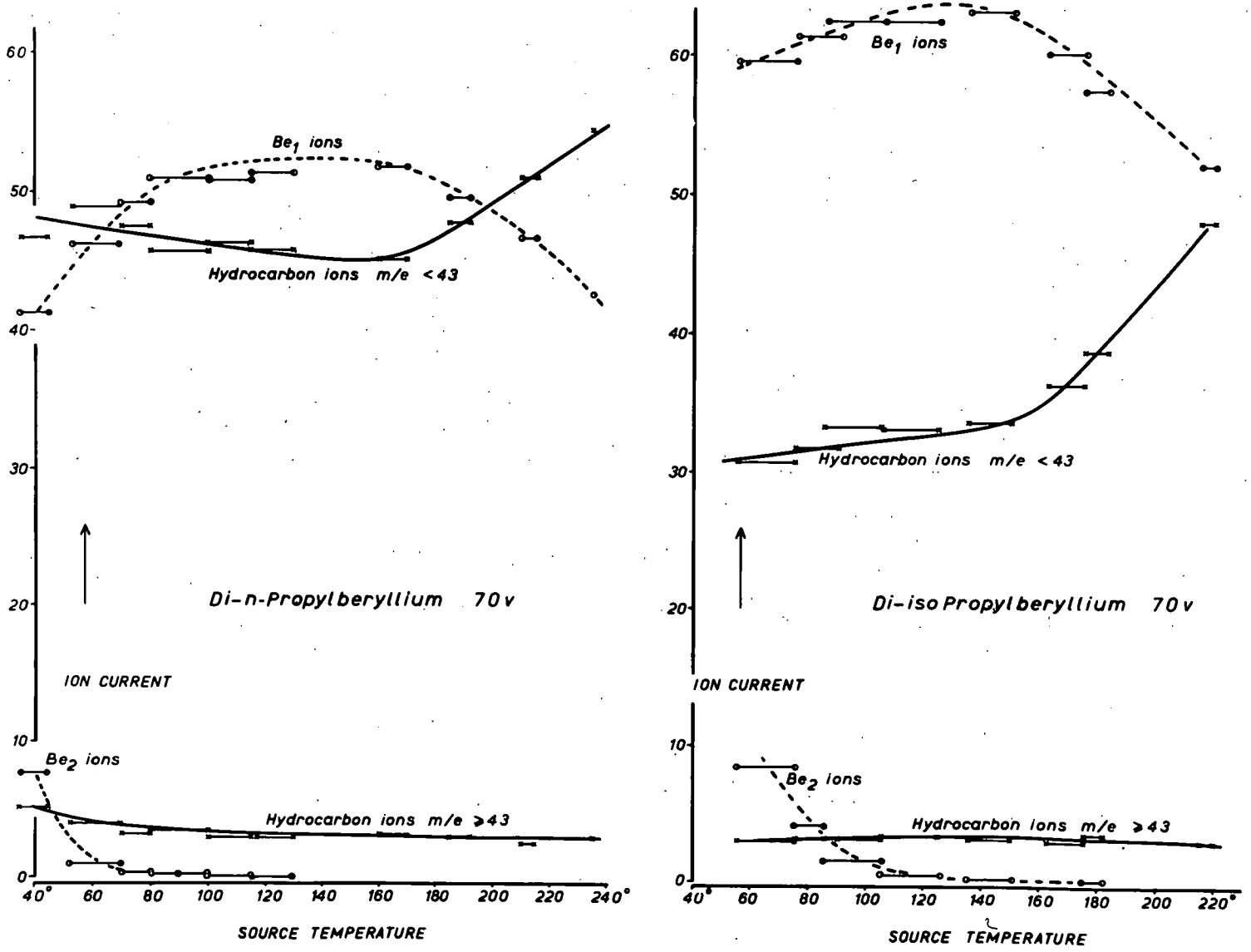
Be1 ions
Hydrocarbon ions m/e < 43
Di-n-Propylberyllium 70 v
ION CURRENT
Be2 ions
Hydrocarbon ions m/e ⩾ 43
SOURCE TEMPERATURE
Be1 ions
Hydrocarbon ions m/e < 43
Di-iso Propylberyllium 70 v
ION CURRENT
Be2 ions
Hydrocarbon ions m/e ⩾ 43
SOURCE TEMPERATURE

Table 4.3.1.

Variation of ion abundances with source temperature for diethylberyllium (70eV)

Source temp. °C	% of total ion-current carried by:-				
	$C_dH_eBe_3^+$ ions	$C_aH_bBe_2^+$ ions	$C_xH_yBe^+$ ions	Hydrocarbon m/e > 30	Hydrocarbon m/e ≤ 30
45-55	0.45	25.67	47.29	1.38	25.06
55-65	0.14	11.74	60.35	0.90	26.86
70-85	0.03	2.57	67.43	0.94	29.00
85-100	0.006	2.14	67.23	1.21	29.43
110-122	0.003	1.93	66.22	1.20	30.68
135-142	0	1.60	64.98	1.32	32.09
150-155	0	1.87	67.25	1.32	29.51
167-170	0	1.59	67.52	1.40	29.47
184-186	0	0.79	68.02	1.60	29.58
196	0	0.72	67.29	1.11	30.65

The greater importance of hydrocarbon ions at higher source temperatures is in agreement with the thermal decomposition of diethylberyllium which produces ethane, ethylene and butane from about 85°C.

The two propyl compounds also produce dimeric ions (tableA23.p. and fig. 15).

At corresponding source temperatures such ions are of much lower abundance than with diethylberyllium and this reflects the decreasing degree of association of beryllium dialkyls as the size of the alkyl group increases.[91] Like the ethyl compound the abundance of dimeric ions falls with increasing source temperature and there is a complementary increase in the intensity of monomeric ions. Again this is because associated molecules dissociate to monomer molecules prior to ionization at high source temperatures.

Dimeric ions, $C_aH_bBe_2^+$, are more abundant at corresponding source temperatures for $(i\text{-}Pr)_2Be$ than for $(n\text{-}Pr)_2Be$ from which it may be inferred that dimer molecules are more abundant in the vapour for the iso compound.

A tentative explanation of this observation is that the inductive effect of methyl groups attached to the bridging carbon atom in the dimer molecule

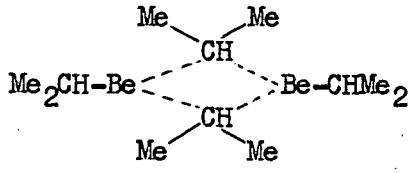

increase the electron density in the Be-C-Be bridging bonds. Inductive effects should be less pronounced with the n-propyl compound. Extending this argument to the butyl compounds one would expect di-tert-butylberyllium to be more associated than di-n-butylberyllium which is not the case; the tertiary compound being monomeric in benzene solution [13] and the normal compound dimeric [154]. Steric effects must also be considered to influence the degree of association and with di-tertiary-butyl beryllium the size of the organic group probably inhibits association. Steric hindrance has been postulated to explain why diethylberyllium unlike dimethylberyllium does not form a polymer.[155]

With di-iso-propylberyllium the abundance of hydrocarbon ions $m/e \leqslant 42$ increases from a source temperature of 55°C and rapidly above $\sim$150°C. Since this compound is known to decompose thermally giving propene from about 50°C, the reaction becoming rapid at 200°C, these observations may be ascribed to thermal decomposition prior to ionization. Although hydrocarbon ions $m/e \leqslant 42$ are more abundant for di-n-propylberyllium they do not increase in abundance until about 165°C, source temperature, indicating that the n-propyl compound is somewhat more stable to thermal decomposition than the iso compound. The initial high abundance of hydrocarbon ions for the normal compound is probably because of a high

Table 4.3.2.

Variation of ion abundances with source temperature (70eV).

di-iso-butylberyllium.

Source temp. °C	% of total ion current carried by:-		
	$C_xH_yBe^+$ ions	hydrocarbon ions m/e $>$ 56	hydrocarbon ions m/e $\leqslant$ 56
75-90	43.46	1.74	54.80
95-130	41.88	1.56	56.56
160-170	36.61	1.53	61.86
200-210	29.61	1.30	69.09
235	20.70	1.34	77.50

di-tert-butylberyllium.

Source temp. °C	% of total ion current carried by:-		
	$C_xH_yBe^+$ ions	hydrocarbon ions m/e $\geqslant$ 57	hydrocarbon ions m/e $\leqslant$ 56
55-75	52.31	10.77	35.27
75-80	51.94	11.21	36.72
125-135	47.86	11.37	40.70
140.155	51.14	11.90	37.66
155-165	45.86	12.05	41.89
165-175	44.00	10.32	45.71
240	27.11	7.27	65.69

concentration of dissolved propene in the sample of di-n-propylberyllium when the spectra was recorded.

Even though di-iso-butylberyllium is dimeric in benzene [13] only monomeric ions $C_xH_yBe^+$, are detected in the mass spectrum. As with di-tertiary-butyl beryllium, the abundance of these monomeric ions falls with increasing source temperature while hydrocarbon ions m/e $\leqslant$ 56 increase in abundance. (table 4.3.2.). This reflects thermal decomposition to involatile hydride and butene prior to ionization.

Although solid dimethylberyllium is a long chain electron deficient polymer as revealed by X-ray analysis [156]

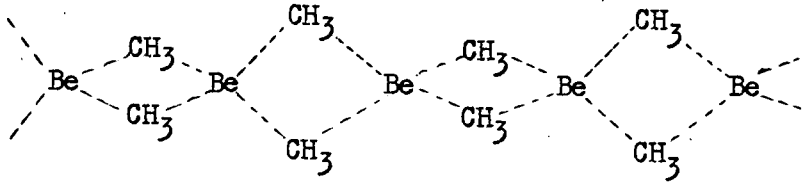

ions containing two or more beryllium atoms are of low abundance in the mass spectrum at 70eV and low source temperatures. This may be because only discrete monomer units can escape easily from the polymeric solid in contrast to liquid diethylberyllium which probably contains dimer and trimer molecules which can leave the surface of the liquid as complete entities. The infra-red spectrum of dimethylberyllium also indicates that the unsaturated vapour consists mainly of monomer while the saturated vapour gives a complex spectrum due to the presence of dimers and trimers.[91]

Since thermal decomposition of dimethylberyllium giving mainly methane does not occur until above $\sim$ 200°C[91] it is not surprising that the abundance of hydrocarbon ions in the mass spectrum of this compound increase only slowly as the source temperature rises to 210°C (table 4.3.3.)

Table 4.3.3.

Variation of ion abundances with source temperature for dimethylberyllium (70eV).

Source temp. °C	% of total ion current carried by			
	$C_xH_yBe^+$ ions	$C_aH_bBe_n^+$ ions	Hydrocarbon ions m/e > 16	Hydrocarbon ions m/e ≤ 16
37-50	83.28	3.45	4.01	9.27
73-87	83.86	0.97	3.92	11.17
115-127	84.86	0.63	3.87	10.64
164-170	84.57	0.60	3.90	11.01
195-198	83.64	0.24	2.02	12.35
210	81.10	0.41	3.78	14.52

With dimethyl-,di-iso-butyl- and di-tert-butyl-beryllium which show essentially only $C_xH_yBe^+$ ions, the monomeric parent ions, $R_2Be^{+\cdot}$, are most abundant at low source temperatures. In this respect they are like hydrocarbons [1,157] which show a similar trend. As with hydrocarbons the effect is most pronounced in the highly branched molecules such as di-tert-butyl-beryllium. (table 4.3.2.).

4.3.2. Mass Spectra and Modes of Decomposition.

Unlike the organo derivatives of Group IVb elements, even-electron ions of the type, $C_xH_yBe^+$, are not outstandingly more abundant than odd-electron ions, as is illustrated in the following table calculated from the spectrum obtained at high source temperatures at 70eV.

The high abundance of odd-electron ions is mainly because of two factors:-

a) Monomer parent ions, $(C_nH_{2n+1})_2Be^{+\cdot}$, are abundant for all beryllium dialkyls except the butyl compounds. As the size of the alkyl

	Abundance of odd-electron $C_xH_yBe^+$ ions			Abundance of even-electron $C_xH_yBe^+$ ions
$(C_nH_{2n+1})_2Be$	$(C_nH_{2n+1})_2Be^{+\cdot}$	$C_nH_{2n}Be^{+\cdot}$	Total	
Me_2Be	17.91	15.14	39.63	41.47
Et_2Be	8.02	23.05	38.75	28.83
$(i\text{-}Pr)_2Be$	2.36	13.80	24.93	26.94
$(n\text{-}Pr)_2Be$	1.34	11.09	16.85	25.21
$(i\text{-}Bu)_2Be$	0.08	3.34	5.26	15.44
$(t\text{-}Bu)_2Be$	0.37	2.70	6.36	20.78

group increase so the abundance of the monomer parent ion decreases.

b) The odd-electron ion, $C_nH_{2n}Be^{+\cdot}$, is produced in high abundance by elimination of the alkane, C_nH_{2n+2}, from the parent monomer ion. This process is discussed in more detail when the decomposition modes of the monomeric ions, $C_xH_yBe^+$, are discussed.

In contrast abundant associated ions, $C_fH_gBe_n^+$, areeven-electron and maintain themselves even-electron by eliminating a molecule such as hydrogen or a hydrocarbon. (Figs. 16 and 17).

Modes of Decomposition of Associated Ions at 70eV.

$C_fH_gBe_n^+$ ions are observed in the spectra of dimethyl-, diethyl- and di-propyl-beryllium compounds at low source temperatures. The observed metastable transitions for these ions are given in figures 16, 17 and 18.

The decomposition of these ions is very simple. The parent ion of the associated species, $R_{2n}Be_n^{+\cdot}$, first loses an alkyl group R, giving an even-electron ion which maintains its even-electron character by

Fig. 16.

Metastable confirmed decompositions for $C_aH_bBe_2^+$ and $C_dH_eBe_3^+$ ions in spectra of diethylberyllium.

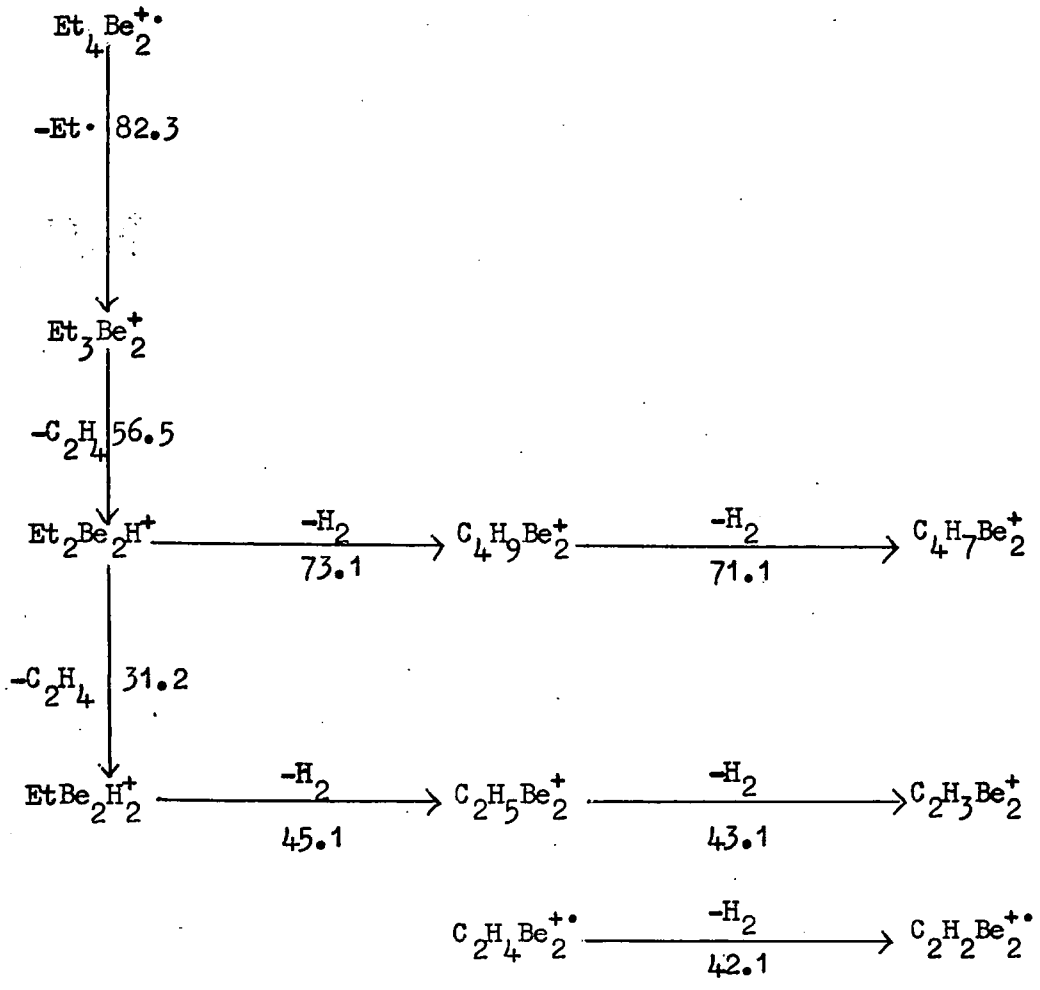

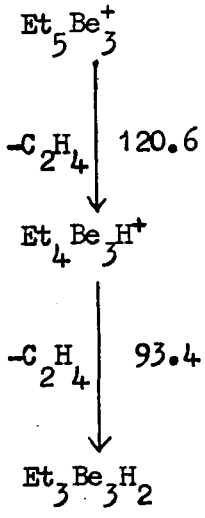

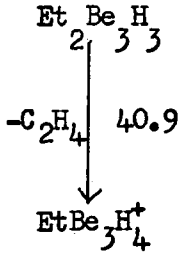

70eV; numbers are mass of observed metastable peak.

Fig. 17.

Metastable confirmed decompositions for di-propylberyllium compounds.

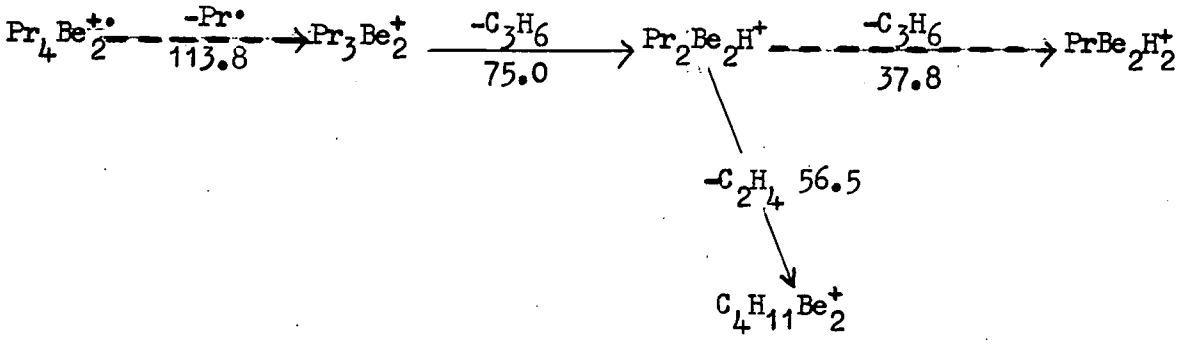

70eV; numbers are observed mass of the metastable peak. Solid arrows indicate metastable transitions common to both propyl compounds. Arrow ——→ indicate transitions observed only for $(i\text{-}Pr)_2Be$

Fig 18.

Metastable confirmed decompositions for dimethylberyllium

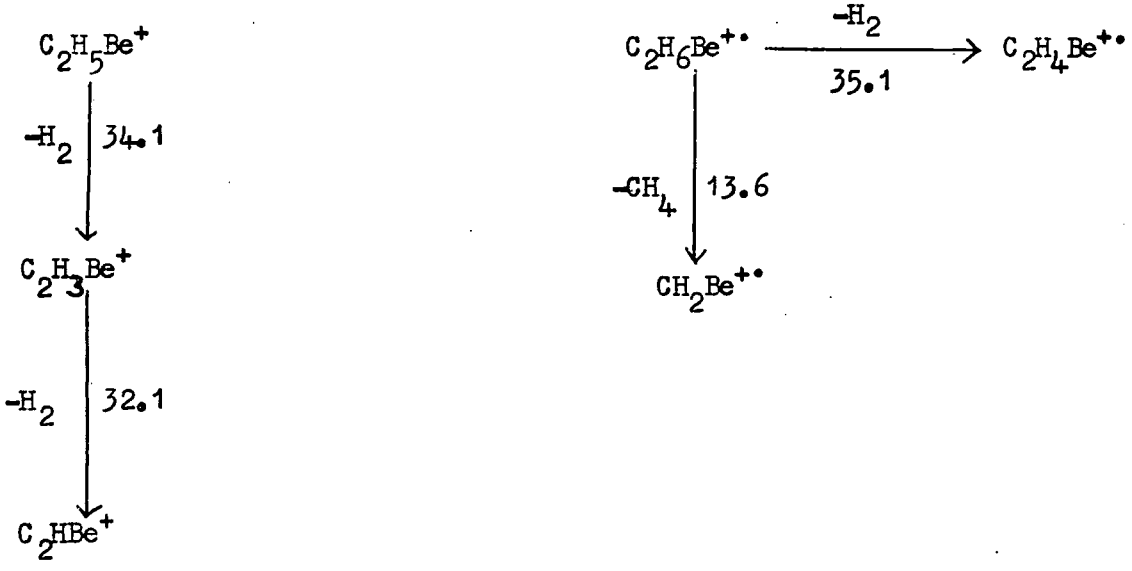

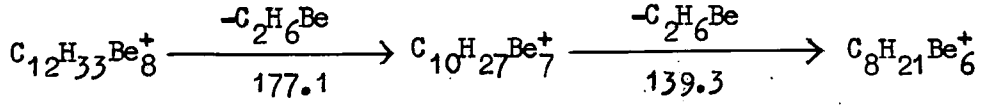

70eV; numbers are observed mass of metastable peak.

successive loss of neutral molecules.

With the ethyl compound successive elimination of ethylene from $Et_3Be_2^+$ and $Et_5Be_3^+$ yields hydride ions in high abundance at low source temperatures

$$Et_3Be_2^+ \longrightarrow Et_2Be_2H^+ \longrightarrow EtBe_2H_2^+ \dashrightarrow H_3Be_2^+$$

$$Et_5Be_3^+ \longrightarrow Et_4Be_3H^+ \longrightarrow Et_3Be_3H_2^+ \dashrightarrow$$

$$\dashrightarrow Et_2Be_3H_3^+ \longrightarrow EtBe_3H_4^+$$

(metastable confirmed decompositions are given as solid arrows)

Such rearrangement may involve an intermediate similar to that postulated for ethylene elimination from even-electron ions of the Group IVb metals (p. 107)

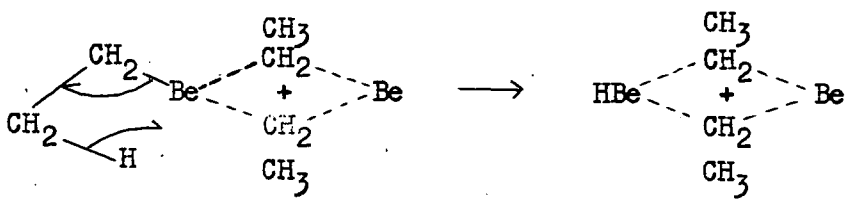

Alternatively or in addition a more complex mechanism involving a bridging ethyl group may apply.

The resulting ions can obviously be formulated in a variety of ways depending whether a hydrogen atom or ethyl group is involved in a bridge between two beryllium atoms. For example $EtBe_2H_2^+$ could be

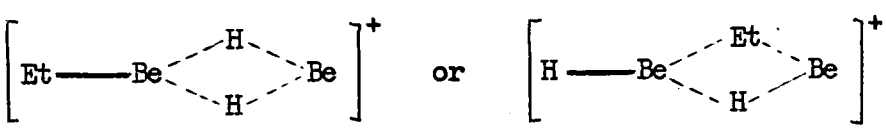

In addition trimer ions can be formulated as a 6-membered ring or a spiro structure:

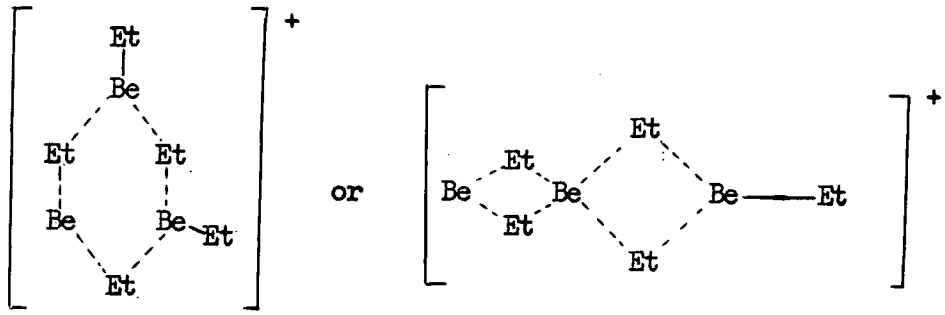

The hydride ions $Et_2Be_2H^+$ and $EtBe_2H_2^+$ also decompose by H_2 loss producing low abundance ions.

$Pr_3Be_2^+$ produced in the spectra of both propyl compounds shows successive elimination of propene giving $Pr_2Be_2H^+$ and $PrBe_2H_2^+$. In addition loss of ethylene is observed from $Pr_2Be_2H^+$ which may involve formation of a methyl group. e.g.

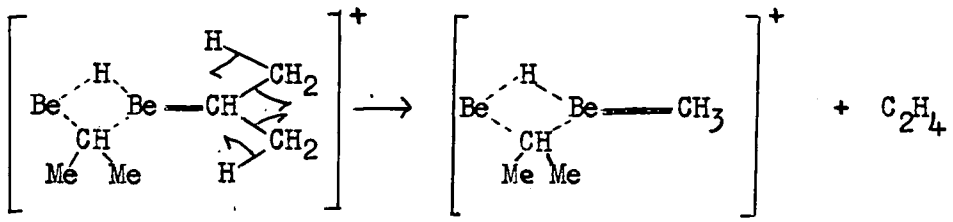

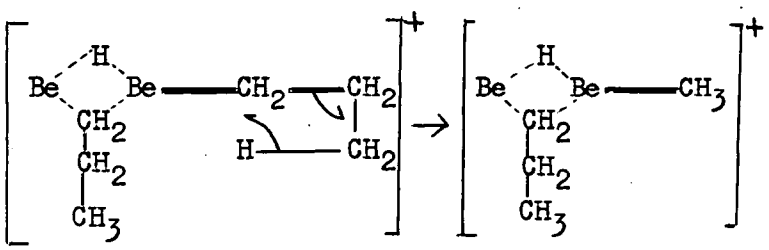

The bridging propyl group may also be involved.

Ions of very low abundance are observed at low source temperatures which could be produced by methane loss

$$Pr_3Be_2^+ \longrightarrow C_8H_{17}Be_2^+ + CH_4$$

$$Pr_2Be_2H^+ \longrightarrow C_5H_{11}Be_2^+ + CH_4$$

Although the mass spectrum of dimethylberyllium shows no ions of the type $Me_{2n}Be_n^{+\cdot}$, $Me_3Be_2^+$ carries 0.82% of the total ion current at low

Fig. 19.

Metastable confirmed decompositions for $C_xH_yBe^+$ ions for diethylberyllium

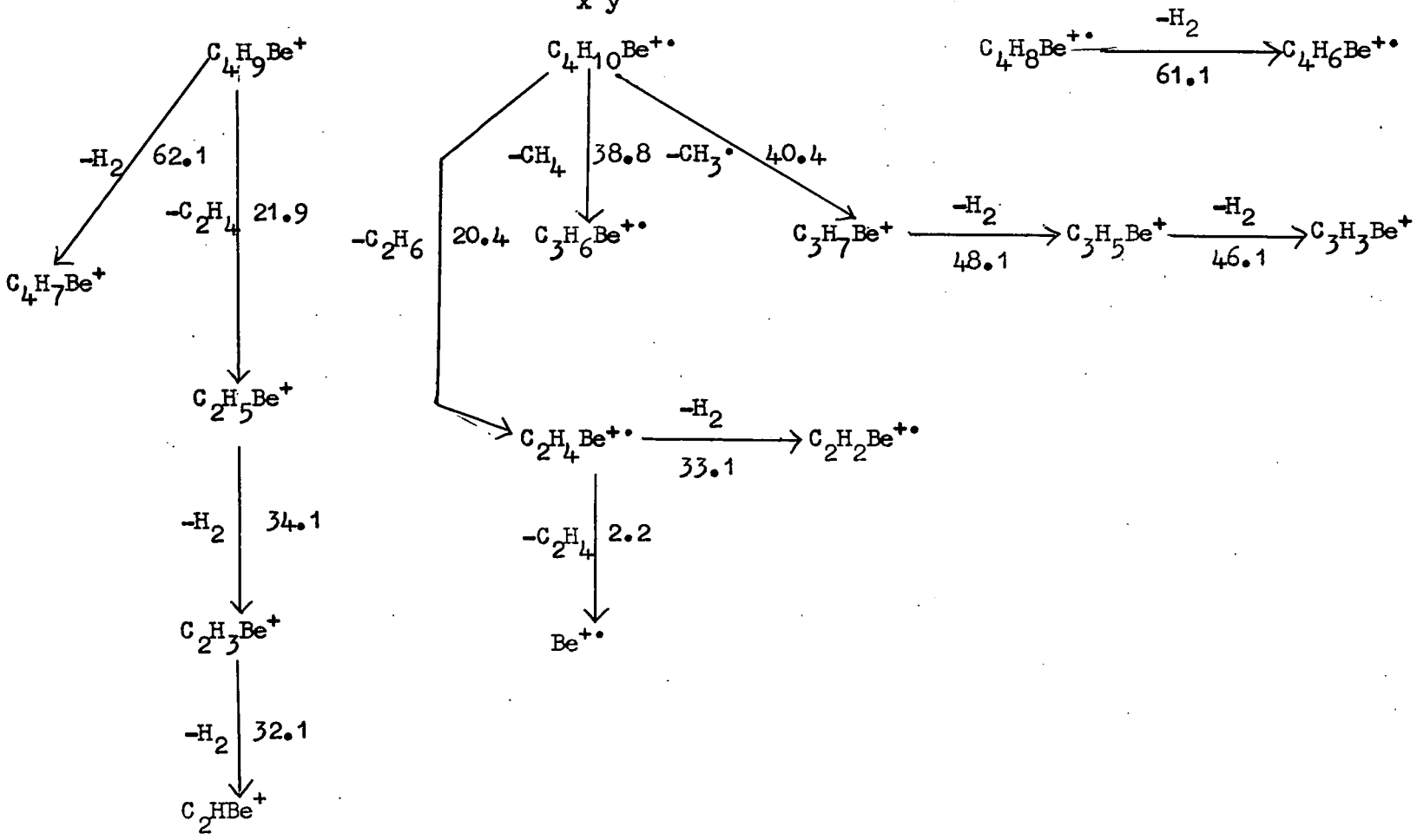

70eV; numbers are observed mass of metastable peak.

Fig. 20.

Metastable confirmed decompositions for $C_xH_yBe^+$ ions for di-propylberyllium compounds.

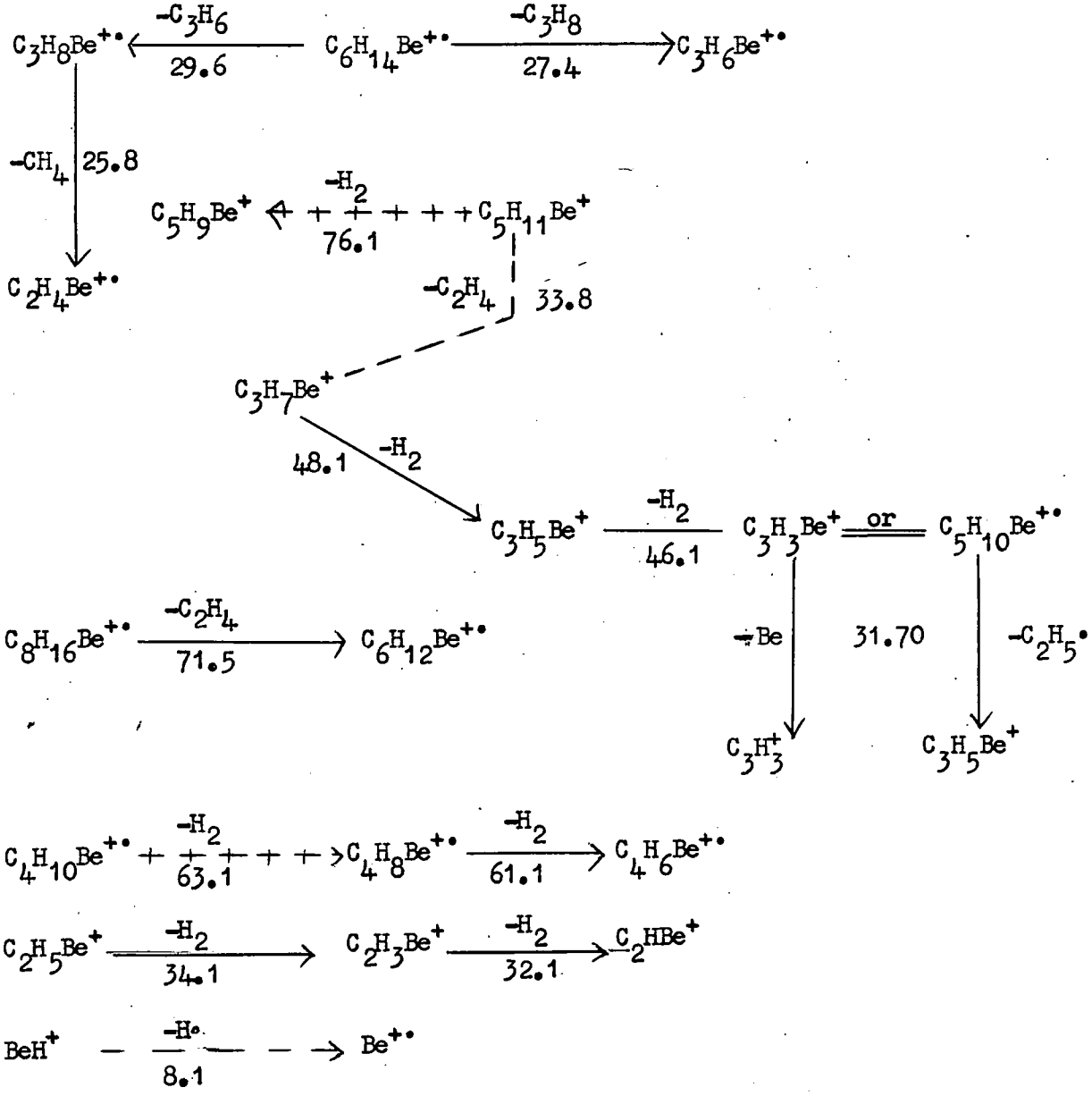

70eV; numbers are observed mass of the metastable peak. Solid arrows indicate metastable transitions common to both $(n\text{-Pr})_2Be$ and $(i\text{-Pr})_2Be$
Arrows ——→ indicate transitions observed only for $(i\text{-Pr})_2Be$.
Arrows + + + indicate transitions observed only for $(n\text{-Pr})_2Be$.

Fig. 21.

Metastable confirmed decompositions for di-tertiary-butylberyllium

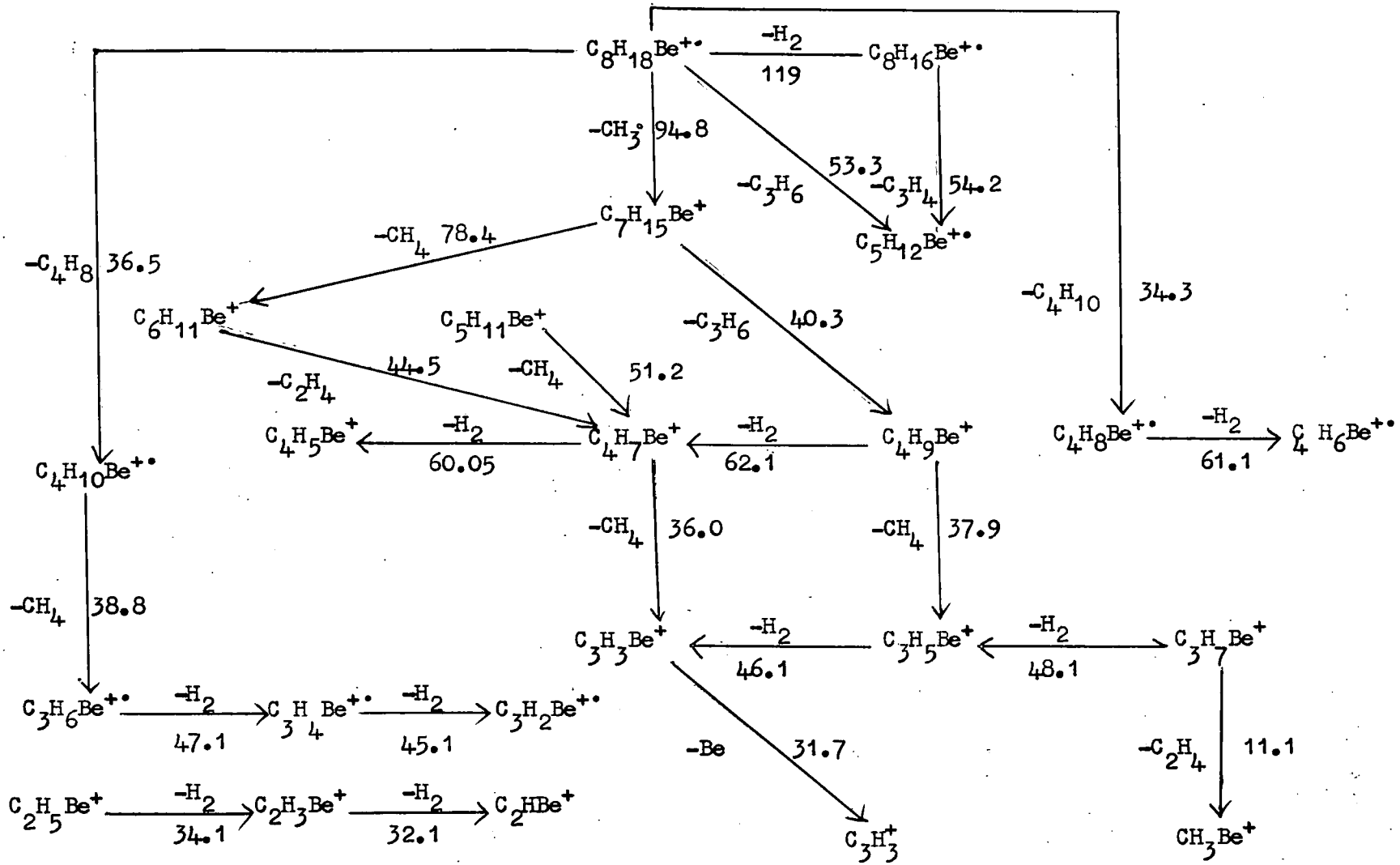

At 70eV; numbers are mass of observed metastable peak.

Fig. 22.

Metastable confirmed decompositions for di-iso-butylberyllium.

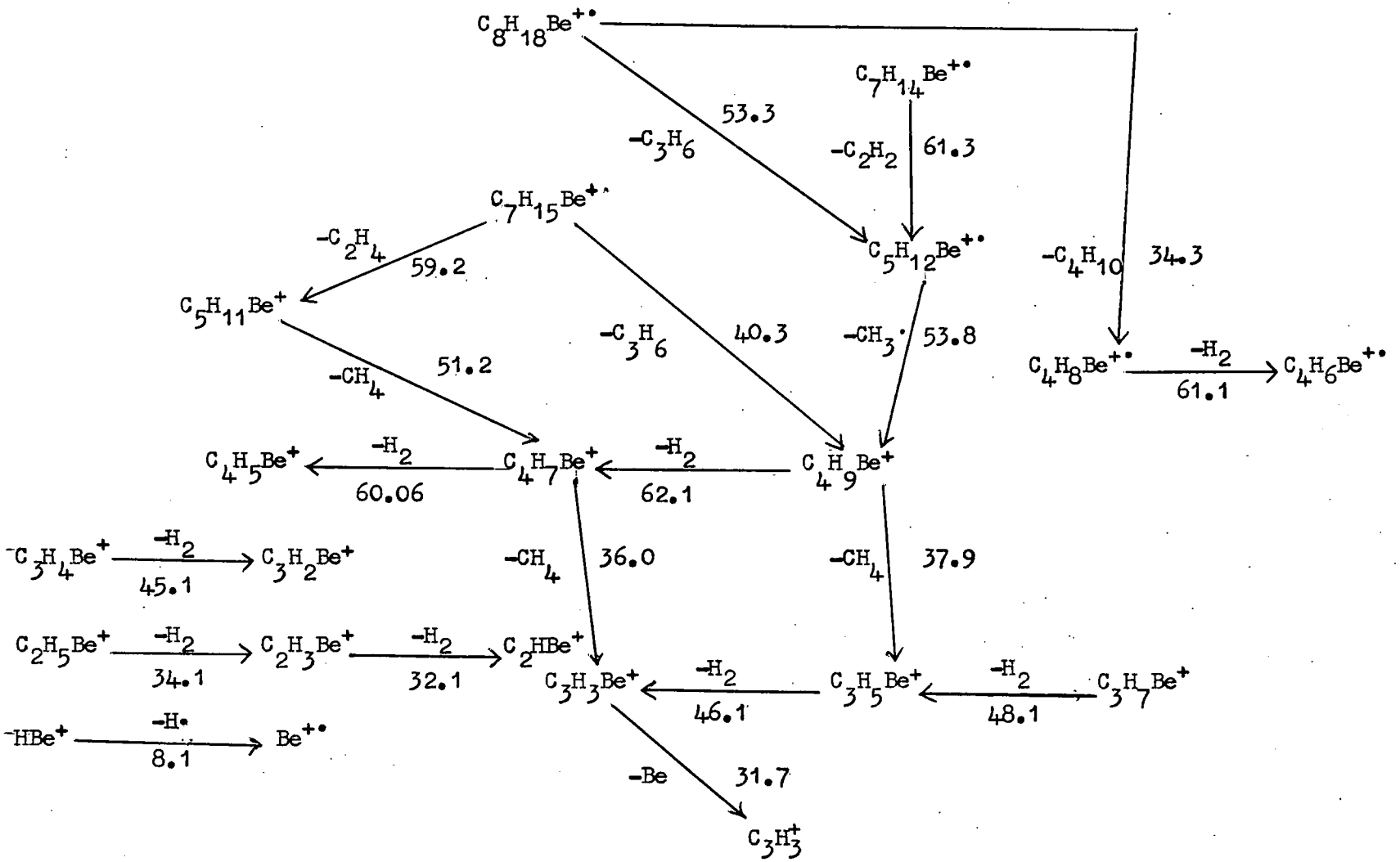

at 70eV; numbers are mass of observed metastable peak.

source temperatures. The ion $C_2H_5Be_2^+$ could be produced by methane loss from $Me_3Be_2^+$. With this compound the ions $C_{12}H_{33}Be_8^+$, $C_{10}H_{27}Be_7^+$, $C_8H_{21}Be_6^+$ and $C_6H_{15}Be_5^+$ are observed in low abundance together with metastable confirmed eliminations of C_2H_6Be (Me_2Be?)

$$C_{12}H_{33}Be_8^+ \xrightarrow{-C_2H_6Be} C_{10}H_{27}Be_7^+ \xrightarrow{-C_2H_6Be} C_8H_{21}Be_6^+$$

Since these are all even-electron they must be fragment ions of some unobserved parent ion. It seems unlikely that $(Me_2Be)_8^{+\cdot}$ is the parent ion since four carbon atoms and fifteen hydrogen atoms must then be lost either as radicals or molecules to give $C_{12}H_{33}Be_8^+$. It is possible that these ions are produced by ionization of a complex associated beryllium molecule formed during slight thermal decomposition of the dimethylberyllium polymer at 50°C (i.e. the sample temperature required) involving methane and hydrogen loss.

Obviously many structures can be postulated for these ions. However it does reflect the polymeric nature of solid dimethylberyllium that ions containing up to eight beryllium atoms are observed.

Modes of Decomposition of $C_xH_yBe^+$ ions.

Metastable confirmed decompositions for these ions are given in figures 18,19,20,21 and 22. The modes of decomposition observed for parent monomeric ions, $R_2Be^{+\cdot}$ are first discussed since these are similar for all compounds.

Parent Ion Decompositions.

The simple bond cleavage decomposition

$$R_2Be^{+\cdot} \longrightarrow RBe^+ + R\cdot$$

with formation of the abundant even-electron ion RBe^+, is not confirmed by a metastable peak for any compounds studied. With di-tert-butylberyllium

$C_4H_9^+$ is produced in much higher abundance than for di-iso-butylberyllium which suggests that for this compound the fragmentation:-

$$(t\text{-}Bu)_2Be^{+\bullet} \longrightarrow Me_3C^+ + C_4H_9Be\bullet$$

is important.

Carbon-carbon bond cleavage is also observed, the following decompositions being metastable confirmed:

$$Et_2Be^{+\bullet} \longrightarrow EtBeCH_2^+ + CH_3\bullet$$

$$(t\text{-}Bu)_2Be^{+\bullet} \longrightarrow t\text{-}Bu\text{-}Be\text{-}CMe_2^+ + CH_3\bullet$$

For di-tert-butylberyllium the resulting ion is of high abundance especially at 12eV. This is perhaps expected in view of the fact that hydrocarbons cleave readily at the carbon atom of greatest branching [1,9]. With the iso-butyl compound the $(p\text{-}Me)^+$ ion (i.e. parent ion minus methyl) is only of low abundance.

In contrast the $(p\text{-}Me)^+$ ion for di-iso-propylberyllium is lower than for the normal compound. (i.e. $(p\text{-}Me)^+$ constitutes 0.23% of the total beryllium-containing ions for di-iso-propylberyllium and 0.55% for di-n-propylberyllium). Surprisingly diethylberyllium gives an abundant $(p\text{-}Me)^+$ ion especially at 12eV.

Parent ions also decompose by processes which involve rearrangement. All the dialkyls show a metastable peak for

$$(C_nH_{2n+1})_2Be^{+\bullet} \longrightarrow C_nH_{2n}Be^{+\bullet} + C_nH_{2n+2}$$

The ion $C_nH_{2n}Be^{+\bullet}$ is a major beryllium-containing ion. A simple hydrogen migration can be postulated; thus for the methyl compound a 4-centre intermediate can be invoked.

Table 4.3.4.

Abundances of parent monomeric ions and major Be-containing ions for beryllium dialkyls.

	Me_2Be		Et_2Be		$(i\text{-}Pr)_2Be$		$(n\text{-}Pr)_2Be$		$(i\text{-}Bu)_2Be$		$(t\text{-}Bu)_2Be$	
	70eV	15eV	70eV	12eV	70eV	12eV	70eV	12eV	70eV	12eV	70eV	12eV
parent ion $(C_nH_{2n+1})_2Be^{+\bullet}$	17.99	78.37	8.02	21.28	2.76	6.91	1.34	3.75	0.08	0.23	0.37	3.36
$(p\text{-}Me^{\bullet})^+$	(see below)		2.02	4.03	0.12	0.16	0.17	0.56	0.08	0.28	1.95	15.29
$(p\text{-}C_nH_{2n})^{+\bullet}$	-	-	2.76	0.43	0.61	1.34	0.69	0.89	0.44	0.55	0.47	2.28
$(p\text{-}C_nH_{2n+1}^{\bullet})^+$	31.93	2.52	14.92	9.33	9.99	12.04	14.67	15.94	7.87	8.86	4.59	8.62
$(p\text{-}C_nH_{2n+2})^{+\bullet}$	15.14	6.89	23.04	30.67	13.70	30.76	11.09	24.53	3.34	7.34	2.70	9.54
% of total ion current due to $C_xH_yBe^+$ ions carried by above ions	80.1	96.8	75.1	93.5	51.6	83.2	66.5	84.4	54.0	87.4	37.2	82.5
Source temp. °C	210°		196°		215-220°		210-215°		235°		240°	

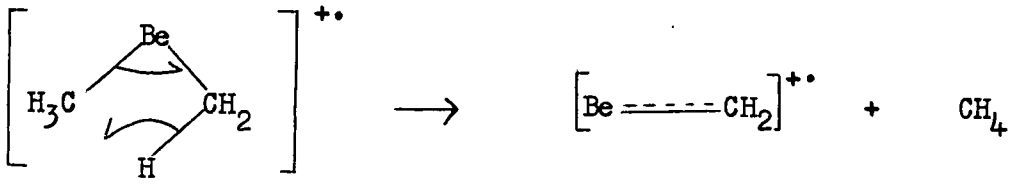

For the other dialkyls the position of hydrogen atoms involved can only be found by deuterium labelling in the alkyl group.

From the energy of dissociation

$$C_nH_{2n+1}Be^+ \longrightarrow C_nH_{2n}Be^{+\bullet} + H^\bullet$$

found from appearance potentials (p.98) it has been tentatively suggested that the ion $C_nH_{2n}Be^{+\bullet}$ ($n \geqslant 2$) formed by the above process may have a ring structure.

A metastable peak corresponding to loss of the alkene, C_nH_{2n}, is observed from parent ions, $(C_nH_{2n+1})_2Be$, of di-iso-propyl-, di-n-propyl - and di-tert-butylberyllium. Such rearrangement probably involves hydride formation. For example:

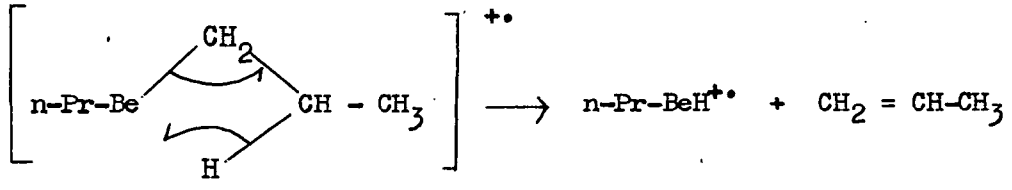

Although no metastable peak is present, the ions $RBeH^{+\bullet}$ (R = Et or i-Bu) are probably produced in a similar way in the spectra of diethyl- and di-iso-butylberyllium. With dimethylberyllium the ion $CH_3BeH^{+\bullet}$ is not observed, probably because its formation from $Me_2Be^{+\bullet}$ would involve CH_2: elimination.

In table 4.3.4. it will be seen that parent ions and fragment ions formed by the decompositions of parent ions discussed above account for most of the ion current due to $C_xH_yBe^+$ ions observed at high source

temperatures. This is especially true at low electron voltages when the number of types of ions formed is far less.

In addition to the decompositions discussed above, $(t\text{-Bu})_2Be^{+\bullet}$ and $(i\text{-Bu})_2Be^{+\bullet}$ show a metastable peak for propene elimination producing $C_5H_{12}Be^{+\bullet}$ in low abundance. A low abundance ion is also produced for methane elimination from $Et_2Be^{+\bullet}$

Fragment Ion Decompositions.

Elimination of H_2 from $C_xH_yBe^+$ ions is very favourable and many metastable peaks for such decompositions are observed. (Figs. 18-22) Whenever an abundant $C_xH_yBe^+$ ion occurs, then ions of much lower abundance are also observed 2,4,6 etc. mass units below formed by loss of hydrogen. Loss of a hydrogen atom gives a metastable peak in one case only:

$$HBe^+ \longrightarrow Be^{+\bullet} + H\bullet$$

The propyl and butyl compounds produce ions which show metastable peaks for methane loss. Such decomposition is present for both odd- and even-electron ions. It is interesting to note that methane loss is the only alkane elimination from fragment ions that gives a metastable peak.

Both ethylene and propene on the other hand are eliminated from fragment ions (figs. 20,21,22) e.g.

$(t\text{-Bu})_2Be$	$C_7H_{15}Be^+ \rightarrow C_4H_9Be^+ + C_3H_6$;	
$(i\text{-Bu})_2Be$	$C_6H_{11}Be^+ \rightarrow C_4H_7Be^+ + C_2H_4$	
$(i\text{-Pr})_2Be$	$C_5H_{11}Be^+ \rightarrow C_3H_7Be^+ + C_2H_4$	
Et_2Be	$C_2H_4Be^+ \rightarrow Be^{+\bullet} + C_2H_4$	

The elimination of Be is observed only from $C_3H_3Be^+$ produced by the propyl and butyl compounds.

$$C_3H_3Be^+ \rightarrow C_3H_3^+ + Be \qquad m^* \quad 31.7$$

With the two butyl compounds the metastable peak at 31.7 can only be assigned to the above process but for the propyl compounds the transition

$$C_5H_{10}Be^{+\bullet} \rightarrow C_3H_5Be^{+} + C_2H_5\bullet$$

can also apply.

If $C_3H_3^+$ formed is identical to that produced by ionization of $\cdot CH_2 - C\equiv CH$ then it is not surprising that the charge is retained by the hydrocarbon species since

$$\left.\begin{aligned} I\ (\cdot CH_2 - C\equiv CH) &= 8.25 \pm 0.08eV \\ I\ (Be) &= 9.32eV \end{aligned}\right\} \text{ ref. 102.}$$

and the charge would be expected to reside on the fragment of lowest ionization potential. [1,4]

Obviously the $C_3H_3^+$ ion could also have a ring structure especially if the ion $C_3H_3Be^+$ has the structure 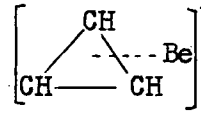 . In the spectra of diethylberyllium the ion $C_3H_3Be^+$ is only of low abundance, which may account for the absence of a metastable peak corresponding to Be elimination. More probably this is because the ion, $C_3H_3Be^+$, has a different structure for this compound. It could for example be $(CH_2 - Be - C\equiv CH)^+$ rather than structures discussed earlier which involve all three carbon atoms bonded together.

Distinguishing Isomers.

The 70eV spectra of the two propyl compounds differ mainly in the relative intensities of the ions $C_3H_6Be^{+\bullet}$ and $C_3H_7Be^+$. At 12eV the spectra are almost identical. In contrast di-iso-butyl- and di-tert-butyl beryllium are most easily identified from their mass spectra at 12eV. At this voltage the tertiary-butyl compound gives an intense ion formed by carbon-carbon

cleavage in the parent ion:

$$(t\text{-}Bu)_2Be^{+\bullet} \longrightarrow t\text{-}Bu\text{-}Be\text{-}CMe_2^{+} + Me\bullet$$

For the iso-butyl compound the ion $C_7H_{15}Be^{+}$ although observed is always of low abundance.

4.4. Mass Spectra of Organoaluminium Compounds.

In view of the considerable effect of source temperature in the mass spectrometry of organoberyllium compounds, it is desirable to determine the effect of this instrument parameter on the mass spectra of organoaluminium compounds which, like the beryllium compounds, form electron deficient molecules. It is also of interest to compare the decomposition modes of the organoderivatives of this metal with those observed for beryllium and group IV derivatives.

Ion abundances of the compounds studied are shown in tables 4.4.1, 4.4.2. and 4.4.3. Unfortunately the sample of triethylaluminium used was contaminated by diethylaluminium ethoxide and so it was not certain which of the peaks in the mass spectrum obtained are due to the ethoxide. Since the major peaks in the spectrum of mixture of diethylaluminium ethoxide and other oxides all contain oxygen, it was assumed that all ions not containing oxygen are due to triethylaluminium. The mass spectra given in table 4.4.3. are thus obtained. Abundances are expressed as a percentage of the base peak rather than as percentage of total ion current because hydrocarbon peaks can come from both triethylaluminium or the ethoxide.

4.4.1. Effect of Source Temperature.

a) Trimethylaluminium.

The mass spectrum of trimethylaluminium has been recorded at 70eV and dimeric ions $Me_5Al_2^+$ detected in extremely low abundance.[12] The effect of source temperature was not considered.

The present study shows that dimeric ions $Me_5Al_2^+$ and $Me_3Al_2^+$ are

Table 4.4.1.

Ion abundances * for Me_3Al and Me_2AlH.

	Me_3Al				Me_2AlH		
m/e	Ion$^+$	Source Temp. °C		m/e	Ion$^+$	Source Temp. °C	
		195	45 - 50			210	50 - 70
129	Me_5Al_2	.14	2.97	159	$Me_5Al_3H_3$	.01	.45
99	Me_3Al_2	.04	.55	115	Me_4Al_2H	.79	4.93
72	Me_3Al•	4.60	6.13	101	$Me_3Al_2H_2$	4.18	24.72
57	Me_2Al	64.78	67.15	72	Me_3Al•	3.06	0.44
56	C_4H_8•	.45	1.14	58	Me_2AlH•	1.51	0.99
	C_2H_5Al•	.69	.66	57	C_4H_9	1.64	0.23
43	C_3H_7	.43	.74		Me_2Al	60.68	39.38
	CH_4Al	3.07	2.37	56	C_4H_8•	1.51	1.97
42	C_3H_6•	.15	.29		C_2H_5Al•	0.54	0.67
	CH_3Al•	5.06	3.49	55	C_4H_7	.32	.37
41	CH_2Al	.75	.60		C_2H_4Al	.09	.20
29	C_2H_5	.20	.41	44	C_3H_8•	.05	.05
	H_2Al	.88	.83		CH_5Al•	.07	.06
28	C_2H_4•	.15	.29	43	C_3H_7	1.48	1.59
	HAl•	.44	.41		CH_4Al	2.85	2.23
27	C_2H_3•	.30	.41	42	C_3H_6•	.64	.74
	Al	12.00	8.29		CH_3Al•	3.86	3.14
26	C_2H_2•	.12	.19	41	C_3H_5	1.19	1.50
16	CH_4•	2.58	1.17		CH_2Al	.50	.18
15	CH_3	2.54	1.46	29	C_2H_5	.67	.65
14	CH_2•	.31	.33		H_2Al	.83	.37
13	CH	.11	.10	28	C_2H_4•	.19	.20
12	C•	.08	.02		HAl•	.33	.20
				27	C_2H_3	.21	.24
					Al	7.33	7.71
				26	C_2H_2•	.13	.12
				16	CH_4•	2.63	1.97
				15	CH_3	2.27	1.78
				14	CH_2•	.30	.31
				13	CH	.09	.12
				12	C•	.03	.05

* expressed as % of total ion current at 70eV.

Table 4.4.2.

Ion abundances * for Et_2AlH

m/e	Ion$^+$	Source Temp. 214°C	Source Temp. 32–45°C	m/e	Ion$^+$	Source Temp. 214°C	Source Temp. 32–45°C
229	$Et_5Al_3H_3$	.02	.27	42	CH_3Al	.53	.16
172	$Et_4Al_2H_2$	.05	.90	30	C_2H_6	.99	4.37
171	Et_4Al_2H	.18	1.54	29	C_2H_5	1.41	3.87
143	$Et_3Al_2H_2$	1.16	12.79		H_2Al	4.72	2.50
115	$Et_2Al_2H_3$	.91	5.83	28	C_2H_4	11.84	14.71
114	Et_3Al	3.54	1.21		HAl	1.18	.39
113	$C_6H_{14}Al$	.05	.32	27	C_2H_3	7.22	5.80
87	$EtAl_2H_4$	.07	.18		Al	8.56	5.71
86	Et_2AlH	1.13	.78	26	C_2H_2	5.89	3.33
85	Et_2Al	19.18	19.27	25	C_2H	.64	.86
71	C_3H_8Al	.88	.47	24	C_2	.24	.20
70	C_3H_7Al	.07	.08	16	CH_4	.11	.40
69	C_3H_6Al	.06	.21	15	CH_3	.23	.71
57	C_2H_6Al	22.26	10.27	14	CH_2	.27	.38
56	C_2H_5Al	2.36	.86	13	CH	.11	.13
55	C_2H_4Al	2.36	.86	12	C	.05	.06
43	CH_4Al	1.75	.62				

* expressed as % of total ion current at 70eV.

Table 4.4.3.

Ion abundances * for Et_3Al and $Et_2Al(OEt)$

m/e	Ion$^+$	Abundance	m/e	Ion$^+$	Abundance
		Et_3Al			
114	$Et_3Al\cdot$	12.5	57	HAlEt	100
99	Et_2AlCH_2	3.4	56	$EtAl\cdot$	6.07
85	Et_2Al	69.7	55	C_2H_4Al	7.18
84	$C_4H_9Al\cdot$	.20	43	CH_4Al	4.29
83	C_4H_8Al	.74	42	$CH_3Al\cdot$	1.48
71	C_3H_8Al	2.74	29	H_2Al	14.29
70	$C_3H_7Al\cdot$	.93	28	$HAl\cdot$	2.07
69	C_3H_6Al	.99	27	Al	23.83
		Et_2AlOEt			
260	$Et_4Al_2(OEt)_2$ °	.45	131	$C_4H_{13}Al_2)$	2.62
259	$C_{12}H_{29}Al_2O_2$	1.35	129	$C_4H_{11}Al_2O$	3.49
231	$C_{10}H_{25}Al_2O_2$	100.	117	$C_2H_7Al_2O_2$	9.28
215	$C_9H_{21}Al_2O_2$	1.23	115	$C_2H_5Al_2O_2$	5.47
	$C_{10}H_{25}Al_2O$	3.67	101	$EtAl(OEt)$ or $[EtAl(OEt)]_2^+$	10.30
203	$C_8H_{21}Al_2O_2$	74.1			
187	$C_7H_{17}Al_2O_2$	6.54		$C_2H_7Al_2O$	4.23
	$C_8H_{21}Al_2O$	2.50	89	$H_3Al_2O_2$	8.60
175	$C_6H_{17}Al_2O_2$	51.0	73	$HAl(OEt)$	11.20
173	$C_6H_{15}Al_2O_2$	14.0			
159	$C_6H_{17}Al_2O$	2.86			
147	$C_4H_{13}Al_2O_2$	28.80			
145	$C_4H_{11}Al_2O_2$	9.08			
143	$C_4H_9Al_2O_2$	2.94			

* expressed as % of total ion current at 70eV.

Table 4.4.4.

Variation of ion abundances * of Me_3Al with source temperature.

Ion type	Source Temperature °C								
	44–50	50–57	60–75	75–85	85–98	120–128	155–160	175–178	195
Me_3Al^+	6.13	7.06	6.93	6.72	6.07	5.82	5.31	4.88	4.60
Monomer $AlC_wH_x^+$	89.93	91.82	92.02	91.17	91.91	90.50	90.91	90.37	92.27
Dimer $Al_2C_yH_z^+$	3.52	2.16	0.99	0.62	0.40	0.29	0.22	0.16	0.18
Hydrocarbon m/e > 16	3.44	3.02	3.07	2.81	2.52	2.96	2.58	2.61	1.80
m/e ≤ 16	3.08	3.00	3.92	5.40	5.16	6.24	6.29	5.41	5.62

* expressed as percentage of total ion current at 70eV.

Table 4.4.5.

Variation of ion abundances * of Me_2AlH with source temperature.

Ion type	Source Temperature °C							
	50–70	70–85	90–102	125–135	135–160	175–180	195	210
Dimer $Al_2C_yH_z^+$	29.65	24.34	22.80	20.00	16.56	7.40	4.39	4.97
Trimer $Al_3C_wH_x^+$	0.45	0.05	0.04	0.05	0.05	0.04	0.06	0.01
Monomer $AlC_aH_b^+$ except Me_3Al^+	56.13	50.33	62.07	60.57	67.96	71.20	77.80	78.59
Me_3Al^+	0.44	0.52	0.45	1.02	1.66	2.30	3.07	3.06
Hydrocarbon m/e > 16	7.66	9.43	9.53	12.62	9.28	10.47	10.33	8.03
m/e ≤ 16	4.23	5.32	5.11	6.77	4.49	8.60	4.35	5.32

* expressed as percentage of total ion current at 70eV.

quite abundant at source temperatures of ~40°C but their abundance rapidly diminishes as the source temperature increases (table 4.4.4.). Such variation is adequately explained by decomposition of dimer molecules to monomer molecules, prior to ionization, becoming increasingly important as the source temperature increases. The low heat of dimerisation of trimethylaluminium is in agreement with this.[148]

$$2Me_3Al \rightleftharpoons Me_6Al_2 \quad \Delta H = -20.2 \text{ Kcal. mole.}^{-1}$$

The pyrolysis of trimethylaluminium at 200 - 250°C has been studied[149] and proceeds by the elimination of methane and formation of aluminium carbide. The variation given in table 4.4.4. shows that as the source temperature increases so hydrocarbon ions m/e ≤ 16 become more important. However even at 195°C all hydrocarbon ions constitute only 7.5% of the total ion current.

b) Dimethylaluminium Hydride.

The variation of the 70eV mass spectrum with source temperature is given in table 4.4.5. At low source temperatures dimeric ions constitute a large proportion of the ion current and the trimeric ion $Me_5Al_3H_3^+$ carries 0.45% of the total ion current. As the temperature increases so monomeric ions, $C_aH_bAl^+$, become more predominant, and this may be partly due to the thermal decomposition of associated molecules into monomer molecules prior to ionization. However from the marked increase in abundance of $Me_3Al^{+\bullet}$ with increase in source temperature, thermal rearrangement of $(Me_2AlH)_n$ species to trimethylaluminium prior to ionization is mainly responsible for the high abundance of monomer ions, $C_aH_bAl^+$, at high source temperatures. The presence of $Me_3Al^{+\bullet}$ at low source temperatures

Table 4.4.6.

Abundances of monomer ions, $C_aH_bAl^+$, due to trimethylaluminium and dimethylaluminium hydride in the spectrum (70eV) of dimethylaluminium hydride at various source temperatures.

	Source Temperature °C.						
	50–70	75–85	85–98	120–128	155–160	175–180	195
$Me_3Al^{+\cdot}$ plus decomposition ions $C_aH_bAl^+$	5.72	7.05	6.81	16.04	28.53	42.57	60.09
$Me_2AlH^{+\cdot}$ plus decomposition ions $C_aH_bAl^+$	50.41	53.28	55.26	44.53	39.43	28.63	17.71

Table 4.4.7.

Variation of ion abundances * in 70eV spectrum of diethylaluminium hydride with source temperature.

	32–45	45–63	70–87	90–105	105–120	130–140	158–165	189–192	214
Dimer $Al_2C_yH_z^+$	21.24	18.90	17.08	16.55	14.98	14.36	10.26	4.27	2.37
Trimer $Al_3C_wH_x^+$	0.27	0.19	0.08	0.06	0.05	0.06	0.04	0.03	0.02
Monomer $AlC_aH_b^+$ except $Et_3Al^{+\cdot}$	42.50	44.79	47.19	48.57	50.12	53.94	58.43	63.74	64.09
$Et_3Al^{+\cdot}$	1.21	1.57	1.55	2.12	2.27	2.55	2.66	3.18	3.54
Hydrocarbon $C_2H_6^{+\cdot}$	4.37	4.22	3.46	3.31	2.80	2.11	1.55	0.98	0.99
$m/e \leqslant 29$	30.45	30.34	30.65	29.38	29.77	26.99	27.05	27.80	28.03

* expressed as percentage of total ion current.

Rearrangement of dimethylaluminium hydride with increasing Source Temperature.

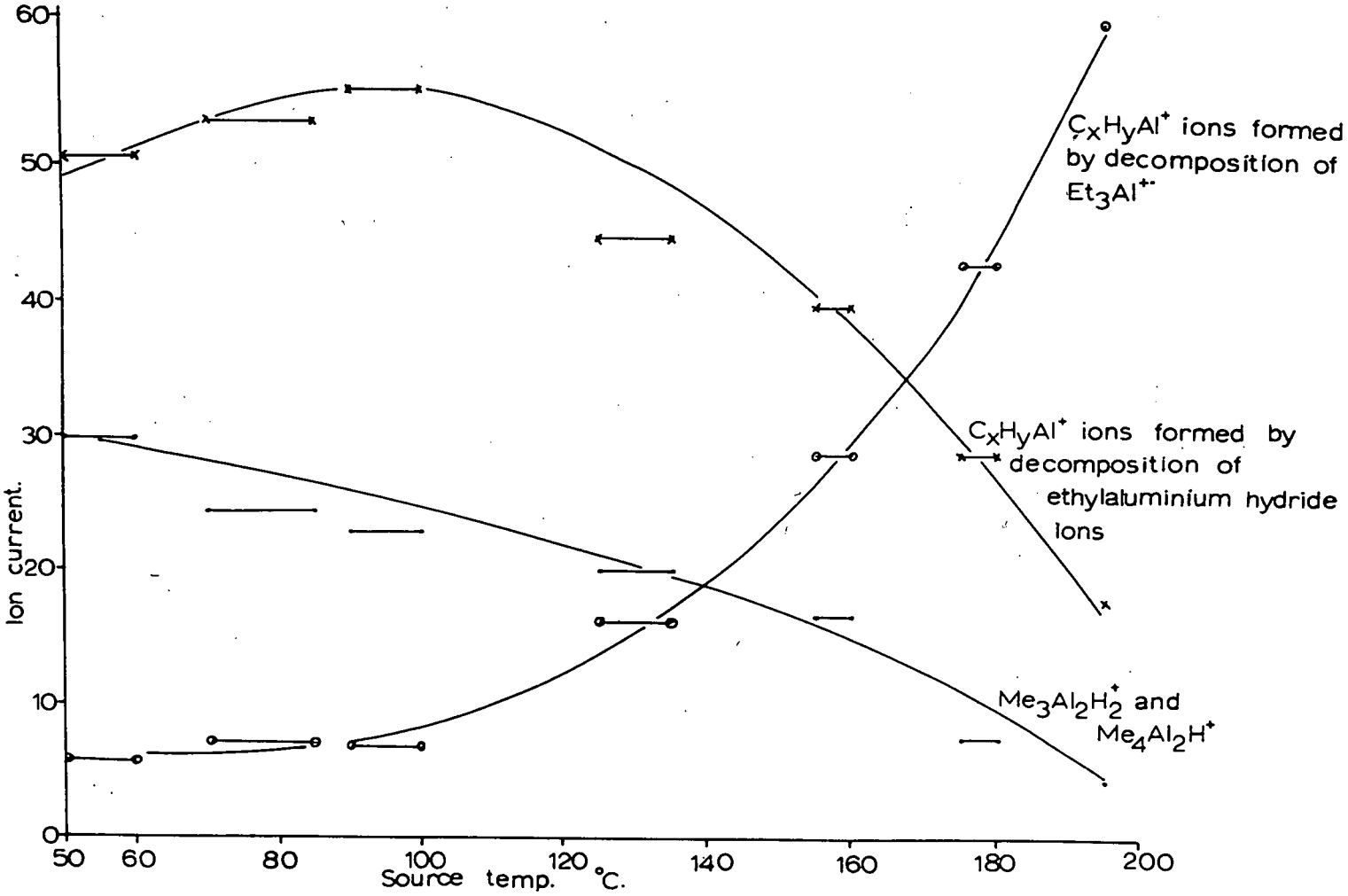

may indicate that the sample of dimethylaluminium hydride used was contaminated with trimethylaluminium or that the ion originates partly from dimer or trimer ions in which transfer of methyl groups from one aluminium atom to another occurs. Certainly in view of the ready transfer of organic groups occurring in the ionization and subsequent decomposition of $A_3M\text{-}M'B_3$ compounds (M,M' = Si,Ge, or Sn) this possibility cannot be ignored entirely.

For trimethylaluminium the variation of the abundances of Me_3Al^+ and other $C_aH_bAl^+$ ions with source temperature is known (table 4.4.4.) Thus from the abundance of $Me_3Al^{+\bullet}$ in a spectrum of dimethylaluminium hydride the percentage of total ion current carried by $C_aH_bAl^+$ ions formed by ionization and subsequent decomposition of trimethylaluminium can be found. In table 4.4.6. the abundances of monomer ions, $C_aH_bAl^+$, due to trimethylaluminium and $C_aH_bAl^+$ ions due to dimethylaluminium hydride in the spectrum of dimethylaluminium hydride at various source temperatures are given.

The abundances of $C_yH_zAl_2^+$ and $C_aH_bAl^+$ ions from dimethylaluminium hydride and $C_eH_fAl^+$ ions from trimethylaluminium are plotted as a function of source temperature in fig 23.

Up to 100°C as dimer ions decrease in abundance so monomer ions from dimethylaluminium hydride become more important. This is because dissociation of associated molecules to Me_2AlH becomes more important as the source temperature increases. At 100°C the thermal rearrangement of $(Me_2AlH)_n$ species begins to increase in importance and ions formed by ionization and subsequent decomposition of trimethylaluminium become significant. At 200°C the mass spectrum recorded is predominantly that

of trimethylaluminium.

Thermal rearrangement of dimethylaluminium hydride was not observed when the vapour density was measured [150] within the temperature ranges 83 - 95°C and 160 - 167°C. The apparent molecular weights obtained were:

Temperature °C.	82.9	88	89	90.8	95.05	160.1	167
Measured molecular weight.	141.6	141.6	139.5	143.3	142.6	118.8	118.5

The little variation of the apparent molecular weight in the temperature range 83 - 95°C was noted by the authors as disturbing. Their results would obviously be greatly influenced by any disproportionation of dimethylaluminium hydride to trimethylaluminium and involatile aluminium hydride.

c) Diethylaluminium Hydride.

Diethylaluminium hydride appears to behave similarly to dimethylaluminium hydride (table 4.4.7.) in that the abundances of dimeric and trimeric ions fall rapidly with increasing source temperature. The ion $Et_3Al^{+\cdot}$ becomes more abundant as the source temperature increases but it is also significant at lower temperatures. This may indicate that transfer of ethyl groups from one aluminium atom to another occurs in dimer or trimer ions or that the sample of hydride used contained some triethylaluminium.

The proportion of ion current carried by dimer and trimer ions falls off rapidly with increasing source temperature. Although the mass spectrum of triethylaluminium has been recorded the sample used was contaminated with ethoxide. Thus the proportion of monomer ions, $C_aH_bAl^+$ due to triethylaluminium in the spectrum of diethylaluminium hydride

cannot be calculated. At 214°C the proportion of triethylaluminium is significant however since the mass spectrum obtained is very similar to that of triethylaluminium (table 4.4.3.). Whereas at a source temperature of 32 - 45°C the most abundant ion is Et_2Al^+, at 214°C the base peak is the same as for triethylaluminium i.e. $EtAlH^+$.

Disproportionation of diethylaluminium hydride giving triethylaluminium has been observed in the purification of this hydride by distillation [151]. The bath temperature should not exceed 80°C and the presence of solid phase in the still pot avoided since this appears to accelerate the disproportionation. In a study of the thermal decomposition of triethylaluminium in a glass vessel disproportionation reactions occurring in rapid succession were purported to lead to the deposition of aluminium as a mirror.[152]

$$2Et_2AlH \longrightarrow Et_3Al + EtAlH_2$$

$$2EtAlH_2 \longrightarrow Et_2AlH + H_3Al$$

4.4.2. Modes of Decomposition.

With the limited number of compounds studied, major ions are predominately even-electron. The ratio of the abundances of even-electron aluminium-containing ions to odd-electron aluminium-containing ions for the following compounds is:

	Abundance of even-electron Al - containing ions	Abundance of odd-electron Al - containing ions	Ratio $\frac{\text{even-electron ions}}{\text{odd-electron ions}}$
Me_3Al	82.76	10.69	7.74
Me_2AlH	60.84	4.38	13.89
Et_2AlH	81.17	5.50	14.20

(c.f. organoberyllium compounds p. 151)

Only for diethylaluminium hydride is a parent ion of an associated organoaluminium molecule detected. At low source temperatures this ion, $(Et_2AlH)_2^{+\cdot}$, constitutes 0.90% of the total ion current. Although ions corresponding to the parent monomer ion may be fragment ions derived by decomposition of dimer and trimer ions, such ions are quite abundant at both low and high source temperatures.

The modes of decomposition for organoaluminium compounds are very similar to those of the group IV organo compounds and may be classified in a similar way.

a) Bond Cleavage by Radical Elimination.

With all compounds a major even-electron ion is produced by loss of a group bonded to aluminium in either parent monomeric, dimeric or trimeric ions.

$$R_3Al^{+\cdot} \longrightarrow R_2Al^{+} + R^{\cdot} \qquad m^* \begin{array}{l} 45.1 \quad R = Me, \\ 63.4 \quad R = Et, \end{array}$$

$$Et_4Al_2(OEt)_2^{+\cdot} \begin{array}{l} \nearrow Et_3Al_2(OEt)_2^{+} + Et^{\cdot} \qquad m^* \; 205.2 \\ \searrow Et_4Al_2(OEt)^{+} + OEt^{\cdot} \qquad m^* \; 177.8 \end{array}$$

With dimethyl - and diethyl-aluminium hydride loss of both alkyl and hydrogen from the parent dimer ion occurs but loss of alkyl occurs to the greater extent. This H· loss probably results from cleavage of the aluminium-hydrogen bond since in the spectra of trimethyl - and triethyl-aluminium loss of H· from $C_aH_bAl^+$ ions by cleavage of a carbon-hydrogen bond is not significant.

With the methyl compounds a methyl group is lost from the even-electron ion Me_2Al^+ but the resulting odd-electron ion is not of high abundance.

$$Me_2Al^{+} \longrightarrow MeAl^{+\cdot} + Me^{\cdot} \qquad m^* \; 30.9$$

The appearance potentials of the ions Me_2Al^+, $MeAl^{+\cdot}$ and Al^+ in the spectrum of trimethylaluminium correspond to simple bond cleavage decompositions. [12]

$$Me_3Al^{+\cdot} \rightarrow Me_2Al^+ \rightarrow MeAl^{+\cdot} \rightarrow Al^+$$

Rearrangement Processes.

b) Alkene Elimination.

With the ethylcompounds the elimination of ethylene from even-electron ions is a major process. For example with diethylaluminium ethoxide eleven metastable peaks are present corresponding to ethylene elimination from even-electron ions. (fig. 25). Also

$$Et_2Al^+ \longrightarrow HAlEt^+ + C_2H_4 \qquad m^* \; 38.2$$

$$Et_4AlH^+ \longrightarrow Et_3Al_2H_2^+ + C_2H_4 \qquad m^* \; 119.6$$

$$Et_3AlH_2^+ \longrightarrow Et_2Al_2H_3^+ + C_2H_4 \qquad m^* \; 92.5$$

$$Et_2AlH_3^+ \longrightarrow EtAl_2H_4^+ + C_2H_4 \qquad m^* \; 65.8$$

As with $>M^+$-Et ions (M = Si,Ge,Sn,Pb) a mechanism involving transfer of a β - hydrogen may be envisaged for elimination of ethylene from $-Al^+$-Et ions. With diethylaluminium ethoxide ethylene may be lost from both ethyl or ethoxy groups attached to aluminium. The formation of $H_3Al_2O_2^+$ must involve loss of ethylene from both. The high abundance of H_2Al^+ with the ethyl compounds is readily ascribed to

$$Et_2Al^+ \longrightarrow EtAlH^+ \longrightarrow H_2Al^+$$

Me_2Al^+ also loses ethylene:

$$Me_2Al^+ \longrightarrow H_2Al^+ + C_2H_4 \qquad m^* \; 14.75$$

This elimination is probably very similar to the elimination of ethylene from Me_3Si^+ and Me_3Ge^+. The ion H_2Al^+ is not as abundant for the methyl

compound as the ethyl.

c) Methane Elimination.

In addition to ethylene elimination Me_2Al^+ ions show a metastable peak for methane loss. The resultant ion although even-electron is of only low abundance.

$$Me_2Al^+ \longrightarrow CH_2Al^+ + CH_4 \qquad m^* \ 29.5$$

In the spectrum of diethylaluminium ethoxide an ion m/e 215 corresponds to methane loss from $Et_3Al_2(OEt)_2^+$.

d) Molecule Elimination by Cleavage of two Al-X Bonds.

Two metastable peaks which may correspond to this process are given below:-

$$Me_2Al^+ \longrightarrow Al^+ + C_2H_6 \qquad m^* \ 12.8$$

$$EtAlH^+ \longrightarrow Al^+ + C_2H_6 \qquad m^* \ 12.8$$

The first process is observed with trimethylaluminium and dimethylaluminium hydride, the second with triethylaluminium and diethylaluminium hydride. Since the presence of a metastable peak does not necessarily indicate an elimination in a single step [128] the two processes above could involve elimination of $2CH_3\cdot$ and $(H\cdot$ and $C_2H_5\cdot)$ respectively. With trimethylaluminium the appearance potential of Al^+ corresponds to the process [12]

$$e + Me_3Al \longrightarrow Al^+ + 3Me\cdot + 2e$$

e) Hydrogen Loss (H_2)

This is observed with the ethyl compounds studied.

$$Et_2Al^+ \longrightarrow C_4H_8Al^+ + H_2 \qquad m^* \ 81$$

$$C_2H_6Al^+ \longrightarrow C_2H_4Al^+ + H_2 \qquad m^* \ 53.1$$

Similarly with diethylaluminium ethoxide ions are present which could result by H_2 loss. (fig. 25)

Fig. 24.

Decomposition diagrams for Me_3Al, Et_3Al, Me_2AlH, and Et_2AlH .

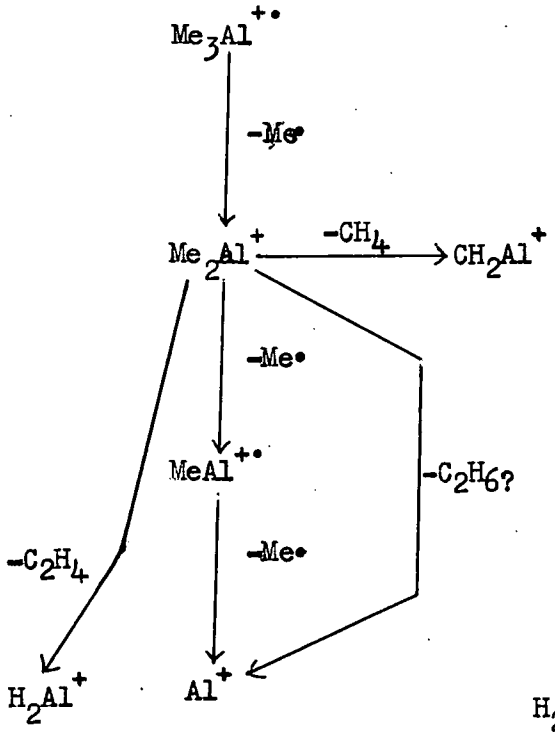

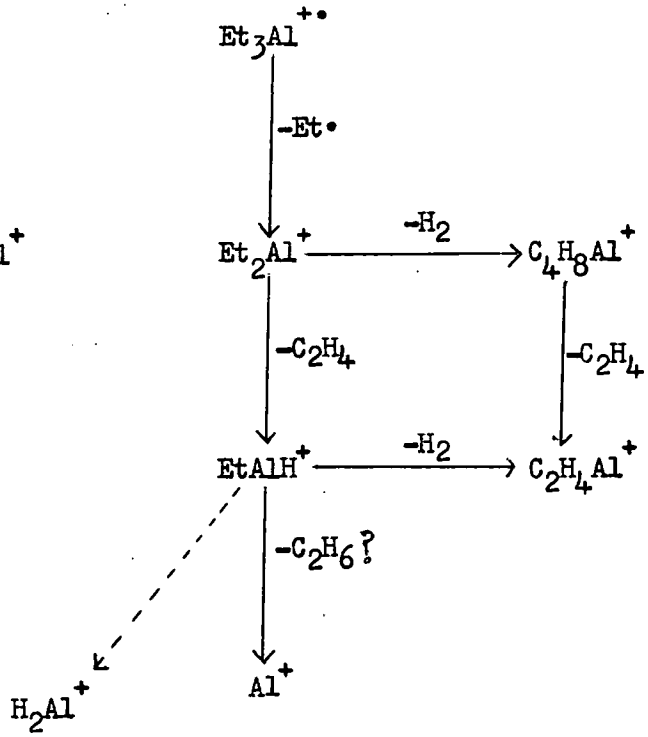

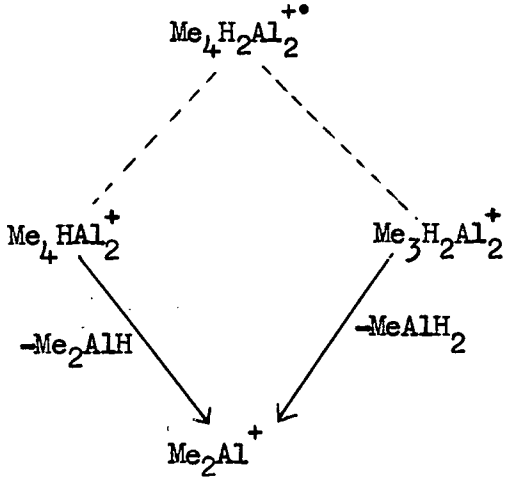

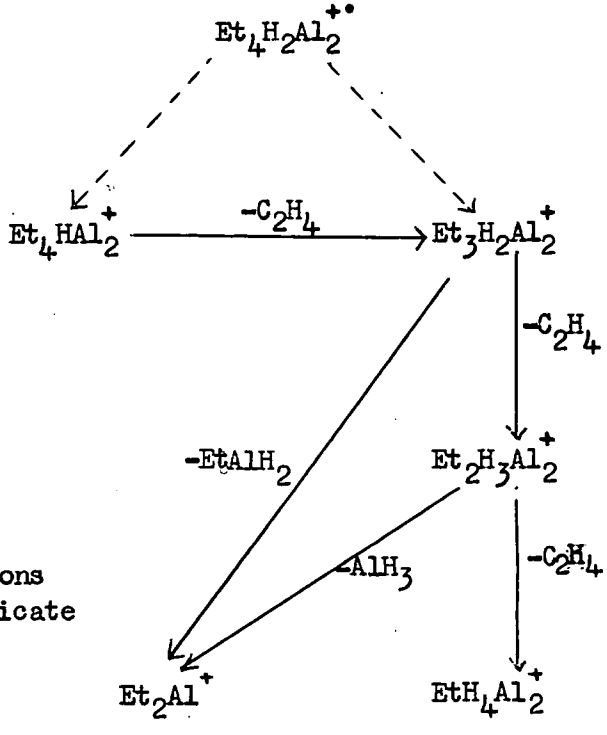

Fragmentations common to two or more ions are shown only once . Solid arrows indicate metastable confirmed decompositions.

Fig. 25.

Decomposition diagram for diethylaluminium ethoxide.

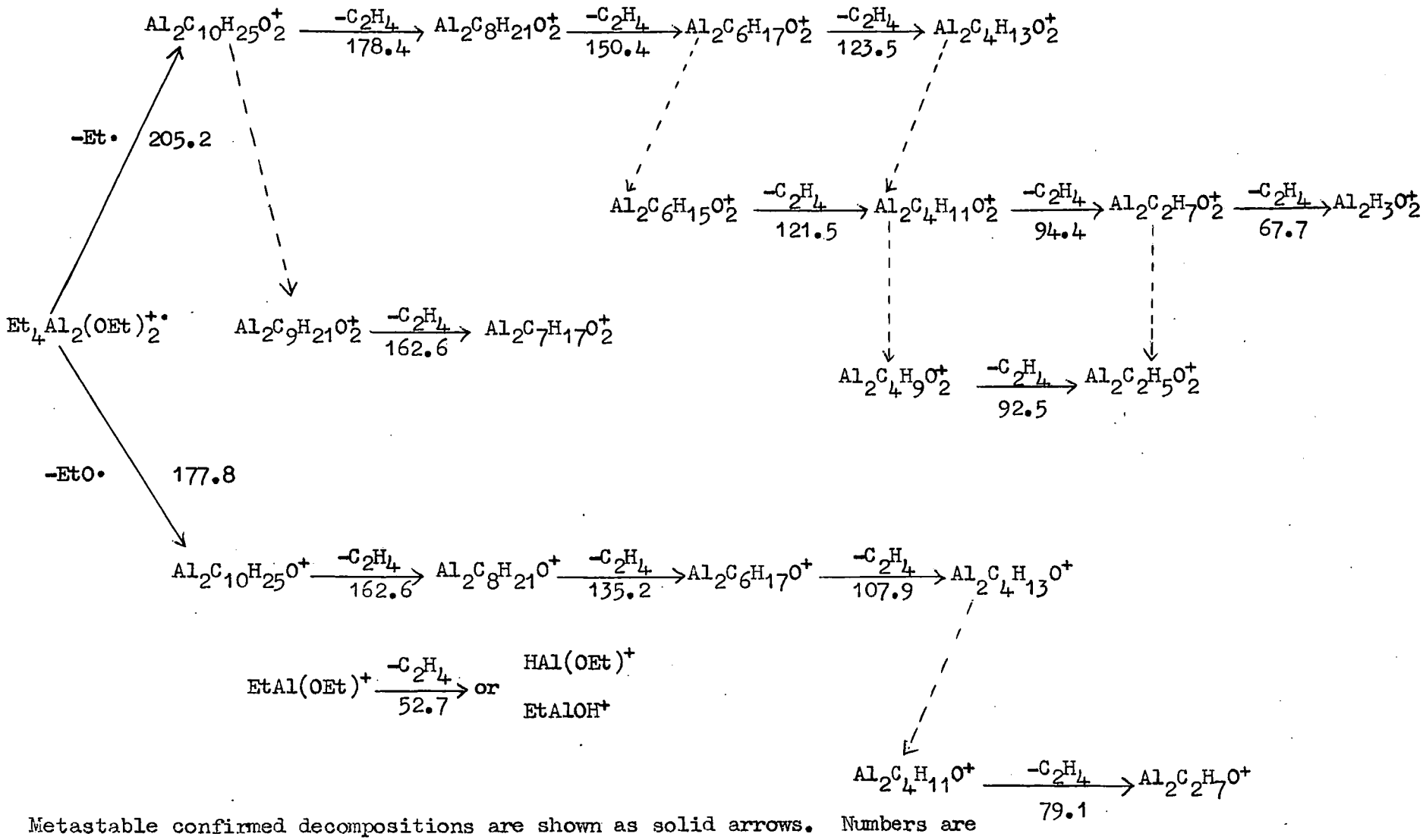

Metastable confirmed decompositions are shown as solid arrows. Numbers are mass of observed metastable peak.

f) Elimination of R_3Al (R = Me, Et or H)

Unlike dimer ions of beryllium but like dimeric ions of group IV metals $Al_2C_xH_y^+$ ions decompose to $AlC_aH_b^+$ ions by loss of R_3Al molecules. The process is metastable confirmed only for dimethyl - and diethyl - aluminium hydride; a fact that may be accounted for by the high abundance of dimer ions with these compounds.

$Me_4Al_2H^+$	$\longrightarrow$	Me_2Al^+	+ $HAlMe_2$	m*	28.25
$Me_3Al_2H_2^+$	$\longrightarrow$	Me_2Al^+	+ $MeAlH_2$	m*	32.2
$Et_3Al_2H_2^+$	$\longrightarrow$	Et_2Al^+	+ $EtAlH_2$	m*	50.5
$Et_2Al_2H_3^+$	$\longrightarrow$	Et_2Al^+	+ H_3Al	m*	62.8

4.4.3. Mass Spectra.

The decomposition diagrams of the compounds studied are shown in figs. 24 & 25 and the abundances of ions in tables 4.4.1., 4.4.2. and 4.4.3.

The spectra recorded for trimethylaluminium at 70eV and source temperature of 195°C is virtually identical to that previously reported.[12]

Hydride ions are far more abundant for the ethyl compounds than the methyl which reflects the ease of ethylene elimination from ions containing Al - C_2H_5 bonds.

A variety of structures may be written for ions containing two aluminium atoms. For example $Et_3H_2Al_2^+$ may involve hydrogen or ethyl bridges or both:

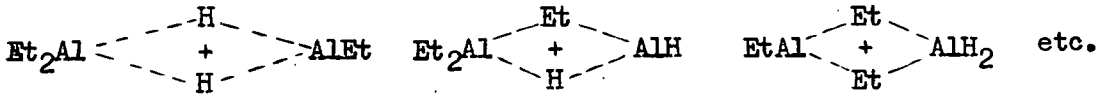

With oxygen containing ions structures involving oxygen bridges are probably more likely because of the ability of oxygen to donate a lone pair of electrons to the aluminium atom.

APPENDIX 1.

Tin and Lead Isotope Masses and Abundances.

Calculated Mass and Abundance Data for

Sn_2, SnGe, Ge_2, SnCl and SnBr.

Tin and lead isotope masses and abundances

	Mass *	Abundances (%) †		
^{112}Sn	111·90494	0·95		
^{114}Sn	113·90296	0·65		
^{115}Sn	114·90353	0·34		
^{116}Sn	115·90211	14·24		
^{117}Sn	116·90306	7·57		
^{118}Sn	117·90179	24·01		
^{119}Sn	118·90339	8·58		
^{120}Sn	119·90213	32·97		
^{122}Sn	121·90341	4·71		
^{124}Sn	123·90524	5·98		
		$PbPh_4$	$PbEt_4$	
^{204}Pb	203·97307	1·69 ± 0·08	1·42 ± 0·09	
^{206}Pb	205·97446	24·77 ± 0·08	25·17 ± 0·08	
^{207}Pb	206·97590	22·52 ± 0·06	21·90 ± 0·08	
^{208}Pb	207·97660	51·02 ± 0·07	51·51 ± 0·06	

* L. A. Konig, J. H. E. Mattauch, and A. E. Wapstra, *Nuclear Phys.*, 1962, **31**, 18. † J. H. Beynon, 'Mass Spectrometry and its applications to Organic Chemistry,' Elsevier, Amsterdam, 1960.

Nominal mass	Multiplicity	Spread p.p.m.	Peak mass (wtd. mean)	Relative abundance
		GeSn		
182	1		181·82922	0·95
184	2	3·0	183·82687	1·92
185	2	2·7	184·82806	0·70
186	3	9·1	185·82627	16·81
187	3	11	186·82719	8·28
188	5	16	187·82508	44·69
189	4	16	188·82594	24·70
190	5	17	189·82456	93·46
191	4	4·9	190·82477	34·13
192	5	25	191·82372	100·00
193	3	5·5	192·82492	30·60
194	4	33	193·82388	79·89
195	2	10	194·82547	5·03
196	3	18	195·82477	28·80
197	1		196·82860	2·27
198	2	8·2	197·82616	12·40
200	1		199·82660	2·26
		GeSi		
98	1		97·90120	54·40
99	1		98·90077	2·78
100	2	6·3	99·89865	74·39
101	2	20	100·89997	24·32
102	3	43	101·89803	100·00
103	2	5·1	102·89758	5·63
104	2	32	103·89782	23·80
105	1		104·89785	1·05
106	1		105·89512	0·69
		Ge_2		
140	Singlet		139·848554	17·76
141	No combination			
142	Singlet		141·846017	47·37
143	Singlet		142·847637	13·46
144	2	14	143·844776	94·61
145	Singlet		144·845099	17·95
146	3	26	145·843356	100·00
147	Singlet		146·844510	23·88
148	2	5·4	147·842494	73·77
149	Singlet		148·844720	5·08
150	Singlet		149·842509	23·78
151	No combination			
152	Singlet		151·842719	2·53

Nominal mass	Multiplicity	Spread (p.p.m.)	Peak mass (wtd. mean)	Relative abundance
		Sn_2		
224	singlet		223·80988	0·05
225	no combination			
226	singlet		225·80790	0·07
227	singlet		226·80847	0·04
228	2	5·0	227·80703	1·53
229	2	6·6	228·80796	0·82
230	3	8·7	229·80625	3·57
231	3	12	230·80697	1·99
232	4	12	231·80491	16·78
233	3	5·1	232·80523	13·51
234	5	19	233·80419	44·41
235	3	3·4	234·80513	35·04
236	5	28	235·80423	92·44
237	3	7·4	236·80519	50·83
238	4	18	237·80417	100·00
239	3	14	238·80565	35·64
240	3	13	239·80476	82·47
241	2	6·2	240·80759	9·53
242	2	6·2	241·80626	33·23
243	singlet		242·80863	5·70
244	2	2·3	243·80734	23·16
245	no combination			
246	singlet		245·80865	3·13
247	no combination			
248	singlet		247·81048	1·99
		SnCl		
147	singlet		146·87380	2·33
148	no combination			
149	2	6·6	148·87150	2·35
150	singlet		149·87239	0·83
151	2	14	150·87093	35·46
152	2	16	151·87188	18·85
153	2	17	152·87022	70·24
154	2	21	153·87152	27·07
155	2	21	154·87036	100·00
156	singlet		155·86929	6·82
157	2	27	156·86932	37·77
158	no combination			
159	2	30	158·87312	18·42
160	no combination			
161	singlet		160·87114	4·75
		SnBr		
191	singlet		190·82329	1·68
192	no combination			
193	2	0·13	192·82129	2·80
194	singlet		193·82188	0·60
195	2	5·9	194·82041	26·34
196	2	7·8	195·82134	13·99
197	2	8·6	196·81952	67·20
198	2	12	197·82066	28·32
199	2	12	198·81950	100·00
200	singlet		199·81973	14·88
201	2	16	200·81889	65·51
202	no combination			
203	2	19	202·82192	18·75
204	no combination			
205	singlet		204·82158	10·37

APPENDIX 2.

Ion Abundances, as Percentage of Total Ion Current, for Beryllium Dialkyls at 70, 15 or 12eV and High and Low Source Temperatures.

Table A.2.1.

Ion abundances for Me_2Be•

Ion+	70eV *37-50°	70eV *210°	15eV *210°	Ion+	70eV *37-50°	70eV *210°	15eV *210°
$C_{12}H_{33}Be_8$	.48	.09	2.50	C_2H_6•	.11	.07	
$C_{10}H_{27}Be_7$	.67	.23	1.21	C_2H_5	.18	.15	
$C_8H_{21}Be_6$	.15	.06		C_2H_4•	.78	1.00	.31
$C_6H_{15}Be_5$	.48	.03		C_2H_3	1.10	1.02	
Me_3Be_2•	.82			C_2H_2•	.40	.37	
C_4H_9	.13	.12	.16	C_2H	.40	.45	
C_4H_8•	.11	.15	.24	C_2•	.20		
C_4H_7	.10	.13		CH_3Be	30.13	31.93	2.52
$C_2H_5Be_2$	.85			CH_2Be•	16.02	15.14	6.89
C_3H_7	.13	.12	.15	CHBe	1.30	1.61	
C_3H_6•	.09	.12	.29	CBe•	.17	.29	
C_3H_5	.28	.08		CH_4•	3.29	5.95	.13
C_2H_6Be•	22.19	17.91	78.37	CH_3	4.47	6.61	4.35
C_2H_5Be	.54	.40	.09	CH_2•	1.22	1.45	
C_2H_4Be•	3.43	2.65	2.69	CH	.24	.40	
C_2H_3Be	1.66	1.45		H_3Be	< .01	< .01	
C_2H_2Be•	.79	.72		C•	.05	.11	
C_2HBe	3.59	3.90		H_2Be•	< .01	< .01	
C_2Be•	.18	.29		HBe	1.68	2.18	
				Be•	1.60	2.63	.11

* Source temp. °C

Ions with same integer m/e ratio are linked by {

Table A.2.2.

Ion abundances for Et_2Be

Ion$^+$	70eV *45-55°	70eV *196°	12eV *196°	Ion$^+$	70eV *45-55°	70eV *196°	12eV *196°
Et_5Be_3	.14			C_4H_9	.23	.05	.03
Et_4Be_3H	.06			C_4H_8•	.04	.04	.09
Et_4Be_2•	.38			C_4H_7	.07	.05	.04
$Et_3Be_3H_2$	.06			C_4H_6•	.03	.03	
Et_3Be_2	5.46	.18	.26	C_3H_8Be•	.05	.07	
$C_6H_{14}Be_2$•	.30			C_4H_5	.03	.03	.12
$Et_2Be_3H_3$	.06			C_3H_7Be	1.19	2.02	4.03
Et_2Be_2H	11.11	.42		C_3H_6Be•	.31	.48	.95
$C_4H_9Be_2$	.22		.16	C_3H_5Be	.46	.48	1.57
$C_4H_7Be_2$	.29			$C_2H_7Be_2$	6.02	.19	
C_5H_{10}•	.02		.04	C_3H_4Be•	.24	.14	.40
C_5H_9	.02		.04	$C_2H_6Be_2$•	.27	.06	
$C_4H_{10}Be$•	3.72	8.02	21.28	C_3H_3Be	.50	.41	
C_4H_9Be	.48	.34	.41	$C_2H_5Be_2$	.72	.02	
C_4H_8Be•	.31	.19	.28	C_3H_2Be	.20	.15	
C_4H_7Be	.24	.10	.04	$C_2H_4Be_2$•	.08		
$C_3H_9Be_2$	.12			C_3HBe	.05	.06	
C_4H_6Be•	.31	.28	.16	$C_2H_3Be_2$	.45	.03	
C_4H_5Be	.19	.18		$C_2H_2Be_2$•	.24	-	
C_4H_4Be•	.12	.03		C_3H_7	.14	.05	.03
$EtBe_3H_4$	.13			C_3H_6•	.06	.05	.07
C_4H_3Be	.13	.11		C_3H_5	.26	.15	.06
C_4HBe	.07			C_2H_7Be	.06	.10	.10
C_4H_{10}•	.07	.06	.07	C_3H_4•	.04	.28	.44

Table A.2.2. continued.

Ion abundances for Et_2Be

Ion$^+$	70eV *45-55°	70eV *196°	12eV *196°	Ion$^+$	70eV *45.55°	70eV *196°	12eV *196°
$C_2H_6Be\bullet$	1.72	2.76	.43	$C_2\bullet$	0.31	.28	
C_3H_3	.37	.32		CH_3Be	1.07	1.09	.09
C_2H_5Be	10.25	14.92	9.33	$CH_2Be\bullet$	.54	.56	.04
$C_2H_4Be\bullet$	13.13	23.05	30.67	$CHBe\bullet$	.07	.08	
C_2H_3Be	4.54	5.15	.37	H_3Be_2	.11	<.01	
$C_2H_2Be\bullet$	1.38	1.66	.19	$CBe\bullet$	.01	<.01	
C_2HBe	2.39	2.50		$CH_4\bullet$	.02	.01	
$C_4H_8Be^+$	.01	.02		CH_3	.14	.11	
$C_4H_6Be^+$	.05	.11		$CH_2\bullet$	.33	.21	
$C_4H_4Be^+$	.09	.17		CH	.12	.08	
$C_2H_6\bullet$	.10	.10	.23	H_3Be	<.01	<.01	
C_2H_5	1.00	.84	.73	$C\bullet$	.06	.04	
$C_2H_4\bullet$	9.47	13.58	25.32	$H_2Be\bullet$	<.01	<.01	
C_2H_3	7.02	8.06	.52	HBe	1.64	1.05	
$C_2H_2\bullet$	5.44	6.42	1.21	$Be\bullet$	1.82	1.30	
C_2H	1.05	0.92					

* Source temp. °C

Ions with same integer m/e ratio are linked by {

Table A.2.3.

Ion abundances for $(i\text{-Pr})_2Be$ and $(n\text{-Pr})_2Be$

Ion$^+$	$(i\text{-Pr})_2Be$ 70eV *55–75°	70eV *215–220°	12eV *215–220°	$(n\text{-Pr})_2Be$ 70eV *35–45°	70eV *210–215°	12eV *210–215°
Pr_4Be_2•	.36					
Pr_3Be_2	1.61	.02	.06			
$C_8H_{17}Be_2$	.04					
Pr_2Be_2H	2.43	.04	.06	3.12	.04	
$C_6H_{14}Be$•	3.96	2.36	6.91	3.12	1.34	3.75
$C_6H_{13}Be$	.09	.23	.18	.07	.10	.56
$C_6H_{12}Be$•	.16	.08	.59	.17	.05	.13
$C_5H_{11}Be_2$	.23					
$C_5H_{11}Be$	.17	.12	.16	.29	.17	.56
$C_5H_{10}Be$•	.17	.11	.09	.15	.04	.05
C_5H_9Be	.31	.25	.18	.12	.06	.09
C_5H_8Be•	.30	.24	.12	.12	.04	.08
$C_4H_{11}Be_2$	1.50			1.10	.02	
$C_4H_{10}Be$•	.78	.82	2.36	1.36	1.22	4.10
C_4H_9Be	.86	.60	.64	1.03	.76	1.19
C_4H_8Be•	.28	.17	.23	.21	.15	.19
C_4H_7Be	.66	.63	.42	.16	.14	
C_4H_6Be•	.37	.26	.17	.15	.06	
$PrBe_2H_2$	2.27	.12		.83	.02	
C_4H_5Be	.17	.17		.06	.06	
C_4H_3Be	.04	.08		.08	.07	
C_4H_9				.82	.33	.31
C_4H_8•				.54	.25	1.11
C_4H_7	.17	.23	.03	.51	.25	.18
C_3H_9Be	.58	.17	.29	.15	.11	
C_4H_6•	.17	.06		.11	.05	.28
C_3H_8Be	.96	.61	1.34	.69	.69	.89
C_3H_7Be	11.65	9.99	12.04	11.42	14.67	15.94
C_3H_6Be•	13.96	13.80	30.86	8.83	11.09	24.53
C_3H_5Be	8.15	7.23	2.13	3.57	5.09	.88

Table A.2.3. continued

Ion abundances for $(i\text{-Pr})_2Be$ and $(n\text{-Pr})_2Be$

Ion$^+$	$(i\text{-Pr})_2Be$			$(n\text{-Pr})_2Be$		
	70eV *55-75°	70eV *215-220°	12eV *215-220°	70eV *35-45°	70eV *210-215°	12eV *210-215°
$C_3H_4Be^\bullet$	.58	.44	.06	.65	.45	
C_3H_3Be	2.61	2.38	.10	1.83	1.71	
$C_3H_2Be^\bullet$	.37	.40		.31	.32	
C_3HBe	.08	.11		.10	.09	
$C_3H_8^\bullet$	.27	.19	.15	.76	.30	.39
C_3H_7	2.33	2.43	2.14	2.34	1.30	2.02
$C_3H_6^\bullet$	6.92	8.80	30.30	9.01	10.49	33.12
C_3H_5	9.91	13.90	4.32	13.72	14.94	5.49
$C_3H_4^\bullet$	2.18	3.24	.96	2.94	3.35	1.53
$C_2H_6Be^\bullet$	.97	.66		.09	.11	
C_3H_3	4.31	6.40	.03	7.33	8.78	
C_2H_5Be	.97	1.03		.50	.78	.23
$C_3H_2^\bullet$	1.13	2.33	.25	1.89	1.94	
$C_2H_4Be^\bullet$	2.74	2.78	2.15	.70	.93	1.00
C_3H	.58	1.37		1.70	1.33	
C_2H_3Be	.95	.82	.03	.66	1.02	
$C_2H_2Be^\bullet$	1.57	1.83	.21	.72	.98	.17
C_2HBe	.80	.77		.60	.66	
$C_5H_{10}Be^+$	.05	.02		.08	.07	
$C_5H_8Be^+$	.08	.04		.05	.07	
$C_5H_6Be^+$	.05	.02		.05	.06	
$C_5H_4Be^+$	.02	.01			.04	
$C_4H_6Be^+$	.13	.02		.21	.18	
$C_4H_4Be^+$	.13	.02		.09	.15	
C_2H_5	.73	.79	.10	1.79	1.74	.43
$C_2H_4^\bullet$	.60	.85	.18	2.45	1.17	.72
C_2H_3	2.67	5.09	.10	3.48	4.42	.11
C_2H_2	.45	.96		1.03	.98	

Table A.2.3. continued

Ion abundances for $(i\text{-Pr})_2Be$ and $(n\text{-Pr})_2Be$

	$(i\text{-Pr})_2Be$			$(n\text{-Pr})_2Be$		
Ion$^+$	70eV *55-75°	70eV *215-220°	12eV *215-220°	70eV *35-45°	70eV *210-215°	12eV *210-215°
C_2H	.06	.13		.18	.16	
$CH_4Be\cdot$	.03	.04		.02	.03	
CH_3Be	1.98	1.94	.03	1.28	2.00	
$CH_2Be\cdot$	.14	.20		.18	.29	
$CHBe$	.10	.01		.02	.02	
$C_3H_5^+$	.05	.06		.10	.08	
$C_3H_4^+$	.14	.24		.27	.30	
$C_3H_3^+$	.10	.12		.19	.25	
$C_3H_2^+$	.15	.25		.30	.34	
$CH_4\cdot$	.06	.04		.04	.04	
CH_3	.20	.36		.49	.43	
$CH_2\cdot$	.06	.14		.19	.16	
CH	.02	.04		.05	.04	
$C\cdot$	.01	.02		.03	.02	
H_3Be	.01	.01		.01	.01	
HBe	.15	.27		.19	.29	
$Be\cdot$	.14	.23		.19	.28	

* Source temperature °C

Ions with the same integer m/e ratio are linked by {

Table A.2.4.

Ion abundances for $(t\text{-Bu})_2Be$ and $(i\text{-Bu})_2Be$

	$(i\text{-Bu})_2Be$			$(t\text{-Bu})_2Be$		
Ion^+	70eV *75–90°	70eV *235°	12eV *240°	70eV *55–75°	70eV *240°	12eV * 240°
$C_8H_{18}Be^{\bullet}$	.89	.08	.23	5.01	.37	3.36
$C_8H_{16}Be^{\bullet}$	.05	.02	.06	.12	.03	.22
$C_7H_{15}Be$	.19	.08	.28	5.71	1.95	15.29
$C_7H_{14}Be^{\bullet}$	.06	.02				
$C_7H_{13}Be$	.04	.02				
$C_6H_{11}Be$	.05	.02		1.48	.65	.15
$C_6H_{10}Be^{\bullet}$	.08	.03				
C_6H_9Be				.36	.17	.11
$C_6H_8Be^{\bullet}$	.01					
$C_5H_{12}Be^{\bullet}$	.48	.19	.47	.74	.30	2.87
$C_5H_{11}Be$	2.02	.76	1.11	1.70	.62	2.44
C_5H_7Be				.05	.03	
$C_4H_{10}Be^{\bullet}$	.94	.44	.55	1.00	.47	2.28
C_4H_9Be	16.54	7.87	8.86	8.43	4.59	8.62
$C_4H_8Be^{\bullet}$	8.17	3.34	7.34	4.59	2.70	9.54
C_4H_7Be	3.51	2.04	.36	6.49	4.01	1.36
$C_4H_6Be^{\bullet}$	.47	.25		.82	.51	
C_4H_5Be	.26	.08		.43	.25	
C_4H_3Be	.19	.14		.17	.09	
$C_4H_{10}^{\bullet}$	.20	.09	.18	.79	.49	.54
C_4H_9	1.54	1.25	3.45	9.98	6.78	6.78
$C_4H_8^{\bullet}$	9.13	12.30	58.76	4.58	8.55	32.48
C_4H_7	3.56	5.88	2.28	1.77	3.30	1.03
$C_4H_6^{\bullet}$	.41	.52		.20	.40	.81
C_4H_5	.89	1.28		.57	1.03	
C_3H_7Be	.34	.21	.13	1.21	.79	.54
$C_4H_4^{\bullet}$	.19	.28		.14	.29	
$C_3H_6Be^{\bullet}$	.36	.26	.12	1.04	.81	.38
C_4H_3	.35	.97		.40	.79	

Table A.2.4. continued

Ion abundances for $(t\text{-Bu})_2Be$ and $(i\text{-Bu})_2Be$

	$(i\text{-Bu})_2Be$			$(t\text{-Bu})_2Be$		
Ion$^+$	70eV *75-90°	70eV *235°	12eV *240°	70eV *55-75°	70eV *240°	12eV *240°
C_3H_5Be	2.98	1.91	.22	3.27	2.26	.22
$C_4H_2\cdot$	.69	1.27		.46	1.09	
$C_3H_4Be\cdot$	.32	.07		.61	.39	
C_4H	.16	.34		.13	.25	
C_3H_3Be	2.29	1.28		4.95	3.34	
$C_3H_2Be\cdot$	.19	.12		.33	.21	
$C_6H_{12}Be^+$	.52	.24		.06	.03	
C_3H_7	2.55	1.79	1.13	3.72	5.83	2.33
$C_3H_6\cdot$	1.70	1.58	1.27	2.21	2.86	1.46
C_3H_5	15.97	23.91	10.75	8.78	18.87	4.56
$C_3H_4\cdot$	1.31	1.91	.84	.92	1.82	.54
C_3H_3	5.00	8.04		4.05	7.18	
$C_2H_6Be\cdot$	.60	.21				
$C_5H_8Be^+$	.42	.22		.16	.09	
$C_5H_6Be^+$				.10	.06	
C_2H_5Be	.15	.11		.21	.26	
$C_3H_2\cdot$	.66	1.07		.46	.97	
$C_2H_4Be\cdot$				.28	.19	
C_3H	.33	.55		.23	.53	
C_2H_3Be	.37	.22		.53	.37	
$C_2H_2Be\cdot$	.18	.11		.27	.19	
C_2HBe	.36	.22		.68	.43	
$C_2H_6\cdot$	.15	.14				
C_2H_5	3.77	4.59	.18	2.35	3.37	.05
$C_2H_4\cdot$	2.84	4.60	1.45	1.12	3.10	.70
C_2H_3	3.15	4.54		2.35	3.81	
$C_2H_2\cdot$	.69	.93		.32	.67	
C_2H	.08	.14		.04	.08	

Table A.2.4. continued

Ion abundances for $(t\text{-Bu})_2Be$ and $(i\text{-Bu})_2Be$

	$(i\text{-Bu})_2Be$			$(t\text{-Bu})_2Be$		
Ion^+	70eV *75-90°	70eV *235°	12eV 240°	70eV 55-75°	70eV 240°	12eV 240°
CH_3Be	.73	.42		1.06	.85	
$CH_2Be^\bullet$	.09	.06		.11	.07	
CHBe	.01			.01	.01	
$CH_4^\bullet$	.05	.05		.05	.06	
CH_3	.42	.62		.33	.39	
$CH_2^\bullet$	.12	.15		.06	.10	
CH	.02	.04		.02	.03	
$C^\bullet$	.01	.02		.01	.02	
HBe	.09	.06		.14	.11	
$Be^\bullet$	.09	.06		.11	.09	

* Source temperature °C

Ions with the same integer m/e ratio are linked by {

APPENDIX 3.

Primary Experimental Data for Appearance Potential Measurements.

Throughout the following abreviations are used:-

S.T. = Source temperature; I.R. = ion repeller voltage;

I(A) = Ionization potential of A.

$A(X^+)XY$ = Appearance potential of ion X^+ from XY.

For beryllium diakyls:-

i(Be) = Ion current of parent ion $(C_nH_{2n+1})_2Be^+$

i(Be') = Ion current of fragment ion $C_nH_{2n+1}Be^+$

i(Be") = Ion current of fragment ion $C_nH_{2n}Be^{+\cdot}$

For organotin compounds:-

i(Et) = Ion current of Et_3Sn^+

i(Ph) = Ion current of Ph_3Sn^+

i(Ph') = Ion current of $PhSnEt_2^+$

i(Ph") = Ion current of Ph_2SnEt^+

i(PhEt) = Ion current of $Ph_2SnEt_2^{+\cdot}$

i(4Et) = Ion current of $Et_4Sn^{+\cdot}$

$I(Me_2Be)$

(eVx5)	i(Be)	i(Ar)	i(Be)	i(Ar)	i(Be)	i(Ar)	i(Be)	i(Ar)	i(Be)	i(Ar)	i(Be)	i(Ar)
100	2800	1690	4400	1220	3150				1058	510	349	187
99		1580		1080						470		163
98		1500		994			3050	1370		430		145
97		1390		910				1215		390		133
96		1270		812		1270		1140		350		117
95	2950	1170	4150	714		1130	3025	1030	1080	310	349	100
94		1060		616		1000		940		275		90
93		940		525		920		840		230		76
92		820		427		800		730		195		64
91		713		361		700		564		160		54
90	2850	630	3250	298	2825	600	2975	530	1070	130	334	44
89		505		221		500		434	1045	100		32
88		400		171		400		374	1030	79		24–5
87		320		129		320		271		58		18–2
86		230		91		250		195	983	37		10.5
85	2600	170	2575	59.5	2600	178	2675	135		25		7.4–8
84		108		36		122		90		13.5–14.5		4.2–4.8
83		66		23		80		54		6.8–7.4		2.0–2.4
82		36.5		10.5–11.1		45		31		3.3–3.7		.8–.1
81		19.1		4.4–4.6		26		16		1.5–1.8		.3–.5
80	2200	11.1		2.3	2250	11.4	2250	7.9	756	.4–.6	230	
79		4.9		.9–.1	2100	5.4		3.8	718		214	
78		2.2–2.4		.5	2050	2.7		1.7	668		200	
77		1.0–1.2			1960	.9		.9	617		184	
76		.6–.7	1860						573		169	
75	1650		1720		1700		1560		529		158	
74	1520		1620		1640		1430		479		143	
73	1400		1480		1540		1350		441		131	
72	1260		1340		1400		1250		397		118	
71	1160		1220		1260		1120		353		105	
70	1040		1110		1140		1010		315		94	
69	940		920		1040		920		272		83	
68	830		815		940		805		232		72	
67	730		725		830		675		197		62	
66	610		610		720		600				53	
65	520		510		610		480		146		43	
64	420		415		530		390–450		116		35	
63	300		337		430		342		93.2		29	
62	270		252		340		257		70.6		21	
61	208		183		262		192		55		17	
60	155		132		202		132		38		11.8	
59	98		89		130		90		25		8.1	
58	64		55		84		48		15		4.4	
57	37		31		52		36		8.8		2.5	
56	19		14		27.5		18		5.0		1.37	
55	9.5		6–6.7		12.2–13.4		8.5		2.4		.7	
54	4–4.3		2.8–3.2		4.5–5.5		3.3		.9			
53	1.7–2.1		1.4–1.7		.5		2.0		.4			
52	.6–.9		.5–.9				.5–.9					
51	.2–.4											
S.T.	193		187		215		18		217		220	
I.R.	-.2		-.2		0.2		-.2		0		0	

$I(Et_2Be)$

eVx5	i(Be)	i(Kr)	i(Be)	i(Kr)	i(Be)	i(Kr)	i(Be)	i(Kr)	i(Be)	i(Kr)	i(Be)	i(Kr)
98		900		570		1270		1580		840		1000
96		780		520		1150		1480		760		890
94		670	2400	470		1000		1340		680		750
92		580	2350	400		840		1150		590		640
90	3100	480		360	1800	720		980		510		540
88		420	2350	310		595		810		405		450
86		340		255		490		665		343		380
84		270		200		390		530		255		300
82		200		146		300		415		180		220
80	2600	140	2275	98	1490	200	1695	288	1020	118	1170	155
79		105		75		163		233		86		120
78	2350	84	2250	55	1400	120	1580	172	950	62		92
77		61		39		89		132		40		64
76		39	2250	23	1300	62	1480	94	870	25.5	943	43
75	2100	24.5		12.-13.4		36		62		15-16.4		28
74		16.5		6.5-7.2	1160	24	1330	375		6.5-7.6		16
73		6.6-7.4		2.6-3.1		11.9		22		2.9-3.5		8.2
72	1850	3.2-3.7		1.1-1.4		5.5-6.2	1200	11.1		1.4-1.9	859	4-4.5
71		1.2-1.6		.5-.7		2.6-3.1		5.4-5.7		.5-.8		1.7-2
70	1700	.5-.7	1900			.9-1.1		2-2.5	625		775	.6-.8
69		.1-.3	1780		900	.3-.5		.8-1	520			.2
68	1500		1670		816		1000	.2-.4			681	
67	1380		1550		760		915				616	
66	1280		1440		690		853		426		561	
65	1160		1300		620		770				511	
64	1070		1160		570		703		358		469	
63	1000		1010		530		632				440	
62	900		860		474		570		267		402	
61	840		760		440		512				360	
60	710		585		382		440		193		318	
59	590		460		320		370		156		268	
58	480		380		268		310		123.5		218	
57	360		250		211		260		99		163	
56	270		167		154		200		70		126	
55	190		108		111		148		47-48		86	
54	130		59		80		108		28.5		60	
53	84		34		53		70		18		40.5	
52	52		16.5		33		46		10		24.3	
51	30		9.2-10		20		31-32		5.5-6		14-15	
50	16		4.5-5		12.7-13.2		20		2.4-2.8		8.2-8.6	
49	7.6-8.4		1.9-2.2		6.6		10.6-11.6		1-1.3		4-4.4	
48	3.6-4.2		.6-1		3.3		5.4-5.9		.5-.6		1.8-2.2	
47	1.8-2.2		.2-.4		1.2-1.4		2.5-3.0				.8-1	
46	.5-.8				.4-.5		1-1.2				.3	
S.T.	195		230		197-213		213-230		230		215	
I.R.	.4		-1		.4		.4		-1		-1	

I(i-Pr_2Be) eV x 5	i(Be)	i(Kr)	i(Be)	i(Kr)	i(Be)	i(Kr)	i(Be)	i(Kr)
100		720	1215	655	3560	1609	1210	600
98		645	1190	575		1363	1200	540
96	1100	565		510		1210		470
94	1050	485		440	2600	1086		400
92		408		380	2410	937		350
90		350	1000	330	2343	790	1040	295
88	910	287		270	2215	680		250
87	885	260		242		607		215
86		237		220		554		205
85		208		193		479	900	177
84	795	183	837	167	1960	437		133
83		157		143		350		129
82		132		122		315		113
81		112		106		260		93
80	595	93	700	82	1683	217	730	75
79		69		66		170		61
78		55		47		129		46
77		40		35		97		31
76	585	28		24	1470	68		23.5
75		16	550	16		38	575	15–17
74		9–11		7.8–8.8		20.5		7.6–9
73		5–6		4.4–5.4	1220	12		3.5–4.5
72		2–2.6		2.3–3		4		1.8–2.4
71		.9–1.4		.9–1.5		2		.8–1.4
70		.4–.9		.4–1				.1–.5
69					965			
68	365				897		372	
66	310		302		784		306	
64	262		254		684		264	
62	223		213		570		222	
60	181		175		460		186	
58	143		140		354		141	
56	102		102		277		106	
54	71		67		177–187		70	
52	41		36.7–40		104–109		36–41	
50	19		17.3–19		51–53		19	
51.5	34.5–35.5		31–34		91–96		30–34	
50	20–21.5		20–21.6		59–61		21–23	
49	11–12.25		11.3–13.2		34–36		11–12.9	
48	6–7		5.4–7		18–19		6–6.7	
46.5	2.5–3.25		2.7–3.5		6–9		2.4–2.6	
46	1–1.75		1.1–1.6		3–4.7		1.1–1.7	
45	.3–.5							
S.T.	205		205		205		205	
I.R.	–.7		–.7		–.7		–.7	

I(n-Pr_2Be) eVx5	i(Ar)	i(Be)	i(Ar)	i(Be)	i(Ar)	i(Be)	i(Ar)	i(Be)	i(Ar)	i(Be)
98	1525				3150					
96	1375				2800					
94	1213				2475					
92	1075		1188		2175		3050			
90	925		1038		1850		2550		775	
88	780		875		1540		2100		670	
86	650		725		1280		1700		534	
84	520		570		1000		1280		410	
82	410		440		800		940		305	
81	350		375		680		805		259	
80	300		305		570		645		181	
79	245		250		460		505		173	
78	200		195		380		375		138	
77	153		148		280		260		103	
76	109		104		203		190		81	
75	76		67		130		115		57	
74	47.5		46		88		70		37	
73	28.3		29		54		42		26	
72	15.8		15.5		30		23.5		16	
71	8.2-9		8.3		16		12		10.3	
70	4.8-5.2		4.1		8.6		5.7-6.2		6.11	
69	2.4-2.7		2-2.2		4.2		2.7-3		3.8-4.1	
68	1.3-1.5		1-1.2		2.3		1.4-1.7		2.2-2.4	
67	.6-.8		.6-.7		1.2		.5-.8		1.5-1.8	
64		1540		1560		1480		1720		
62		1400		1430		1360		1580		
60		1290		1300		1250		1440		1040
58		1130		1130		1100		1250		980
56		960		970		930		1070		900
54		830		870		780		900		800
52		680		670		650		730		720
50		540		540		520		600		585
48		420		415		410		450		500
47		355		350		340		380		440
46		295		300		293		320		375
45		250		250		240		255		320
44		205		195		190		205		270
43		158		150		136		150		220
42		122		108		119		114		175
41		85		82		82		80		130
40		61		56		60		52		100
39		41		35		31		32		74
38		23		22		22		18.5		51
37		12-13.6		11.8		10-12		10.3		32
36		6.5		6.4-6.9		6.8-7.5		5.3-5.7		22
35		3.5-3.9		3.4-3.8		3.5-3.9		2.9-3.4		13-13.6
34		1.9-2.2		1.5-1.8		1.7		1.3-1.7		7-7.6
33		.8-1.2		.7-1.1		.5-.8		.5-.8		4.4-4.9
S.T.		185		185		185		185		185
I.R.		5		5		5		5		5

$I(n\text{-}Pr_2Be)$			$I(i\text{-}Bu_2Be)$				
	i(Ar)	i(Be)		i(Be)	i(Xe)	i(Be)	i(Xe)
eVx5			(eVx5)				
92	3000		100	265	7600	32–34.5	675
90	2600		98	260	7200		620
88	2000		96	260	6800	28–31	560
86	1750		94	255	6500	27–28.5	490
84	1300		92	250	6100	24.5–27	455
82	950		90	235–240	5800	24–25	400
87	800		88	225–235	5400	21–23	377
80	675		86	220–230	5100	21–23	335
79	500		84	215–220	4700	21–23	310
78	380		82	205–215	4400	21–22.5	300
77	260		80	195–205	4000	18.5–22	278
76	186		78	190–200	3650	18.20.5	247
75	120		76	185–195	3100	16–17.5	217
74	65		74	175–185	2900	1 15–17	190
73	40		72	165–175	2500	13.8–16	160
72	22		70	160–165	2100	12–14.2	136
71	10		68	145–155	1700	12–13.2	113
70	6		66	135–145	1320	10.8–12.4	83
69	3		64	124–130	920	10.4–12	61
68	1.4–1.7		62	114–120	620	9.6–11	37.5
67	.5–.8		60	102–108	350	8.4–10.2	22
64		1700	58	90–94	160	7.6–9.2	9–10
62		1500	56	80–84	50–52	7.5–9	3–3.4
60		1420	54	70–73	20–22	6–7.5	.6–.8
58		1200	52	58–61	1.5–2	4.4–5.6	
56		1000	50	48–51	.3–.5	3.5–4.5	
54		950	48	37–41		2.2–3.3	
52		700	46	27–29		1.5–2.4	
50		550	44	18–19.5		.9–1.9	
48		425	42	9.8–11		.3–.7	
47		370	40	4–4.7			
46		310	38	1–1.6			
45		250	36	.1–.4			
44		203	34	0–.2			
43		145					
42		110					
41		75					
40		50					
39		30					
38		19					
37		9					
36		5–5.5					
35		3–3.2					
34		1.3–1.7					
33		.5–.6					
S.T.		210		205		205	
I.R.		–.5		5		5	

I(i-Bu_2Be)

eVx5	i(Be)	i(Xe)	i(Be)	i(Xe)	i(Be)	i(Xe)	i(Be)	i(Xe)
100	36–38.5	720	22.5–25	550	110–114	1000	25–27	116–122
98	33.5–36	650	22.5–25	500	110–114	950	24–27	106–110
96	31.5–34	580	22.5–25	460	108–112	910	22–25	98–100
94	29–31.5	520	21–23	440	104–110	870	23–25	90–95
92	26–30	470	19.5–22	380	104–106	850	17–18	79–82
90	24–27	430	18.5–20.5	360	102–108	870	17–18.5	67–69
88	22.5–26	400	17–18.5	330	98–102	790	17–19.5	60–64
86	22.5–26	360	18–20.5	305	96–102	740	15.5–18	64–66
84	22–25	330	17.5–20	305	86–90	695	15.5–17	56–60
82	21.5–24	310	17.5–20	270	86–90	620	14.5–16	50–52
80	21.5–24	290	17.5–20	260	82–86	575	14.5–16	47–50
78	21.5–24	270	16–18	240	80–84	505	13.5–16	42–44
76	21–22.5	250	14.5–17	205	70–74	465	14.5–15.5	36–39
74	19–21.5	215	13–14.6	185	69–72	387	14–16	35–38
72	17–19	185	12.4–14	155	65–78	343	12.5–15	33–35
70	16–17.5	154	12–14	136	60–64	282	12–14	27–30
68	12–15.5	120	12–14	122	57.5–62	238	11–13	22–29
66	11.4–13.4	90	11.4–12.8	100	52–56	178	10–12	15–17
64	11–13	62	10.4–12	74	49–53	130	9–10	10–12
62	9.8–11.4	41	9–10.8	52	45–48	87	8–10	6.2–7.2
60	8.6–10	21.5	7.6–8.6	32	42–49	52.5	7.6–8.8	3.2–4
58	7.8–9	8.5–10	7–8.4	16.5	38–40	23	6.2–8	1.6–2.1
56	6.6–8.2	2.4–3.1		6.8–7.2	33–35	12–13.6	4.5–6	.5–.7
54	7–8.4	7–1.1		1.6–2.4	26.5–28	2.2–3.2	4–5	
52	5.6–6.6		4.8–5.8	.3–.7	22.5–23.5	.3–.4	3.5–4.5	
50	4.2–5		4–4.9		17–19.2		2.5–3.5	
48	2.8–3.8		3–4		13–15		1.9–2.9	
46	2–2.8		2.6–3.1		9–11		1–1.7	
44	.9–1.7		1.5–1.9		5.5–6.3		.5–1.3	
42	.4–.8		.8–1.2		2.5–3.4		.3–.8	
40	.2–.5		.3–.7		1–1.4			
38			.1–.3		.4–.5			
36								
S.T.	205		205		205		196 – 205	
I.R.	5		5		5		2.4	

$A(CH_3Be^+)Me_2Be$; $A(CH_2Be^+)Me_2Be$.

eVx5	i(Be')	i(Be'')	i(Ar)	i(Be')	i(Be'')	i(Ar)	i(Be')	i(Be'')	i(Ar)	i(Be')	i(Be'')	i(Ar)
100	2900	1350	600	3050	1450	870	2800	1350	780	2900	1800	760
99			562			800			730			715
98			530			750			680			670
97			500			700			630			620
96			460			640			580			572
95	2600	1300	417	2740	1350	590	2600	1230	540	2400	1200	539
94			370			520			490			470
93			335			480			440			420
92			300			430			390			380
91			257			361			330			310
90	2150	1120	215	2200	1175	300	2100	1080	286	2000	1070	279
89			172			260			230			215
88			137			206			182			180
87			109			155			140			120
86			80			118			104			102
85	1550	900	58.51	1580	930	85	1490	860	75	1400	840	72
84			37.4			58			48			45
83			22.6			35			31			29
82			12.1			18.5			16.17			15.17
81			6.9			11.1			8.9			8.1
80	880	620	3.0	920	640	5.2	860	600	4.1	830	550	4.0
79			1.5			2.3			2.0			2.0
78			.7			1.2			.95			.8
77			.4			.5			.45			.4
75	370	355		390	370		338	330		325	300	
74	300	300		305	320		275	285		270	270	
73	220	260		240	275		210	250		205	230	
72	160	215		175	233		146	203		140	200	
71	120	180		127.6	190		114	168		108	161	
70	80	135		86	150		78	136		70	125	
69	56	112		60	118		53	109		50	101	
68	37	88		41	94		35	86		31	78	
67	23.5	67		25	69		22	62		20	60	
66	14	46		14.4	49		12.4	44		12	42	
65	7.6–8.2	31.5		9			5.75	28–29		4	27	
64	3.9–4.3	20.5		5–5.6	23–24		4.0	19–20		3	18	
63	2.0–2.5	12–13		2.4–2.7	13–14		2.0	11–12		2	10–11	
62	.9–1.3	6.6–7.2		1.0–1.3	7.2–8.0		.8–1.1	5.9–6.0		.9–1.0	5.7	
61		3.–3.4		.5–.8	3.9–4.3		.4–.6	3–3.5		.5	3.2	
60		1.5–1.8			1.8–2.1			1.4–1.7			1.2–1.6	
59		.6–.8			.7–.9			.5–.7			.4–.6	
58		.1–.3			.3–.4			.1–.2			.1	
S.T.		193			193			193			199	
I.R.		–.2			–.2			–.2			0	

$A(C_2H_4Be^{+\bullet})Et_2Be^{\bullet}$, $A(C_2H_5Be^{+})Et_2Be$.										$\frac{A(CH_2Be^{+\bullet})Me_2Be}{A(CH_3Be^{+})Me_2Be}$		
eVx5	i(Be")	i(Be')	i(Ar)	i(Be")	i(Be')	i(Ar)	i(Be")	i(Be')	i(Ar)	i(Be")	i(Be')	i(Be)
100	4200	2150	500	5600	2400	800			1120	3850	6800	10000
98			450			710			990	3650	6250	9600
96			400			630			890	3400	5700	9350
94			350	5000	2450	560			730	3150	5200	8950
92			305	4800	2250	460			630	2900	4700	8600
90	3400	1600	260			390	4600	2100	540	2600	4050	8000
88			215	4250	1950	320			430	2350	3500	7600
86			170			235	4000	1740	335	2070	2950	6900
84		1300	135	3850	1650	180	3750	1590	243	1800	2400	6400
83		1220	118	3700	1575	150			200			
82			100			120	3500	1440	165	1550	1900	5800
81			84			94			132			
80	2600	1060	68	3300	1325	72	3300	1310	102	1300	1500	5300
79	2550	1010	55	3200	1250	57			71			
78			42			37.5	3050	1150	48	1000	1010	4550
77	2400	900	31			23			29			
76	2325	860	21	2800	1020	15.5			16.3	770	680	4000
75			13	2625	920	7.4			8.8–9.4	680	550	
74			6.4			3.2–3.5			3.4–3.9	570	420	3325
73			3.3			1.3–1.7			1.5–1.7	480	320	3050
72			1.2–1.5			.3–.5			.4–.7	400	225	2725
71			.6–.7	2050	620		2050	610		325	165	2500
70	1600	500	.2–.3	1900	550		1870	540		265	115	2200
68	1380	395		1625	430		1580	415		160	51	1770
66	1200	315		1320	320		1290	295		76	17.3	1280
65	1100	265		1200	270		1180	255		54	11	1140
63	900	190		960	185		920	169		18.5	2.5–2.8	740
62	800	155.5		850	150		800	128		8.9	.9–1.0	510
61	720	130		740	117		690	103		4.4	.3–.5	430
60	630	105		640	89		600	78		1.7–2.0		305
59	535	78		530	64		515	685		.6–.9		195
58	450	58		430	44		407	39.5				120
57	370	40		360	31		330	27				68
56	308	29		290	21		260	16.8–17.8				37
55	255	21		225	14		210	12.4				18
54	195	13.5		175	9–9.8		152	7.4–7.9				9.2
53	155	8.8		128	5.4–5.6		109	4.5–4.9				3.4
52		5.6		94	1.8–1.9		77	2.9–3.2				1.2
51	90	3.8			1.1–1.2		53	1.9–2.1				.3–.6
50	62	2.4–2.7		41	.7		34.5	.9–1.1				
49	42	1.5–1.8					23	.6–.8				
48	29	.9–1.1		16.5								
47	16.5	.6–.8										
46	9–9.4			4.4								
45	4.8–5.0			2.1								
44	3.0–3.3			.8–1.0								
43	1.4–1.5											
S.T.	200			200			225			194		
I.R.	.2			.2			.5			0		

$A(C_2H_4Be^{+\cdot})Et_2Be$; $A(C_2H_5Be^{+})Et_2Be$

eVx5	i(Be")	i(Be')	i(Ar)	i(Be")	i(Be')	i(Ar)	i(Be")	i(Be')	i(Ar)	i(Be")	i(Be')	i(Ar)
100			1580	3050	3100	1440	9400	4900	2350			1400
98			1430			1280			2175			1240
96			1280			1150			1920			1140
94			1100			1020			1710			1000
92			970			900			1480			865
90	6000	2750	795	5100	2400	760	8000	3700	1270	4300	2000	735
88			650			610			1080			610
86			510	4700	2100	510	7300	3225	845	3900	1730	500
84		2300	385	4400	1900	380	6900	2960	640	3675	1600	363
83		2200	330			330			550			315
82		2150	270	4150	1750	270	6520	2700	455	3450	1450	260
81		2050	210			225			368			218
80	5000	1740	156	3856	1560	183	6150	3450	300	3250	1320	173
79			122			132			220			129
78	4600	1740	81	3550	1380	98	5700	2175	163	3000	1170	99
77			55			68			110			67
76	4325	1540	28.5	3300	1240	46	5200	1840	67	2750	1010	39.5
75			15			26			41.5			23
74			7.1			14			22			13
73			3.2–3.6			5.6			9.4–10.8			4.8–5.2
72			1.4–1.7			2.4			4.5–5.0			1.9–2.1
71			.5–.7			.7–1.0			2–3			.95
70	3150	900		2300	700		3850	1020	1.5–2			.3–.4
68	2675	700		2000	560		3300	900		1560	440	
66	2250	530		1650	420		2700	660		1320	328	
65	2050	450		1500	350		2450	560		1200	280	
63	1600	310		1240	255		2000	400		970	195	
62	1440	250		1100	210		1730	302		860	160	
61	1260	197		970	165		1560	252		760	125	
60	1110	145		840	128		1320	193		640	96	
59	930	108		720	98		1130	143		550	72	
58	765	76		600	70		950	102		460	52	
57	660	56		500	56		785	75		380	37	
56	540	38		400	34		630	54		305	25	
55	425	26		320	22.5		515	38		245	17.5	
54	320	148–16		250	15.3		372	24		190	11	
53	235	10.4		195	10		305	16		138	6.4–7	
52	175	6–6.8		138	6.0–6.3		220	10.5		106	4.5	
51	117	3.5–3.9			4.5–5		160	8–9.5		82	2.7–3	
50	84	2–2.5		82	2.8–3.0		106	4.5–6		54	1.5–1.8	
49	51	1–1.4		51	1.5–1.8		68	3.5–5		35	.8	
48	26	.3–.6		29	1.0–1.1		44			20		
47	15.5			17.5	.5		31			12.4		
46	5.7–6.7			10–10.4			17			6		
45	2.9–3.4			5–5.4			10.5			3.4–3.7		
44	1.3–1.6			2.6–2.9			6–8			1.3–1.5		
S.T.		200			200			200			200	
I.R.		.5			1.4			1.4			1.4	

$A(C_3H_6Be^{+?})i\text{-}Pr_2Be$; $A(C_3H_7Be^{+})i\text{-}Pr_2Be$.

eV	i(Ar)	i(Be")	i(Be')	i(Ar)	i(Be")	i(Be')	i(Ar)	i(Be")	i(Be')	i(Ar)	i(Be")	i(Be')
19.43	900	5720	3700	820	5350	3410	8770			780		
19.05	800			750			720			730		
18.65	715			680			650			662		
18.27	630			610			585			590		
17.90	560			545			520			510		
17.50	465	5300	3100	460	5100	3000	435			432		
17.12	405			390			365			370		
16.73	315			315			298			305		
16.35	245			235			225			235		
16.00	172.5			170			154			160		
15.60	114	4650	2500	108	4325	2225	107	4330	2320	110		
15.4	82			82			77			79		
15.2	55			62			51			55		
15.0	39.5			39.5			38			41		
14.8	25			26			24			29		
14.63	13			12.8			15.6			16		
14.43	6.4–6.7			7.4			7.6			8		
14.23	2.8–3.2			2.9–3.1			3.7–4			3.9		
14.0	1.4–1.6			1.0–1.3			1–1.4			1.7		
13.84	.4–.5			.3–.4			.6–.7			.6		
13.64		3200	1400		3000	1320		2750	1200		2760	1300
13.25			1180			1120			1020			1050
12.87		2500	960		2365	910		2150	820		2200	850
12.48		2135	770		2000	700		1800	625		1900	630
12.10			575			530			480			490
11.7		1480	415		1380	390		1240	350		1270	370
11.32		1180	263		1080	250		1000	233		1050	245
10.93		870	168		870	150		760	146		790	152
10.53		655	94		630	94		560	84		600	89
10.14		466	53		443	52		383	46		390	49
10		435	47		410	47						
9.8		335	29		325	30		305	30		310	31
9.6		262	20.5		248	19.5		233	19.3		243	20
9.4		192	12.9		188	12.2		185	12.8		192	13
9.2		136	7.1		133	6.8–7.6		127	7.6		131	8.1
9.0		95	4.7		96	2.8–3.1		96	5–5.4		98	5.2
8.8		63	2.8–3.1		67	1.3–1.4		64	2.9–3.2		65	3.1
8.6		42.5	1.7–1.9		43	.7–.9		43.5	1.8–2.1		44	1.9
8.4		275	1.0–1.2		27.5	.4–.6		29	1.1–1.2		30	1.2
8.2		16.2	.5–.7		15	.1–.2		16	.45		16	.5
8.0		8.4–8.9			8.4–9.1			9.2	.15		9.4	.2
7.8		4.2–4.4			4.1–4.6			4.7			5.0	
7.6		1.9–2.1			1.7–2.1			2.2			2.2	
7.4		.8–1.1			.5–.8			.9–1.1			1.0	
7.2		.4–.6			.3–.4			.3–.4			.4	
S.T.		205			205			205			190	
I.R.		–.5			–.5			–.5			1.0	

$(C_3H_6Be^{++})n\text{-}Pr_2Be$; $(C_3H_7Be^{+})n\text{-}Pr_2Be$												
eVx5	i(Ar)	i(Be")	i(Be')	i(Ar)	i(Be")	i(Be')	i(Ar)	i(Be")	i(Be')	i(Ar)	i(Be")	i(Be')
96	4950			3475						2450		
94	4400			3050			3200			2150		
92	3800			2650			2800			1850		
90	3200			2250			2425			1600		
88	2700			1900			2075			1325		
86	2100			1460			1700			1050		
84	1600			1090			1328			800		
82	1070			750			1000			565		
80	680			475			690			360		
79	490			360			435			363		
78	340			256			330			183		
77	230			166			220			122		
76	128			109			110			76		
75	74			62			86			43		
74	43			33			49			24		
73	20			16			25.8			11.1		
72	11.1			10.2			12.9			5.5		
71	6.3–6.5			5.1			6.8–6.9			2.75		
70	3.5–3.7			2.5–2.7			3.7–3.8			1.55		
69	2.2–2.3			1.7–1.8			1.9–2.1			.9–1		
68	1.6–1.8			1.1			1.2–1.3			.7		
67	1.3–1.5			.9			.8–.9			.5–.6		
66		2175	1325		2075	1325		1940	1240		2000	1280
65		2025	1130		1950	1175		1780	1060		1820	1120
64		1850	970		1800	1000		1620	920		1680	980
63		1680	820		1650	890		1500	785		1560	840
62		1510	690		1480	700		1370	650		1420	710
61		1350	560		1340	590		1240	540		1320	590
60		1220	460		1200	475		1120	450		1160	490
59		1060	355		1050	375		935	325		1040	390
58		910	260		890	275		830	258		890	300
57		760	195		760	208		720	195		770	228
56		625	134		630	143		600	145		660	160
55		495	92		515	107		495	101		550	120
54		393	64		410	71		370	63.5		445	82
53		285	40		302.5	49		295	43.5		355	59
52		225	26		230	30		225	29		260	37
51		156	18		165	20		162	19.5		210	27
50		106	10.6		119	12.6		114	11.7		148	16.6
49		72	6.7		81.5	8		68	6.6		103	10.4
48		44	3.7		56	5		48	4.4		63	5.7
47		23	2.2–2.4		39	3.5		32.5	3		42	3.5
46		20	1.5–1.7		27.5	2.2		20.5	1.9		25	2.2
45		14.1	1.1–1.2		19	1.6		13.9	1.25		14.4	1.3
44		8.5	.7–.8		10.6	.9		10	.95		8.4	.8–.9
43		5.0	.5		5.8	.6		6.1–6.3	.6		5.15	.6
42		3			3.4			3.6–3.7			2.35	
41		1.95			1.95			2.3			1.7–1.8	
40		1.15			1.1–1.2			1.25			1.1–1.2	
S.T.		185			185			185			185	
I.R.		4.6			4.6			4.6			4.6	

$A(C_3H_6Be^{+\bullet})$n-Pr_2Be;		$A(C_3H_7Be^{+})$n-Pr_2Be.	
eV x 5	i(Ar)	i(Be'')	i(Be')
96	2075		
94	1825		
92	1600		
90	1375		
88	1100		
86	880		
84	660		
82	470		
80	305		
79	220		
78	165		
77	106		
76	66.5		
75	36.5		
74	19.5		
73	9.4		
72	5.2		
71	2.6		
70	1.4		
69	.8		
68	.6–.7		
67	-		
66		1860	1220
65		1720	1060
64		1600	930
63		1450	790
62		1340	670
61		1210	560
60		1110	460
59		970	365
58		840	280
57		720	210
56		615	165
55		515	113
54		420	77
53		323	53
52		260	36.5
51		205	26.5
50		140	15.6
49		98	9.6
48		67	5.9–6.1
47		42	3.4–3.6
46		26.5	2.2–2.3
45		15.4	1.3
44		8.8	.8
43		5	.5–.6
42		2.9	
41		1.5–1.6	
40		.9–.95	
39		.6	
S.T.		1.85	
I.R.		4.6	

$A(C_4H_8Be^{+\bullet})$i-Bu_2Be;		$A(C_4H_9Be^{+})$i-Bu_2Be
i(Be'')	i(Be')	i(Ar)
		2120
		1925
		1720
		1450
		1320
		1140
2500	4200	950
2375	3675	775
2350	3725	620
2200	3000	420
		340
1630	2425	268
		215
1560	2075	161
		127
1440	1870	84
		55
1330	1470	30
		17–17.5
1080	1180	8–8.2
		3.5–3.9
870	860	1.3–2.5
		0.4–0.5
750	660	.1–.2
590	470	
452	297	
403	225	
333	175	
292	132	
270	104	
223	84	
182	60.5	
147	42.5	
128	34	
101	25–26	
71	16–17	
54	12–12.5	
42	7.8–8.2	
30	5.5–5.8	
20.5	3.1–3.5	
10.4–11	1.7–2.0	
5.7–6.1	.8–1.1	
2.9–3.2	.4–.6	
1.3–1.6		
.5–.7		
	205	
	+5	

$A(C_4H_8Be^{+?})i\text{-}Bu_2Be$; $A(C_4H_9Be^{+})i\text{-}Bu_2Be$.

eVx5	i(Be″)	i(Be′)	i(Kr)	i(Be″)	i(Be′)	i(Kr)	i(Be″)	i(Be′)	i(Kr)	i(Be″)	i(Be′)	i(Kr)
90			1290			1040	2250	4500	1550	2250	4450	1400
88			1180			920	2150	4125	1230	2150	4150	1310
86			1060			840	1975	3775	1140	2050	3800	1130
84	2600	4300	900	3900	6600	740	1900	3500	920	1920	3550	1030
82	2478	3950	730	3800	6300	620	1780	3200	840	1810	3325	825
80	2425	3850	620	3750	5900	520	1720	2950	700	1720	3050	755
79			580	3650	5400	410	-		650			
78	2150	3375	510	3000	4700	370	1620	2750	590	1600	2700	590
77			345	2950	4400	290			510			
76	1500	2250	273	3100	4450	265	1500	2450	430	1520	2500	460
75			215	3000	4200	230			350			
74	1250	1820	162	2950	4100	190	1380	2100	300	1400	2250	345
73			128	2650	3700	140			255			290
72	1150	1610	90	2300	3150	104	1310	1920	205	1280	1910	233
71			66	2150	2750	64			159			187
70	1130	1360	47	2050	2500	44	1190	1630	117	1170	1680	143
69			28.5	1950	2450	30			88			107
68	780	930	12.4	1900	2150	14.5	1090	1370	53.5	1090	1460	75
67			5.6–6.1	1800	1950	7.2–7.8			32			48.5
66	660	705	1.9–2.1			3.4–3.8	890	1070	17	935	1150	27.5
65			1–1.3			.9–1.3			9.8–11			15.5
64	510	530	.4–.5			.3–.6			4.9–5.6	810	900	7–8
62	410	345		1200	1000				2.3–3.1			1.4–1.8
60	332	245		940	640		630	555	1.3–1.6	585	525	
59	295	205		840	550				.7–1			
58	255	165		720	420		535	390		480	375	
57	225	127		630	340							
56	208	99		550	270		440	272		410	270	
55	176	77		500	215		410	235				
54	148	575		430	160		355	195		342	176	
53	131	47		340	122		308	153				
52	108	34		290	91		263	116		250	108	
51	94	28		235	68		228	88				
50	71	q9.3		180	42		186	63		186	63–64	
49	52	15.2		142	32.5		148	52.5		154	51	
48	44	9.3		102	21		128	40		122	38	
47	33	6.5–7		75	14.5–16		97	27		103	29	
46	25.5	4.1–4.6		48	8.8–9		70	17		79	21	
45	17.5	3–3.6		33	5–5.4		56	13.5		61.5	14.5	
44	10.6	1.5–1.8		19	2.6–3.1		41	8.4–9.4		39	8.8–10	
43	6–6.5	.9–1.1		9.6	1.2–1.6		26	5.5–6.5		31.5	6.5–7.3	
42	2.8–3.1	.4–.6		4.8–5.4	.6–.9		15	3.3–3.9		19.5	3.8–4.5	
41	1.4–1.7			2.2–2.6	.2–.4		9.6	2.2–2.5		12.4–13.2	2.0–2.4	
40	.6–.8			.9–1.2			4.1–4.7	1.4–1.3		6.4–7.1	1–1.4	
39							2.3–3.0			4–4.8	.6–1.0	
S.T.		205			198			205			205	
I.R.		3			2.5			5			3	

$A(Ph_3Sn^+)Ph_3SnI$ vs. $A(Et_3Sn^+)Et_4Sn$

eV	i(Et)	i(Ph)	i(Et)	i(Ph)	i(Et)	i(Ph)	i(Et)	i(Ph)
70	840	860	850	960	1060	1080	900	1520
19.6	730	918	818	1160	720	613	619	880
18.9	720	804	806	1020	550	523	473	750
18.1	700	772	784	980	530	488	456	700
17.3	680	725	760	920	520	474	447	680
16.5	630	677	706	860	490	432	421	620
15.7	590	615	660	780	460	411	396	590
14.9	540	575	605	730	430	397	370	570
14.1	480	527	538	670	410	383	353	550
13.4	400	433	448	550	330	293	284	420
12.6	315	335	353	425	270	247	232	355
11.8	240	200	269	355	185	184	159	265
11.4	205	232	230	295				
11.0	165	193	185	245	126	118	108	170
10.6	134	155	150	196	106	109	91.2	156
10.2	88	118	98.6	150	64	66.9	55	96
10	70	98.1	76.1	125	52	58.5	44.7	84
9.8	52	75.6	59.4	96	40	44.6	34.4	64
9.6	37	55.9	41	71	26	31.4	22.4	45
9.4	25	38.6	28	49	16.5	20.2	14.2	29
9.2	17	27.2	19	34.5	10	12.5	8.6	18
9.0	10–10.2	17.7	11–11.4	22.5	5.6–5.8	74	4.8–5	10.6
8.8	5.6	9.9–10.1	6.3	12.7	3.6	4.5	3.1	6.4
8.6	3.1–3.2	5.2–5.3	3.5–3.6	6.6–6.7	1.5	.2	1.3	3
8.4	1.5–1.6	2.4–2.5	1.7–1.8	3.1–3.2	.7	.1	.6	1.5
8.2	.7–.8	1.2	.8–.9	1.5–2.6	.3	.4	.3	.6
8.0	.1–.4	.45	.1–.4	.6	.2	.2		.3
7.8		.15		.2				
S.T.	195		205		197		210	
I.R.	0.4		0.4		0.5		0.6	

$A(Ph_3Sn^+)Ph_4Sn$ vs. $A(Et_3Sn^+)Et_4Sn$

eV	i(Et)	i(Ph)	i(Et)	i(Ph)	i(Et)	i(Ph)	i(Et)	i(Ph)
67.3	191	191	157	270	650	660	1480	1490
19.6	370–375	368	305	520	475	410	1080	930
18.9	362	361	297	510				
18.5					444	350	1015	800
18.1	355	336	291	474				
17.7					418	315	950	712
17.3	347	311	285	440				
16.9					396	270	900	610
16.5	334	272	274	385				
16.1					374	235	855	530
15.7	320	244	262	345				
15.3	305	205	250	290	354	190	805	430
14.5	290	177	238	250	328	154	745	350
13.7	262	136	214	192	292	118	665	270
13.0	227	97.6	187	138	244	82–100	555	190

eV	i(Et)	i(Ph)	i(Et)	i(Ph)	i(Et)	i(Ph)	i(Et)	i(Ph)
12.6	205	79.2	168	112				
12.2	179	61.5	147	87	195	53	442	120
11.8	156	48	128	68				
11.4	133	37	109	52	143	31–33	325	71
11.0	105	24	86	34	121	24	275	54
10.6	80.3	16.5	65.8	23.5	95–97	16.4	217	37
10.2	63	11.3	51.7	15.4–16	73.9	11.4–12.2	168	25.8
9.8	45	7	36–37	9.8–10	58.1	8.2	132	18
9.6	39.5	64–65	32.4	9–9.2	47.5	5.9	108	13.3
9.4	31.5–32	4.6–4.7	26	6.5–6.7	40.5	4.9	92	11
9.2	23.5–24	3.1–3.3	19–19.7	4.4–4.6	28.2	3.7	64	8.4
9.0	17–17.4	2.0–2.1	14–14.3	2.8–2.9	26	2.85	58.5	6.4
8.8	12–12.4	1.3	9.8–10.2	1.8–1.9	19	1.9–2.2	43	4.3–5
8.6	8.2–8.4	.9	6.7–7	1.2–1.3	15.2	1.4–1.6	35	3.2–3.6
8.4	5.1–5.4	.4	4.2–4.4	.6	10.8–11	.9–1.1	24.7	2–2.5
8.2	3.1–3.3	.2–.3	2.5–2.7	.3–.4	7–7.4	.7	16–16.8	1.6
8.0	1.9–2.0		1.6	.2–.3	4.6–4.8	.3	10.4–10.8	.7
7.8	.9–1		.7–.8	.1	2.9–3.1	.1–.2	6.5–7	
7.6	.4		.3		1.6–1.8		3.6–4	
7.4	.2		.2		.8		1.8	
7.2	.1		.1		.4		.8	
7.0					.2		.4–.5	
S.T.	195		210		195		203	
I.R.	.4		.4		.4		1.5	

$A(Ph_3Sn^+)Ph_3SnEt$ vs. $A(Et_3Sn^+)Et_4Sn$

eV	i(Et)	i(Ph)	i(Et)	i(Ph)	i(Et)	i(Ph)	i(Et)	i(Ph)
67.3	170	170	180	140	670	670	870	900
18.9	705	640			580	618	700	830
18.5								
18.1	709	680						
17.3	721	720			540	551	660	740
16.5	705	760						
16.1					480	469	580	630
15.7	689	800	700	630				
14.9	640	790	670	620				
14.5					365	327	440	440
14.1	583	760	590	600				
13.7	559	730	540	580				
13.4	518	690	510	540				
12.9	478	640	460	500	270	234	330	315
12.6	437	580	435	460	205	175	250	235
12.2	387	515	382	400				
11.8	332	455	310	360	132	115	160	154
11.4	279	385	280	304	102	95.2	120	128
11.0	233	325	240	256	74	71.4	90	96
10.6	186	265	171	209	44	46.1	53	62
10.2	143	198	135	156	25	27.9	30	37.5
10	112.5	156	110	123	16.5	23.8	20	32
9.8	93.5	133	92	105	10.4–11.2	16.4	12.6–13.6	22

eV	i(Et)	i(Ph)	i(Et)	i(Ph)	i(Et)	i(Ph)	i(Et)	i(Ph)
9.6	78.5	108	75	85	5.6	9.1	6.8	12.2
9.4	62	85–86	60	67.5	3	5.6	3.6	7.5
9.2	48.5	65–67	49	52	1.4–1.5	3.1	1.7	4.1
9.0	36.5	51–52	39	40.5	.6	1.6	.7	2.2
8.8	27	37	25	29	.1–.2	.6–.7	.1–.2	.8–.9
8.6	18.5–18	26	18	20.3		.4		.5
8.4	11.5–12	16.6–17	11.5	13.2		.15		.2
8.2	7.3–7.6	10.2–10.4	7–8	8–8.2				
8.0	4.1–4.6	3.2–3.4	4–5	4.7–5				
7.8	1.9–2.3	1.4–1.5	2–2.2	2.5–2.7				
7.6	.7–.8	.6–.7	.6–.9	1.1–1.2				
7.4	.2–.3	.2–.3	.2–.3	.5–.6				
S.T.	200		195		195		195	
I.R.	2.0		2.0		2.0		2.0	

$A(Ph_3Sn^+)Ph_3SnSPh$ vs. $A(Et_3Sn^+)Et_4Sn$

eV	i(Et)	i(Ph)	i(Et)	i(Ph)	i(Et)	i(Ph)	i(Et)	i(Ph)
70	1000	1360	930	2400	980	1240	920	1860
19.6	1000	1180			980	1060	900	1580
17.7	1000	1140	1080	1950	900	900	840	1360
15.7	740	760	800	1400	780	680	740	1040
13.7	500	460	540	860	590	420	520	610
11.8	250	200	270	380	295	175	260	260
11.4	205	150	225	305	230	127	210	200
11.0	154	111	180	240	186	100	165	148
10.6	119	80	130	166	135	72	120	100
10.2	80	51–52	89	108	102	48.5	84	66
10	65	39–40	74.5	86.5	81	36.5	70	53–55
9.8	53	30–32	59	65.5	65	28	53–55	38
9.6	37.5	21	43	47	47	19.5	39–41	26
9.4	28	14–14.6	31	32.5	33	12–12.8	27.5	16.8–17.2
9.2	17.8–18.6	8.8–9.2	21–22	21	23.5	7.6–8.1	16.5	8–8.8
9.0	11.4–12.2	4.5–4.8	13–13.4	12.6–13	13.2–14	4.2–4.6	11.3	3–3.3
8.8	6.8–7.5	2.6–2.9	8–8.5	7.5–8	8–8.7	2.4–2.8	6–.65	1.7
8.6	4.4–4.6	1.4–1.7	4.8–5.2	4.4–4.7	4.5–4.9	1.4–1.6	3.9–4.1	.9–1.1
8.4	1.9–2.2	.6–.8	2.6–2.9	2.4–2.5	2.5	.8	2–2.4	.4–.5
8.2	.9–1.1	.3	1.2–1.5	1–1.3	1.2–1.4	.4	.9–1	.2
8.0	.3–.5				.6			
S.T.	197		202		203		203	
I.R.	.9		.8		.8		.8	

eV	i(Et)	i(Ph)	eV	i(Et)	i(Ph)	eV	i(Et)	i(Ph)
70	1400	2400	10.6	127	133	8.8	7.8–8.4	5.2
19.6	1380	1980	10.2	87	85	8.6	4–4.4	2.7
17.7	1250	1720	10	66	63.5	8.4	2.2–2.5	1.4
15.7	800	1300	9.8	56	49	8.2	.9–1.1	.55
13.7	540	770	9.6	40	33	8.0	.4–.6	.1
11.8	270	330	9.4	29.5	23			
11.4	212	247	9.2	20	14–15			
11.0	163	181	9.0	12.6	9			
S.T.	203		200		200		200	
I.R.	.8		1		1		1	

$A(Ph_3Sn^+)Ph_3SnMe$ vs. $A(Et_3Sn^+)Et_4Sn$

eV	i(Et)	i(Ph)	i(Et)	i(Ph)	i(Et)	i(Ph)	i(Et)	i(Ph)
70	2450	1200	858	1120	3050	1580	1250	2100
19.6	3050	1360	1067	1400	3500	1680	1430	2240
18.8	3100	1400	1067	1360	3450	1660	1420	2210
17.6	3000	1250	1090	1300	3300	1580	1350	2100
16.9	2950	1200	1050	1220	3200	1480	1310	1970
15.7	2600	1040	1030	1020	2800	1280	1150	1705
14.9	2300	885	910	880	2450	1100	1000	1460
13.7	1700	620	805	620	1950	830	800	1090
12.9	1340	500	595	490	1540	655	631	875
11.8	800	300	469	310	1000	450	410	600
11.4	620	250	280	245	800	365	328	478
11.0	450	185	214	180	620	293	254	390
10.6	305	126	158	124–128	430	207	176	273
10.2	210	83	107	81–86	265	133	109	177
10	154	67	73.5	65 –69	210	106	84–88	139
9.8	110	50	38–39	46–49	141	73	57–59	93–100
9.6	74	30	25–27	29–31	92–100	50–54	38–41	67–72
9.4	47.5	19	16–17	18–21	57–62	32–35	21–25	43–47
9.2	39	12–14	14	12–14	34–37	21–23	14–15	27–31
9.0	16	6–8	5.3–6	6.5–7.5	17–20	11–13	8–8.2	15–17
8.8	9.6	3–4.5	3–3.7	3.5–4.4	8–11	5–6.5	3.3–4.5	6–8
8.6	4–6	1.9–2.5	1.4–2.1	1.8–2.7	3–4.5	2–3.5	1.2–1.9	2.7–4.7
8.4	2.2–3.6	.5–1.3	.8–1.3	.5–1.4	1–2.3	.9–1.7	.4–.9	1.2–1.3
8.2	.9–1.9	.2–.7	.3–.7	.2–.7	.2–.5	.1–.9	.2–.5	.1–1.2
8.0	.2–1.1							

S.T.	195		200		195		200	
I.R.	.4		1.6		.4		1.6	
70	2100	2650	2600	2700	780	800	1560	850
19.6	2380	2900	3000	3000	960	860	1920	780
18.4	2330	2800	2950	2900	860	850	1720	800
17.6	2050	2400	2580	2450	850	820	1700	810
16.5	1850	2050	2330	2000	780	730	1560	715
15.7	1700	1800	2142	1820	720	670	1440	660
14.5	1520	1620	1920	1600	580	520	1160	500
13.7	1300	1320	1640	1290	490	420	980	400
12.5	875	910	1100	890	335	295	670	300
11.8	620	650	781	640	238	220	480	210
11.4	500	530	630	510	193	180	390	190
11	370	405	466	400	140	134	280	130
10.6	255	275	320	275		99	200	95
10.2	149	172	185	168	60–63	64	123	60
10	114	135	144	130–140	49.5	52.5	99	51
9.8	79–82	94	101	90–98	31.5	36.5	65	37
9.6	49–54	62–66	64.7	63	21	24	42	23
9.4	32–33	40–45	40–42	42	12–13	14–16	25–27	13–17
9.2	17–19	23–27	22–24	20–25	6–7	8–9.4	13.5	8–9
9.0	7.5–10	13–15	9.5–12.6	12–14	3–4	5–5.5	6–8	4–6

	i(Et)	i(Ph)	i(Et)	i(Ph)	i(Et)	i(Ph)	i(Et)	i(Ph)
8.8	4.5–5	6–8	5.7–6.3	5–9	1–2.2	2.6–3	3.2–4.4	2–2.5
8.6	1.3–2.3	1.5–2.5	1.6–2.8	1–3	.7–1	1–1.4	.5–.9	1–1.2
8.4	.3–.8		.3–.1		.2–.5	.3–.7	.3–.5	.3–.6
8.2								
S.T.	200		200		205		206	
I.R.	.7		.8		1.2		1.5	

$A(Ph_3Sn^+)Ph_3Sn\cdot GeMe_3$ vs. $A(Et_3Sn^+)Et_4Sn$

eV	i(Et)	i(Ph)	i(Et)	i(Ph)	i(Et)	i(Ph)	i(Et)	i(Ph)
70	3700	3000	2800	2750	3200	2600	2900	2900
19.6	3250	2150	2720	2200	2700	1850	2630	2120
18.9	3150	1950	2560	2080	2650	1640	2550	1900
18.1	3050	1720	2510	1700	2600	1470	2470	1700
17.3	2750	1460	2460	1550	2450	1260	2230	1400
16.5	2600	1240	2320	1350	2300	1040	2110	1200
15.7	2425	980	2160	1075	2150	860	1970	950
14.9	2125	740	1960	800	1840	670	1720	720
14.1	1780	520	1680	610	1480	470	1440	510
13.4	1460	350	1344	380	1300	310	1180	340
12.6	1120	225	1064	243	1000	193	907	240
11.8	820	120	768	140	680	110	664	130
11.4	630	81	608	110	550	76	510	85
11.0	460	54	452	68	400	53.5	373	56
10.6	335	36	320	45	290	33	271	39
10.2	207	21	208	27	178	18–20	168	20
10.0	174	16.6–17.2	166	20.5–19	148	15–17	141	16–17
9.8	120	11.6–12.8	110	12–13.5	102	9.8–10.8	96–97	12
9.6	82–84	8.4–9.2	82	8.6–9.6	74	6.5–7.2	67	8.8
9.4	51–54	5.1–5.5	51	5.4–6.4	44	4–4.7	41–44	5–5.7
9.2	30–33	3.3–3.5	31–32.8	3.2–4.1	28.5	2.5–3.1	25–26	3–3.5
9.0	17–17.8	1.6–2.1	16.8–18	1.9–2.5	14–16	1.4–1.9	13.6–14.3	1.6–2.1
8.8	9–10.2	1–1.3	9.6–10.4	1.2–1.5	7–8	.6–.9	7.3–8.3	1–1.4
8.6	4.4–5.1	.5–.7	4.4–4.9	.5–.9	3.5–4.5	.4–.5	3.6–4.1	.5–.6
8.4	2.5–2.8	.2–.4	1.8–2.5	.3	1.8–2.1	.2–.4	2–2.3	.2–.4
8.2	.9–1.3		.8–1.2		.8–1.4	.1–.2	.7–1.1	
8.0	.4–.7		.4		.4–.6		.3–.6	
S.T.	205		210		195		205	
I.R.	1.2		1.6		2.0		1.7	

$A(Ph_3Sn^+)Ph_6Sn_2$ vs. $A(Et_3Sn^+)Et_4Sn$

eV	i(Et)	i(Ph)	i(Et)	i(Ph)	i(Et)	i(Ph)	i(Et)	i(Ph)
70	2380	4100	5000	5600	8600	8300	7000	4000
19.6	1770	3750	4050	6500	7000	9600	5200	3700
17.6	1460	2750	3200	4100	5600	6050	4300	2700
15.6	1160	1500	2204	2600	3850	3850	2140	1450
13.7	748	900	1570	1480	2700	2190	1390	850
11.7	415	450	870	800	1500	1180	769	420
11.3	354	390	789	660	1360	977	655	380
10.9	282	315	673	550	1160	814	523	310
10.5	228	250	545	440	940	651	422	245
10.1	173	190	418	330	720	489	321	180
10	170	166	412	290	710	429	315	167
9.8	124	122	336	235	580	348	230	123
9.6	109	108	270	190	465	281	202	109
9.4	90.1	86	218	146	375	216	167	85
9.2	64.6	65	168	112	290	166	120	65
9	47.6	47–51	131	84	225	124	88.2	50
8.8	34–35	34–36	90	59–63	155	87–93	63–65	35
8.6	22.8–24.8	23–25	62.6	42–44	108	63.6	43–46	24.5
8.4	14.6	15	39.7	27	67–70	40	27.1	15–16
8.2	9.4	9–10.2	24.4	17–18	42	25.2	17.3	9–10
8.0	4.9–5.4	5–6	13.1–14.5	9–11	22.5–25	13.3	9.2–10	5–6
7.8	2.2–2.5	2.4–3.2	5.2–7	4.5–5.5	9–12	6.7–8.1	4–4.7	2.3–3.1
7.6	1–1.4	1–2	2–2.9	2–3	3.5–5	3–4.4	1.9–2.5	1–2.2
7.4	.3–.5	.5–.7	.9–1.7	.5–1.5	1.5–3	7–2.2	.6–1	.5–.7
7.2			.3–.9		.5–1.5			.1–.4
S.T.		205		205		205		205
I.R.		.4		.4		.4		.4
70	6900	2300	2620	4700	3300	3000	2150	3450
19.6	5700	1800	1940	3600	1600	1800	800	1640
17.6	4500	1340	1710	1680	1280	1140	620	980
15.6	3650	860	1390	1650	1060	610	520	600
13.7	2450	460	931	920	860	225	430	340
11.7	1300	220	494	450	440	155	235	134
11.3	1100	185	418	370	340	106		
10.9	880	148	334	300	250	66	140	70
10.5	690	118	262	235	160	34	96	43
10.1	510	88	194	175	94	35	58	22.5
10.0	510	80	194	160	78	23	50	25
9.8	410	64	156	125	57	13.4	34	15–16.5
9.6	315	49.5	120	100	31.5	7.2	22	10.4
9.4	245	38–40	93	80	17–19	3.7	12	5.4
9.2	190	29–31	72	60	9.6–10.2	1.9–2.4	5.8	2.6
9.0	137	22.5	52	45	5–5.5	.9–1.1	3.7	1.7
8.8	92	15–16	35	30–32	2.2–2.6	.5	1.7	.8
8.6	62	10–10.8	23.6	20–21	1–1.3		.8–1	.4–.5
8.4	35–38	5.5–6.5	13.3–14.3	11–13	.3–.5			
8.2	20.5	3.5	7.6–8	7				
8.0	10–12	1.5–2	3.8–4.6	3–4				
7.8	5–6.4	.7–1.3	1.9–2.4	1.5–2.5				
7.6	2.2–2.7	.4–.8	.8–.1	.8–1.5				
7.4	.7–.1		.3–.4	.4–.7				

S.T.	200	210	195	200
I.R.	1.7	1.7	1.7	1.7

$A(Ph_3Sn^+)Ph_3Sn{\cdot}SnMe_3$ vs. $A(Et_3Sn^+)Et_4Sn$

eV	i(Et)	i(Ph)	i(Et)	i(Ph)	i(Et)	i(Ph)	i(Et)	i(Ph)
70	274	274	1160	319	620	620	2200	691
19.2	352	275	1180	330	400	380	1420	430
17.3	287	220	960	264	321	285	1140	325
15.4	212	162	710	194	248	225	880	255
13.4	150	110	500	132	161	140	570	158
11.5	65.8	40–43	220	50	87.4	60	310	68
11.1	59.8	34–38	200	43	74.7	47	265	53
10.8	40.1	24–27	140	30	60.6	40	215	44.7
10.4	34.5–37	18–21	120	22	49.4	30–33	170	35.1
10	29.9	14–16	95	17–19	39.2	22.5–25	145	25.5–28.3
9.8	23.9–24.5	11–13	82	16–17	32.4	16–19	115	18.1–21.5
9.6	19.4–22.4	10–12.4	70	13	26.8	13–15	90–100	14.7–17
9.4	17.9–20.9	8–10	65	12–15	20.4	9–12	70–75	10.2–13.6
9.2	15–16.4	7–8	53	9.6–12	16.1	6.5–8	54–60	7.4–9
9.0	11–12.7	5–5.5	40	8.4–9.6	13	5–6	45–48	5.7–6.8
8.8	9–9.7	3.5–4.7	30–32.5	6–6.6	8.5	3.4	28–32	3.8–5.2
8.6	6.7–7.5	2.5–4	23–25	4.2–5.6	5.1	2–3	17–19	2.3–3.4
8.4	3.3–3.5	1–2.5	14–15	3–4.8	3.4	.5–1.6	10–14	.6–.8
8.2	2.7–3.6	.5–1.5	9–12	1.2–3	2.1		7–8	
8.0	1.6–2.1	.1–1.5	5.5–7	.6–1.8	1.13		3.4–4.6	
7.8	.9–1.3		3–4.5	.1–1.8	.42		1.5–3	
7.6	.5–.9		1.5–3				.5–1.5	
7.4	.3–.5		.9–1.5					
7.2			.1–1					

S.T.	205		205		210		210	
I.R.	.4		.7		.4		.7	
eV	i(Et)	i(Ph)	eV	i(Et)	i(Ph)	eV	i(Et)	i(Ph)
70	310	430	10.4	94–98	45	8.8	19–21.2	8–9
19.2	308	580	10	77	38	8.6	12.5–13.5	5.5–6.5
173	273	450	9.8	69	28.5–33	8.4	9.6–10.2	3.5–4.5
15.4	235	320	9.6	57	25–26	8.2	5.4–6.2	2.0–3.5
13.4	173	190	9.4	46	19–21	8.0	3.1–3.9	1–2
11.5	135		9.2	35–36	13–15	7.8	1.9–2.5	.5–1
11.1	119	78	9.0	27–29	11–13	7.6	.8–1.2	
10.8	114	58				7.4	.4–.7	

S.T.	205
I.R.	.4

$A(PhSnEt_2^+)Ph_2SnEt_2^+$ vs. $A(SnEt_3^+)Et_4Sn$.

eV	i(Ph')	i(Et)	i(Ph')	i(Et)	i(Ph')	i(Et)	i(Ph')	i(Et)
67.3	475	479	3070	3055	630	630	1970	9700
19.6	395	518	2560	3355	560	590	1750	9200
18.9	380	502	2460	3250	540	578	1680	8900
18.1	360	480	2330	3130	530	558	1650	8600
17.3	340	560	2260	2950	495	526	1540	8100
16.5	290	433	1880	2800	455	493	1420	7600
15.7	255	399	1650	2560	417	454	1300	7000
14.9	220	363	1420	2350	378	409	1170	6300
14.1	182	317	1180	2050	320	350	1000	5400
13.4	146	260	940	1660	265	292	827	4500
12.6	106	201	685	1300	210	227	655	3500
11.8	65	150	420	940	156	169	477	2600
11.0	50	87	325	500	105	109	328	1680
10.6	33	66	215	420	80	82	250	1280
10.2	26	43	170	275	56	56.5	175	870
10	20	34	130	220	44	45.4	137	700
9.8	13.8	25	89.3	161	33–35	33–34	100–109	515
9.6	9.3	17–17.6	60.2	112	25–27	25	78–84	383
9.4	5.9	11–11.7	38.2	75	17.2–17.8	17–17.2	54–56	263
9.2	4.2	6.7–7.0	27.1	43.5–45.5	12.6–13.2	11.7–11.9	39–41	182
9.0	2.45	4.4–4.6	15.9	28–30	7.7–8.3	7.1–7.4	24–26	112
8.8	1.3	2.3–2.4	8.4	14.6–15.8	5.3–5.9	4.7–4.9	17–18.5	74
8.6	.8	1.2–1.4	3.9–5.2	8–9	3–3.5	2.4–2.5	9–11	38
8.4	.35	.5–.6	1.2–3.2	3.5–4.1	1.6–2	1.3–1.4	5–6.2	20–21
8.2		.2–.3		1.5–1.7	.9–1.1	.6–6.7	2.8–3.4	9.6–10.4
8.0		.1–.12		.6–.8	.4–.6	.3	1.2–1.8	4–4.5
7.8				.3–.4	.2–.4		.6–1.2	2
7.6								.9–1.1
7.4								.5–.8
S.T.	200		200		200		200	
I.R.	1.4		1.4		1.4		1.4	

$A(Ph_2SnEt^+)Ph_2SnEt_2$ vs. $A(Et_3Sn^+)Et_4Sn$

eV	i(Ph")	i(Et)	i(Ph")	i(Et)	i(Ph")	i(Et)	i(Ph")	i(Et)
70	5100	5100	625	625	4300	4300	880	640
19.6	5030	4900	781	710	4230	4140	1100	700
18.9	4900	4700	760	690	4140	3950	1070	680
18.1	4770	4550	739	667	4050	3840	1040	660
17.3	4500	4300	689	635	3800	3630	970	640
16.5	4240	4050	646	610	3580	3450	910	620
15.7	3910	3700	597	570	3300	3120	840	590
14.9	3570	3350	540	525	3000	2820	760	515
14.1	3050	2900	479	470	2570	2450	675	465
13.4	2520	2450	419	410	2130	2060	590	405
12.6	2050	1910	348	340	1650	1610	490	330
11.8	1590	1440	270	260	1290	1250	380	255
11.4	1360	1200	234	223	1100	1010	330	221
11.0	1050	920	199	185	850	745	280	180

eV	i(Ph")	i(Et)	i(Ph")	i(Et)	i(Ph")	i(Et)	i(Ph")	i(Et)
10.6	834	720	165	150	675	585	233	140
10.2	596	505			480	410		
10	503	410	112	100	407	335	158	98
9.8	404	330	95.1	84	326	267	134	82
9.6	295	245	78.1	68	240	198	110	69
9.4	222	178	62.5	54	180	144	88	52
9.2	156	122	48.3	41	126	98	68	40
9.0	109.5	83	39.1	33	87.5	67	55	31
8.8	72.9	54	28.8	23.5	59	43.5	40.5	21.5
8.6	46–47	32.5	19.5	15.2–16	37.3	26.4	27.5	15–16
8.4	27.2–27.8	17.8–18.6	13.9–14.1	11	22.4	14.4–15.1	19.7	11.5
8.2	14.9–15.2	8.8–9.2	9.5	6.8–7.2	12.15	7.1–7.5	13.4	6.7–7.1
8.0	7–7.3	3.9–4.1	5.6	3.95	5.8	3.2–3.3	7.9	4
7.8	3.3–3.6	1.8–2	3.1–3.2	2.1–2.2	2.7–2.9	1.5–1.6	4.45	2–2.1
7.6	1.5–1.6	.9–1.1	1.6	1	1.2–1.3	.7–.9	2.2–2.3	1
7.4	.7–.8	.5–.6	.8	.5	.6–.7	.4–.5	1.1	.4–.5
7.2	.7	.4–.5	.4	.2–.3			.5–.6	.1
S.T.	205		210		205		198	
I.R.	1.4		1.2		1.3		.7	

$A(Ph_2SnEt^+)Ph_3SnEt$ vs. $A(Et_3Sn^+)Et_4Sn$

eV	i(Ph")	i(Et)	i(Ph")	i(Et)	i(Ph")	i(Et)	i(Ph")	i(Et)
67.3	254	1400	260	253–268	506	700	260	1500
19.6	490	3150	495	600	957	1600	480	3200
18.9	520	3200	525	590–620	1000	1600	510	3150
18.1	530	3200	535	595	1040	1600	515	3150
17.3	510	3100	540	577	1010	1590	505	3160
16.5	470	2900	468	539	950	1450	465	2850
15.7	435	2780	442	512	890	1400	405	2800
14.9	387	2600	387	484	765	1305	390	2700
14.1	279	2050	282	386	550	1025	281	1950
13.4	165	1400	180	255	340	700	170	1390
12.6	130	1080	128–126	202	255	540	125	1070
11.8	74–79	710	74–80	132	149	355	76	710
11.0	30–35	330	33–35	60–63	65	175	31–36	310
10.6	22–23	210	21–22.5	39	50–52	105	21–23	210
10.2	11–15	129	11.4–13	23–25	21–28	64.5	10–14	130
10	10.5	111	10–11	20–21	21–24	55	11	110
9.8	4–6	70	5–6	12.6–13.4	11	34.3	4–6	65
9.6	3.2–4.1	43	3.5–4.3	7.8–8.4	7–8.6	21.2	3.3–4	40
9.4	2.5–3.1	28	2.5–3	5.1–5.5	5–6	14.5	2.6–3	25
9.2	1–1.7	19.5–21	1.4–1.6	3.6–3.9	2.8–3.6	8.9–10.1	1.1–1.8	19–22
9.0	.7–.9	8.8–10	.75	1.6–1.9	1.4–1.9	4.5–5	.8	8–9.5
8.8	.4–.6	6–7	.5	1.1–1.3	.8–1.2	3–3.9	.5–.6	6.3–7.1

eV	i(Ph^{II})	i(Et)	i(Ph^{II})	i(Et)	i(Ph^{I})	i(Et)	i(Ph^{III})	i(Et)
8.6	.1–.3	3–5	.1	.7	.2–.6	1.4–2.4	.1	3.1–5.1
8.4		1.4–1.8		.3		.7–.9		1.4–1.8
8.2		.4–.6				.15		.42
S.T.	205		197		205		205	
I.R.	.4		.6		.4		.4	

$A(PhSnEt_2^+)PhSnEt_3$ vs. $A(Ph_3Sn^+)Ph_4Sn$

eV	i(Ph)	i(Ph')	i(Ph')	i(Ph)
70	520	520	1950	1950
19.6	350	462	1690	1300
18.9			1640	1160
18.5	300	440		
18.1			1620	1040
17.7	265	433		
17.3			1530	885
16.9	225	411		
16.5			1460	740
16.1	184	383		
15.7			1320	590
15.3	144	361		
14.9			1200	445
14.5	110	314		
14.1			1040	320
13.7	74	267		
13.4			877	215
12.9	47	220		
S.T.	210		205	
I.R.	1.3		1.4	

eV	i(Ph)	i(Ph')	i(Ph')	i(Ph)
12.6			682	128
12.2	27	170		
11.8			501	71
11.4	14.1	116	385	46
11.0			296	31.5
10.6	6.0	65	218	20.5
10.2	3.5	45	139	10.9
10			117	8.9
9.8	1.9	26.7	88	6.2
9.6	1.2–1.4	18.2	61	4.3
9.4	.7	12.3	38.5	2.6
9.2	.3–.4	7.9	22.6	1.45
9.0		4.8		
8.8		2.6	6.75	.4–.5
8.6		1.4	4.8	
8.4		.6	2.1	
8.2		.4	1.05	
8.0			.4–.6	

$A(PhSnEt_2^+)PhSnEt_3$ vs. $A(Ph_3Sn^+)Ph_3SnEt$

eV	i(Ph')	i(Ph)	i(Ph')	i(Ph)
67.27	5000	5000	4950	4500
19.6	5000	5100	5200	5210
18.9	5318	4950	5300	5110
18.1	5181	4800	5200	4910
17.3	5045	4550	5000	4600
16.5	4910	4300	4900	4300
15.7	4480	4000	4500	4000
14.9	4091	3500	4100	3600
14.1	3640	2900	3700	2850
13.4	3050	2350	3100	2400
12.6	2450	1850	2500	1900
11.8	1890	1350	1900	1400
11.0	1380	914	1400	920
8.0	12.0	8.6–9	11.9	9.0

eV	i(Ph')	i(Ph)	i(Ph')	i(Ph)
10.6	1000	750	980	750
10.2	764	588	700	590
10	596	455	600	460
9.8	509	400	500	400
9.6	388	308	400	307
9.4	297	242	300	241
9.2	220	183	210	180
9.0	159	128	165	130
8.8	100	80	105	80
8.6	64.5	51	65	50
8.4	37	29.2	40	30
8.2	22.5	16.8	21	17.5
7.4	1.15	.9–1.1	1.1	.95

eV	i(Ph)	i(Ph')	i(Ph)	i(Ph')	eV	i(Ph)	i(Ph')	i(Ph)	i(Ph')
7.8	5.45	3.8	6.0	4.1	7.2	.4–.6	.3–.5	.5	.40
7.6	2.5	1.45	2.3	1.3	7.0				
S.T.	205		205						
I.R.	1.3		1.3						

$I(Ph_2SnEt_2)$ vs. $A(Et_3Sn^+)Et_4Sn$

eV	i(Et)	i(PhEt)	i(Et)	i(PhEt)	i(Et)	i(PhEt)	i(Et)	i(PhEt)
70	10000	46–48	10000	46–49	9500	49–50	5100	50–51
19.6	9800	70–72	9600	71–72	9100	71–75	5000	70–72
18.9	9500	70–72	9300	71–72	8900	71–75	4900	71–72
18.1	9200	73–75	9020	72–73	8700	71–74	4700	71–72
17.3	8800	72–74	8600	72–73	8300	72–75	4500	72–73
16.1	8400	75–77	8240	72.–73	7900	72–75	4300	72–73
15.7	7800	72–74	7650	72–73	7300	72–75	4000	72–73
14.9	7100	69–71	7000	70–72	6700	69–72	3650	69–71
14.1	6300	67–69	6200	68–70	5900	67–69	3200	68
13.4	5400	62–65	5300	61–64	5090	62–65	28—	63
12.6	4300	55–57	4200	54–56	4050	56–58	2200	55–58
11.8	3250	47–49	3200	48–50	3050	48–49	1650	47–49
11.4	2900	42–44	2850	43–45	2700	43–44	1500	42–45
11.0	2200	36–38	2150	35–39	2070	36–38	1150	37–38
10.6	1680	30–31.5	1650	31–32	1580	30–32	860	30–32
10.2	1280	25–26	1250	25–27	1200	25–26.5	660	25–27
10	1070	22.5–24	1050	23–26	1000	23–24	550	21–24
9.8	820	18.4–19.6	800	18–19	770	19	420	17–18.5
9.6	650	15.4–16.4	640	15–16.5	610	15–16	330	14.5–16.3
9.4	475	12.8–13.4	465	13–13.5	450	12.8–13.3	243	12.7–13.2
9.2	345	10.2–11	340	10–11	330	10.3–11.1	178	10–11
9.0	245	8–8.8	240	8–9	230	8–9	125	8–8.9
8.8	158	5.6–6.4	155	5–6.5	150	5.5–6.5	81	5.4–6.2
8.6	95	3.9–4.5	93	4–4.6	90	3.8–4.4	49	3.9–4.4
8.4	61	2.9–3.3	60	3–3.2	57	3.0–3.4	31	2.9–3.1
8.2	29.5	1.5–1.9	29	1.5–1.8	28	1.6–1.9	15.1	1.5–1.8
8.0	15	.9–1.1	14.5	.9–1	14	.9–1.1	7.6	.9–1.2
7.8	7.5	.4–.6	7.5	.5	7	.5	3.8	.4–.6
7.6	3.2	.2–.3	3.1	.25	3	.2–.4	1.7	.2–.3
7.4	1.7		1.5		1.5		.9	
7.2	.9		.8		.8		.4	
S.T.	205		205		205		200	
I.R.	1.4		1.4		1.4		1.7	

$I(Et_4Sn)$ vs. $A(Et_3Sn^+)Et_4Sn$

eV	i(Et)	i(4Et)	i(Et)	i(4Et)	i(Et)	i(4Et)	i(Et)	i(4Et)
70	3900	106–108	4400	107	3900	107	2000	55–56
19.6	5100	152–156	5700	158–159	5100	158–159	2625	78–79
18.9	5000	152–156	5600	156–157	5000	156–157	2575	78–79
18.1	4850	156–160	5400	154–158	4850	151–157	2500	78–79
17.3	4700	152–154	5260	152–154	4700	151–154	2425	80–81
16.5	4500	150–154	5000	152–154	4500	151–152	2300	78–81
15.7	4350	150–152	4900	152–154	4350	152	2250	77–80

eV	i(Et)	i(4Et)	i(Et)	i(4Et)	i(Et)	i(4Et)	i(Et)	i(4Et)
14.9	4050	154–156	4500	150–153	4000	150–153	2010	78–80
14.1	3625	136–140	4050	139–140	3600	139	1900	70–72
13.4	3150	128–130	3500	130–129	3100	131	1625	66–68
12.6	2550	112–114	2860	110–113	2500	112	1310	58–59
11.8	2150	104	2400	105	2100	105	1100	54
11.0	1460	79–81	1640	80	1500	81	750	41–42
10.2	840	55–56	950	57	850	56	440	28
10	760	53	850	51	750	50	390	27–
9.8	615	46	700	45	600	44	315	24–25
9.6	505	38.5–40.5	560	39	500	38.5	260	19.8–20
9.4	395	33–35	440	34	400	33	200	17–18
9.2	292	27.5–28.5	325	28–29	300	28	150	14–15
9.0	225	23–25	250	22–24	215	24	115	12–13
8.8	159	18–19	175	18–19	160	18.5	82	9–9.5
8.6	111	14.2–15	125	14–15	110	14.7	57	7.3–8
8.4	73	10.4–11	82	10–12	75	10–11	38	5.4–5.7
8.2	41	6.8–7.2	45	6.7–7.5	40	7–7.1	21	3.5–3.7
8.0	25	4.6–5	28	4.7–5.1	20	4–6	13	2.4–2.6
7.8	12.6–13.8	3.1–3.5	14–15.4	3.2–3.6	13.6	3–4	6.7	1.6–1.8
7.6	5.5	1.5–1.8	6.2	1.4–1.9	6.0	2.0	2.8	.8–.9
7.4	2.5	.7–.8	2.8	.7–.8	3	.8	1.3	.4–.5
7.2	.9	.3–.4	1.0	.3	.8	.4	.5	
7.0	.5	.1–.2	.6		.3	.1		
ST		205		205		205		200
I.R.		1.2		1.2		1.4		1.2

$A(Et_3Sn^+)Et_4Sn$

eV	i(Xe)	i(Et)	i(Xe)	i(Et)	i(Xe)	i(Et)	i(Xe)	i(Et)
70	365	250	435	285	420	415	365	370
19.6	217	275	227	290	216	440	215	384
19.2	207	271	213	282	202	428	205	379
18.9	202	268	204	274	195	415	200	374
18.5	189	258	193	269	183	408	190	360
18.1	183	268	184	264	176	400	180	374
17.7	180	271	176	261	168	395	180	379
17.3	183	268	168	257	160	390	182	374
16.9	173	248	158	254	151	385	172	370
16.5	165	241	149	248	141	375	164	360
16.1	155	235	140.5	244	135	370	154	351
15.7	141	220	131	238	125	360	140	328
15.3	131	216	119	231	113	380	130	323
14.9	122	210	105	221	101	335	121	314
14.5	111	204	100	224	95	340	111	304
14.1	99	191	85	213	81	323	99	285
13.7	85	179	695	200	66	303	82	267
13.4	72	166	57.5	188	54.5	285	72	248
13.0	59.5	153	42	168	40.5	255	60	229
12.6	46.5	141	29	155	27.7	235	47	211
12.2	36	129	17.5	139	17.1	210	36	192
11.8	27	114	9.1	119	8.7	180	27	170

eV	i(Xe)	i(Et)	i(Xe)	i(Et)	i(Xe)	i(Et)	i(Xe)	i(Et)
11.4	16.5	99.2	3.0	100	3.0	152	16.5	148
11.0	9.5	86.4	5-.7	85.8	.5-.7	130	9.5	129
10.6	4.2	73.7	.2	72.6	.2	110	4.1	110
10.2	1.4	62.7		55.4		84	1.3	93.6
9.8	.3	50.2		43.6		66	.3	74.9
10	1.0	55		49.5		75	.9-1.1	79-89
9.8	.4	52		41.6		63	.3	81
9.6		48.3		34.3		52		72
9.4		41.4		28.4		43		62
9.2		35.8		22.4		34		53
9.0		30.8		17.2		26		45
8.8		24.1		12.9		19.5		36
8.6		20.4		8.6-8.8		13-13.4		30.4
8.4		17		5.8-6.1		8.8-9.2		25.5
8.2		13.5		3.6-3.7		5.5-5.6		20
8.0		10.3		2.2-2.4		3.4-3.6		15.5
7.8		7.6-8		1.3-1.4		1.9-2		11.5-12
7.6		5.5-5.7		.7		1-1.1		8.2-8.5
7.4		3.8-4.0				.5		5.6-5.9
7.2		2.6-2.8				.25		3.9-4.2
7.0		1.6-1.7						2.3-2.5
6.8		.9-1						1.3-1.5
6.6		.4-.5						.7-.8
6.4		.2-.3						.3
6.2								.1-.2
S.T.		195		195		195		195
I.R.		0.4		0.4		0.4		0.4

REFERENCES.

1. J.H. Beynon, "Mass Spectrometry and its Applications to Organic Chemistry", Elsevier, 1960.

2. "Mass Spectrometry", A N.A.T.O. Advanced Study Institute. ed. R.I. Reed, Academic Press, London 1965.

3. R.I. Reed, Quarterly Reviews, 1966, 4, 527.

4. R.I. Reed, "Ion Production by Electron Impact", Academic Press, London 1962.

5. ~~F.W. McLafferty,~~ "Mass Spectrometry of Organic Ions", ed. F.W. McLafferty, Academic Press, New York 1963.

6. F.H. Field and J.L. Franklin, "Electron Impact Phenomena and the Properties of Gaseous Ions", Academic Press, New York 1957.

7. R.L. Platzman, Vortex, 1962, 23, 372.

8. A.J.C. Nicholson, J. Chem. Phys., 1963, 39, 954.

9. H. Budzikiewicz, C. Djerassi and D.H. Williams, "Mass Spectrometry of Organic Compounds", Holden Day Inc., 1967.

10. J. Berkowitz, D.A. Bafus and T.L. Brown, J. Phys. Chem., 1961, 65, 1380.

11. G.E. Hartwell and T.L. Brown, Inorg. Chem., 1966, 5, 1257.

12. R.E. Winters and R.W. Kiser, J. Organomet. Chem., 1967, 10, 7.

13. P.D. Roberts, Ph.D Thesis, Durham 1968.

14. V.H. Dibeler and F.L. Mohler, J. Res. Nat. Bur. Stand., 1951, 47, 337.

15. L. Friedman, A.P. Irsa and G. Wilkinson, J.Amer.Chem. Soc., 1955, 77, 3689.

16. J. Müller and L. D'Or, J. Organomet. Chem., 1967, 10, 313.

17. A.W. Laubengayer and W.F. Gilliam, J.Amer.Chem. Soc., 1941, 63, 477.

18. K. Wade and B.K. Wyatt, J. Chem. Soc. (A), 1967, 1339.

19. G. Fritz, H. Buhl, J. Grobe, F. Aulinger and W. Reerink, Z. anorg. Chem., 1961, 312, 201.

20. F. Aulinger, Colloq. Spectros. Intern. 8th Lucern, Switzerland, 1960, 1959, 267.

21. F. Aulinger and W. Reerink, Z. anal. Chem., 1963, 197, 24.

22. J. Silbiger, C. Lifshitz, J. Fuchs and A. Mandelbaum, J. Amer. Chem. Soc., 1967, 89, 4308.

23. V.H. Dibeler, F.L. Mohler and R.M. Reese, J. Chem. Phys., 1953, 21, 180.

24. G.P. van der Kelen, O. Volders, H. van Onckelen and Z. Eeckhaut, Z. anorg. Chem., 1965, 338, 106.

25. C.A. Hirt, Anal. Chem., 1961, 33, 1786.

26. N.K. Sokolov, K.A. Andrianov and S.M. Akimova, J. Gen. Chem. U.S.S.R., 1955, 25, 647.

27. A.G. Sharkey, R.A. Friedel and S.H. Langer, Anal. Chem., 1957, 29, 770.

28. J. Diekman, J.B. Thomson and C. Djerassi, J. Org. Chem., 1967, 32, 3904.

29. E.I. Quinn, V.H. Dibeler and F.L. Mohler, J. Res. Nat. Bur. Stand., 1956, 57, 41.

30. V.H. Dibeler, J. Res. Nat. Bur. Stand., 1952, 49, 235.

31. C.P. Johnson and A. Langer, J. Phys. Chem., 1957, 61, 1010.

32. D.E. Bublitz and A.W. Baker, J. Organometal. Chem., 1967, 9, 383.

33. R.G. Kostyanousky and V.V. Yakshin, Izv. Akad. Nauk. S.S.S.R. Ser. Khim., 1967, 2363.

34. R.E. Honig, J. Chem. Phys. 1948, 16, 105.

35. W.B. Nottingham, Phys. Rev., 1939, 55, 203.

36. J.D. Waldron and K. Wood, "Mass Spectrometry." The Institute of Petroleum, London, 1952, p. 16.

37. A.J.C. Nicholson, J. Chem. Phys., 1958, 29, 1312.

38. A.O. Nier and E.E. Hanson, Phys. Rev., 1936, 50, 722.

39. H.D. Hagstrum, J. Chem. Phys., 1948, 16, 848.

40. R.H. Vought, Phys. Rev., 1947, 71, 93.

41. J.W. Warren, Nature, 1950, 165, 810.

42. See. 34.

43. V.H. Dibeler and R.M. Reese, J. Res. Nat. Bur. Stand., 1955, 54, 127.

44. F.P. Lossing, A.W. Tickner and W.A. Bryce, J. Chem. Phys., 1951, 19, 1254.

45. J.D. Morrison, J. Chem. Phys., 1954, 21, 1767.

46. J.D. Morrison, J. Chem. Phys., 1953, 21, 2090.

47. F.H. Dorman and J.D. Morrison, J. Chem. Phys., 1961, 34, 578.

48. E.M. Clarke, Can. J. Phys., 1954, 32, 764.

49. R.E. Fox, W.M. Hickam. T. Kjeldaas and D.J. Grove, Phys. Rev., 1951, 84, 859.

50. R.E. Fox, W.M. Hickam, T. Kjeldaas and D.J. Grove, Rev. Sci. Instr., 1955, 26, 1101.

51. F.H. Field and J.L. Franklin, J. Chem. Phys., 1954, 22, 1895.

52. See. 34.

53. J.D. Morrison, J. Chem. Phys., 1951, 19, 1305.

54. J.D. Morrison and A.J.C. Nicholson, J. Chem. Phys., 1952, 20, 1021.

55. R.E. Fox and W.M. Hickam, J. Chem. Phys., 1954, 22, 2059.

56. J.D. Morrison, J. Chem. Phys., 1954, 22, 1219.

57. J.D. Morrison, J. Chem. Phys., 1963, 39, 200.

58. J.H.D. Eland, P.J. Shepherd and C.J. Danby, Z. Naturforschung, 1966, 21a, 1580.

59. D.P. Stevenson, Disc. Faraday Soc., 1951, 10, 35.

60. G.G. Hess, F.W. Lampe and L.H. Sommer, J. Amer. Chem. Soc., 1965, 87, 5327; 1964, 86, 3174.

61. J.A. Connor, R.N. Haszeldine, G.J. Leigh and R.D. Sedgewick, J. Chem. Soc. (A), 1967, 768.

62. J.A. Connor, G. Finney, G.J. Leigh, R.N. Haszeldine, P.J. Robinson, R.D. Sedgewick and R.F. Simmons, Chem. Comm., 1966, 178.

63. S.J. Band, I.L. Stephenson, I.M.T. Davidson and C.A. Lambert, Chem. Comm., 1967, 723.

64. A.L. Yergey and F.W. Lampe, J. Amer. Chem. Soc., 1965, 87, 4204.

65. D.R. Bidinosti and N.S. McIntyre, Can. J. Chem., 1967, 45, 641.

66. A. Foffani, S. Pignataro, B. Cantone and F. Grasso, Z. physik. Chem., 1965, 45, 79.

67. J. Müller and L. D'Or, J. Organometal. Chem., 1967, 10, 313.

68. R.E. Winters and R.W. Kiser, J. Organometal. Chem., 1965, 4, 190.

69. W.J. Jones, D.P. Evans, T. Gulwell and D.C. Griffiths, J. Chem. Soc., 1935, 39.

70. R. Sasin and G.S. Sasin, J. Org. Chem., 1955, 20, 770.

71. L.A.K. Staveley, H.P. Paget, B.B. Goalby and J.B. Warren, J. Chem. Soc., 1950, 2290.

72. D. Seyforth and F.G.A. Stone, J. Amer.Chem. Soc., 1957, 79, 515.

73. K.A. Kozeschkow, M.M. Nadj and A.P. Alexandrov, Ber., 1934, 1348.

74. G.J.M. Van der Kerk, J.G. Noltes and J.G.A. Luijten, J. Appl. Chem., 1957, 7, 366.

75. E. Krause and R. Becker, Ber., 1920, 173.

76. M. Lesbre, Mrs. R. Buisson, J.G.A. Luijten and G.J.M. Van der Kerk, Rec. Trav. Chim., 1955, 74, 1056.

77. K. Bowden and E.A. Braude, J. Chem. Soc., 1952, 1068.

78. J.F. Norris and A.W. Olmstead, Org. Synthesis Coll. Vol., 1, 138.

79. W.E. Bachmann, Org. Synthesis Coll. Vol., 3, 841.

80. H. Gilman, O.L. Marrs and See-Yuen Sim, J. Org. Chem., 1962, 27, 4232. G. Tamborski, F.E. Ford and E.J. Soloski, J. Org. Chem., 1963, 28, 181.

81. M.V. George, D.J. Peterson and H. Gilman, J. Amer. Chem. Soc., 1960, 82, 403.

82. H. Gilman and C.W. Gerow, J. Amer. Chem. Soc., 1956, 78, 5435.

83. R.J. Cross and F. Glockling, J. Chem. Soc., 1964. 4125.

84. A.L. Smith, Spect. Chim. Acta., 1960, 16, 87.

85. R.D. Kross and V.A. Fassel, J. Amer. Chem. Soc., 1955, 77, 5858.

86. R.C. Poller, J. Inorg. Nuclear Chem., 1962, 24, 593.

87. M.C. Henry and J.G. Noltes, J. Amer. Chem. Soc., 1960, 82, 555.

88. J.S. Thayer and R. West, Inorg. Chem., 1964, 3, 889.

89. M.P. Brown, R. Okawara and E.G. Rochow, Spect. Chim. Acta., 1960, 16, 595.

90. R. Okawara, D.E. Webster and E.G. Rochow, J. Amer. Chem. Soc., 1960, 82, 3287.

91. G.E. Coates, K. Wade and M.L.H. Green, "Organometallic Compounds" vol. 1. 3rd ed., Methuen and Co. Ltd., 1967.

92. H. Gilman and F. Schulze, J. Chem. Soc., 1927, 2663.

93. H. Gilman and R.E. Brown, J. Amer. Chem. Soc., 1930, 52, 4480.

94. W.H. Glaze, C.M. Selman and C.H. Freeman, Chem. Comm., 1966, 474.

95. A.B. Burg and H.I. Schlesinger, J. Amer. Chem. Soc., 1940, 62, 3425.

96. A. Carrick, PhD. Thesis, Durham, 1967.

A. Carrick and F. Glockling, J. Chem. Soc., (A) 1967, 40.

97. J.M. Miller, J. Chem. Soc., (A) 1967, 828.

98. A.E. Williams, Proceedings of the 3rd Annual M.S.9. Users Meeting 1965.

99. J.H. Beynon and A.E. Fontaine, Z. Naturforschung, 1967, 22a, 334.

100. J.H. Beynon, R.A. Saunders and A.E. Williams, "Tables of Meta-Stable Transitions for Use in Mass Spectrometry", Elsevier, 1965.

101. A.J.C. Stevenson, J. Chem. Phys., 1958, 29, 1312.

102. V.I. Vedeneyev, L.V. Gurvich, V.N. Kondrat'yev, V.A. Medvedev, Ye. L. Frankevich, "Bond Energies, Ionization Potentials and Electrom Affinities", Arnold, 1965.

103. A.E. Pope and H.A. Skinner, Trans. Faraday Soc., 1964, 60, 1402.

104. J.A. Kerr, Chem. Rev., 1966,66, 465.

105. J.L. Franklin, Ind. Eng. Chem., 1949, 41, 1070.

106. H.A. Skinner, Adv. Organometal. Chem., 1964, 2, 49.

107. H.E. O'Neal and M.A. Ring, Inorg. Chem., 1966, 5, 435.

108. G.G. Hess, F.W. Lampe and A.L. Yergey, Annals New York Acadamy of Sciences, 1966, 136, 106.

109. S.J. Band, I.M.T. Davidson and C.A. Lambert, J. Organometal. Chem., 1968, 12, 3P.

110. R. Ettinger, Tetrahedron, 1964, 20, 1579.

111. B.G. Hobrock and R.W. Kiser, J. Phys. Chem., 1961, 65, 2186; 1962, 66, 155.

112. B.G. Gowenlock, R.M. Haynes and J.R. Majer, Trans. Faraday Soc., 1962, 58, 1905.

113. R.W. Law and J.L. Margrave, J. Chem. Phys., 1956, 25, 1086.

114. W.C. Steele, L.D. Nichols and F.G.A. Stone, J. Amer. Chem. Soc., 1962, 84, 4441.

115. D.B. Chambers, F. Glockling and M. Weston, J. Chem. Soc., (A) 1967, 1759.

116. W.R. Cullen and D.C. Frost, Can. J. Chem., 1962, 40, 390.

117. R.W. Law and J.L. Margrave, J. Chem. Phys., 1956, 25, 1086.

118. "Handbook of Chemistry and Physics", 46th Edition 1965-1966, The Chemical Rubber Co., Cleveland, Ohio, U.S.A.

119. P.N. Rylander and S. Meyerson, J. Amer. Chem. Soc., 1956, 78, 5799.

120. M.B. Wallenstein, A.L. Wahrhaftig and H. Eyring, "The Mass Spectra of large Molecules I. Saturated Hydrocarbons", University of Utah, Utah, U.S.A. 1951.

121. "Advanced Inorganic Chemistry", F.A. Cotton and G. Wilkinson, 2nd. Ed., Interscience, 1966.

122. E. Heldt, K. Höppner and K.H. Krebs, Z. anorg. Chem., 1966, 347, 95.

123. F. Glockling and J.R.C. Light, J. Chem. Soc., (A) 1968, 717.

124. J.L. Occolowitz, Tetrahedron Letters, 1966, 5291.

125. M. Gielen and G. Mayence, J. Organometal. Chem., 1968, 12, 363.

126. N. Ya. Chernyak, R.A. Khmel'nitskii, T.V. D'yakova, V.M. Vdovin and T.N. Arkhipova, J. Gen. Chem., 1966, 36, 99.

127. A.M. Duffield, C. Djerassi, J. Dubac, G. Manwell and P. Mazerolles, J. Organometal Chem., 1968, 12, 123.

128. K.R. Jennings, Chem. Comm., 1966, 283.

129. P. Brown and C. Djerassi, Angew. Chem. Int. Ed., 1967, 6, 477.

130. W.P. Newman, E. Peterson and R. Sommer, Angew. Chem. Int. Ed., 1965, 4, 599.

131. I.M.T. Davidson and I.L. Stephenson, Chem. Comm., 1966, 746.

132. N. Ya. Chernyak, R.A. Khmel'nitskii, T.V. D'yakova and V.M. Vdovin, J. Gen. Chem., 1966, 36, 93.

133. M. Gielen and J. Nasielski, Bull. Soc. Chim. Belges., 1968, 77, 5.

S. Boue, M. Gielen and J. Nasielski, Bull. Soc. Chim. Belges., 1968, 77, 43.

134. J. Lewis, A.R. Manning, J.R. Miller and J.M. Wilson, J. Chem. Soc., (A) 1966, 1663.

135. A. Carrick and F. Glockling, J. Chem. Soc., (A) 1968, 913.

136. E.H. Brooks, R. Cross and F. Glockling, Inorg. Chim. Acta., 1968, 2, 17.

137. F.J. Preston and R.I. Reed, Chem. Comm., 1966, 51.

138. J.M. Smith, K. Mehner and H.D. Kaesz, J. Amer. Chem. Soc., 1967, 89, 1759

139. H. Svec and G.A. Junk, J. Amer. Chem. Soc., 1967, 89, 2836.

140. M.J. Mays and R.N.F. Simpson, J. Chem. Soc., (A) 1967, 1936.

141. N. Moaz, A. Mandelbaum and M. Cais, Tetrahedron Letters, 1965, 2087.

142. A. Mandelbaum and M. Cais, Tetrahedron Letters, 1964, 3847.

143. R.C. Dobbie and R.G. Cavell, Inorg. Chem., 1967, 6, 1450.

144. R.B. King, J. Amer. Chem. Soc., 1967, 89, 6368.

145. M.I. Bruce, J. Organometal Chem., 1967, 10, 495.

146. H.H. Hoehn, L. Pratt, K.F. Watterson and G. Wilkinson, J. Chem. Soc., 1961, 2738.

147. M.I. Bruce, J. Organometal. Chem., 1967, 10, 95.

148. A.W. Laubengayer and W.F. Gilliam, J. Amer. Chem. Soc., 1941, 63, 477.

D.P. Eyman, Inorg. Chem., 1967, 6, 1461.

149. K. Ziegler, K. Nagel and W. Pfohl, Annal. 1960, 629, 210.

150. T.H. Wartik and H.I. Schlesinger, J. Amer. Chem. Soc., 1953, 75, 835.

151. K. Ziegler, H.G. Gellert, H. Martin, K. Nagel and J. Schneider, Annal. 1954, 589, 91.

152. W.L. Smith and T. Wartik, J. Inorg. Nuclear Chem., 1967, 29, 629.

153. G.E. Coates, A.J. Downs and P.D. Roberts, J. Chem. Soc., (A), 1967, 1085.

154. W.H. Glaze, C.M. Selman and C.H. Freeman, Chem. Comm., 1966, 474.

155. E. Weiss, J. Organometal. Chem., 1965, 4, 101.

156. A.I. Snow and R.E. Rundle, Acta. Cryst., 1951, 4, 348.

157. F. Nakao, Natl. Tech. Rept., 1963, 9, 499. Chem. Abs., 1964, 60, 13985b.